De Sitter Vacua and Black Hole Microstates in String Theory

Dimitrios Toulikas

université PARIS-SACLAY

De Sitter Vacua and Black Hole Microstates in String Theory

Les Vides de Sitter et les Micro-états de Trous Noirs en Théorie des Cordes

Thèse de doctorat de l'université Paris-Saclay

École doctorale n°564 : physique en Île-de-France (PIF)
Spécialité de doctorat: Physique
Graduate School : Physique. Référent : Faculté des Sciences d'Orsay

Thèse préparée à l'**Institut de Physique Théorique** (Université Paris-Saclay, CNRS, CEA), sous la direction de **Iosif BENA**, Directeur de recherche.

Thèse soutenue à Paris-Saclay, le 16 Décembre 2024, par

Dimitrios TOULIKAS

Composition du jury

Membres du jury avec voix délibérative

Ruben MINASIAN Directeur de Recherche, CNRS/CEA, Université Paris Saclay, IPhT	Président
Oscar DIAS Professeur, University of Southampton	Rapporteur & Examinateur
Susha PARAMESWARAN Maitre de conférence (équiv.HDR), University of Liverpool	Rapporteur & Examinatrice
Costas BACHAS Directeur de recherche émérite, École normale supérieure	Examinateur

THESE DE DOCTORAT
NNT : 2024UPASP177

université PARIS-SACLAY | ÉCOLE DOCTORALE Physique en Île-de-France (PIF)

Titre: Les Vides de Sitter et les Micro-états de Trous Noirs en Théorie des Cordes

Mots clés: Théorie des Cordes, Supergravité, Vides de Sitter, Compactification, Trous noirs, Fuzzballs

Résumé: Depuis la découverte que l'expansion de notre univers est probablement entraînée par l'énergie du vide, la recherche de vides de Sitter en quatre dimensions dans la théorie des cordes est devenue un des principaux objectifs de la phénoménologie des cordes. Cependant, malgré deux décennies d'efforts, la construction de vides de Sitter métastables reste un grand défi, et la construction vieille de vingt ans de Kachru, Kallosh, Linde et Trivedi (KKLT), bien que controversée, demeure un des exemples prototypes. Le scénario KKLT est une construction en deux étapes, où, dans un premier temps, la théorie des champs effective en quatre dimensions est utilisée pour obtenir un vide AdS_4 supersymétrique, puis des anti-branes D3 sont ajoutées pour briser la supersymétrie et relever l'énergie du vide à une valeur positive. Dans la première partie de cette thèse, nous étudions en détail certains aspects des deux étapes de cette proposition. D'une part, nous fournissons une description en dix dimensions des vides AdS_4 intermédiaires en utilisant le langage de la géométrie complexe généralisée. D'autre part, nous étudions la rétroaction des anti-branes D3 et découvrons qu'elles génèrent aussi des flux de trois-forme. Nous répertorions toutes les composantes de ce flux, calculons leur effet sur les D7-branes enroulées autour des cycles de quatre dimensions dans la variété de compactification, et élaborons un scénario de type KKLT plus minimaliste.

Dans la deuxième partie de la thèse, nous travaillons sur la nature de la microstructure des trous noirs, un autre problème important que la théorie des cordes devrait résoudre. En relativité générale, les trous noirs sont caractérisés de manière unique par peu de paramètres asymptotiques. Cependant, les trous noirs possèdent aussi une énorme entropie S, qui devrait être expliquée par une description microscopique. Nous examinons cette divergence numérique à travers le prisme de la proposition des fuzzballs, qui affirme qu'il existe e^S solutions sans horizon qui ressemblent au trou noir de loin, mais diffèrent à proximité de l'horizon. Plus précisément, nous travaillons dans le cadre du programme des géométries de microétats, qui concerne les fuzzballs décrits comme des solutions sans horizon en supergravité. Nous étudions le trou noir M2-M5-P, dont l'entropie à faible couplage provient du fractionnement de chaque brane M2 en bandes reliant des branes M5 parallèles. La rétroaction de telles bandes M2 est similaire à un pic de Callan-Maldacena, et pour plusieurs branes M5 et M2, on obtient une structure complexe en forme de labyrinthe à laquelle on peut ajouter des ondes de quantité de mouvement. Globalement, ce «super-maze» préserve quatre supercharges, mais localement, ce nombre est porté à seize. Inspirés par ce résultat, nous montrons que toutes les géométries de microétats connues sont basées sur des «themelia», des configurations de branes présentant cet accroissement local de supersymétrie. Nous expliquons pourquoi les solutions de supergravité rétroagies correspondant aux themelia devraient être lisses et sans horizon, et discutons des progrès récents dans la construction des solutions de supergravité du super-maze. Nous montrons que les solutions de supergravité pour les systèmes d'intersection $\frac{1}{4}$-BPS de branes M2 et M5 sont entièrement caractérisées par une fonction unique satisfaisant une équation non linéaire de type Monge-Ampère, et démontrons que, pour toute solution $\frac{1}{4}$-BPS M2-M5, l'ajout de quantité de mouvement pour arriver à une solution $\frac{1}{8}$-BPS est régi par un système d'équations linéaires. Enfin, comme première étape vers la construction de solutions explicites, nous examinons une limite proche des branes de certaines intersections simples M2-M5, où les équations BPS se linéarisent et l'on obtient des géométries de la forme $AdS_3\times S^3\times S^3\times\Sigma$, avec Σ une surface de Riemann.

université PARIS-SACLAY | ÉCOLE DOCTORALE Physique en Île-de-France (PIF)

Title: De Sitter Vacua and Black Hole Microstates in String Theory

Keywords: String Theory, Supergravity, de Sitter Vacua, Compactification, Black Holes, Fuzzballs

Abstract: Since the discovery that the expansion of our universe is most likely driven by vacuum energy, finding four-dimensional de Sitter vacua in String Theory has been one of the main goals of String Phenomenology, but despite two decades of efforts, constructing metastable de Sitter vacua continues to be a great challenge, and the twenty-year-old construction of Kachru, Kallosh, Linde and Trivedi (KKLT), although not uncontested, remains one of the prototypical examples. The KKLT scenario is a two-step construction, where initially four-dimensional effective field theory is used to obtain a supersymmetric AdS_4 vacuum, and then anti-D3 branes are added to break supersymmetry and uplift the vacuum energy to a positive value. In the first part of this thesis, we study in detail some aspects of both steps of this proposal. On the one hand, we provide a ten-dimensional description of the intermediate AdS_4 vacua using the language of Generalized Complex Geometry. On the other hand, we study the backreaction of the anti-D3 branes and find that they also source three-form fluxes. We tabulate all components of this flux, calculate their effect on the D7-branes wrapping four-cycles in the bulk of the compactification manifold, and devise a more minimalist KKLT-like scenario.

In the second part of the thesis, we work on the nature of the microstructure of black holes, which is another important issue that String Theory should be able to address. In General Relativity, black holes are uniquely characterized by very few asymptotic parameters. However, black holes also have a huge entropy S, which should be explained by a microscopic description. We look at this numerical discrepancy through the lens of the fuzzball proposal, which claims that there are e^S horizonless solutions that resemble the black hole from afar but differ from it in the vicinity of the horizon. More precisely, we work in the context of the microstate geometries programme, which concerns fuzzballs that can be described as horizonless solutions in supergravity. We study the M2-M5-P black-hole, whose entropy at weak coupling comes from the fractionation of each M2-brane into strips connecting parallel M5-branes. The backreaction of such M2-strips is similar to a Callan-Maldacena spike, and for multiple M5- and M2-branes, one gets a complicated maze-like structure to which one can add momentum waves. Globally, this "super-maze" preserves four supercharges, but locally this number is enhanced to sixteen. Inspired by this result, we show that all known microstate geometries are based on "themelia", which are brane configurations that exhibit this local supersymmetry enhancement. We explain why the fully back-reacted supergravity solutions corresponding to themelia should be smooth and horizonless, and then discuss recent progress in constructing the supergravity solutions corresponding to the super-maze. We show that the supergravity solutions for $\frac{1}{4}$-BPS intersecting systems of M2- and M5-branes are completely characterized by a single function that satisfies a non-linear Monge-Ampère-like equation, and we demonstrate that given any M2-M5 $\frac{1}{4}$-BPS solution, the addition of momentum to arrive at an $\frac{1}{8}$-BPS solution is governed by a linear system of equations. Finally, as a first step towards constructing explicit solutions, we look at a near-brane limit of certain single M2-M5 intersections, where the BPS equations linearize and one gets geometries of the form $AdS_3\times S^3\times S^3\times\Sigma$, with Σ a Riemann surface.

To my parents, Nikolaos and Aikaterini,
and my sister, Maria-Iordana.

Acknowledgements

First and foremost, I would like to express my gratitude to my PhD advisor, Iosif Bena, for his unwavering support and continuous guidance. I thank him for the countless discussions that taught me so much and for his contagious enthusiasm that boosted my passion for theoretical physics and helped me overcome various challenges. Moreover, I deeply appreciate his invaluable help with non-scientific matters.

I would like to thank Nick Warner for his outstanding explanations that helped me develop my physical intuition, his willingness to dive into every intricate detail of each calculation, and the conversations on non-research topics that made our long meetings even more enjoyable. I also feel privileged to have started my PhD journey working with Mariana Graña and Emilian Dudas, from whom I learned a great deal of physics and much about how to be a good researcher. I am grateful to them for that.

I would like to thank my other collaborators and friends Nejc Čeplak, Soumangsu Chakraborty, Raphaël Dulac, Shaun Hampton, Anthony Houppe, Nicolas Kovensky, Yixuan Li, and Gabriele Lo Monaco. I thoroughly enjoyed the many stimulating discussions, both on physics and beyond, with all of them.

I would also like to thank the other great friends I made at Saclay: Fabian Bautista, Antoine Bourget, Peng Cheng, Veronica Collazuol, Gabriele di Ubaldo, Bernardo Fraiman, Bogdan Ganchev, Silvia Georgescu, Johan Henriksson, Alvaro Herraez, Dimitrios Mitsios, Hector Parra De Freitas, Salvatore Raucci, Ioannis Tsiares, as well as the entire String Theory group for creating such a wonderful and inspiring environment.

I am grateful to Costas Bachas, Stefano Massai and Ruben Minasian for agreeing to be members of my defense committee, and particularly to Oscar Dias and Susha Parameswaran for fulfilling the role of rapporteur. Moreover, I would like to thank Mariana Graña and Andrea Puhm for taking on the roles of my mentor and tutor. Special thanks also go to Veronique Terras for her invaluable and prompt assistance on many occasions with matters related to my doctoral school obligations.

I appreciate the generous funding from the CEA, and I am grateful to the Alexander S. Onassis Foundation for supporting the final year of my PhD through a scholarship (Onassis Foundation - Scholarship ID: F ZN 078-2/2023-2024). Additionally, I thank the A.G. Leventis Foundation for providing me with an educational grant.

Finally, I am deeply grateful to my parents and my sister for their unconditional love and self-sacrificing support throughout my life, as well as to my long-time friends and to my Melina.

Publications

This thesis is based on the following papers:

Published papers

- **Bare-bones de Sitter vacua**
  I. Bena, E. Dudas, M. Graña, G. Lo Monaco and D. Toulikas
  Phys.Rev.D 108 (2023) 2, L021901 [*arXiv:2202.02327*]
- **Resolving black-hole microstructure with new momentum carriers**
  I. Bena, N. Čeplak, S. D. Hampton, Y. Li, D. Toulikas and N. P. Warner
  JHEP 10 (2022) 033 [*arXiv:2202.08844*]
- **The (amazing) super-maze**
  I. Bena, S. D. Hampton, A. Houppe, Y. Li and D. Toulikas
  JHEP 03 (2023) 237 [*arXiv:2211.14326*]
- **$\overline{\text{D3}}$-branes and gaugino condensation**
  I. Bena, E. Dudas, M. Graña, G. Lo Monaco and D. Toulikas
  JHEP 12 (2023) 019 [*arXiv:2211.14381*]
- **Smearing and unsmearing KKLT AdS vacua**
  M. Graña, N. Kovensky and D. Toulikas
  JHEP 03 (2023) 015 [*arXiv:2212.05074*]

Preprints

- **Themelia: the irreducible microstructure of black holes**
  I. Bena, N. Čeplak, S. D. Hampton, A. Houppe, D. Toulikas and N. P. Warner
  [*arXiv:2212.06158*]
- **Maze Topiary in Supergravity**
  I. Bena, A. Houppe, D. Toulikas and N. P. Warner
  [*arXiv:2312.02286*]
- **Waves on Mazes**
  I. Bena, R. Dulac, A. Houppe, D. Toulikas and N. P. Warner
  [*arXiv:2404.14477*]
- **The M2-M5 Mohawk**
  I. Bena, S. Chakraborty, D. Toulikas and N. P. Warner
  [*arXiv:2407.01665*]

Contents

0 Introduction en Français **1**

1 Introduction **15**

I De Sitter Vacua in String Theory **27**

2 Bare-bones de Sitter **29**
2.1 Introduction . . . 29
2.2 Fluxes generated by $\overline{\text{D3}}$ branes . . . 30
2.3 4d supergravity description . . . 32
2.4 Bare-Bones de Sitter . . . 36
2.5 Conclusions . . . 36

3 $\overline{\text{D3}}$-branes and gaugino condensation **39**
3.1 Introduction . . . 39
3.2 $\overline{\text{D3}}$formed KS geometry . . . 42
3.2.1 Review of the KS solution and its non-supersymmetric deformations 42
3.2.2 Adding $\overline{\text{D3}}$-branes . . . 44
3.3 The flux zoo . . . 45
3.4 Fermion masses . . . 48
3.4.1 Gaugino mass and gaugino condensation . . . 49

4 Smearing and Unsmearing KKLT AdS Vacua **53**
4.1 Introduction . . . 53
4.2 Supersymmetry conditions for type II AdS_4 vacua from 10D . . . 55
4.2.1 Supersymmetric AdS_4 vacua without gaugino condensates . . . 55
4.2.2 Supersymmetry conditions from the 4D EFT and superpotential . . . 57
4.2.3 Kähler potential, cosmological constant, and self-consistency . . . 58
4.2.4 SU(3) structure and Minkowski solutions . . . 59
4.3 Revisiting the effect of the gaugino condensate . . . 60
4.3.1 Supersymmetry conditions with localized terms . . . 61
4.3.2 Motivation . . . 61
4.3.3 Self-consistency and interpretation . . . 63
4.4 Smearing the condensate: KKLT as a proof of concept . . . 66
4.4.1 Summary and effective theory . . . 68

4.4.2 Scale separation . . . 70
4.5 Features of the localized solution . . . 71
4.5.1 Dynamic SU(2) structure and IASD fluxes . . . 71
4.5.2 Cancellation of divergences . . . 72
4.6 Conclusions . . . 76

II Black Hole Microstates in String Theory 79

5 Resolving Black-Hole Microstructure with New Momentum Carriers 81
5.1 Introduction . . . 81
5.2 Momentum carriers on superstrata . . . 85
5.3 Construction of the new three-charge solution . . . 88
5.3.1 Generating an NS5-P solution with local D0-D4 charges . . . 89
5.3.2 Generating the F1-NS5-P solution with local D0-D4 charges . . . 93
5.4 Analysis and comparison . . . 94
5.4.1 The F1-NS5-P three-charge black hole . . . 95
5.4.2 The new three-charge solution with local D0-D4 charges . . . 96
5.4.3 Supersymmetries and singularities . . . 102
5.5 Conclusion and discussion . . . 103

6 The (amazing) Super-Maze 107
6.1 Introduction . . . 107
6.2 Making two-charge bound states out of strings and branes . . . 112
6.2.1 The F1-P bound state . . . 114
6.2.2 The NS5-P bound state . . . 115
6.2.3 The NS5-F1 bound state . . . 116
6.2.4 The relation between the M5-M2 furrow and the Callan-Maldacena spike . . . 118
6.3 The three-charge NS5-F1-P bound state . . . 119
6.3.1 Constructing the projector . . . 119
6.3.2 The M5-M2-P triality . . . 122
6.4 The Brane Content of the Super-Maze . . . 123
6.5 In lieu of a Conclusion: Some thoughts on Super-Maze backreaction . . . 125

7 Themelia: the irreducible microstructure of black holes 131
7.1 Introduction . . . 131
7.2 Themelia . . . 133
7.3 The hyperstratum . . . 137

8 Maze Topiary in Supergravity **141**
8.1 Introduction . . . 141
8.2 The most general solution describing M5-M2 intersections . . . 144
8.2.1 The metric and the three-form potential. . . . 145
8.2.2 The maze function . . . 146
8.2.3 Imposing spherical symmetry . . . 146
8.3 Near-brane M5-M2 intersections . . . 147
8.3.1 Smeared solutions . . . 148
8.3.2 More general families of solutions . . . 150
8.3.3 Mapping the AdS_3 solutions to M5-M2 intersections . . . 152
8.3.4 Verifying the BPS equations for the AdS_3 solutions . . . 156
8.4 String webs . . . 157
8.4.1 The D2-D4 frame . . . 158
8.4.2 Uplifting to M-theory . . . 158
8.5 Floating M2 and M5 branes . . . 159
8.5.1 Floating M2 branes in the intersecting M2-M5 Ansatz . . . 160
8.5.2 Floating M2 branes in the AdS_3 formulation . . . 160
8.5.3 Floating M5 branes in the intersecting M2-M5 Ansatz . . . 161
8.6 Interesting examples of M2-M5 near-horizon solutions . . . 162
8.6.1 No-flip solutions . . . 163
8.7 Adding momentum . . . 164
8.7.1 Adding momentum to spherically symmetric brane intersections . . . 164
8.7.2 Adding momentum charge to the near-brane limit . . . 166
8.7.3 An interesting family of solutions . . . 168
8.8 Conclusions and future directions . . . 169

9 Waves on Mazes **171**
9.1 Introduction . . . 171
9.1.1 Adding momentum to M2-M5 Intersections . . . 172
9.2 Adding momentum to the M2-M5 system - the DBI analysis . . . 173
9.3 The $\frac{1}{8}$-BPS M2-M5-P themelion . . . 176
9.3.1 The Ansatz for the metric and flux . . . 176
9.3.2 The supersymmetries . . . 178
9.3.3 Outline of solving the BPS equations . . . 179
9.3.4 The equations of motion . . . 183
9.3.5 An interesting footnote . . . 184
9.3.6 Summary of the solution . . . 185
9.3.7 A conjecture about multiple momentum waves. . . . 185
9.4 Final comments . . . 186

10 The M2-M5 Mohawk **189**
10.1 Introduction . . . 189
10.2 General M2-M5 intersections and AdS_3 limits . . . 192
10.3 Primary example . . . 193
10.4 Computing the M2 Charges . . . 197
10.4.1 The flux functions . . . 197
10.4.2 Non-trivial cycles and smooth fluxes . . . 198
10.4.3 Computing the flux potential, $\widehat{\Omega}_1$ . . . 199
10.4.4 Computing the flux potential, $\widehat{\Omega}_1$ for the example . . . 201
10.4.5 The brane-intersection mohawk . . . 202
10.5 Final comments . . . 203

Appendices **207**

A Chain of dualities **209**
A.1 Generating the NS5-P-(D0-D4) solution . . . 209
A.2 Adding F1 charge by using a Gibbons-Hawking base . . . 212

B Conventions for Chapter 5 **217**

C Projectors and involutions for branes **221**

D Parameterizing the themelia **223**

E Spherically symmetric $\frac{1}{4}$-BPS M5-M2 intersections **225**
E.1 The Ansatz . . . 225
E.2 Solving the BPS system . . . 227
E.3 Solving the Bianchi equations . . . 228

F The democracy of M5 and M5' branes **231**

G Dualities from the F1-D1 string web to the D2-D4 string web **233**

H The infinite tilted M2-M5 bound state. **239**
H.1 Performing two T-dualities . . . 240
H.2 The democratic formalism . . . 241
H.3 M-theory uplift and matching . . . 242

I Probe M5-branes **245**

Chapter 0

Introduction en Français

Au cours du siècle dernier, il est devenu possible de décrire avec une précision remarquable des phénomènes impliquant des énergies petites et grandes — ou, de manière équivalente, des distances grandes et petites — grâce au développement de deux théories extraordinaires qui constituent aujourd'hui les piliers de notre compréhension du monde. D'une part, on a compris que le microcosme est décrit par les principes de la physique quantique, qui a introduit l'observation surprenante que notre monde est fondamentalement probabiliste. Depuis le début des années 1900, lorsque Planck a introduit le concept de quanta pour expliquer le rayonnement du corps noir, la théorie quantique a considérablement évolué, aboutissant à la création du Modèle Standard de la Physique des Particules. Ce modèle unifie toutes les particules élémentaires connues ainsi que trois des quatre forces fondamentales — l'électromagnétisme, la force faible et la force forte — dans un cadre unique. Bien que ce modèle ne soit pas encore entièrement complet, il a été testé avec une précision extraordinaire et a permis de faire des prédictions significatives, dont beaucoup ont été confirmées bien plus tard, comme le boson de Higgs, découvert au CERN 40 ans après sa prédiction.

Passons maintenant aux grandes distances/faibles énergies : l'autre découverte remarquable du siècle dernier est la Théorie Générale de la Relativité d'Einstein, qui propose que la gravité est un phénomène géométrique. Plus précisément, l'attraction gravitationnelle ressentie entre tous les corps résulte de la courbure de l'espace-temps à quatre dimensions causée par la présence de masse et d'énergie. Cette théorie a également été testée expérimentalement et a conduit à des prédictions extraordinaires, telles que la déviation de la lumière passant près d'un objet massif, les ondes gravitationnelles et, bien sûr, les trous noirs. L'existence des trous noirs a été indirectement confirmée par l'observation des ondes gravitationnelles provenant de fusions de trous noirs en 2016, 100 ans après leur prédiction théorique, et plus récemment, observée directement grâce à la photographie d'un trou noir capturée par le télescope EHT (*Event Horizon Telescope*).

Malheureusement, malgré le succès immense de la Mécanique Quantique et de la Relativité Générale, ces théories sont fondamentalement incompatibles entre elles, et l'un des plus grands défis de la physique moderne est le développement d'un cadre unifié. L'existence d'une telle théorie de la Gravité Quantique est non seulement séduisante sur

le plan philosophique, mais aussi nécessaire pour décrire des phénomènes extrêmes dans l'univers, tels que le Big Bang et les trous noirs, où ni la gravité ni la Mécanique Quantique ne peuvent être ignorées.

La Théorie des Cordes

Notre meilleur espoir pour une théorie de la gravité quantique est la théorie des cordes, qui postule que les constituants fondamentaux de la nature ne sont pas des particules ponctuelles, mais des cordes unidimensionnelles. Les cordes peuvent vibrer à différentes fréquences, et les modes de vibration correspondent aux particules usuelles. Un champ de spin 2 sans masse, le graviton, est toujours présent dans le spectre, ce qui signifie que la gravité est naturellement intégrée à la théorie des cordes. De plus, les théories de jauge de Yang-Mills et une matière semblable à celle du Modèle Standard peuvent également être obtenues. Il existe deux types de cordes : les cordes fermées, qui n'ont pas d'extrémités, et les cordes ouvertes, qui s'étendent entre des objets de dimensions supérieures, les D-branes. Ces objets sont eux-mêmes dynamiques et se couplent à des champs que l'on peut considérer comme des analogues multidimensionnels du champ électromagnétique.

La supersymétrie, une symétrie reliant bosons et fermions, est l'une des idées qui n'ont pas encore été observées expérimentalement, mais que la théorie des cordes intègre naturellement. Contrairement à la plupart des théories, qui ne prédisent pas leurs dimensions d'espace-temps, dans sa formulation supersymétrique, la cohérence interne de la théorie des cordes exige que le nombre de dimensions d'espace-temps soit de dix. Il est possible de construire cinq théories des cordes supersymétriques différentes en dix dimensions, qui sont cependant reliées entre elles par des dualités. De plus, on pense que toutes ces théories descendent d'une théorie en onze dimensions appelée théorie M. Dans ce travail, nous travaillerons principalement dans les limites d'énergie basse des théories des cordes, qui sont des théories de supergravité. Celles-ci sont des extensions de la relativité générale avec d'autres champs issus du spectre des cordes de masse nulle.

Pour établir un lien avec le monde à quatre dimensions que nous observons, nous devons compactifier la théorie des cordes jusqu'à quatre dimensions. Pour cela, il faut choisir une variété interne à six dimensions dont la taille est suffisamment petite pour avoir échappé à la détection. Le choix de cette variété est crucial, car la physique à quatre dimensions dépend fortement de ses propriétés topologiques. Un tore est l'espace interne le plus simple à considérer, mais cela conduit à une grande quantité de supersymétrie en quatre dimensions, ce qui ne semble pas correspondre à nos observations expérimentales. Pour cette raison, d'autres espaces qui conduisent à moins de supersymétrie, comme les variétés de Calabi-Yau, sont généralement utilisés pour des compactifications pertinentes sur le plan phénoménologique. Une autre caractéristique irréaliste de la plupart des compactifications est la présence d'un grand nombre de champs scalaires sans masse appelés modules. Ceux-ci entraînent des interactions à longue portée qui ne sont pas observées dans la nature. Un défi majeur, connu sous le nom de problème de stabilisation des mod-

ules, consiste donc à trouver un mécanisme pour doter ces modules d'un potentiel qui fixe leurs masses.

Les Vides de Sitter

Il y a environ 25 ans, il a été découvert qu'à l'époque actuelle, l'univers est en expansion à un rythme accéléré [1,2], et l'une des plus grandes questions ouvertes en physique concerne la nature de l'énergie qui alimente cette expansion. L'explication la plus simple de cette « énergie noire » est qu'elle provient d'une constante cosmologique, c'est-à-dire une densité d'énergie du vide constante, qui devrait être positive et extrêmement petite (de l'ordre de 10^{-120} en unités de Planck). Actuellement, il n'existe aucune explication dynamique pour justifier pourquoi la constante cosmologique a une valeur aussi infime. Cependant, étant donné que les compactifications en théorie des cordes peuvent donner lieu à un nombre énorme de vides à quatre dimensions, le « paysage de la théorie des cordes », on pourrait recourir à un raisonnement anthropique pour aborder le problème de la constante cosmologique, puisque des énergies du vide beaucoup plus grandes n'auraient pas permis la formation des galaxies (et donc le développement de la vie intelligente) [3]. Il a été avancé qu'il existe au moins environ 10^{500} vides à quatre dimensions en raison du grand nombre de variétés de Calabi-Yau et de toutes les façons possibles d'y appliquer des flux. Il est donc possible que la valeur de la constante cosmologique soit environnementale, déterminée par notre position dans ce multivers de vides.

Le paradigme du multivers pourrait ne pas être particulièrement satisfaisant, car on pourrait espérer que la théorie des cordes pointe vers un vide unique reproduisant exactement la physique que nous observons. Cependant, il existe un problème encore plus grand : il s'avère extrêmement difficile de construire des solutions de de Sitter en théorie des cordes, et on pourrait soutenir qu'il n'existe même pas un seul vide de Sitter à quatre dimensions pleinement rigoureux, encore moins plus de 10^{120} d'entre eux. Par conséquent, la construction de vides métastables de Sitter à quatre dimensions reste un défi majeur, et la construction vieille de vingt ans de Kachru, Kallosh, Linde et Trivedi (KKLT) [4], bien que controversée, demeure l'un des exemples prototypes.

La question de savoir si l'espace de Sitter est réalisable en théorie des cordes a également été explorée du point de vue de l'approche « bottom-up » du programme du swampland, qui vise à déterminer l'ensemble des théories des champs à basse énergie, apparemment cohérentes, mais qui ne peuvent pas être couplées à la gravité quantique. Motivée par les défis significatifs de la construction d'un vide de Sitter en théorie des cordes et par des connexions avec d'autres conjectures du swampland, la conjecture de de Sitter a été proposée [5,6]. Celle-ci exclut les vides de Sitter (méta-)stables en théorie des cordes. Si elle est vraie, cela signifierait que la nature de l'énergie noire dans notre univers ne peut pas être une constante cosmologique.

Il est donc important de continuer à revisiter et à examiner attentivement les propositions existantes pour obtenir des solutions avec une constante cosmologique positive en

théorie des cordes, ainsi qu'à en concevoir de nouvelles, plus solides. Le travail présenté dans la première partie de cette thèse contribue à ces efforts.

Les Trous Noirs et leurs Énigmes

Comme mentionné dans l'avant-propos, la mécanique quantique et la relativité générale sont fondamentalement incompatibles. Ce conflit est particulièrement prononcé dans l'étude des trous noirs, qui servent donc de cadre idéal pour tester toute théorie de la gravité quantique.

Les trous noirs sont des objets astrophysiques qui résultent de l'effondrement gravitationnel d'étoiles supermassives. Ils constituent des solutions classiques aux équations du mouvement de la relativité générale et ne sont décrits que par quelques paramètres macroscopiques : leur masse, leur charge et leur moment angulaire. Ils représentent une région de l'espace-temps où toute la masse est concentrée en une singularité de l'espace-temps, enveloppée par un horizon des événements. Cette hypersurface nulle sépare l'espace-temps extérieur de l'intérieur du trou noir, d'où même la lumière ne peut s'échapper.

Une autre caractéristique remarquable des trous noirs est que, classiquement, ils obéissent à des lois qui ressemblent de près aux lois de la thermodynamique. A priori, il ne s'agit que d'une analogie formelle, mais il s'avère que, lorsque des effets quantiques sont pris en compte, les trous noirs présentent de véritables propriétés thermodynamiques, révélant ainsi une connexion profonde entre la géométrie des trous noirs, la mécanique quantique et la thermodynamique. Sans même invoquer de physique quantique, en considérant que jeter une masse dans un trou noir ne devrait pas entraîner de perte d'entropie, Bekenstein a conjecturé que les trous noirs devraient avoir une entropie proportionnelle à la surface de leur horizon [7]. Peu de temps après, Hawking a confirmé cette intuition en étudiant les champs quantiques près de l'horizon [8]. En particulier, il a montré que les trous noirs émettent un rayonnement thermique à une température $T_H = \frac{\hbar c^3}{8\pi G M k_B}$, qui, en utilisant la deuxième loi de la thermodynamique, peut être utilisée pour dériver leur entropie S :

$$S = \frac{k_B c^3 A}{4\hbar G}\,, \tag{1}$$

où A est la surface de l'horizon du trou noir.

L'entropie dite de Bekenstein-Hawking est énorme, de l'ordre du carré de la masse du trou noir. Par exemple, pour le trou noir au centre de la Voie lactée, Sagittarius A*, ce nombre est d'environ 10^{90}. Selon la formule de l'entropie de Boltzmann $S = \log(N)$, cette entropie devrait correspondre à un nombre encore plus grand de micro-états N partageant les mêmes propriétés macroscopiques. Cependant, en relativité générale, le théorème d'unicité des trous noirs nous dit que $N = 1$, puisqu'un trou noir stationnaire est unique pour une masse, une charge et un moment angulaire donnés. Le grand mystère est donc de savoir où se trouvent tous ces micro-états. La relativité générale ne peut pas répondre à cette question.

Un autre puzzle profond est le paradoxe de l'information, qui apparaît lorsque l'on

considère l'évaporation d'un trou noir via le rayonnement de Hawking. Imaginez qu'un trou noir se forme à partir de l'effondrement gravitationnel d'une étoile. Ce trou noir émet ensuite un rayonnement, perdant progressivement de la masse, et si l'on attend suffisamment longtemps, il finira par s'évaporer complètement, ne laissant derrière lui que du rayonnement. Cependant, ce rayonnement provient de la région de l'horizon et, selon le théorème d'unicité des trous noirs, il devrait être universel et ne peut contenir aucune information sur ce qui a initialement formé le trou noir. Ce processus semble entraîner une perte d'information sur l'état initial et viole donc l'unitarité, l'un des principes fondamentaux de la mécanique quantique.

La Proposition de Fuzzball

Le puzzle de l'origine microscopique de l'entropie des trous noirs et le paradoxe de l'information suggèrent que nous avons besoin d'une théorie quantique de la gravité pour les résoudre. Comme nous l'avons déjà mentionné, la théorie des cordes est notre meilleur espoir pour y parvenir. En effet, l'un des plus grands succès de la théorie des cordes est le dénombrement des degrés de liberté qui donnent naissance à l'entropie des trous noirs supersymétriques en termes d'états liés de cordes et de branes dans le régime des paramètres où les interactions gravitationnelles sont désactivées.

En théorie des cordes, on peut effectuer un développement perturbatif selon deux paramètres : la longueur de corde l_s, qui fixe l'échelle à laquelle les effets des cordes deviennent importants, et le couplage de corde g_s, qui contrôle l'intensité de l'interaction entre les cordes. En termes de ces paramètres, la constante gravitationnelle s'exprime comme $G_N \sim g_s^2 l_s^{d-2}$, où d est le nombre de dimensions. Lorsque $g_s \ll 1$, nous sommes dans le régime (semi)classique, tandis que pour $g_s \sim 1$, nous sommes dans le régime quantique. En présence d'un état lié de N D-branes, le couplage effectif entre cordes ouvertes et fermées, qui est également le couplage entre cordes ouvertes, est donné par $g_s N$. À faible $g_s N$, on peut décrire le système en termes de cordes ouvertes faiblement couplées sur le fond des N D-branes, car, dans ce régime, les cordes ouvertes et fermées se découplent et la gravité peut être négligée. À grand $g_s N$, les D-branes rétroagissent sur la géométrie, et le système est décrit en utilisant la supergravité. Ces deux régimes sont illustrés dans la Fig. 1. Une chose importante à noter est que l'entropie de Bekenstein-Hawking est indépendante du couplage de corde (et de la longueur de corde), ce qui signifie que nous devrions être capables de la reproduire en comptant les états supersymétriques dans le régime $g_s N \ll 1$.

Cela a été réalisé pour la première fois pour le trou noir supersymétrique à deux charges par Sen en 1995 [10]. Dans le cadre de dualité F1-P, où l'on a N cordes fondamentales avec une impulsion P sur elles, l'entropie du système provient des différentes manières dont les cordes fondamentales peuvent transporter l'impulsion, et dans le régime de couplage nul, la dégénérescence des états peut être calculée en utilisant la formule de Cardy dans la théorie conforme des champs sous-jacente. En activant g_s , le système rétroagit et

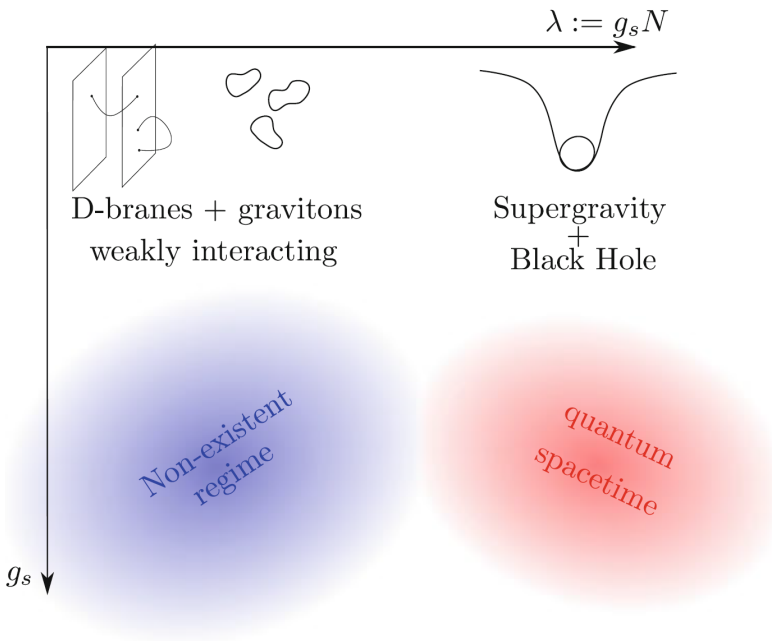

Figure 1: Les régimes des paramètres en théorie des cordes. La figure est tirée de [9].

forme un trou noir, qui possède classiquement une surface d'horizon nulle. Cependant, il a été montré dans [11] qu'en prenant en compte les corrections liées aux cordes, le trou noir développe un petit horizon, dont l'entropie correspond au calcul de Sen. Ce système est très particulier, et on pourrait douter qu'une correspondance similaire tienne pour des trous noirs avec un horizon macroscopique, mais un an après l'article de Sen, Strominger et Vafa ont étendu son résultat au trou noir D1-D5-P [12], montrant que le dénombrement des états dans la CFT pour un couplage nul correspond exactement à l'entropie de Bekenstein-Hawking.

Ces résultats sont remarquables, mais ils ne montrent que quels sont les degrés de liberté microscopiques des trous noirs supersymétriques dans un régime de paramètres où la solution classique de trou noir n'existe pas, laissant ouverte une question importante qui fait encore l'objet de débats : Que deviennent les micro-états du trou noir lorsque le couplage gravitationnel est activé ? Tombent-ils derrière l'horizon, ou restent-ils visibles via une nouvelle physique à l'échelle de l'horizon ?

Puisque l'attraction gravitationnelle est universelle et devient plus forte avec la constante gravitationnelle, la matière ordinaire se compresse à mesure que G_N augmente. Seul l'horizon d'un trou noir croît en taille, et on s'attend donc à ce qu'au fur et à mesure que g_s augmente, un horizon finisse par se former, et que les micro-états responsables de l'entropie pour un couplage nul soient absorbés par cet horizon, devenant indiscernables du trou noir. Cependant, en théorie des cordes, ce n'est pas toujours le cas, car il existe des configurations de branes qui, en réalité, s'étendent et ne forment jamais d'horizon. De plus, leur taille augmente au même rythme que le rayon de l'horizon du trou noir.

La proposition de fuzzball [13] affirme que ce phénomène est générique et non limité à des exemples particuliers. En particulier, elle soutient que lorsqu'on tente de former

un trou noir en théorie des cordes, on n'obtient pas la solution traditionnelle du trou noir, mais un objet sans horizon à l'échelle de l'horizon, appelé fuzzball. Cet objet rayonne depuis sa surface comme un corps normal, et il n'y a donc pas de paradoxe de l'information. Une caractéristique remarquable de cette proposition est que les effets de gravité quantique deviennent importants et modifient la géométrie non pas à l'échelle de la longueur de Planck, mais déjà à l'échelle de l'horizon. Un trou noir doit donc être vu comme une description moyenne des degrés de liberté du fuzzball, et les horizons ainsi que les singularités n'apparaissent que lorsque la gravité est décrite par une théorie qui n'est pas suffisamment riche pour capturer la physique sous-jacente.

Les géométries de micro-états

Pour que la proposition de fuzzball soit valide, il devrait exister environ e^S configurations sans horizon et non singulières pour un trou noir donné d'entropie S. Pour le trou noir à deux charges, cela a été réalisé puisqu'il a été montré que les états BPS de la CFT décrivant la physique basse énergie du système D1-D5 correspondent à certaines configurations non singulières et sans horizon, appelées supertubes, qui possèdent des charges électriques D1 et D5 ainsi qu'une charge dipolaire de monopôle de Kaluza-Klein (KKM). Leurs solutions en supergravité sont paramétrées par une forme arbitraire, et la quantification de leur espace de modules reproduit exactement l'entropie du trou noir à deux charges obtenue par le dénombrement à couplage nul : $S = 2\pi\sqrt{2N_1N_5}$ [14–20].

Cependant, comme nous l'avons déjà souligné, le système à deux charges est un cas assez particulier. Pour faire progresser la proposition de fuzzball, nous devrions considérer des trous noirs avec un horizon macroscopique. Cela nous conduit naturellement à étudier les trous noirs supersymétriques à trois charges. Eux aussi ont une température de Hawking nulle, ce qui signifie qu'ils ne permettent pas d'aborder le paradoxe de l'information. Cependant, il est très important de les étudier afin de comprendre le problème du stockage de l'information.

Les fuzzballs sont les configurations les plus générales sans horizon et avec structure à l'échelle de l'horizon, ayant la même masse, charge et moment angulaire qu'un trou noir donné, et elles peuvent être arbitrairement quantiques et fortement courbées. Cela signifie qu'en pratique, il est difficile de décrire une fuzzball générique. On peut cependant essayer de construire des géométries de micro-états, qui sont des fuzzballs pouvant être décrites comme des solutions lisses et sans horizon en supergravité (voir Fig. 2). Étant donné le nombre immense de micro-états quantiques d'un trou noir, il devrait exister un nombre tout aussi immense de représentations cohérentes de ces micro-états, et l'objectif du programme des géométries de micro-états (voir [22, 23] pour des revues récentes), qui a débuté il y a presque vingt ans, est de les construire.

Un nombre considérable de géométries a été construit pour le trou noir supersymétrique à trois charges, et celles-ci ont également été mises en correspondance avec la CFT duale via l'holographie de précision. Cependant, il n'a pas été possible de construire des états

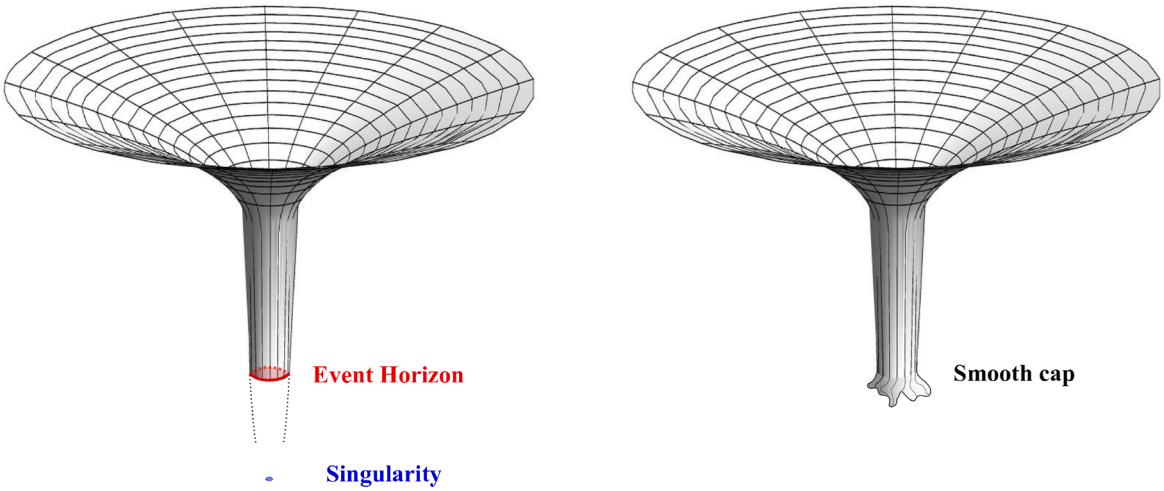

Figure 2: Représentation schématique d'une géométrie de micro-état. À gauche, la géométrie du trou noir se termine par une singularité cachée derrière l'horizon des événements. À droite, la géométrie de micro-état ressemble asymptotiquement exactement à la solution de trou noir, mais la gorge se referme de manière lisse avant l'horizon. La figure est tirée de [21].

rendant compte de l'ensemble de l'entropie du trou noir. En particulier, l'entropie des superstrata [24–26], qui représentent la plus grande famille de géométries de micro-états des trous noirs D1-D5-P, croît comme $\sqrt{N_1 N_5} N_P^{1/4}$ [27, 28], ce qui est paramétriquement plus petit que l'entropie du trou noir, $\sqrt{N_1 N_5 N_P}$. La raison en est que les superstrata sont construites en supergravité à six dimensions, qui ne peut pas résoudre le fractionnement des branes, essentiel pour accéder au secteur tordu (twisted sector) de la CFT duale, d'où provient la majeure partie de la microstructure du trou noir.

Un grand défi consiste donc à décrire le fractionnement des branes en utilisant la supergravité en dix ou onze dimensions. Dans la seconde partie de cette thèse, nous commençons à aborder ce problème en étudiant le trou noir M2-M5-P, dont l'entropie provient du fractionnement de chaque brane M2 en bandes transportant de l'impulsion suspendues entre des branes M5 parallèles.

Themelia

En résolvant la microstructure des trous noirs, on est naturellement amené à se demander: quelles sont les structures fondamentales en théorie des cordes ? La réponse la plus simple et la plus naïve est, bien sûr, les cordes. Cependant, la réponse à cette question doit être invariante sous dualité. La solution évidente est donc d'inclure tous les objets pouvant être obtenus par dualisation des cordes, tels que les branes, les monopôles de Kaluza-Klein et les états liés de branes qui préservent seize supercharges.

On peut alors envisager une extension supplémentaire, pour inclure des objets qui

préservent seize supercharges *localement*, mais qui n'en préservent qu'une fraction (ou éventuellement aucune) lorsqu'on considère l'objet dans son ensemble. Ces objets ont été appelés *themelia* dans [29].

Un exemple simple: une corde portant une impulsion dans le sens droit est $\frac{1}{4}$-BPS, préservant huit supersymétries. C'est un themelion parce que, lorsqu'on « zoome » sur la corde, on ne voit qu'un segment boosté de corde, qui préserve 16 supersymétries. Un autre segment de la corde préserve également 16 supersymétries, mais des supersymétries différentes: celles-ci dépendent de l'orientation du segment de corde [30]. Cependant, chaque ensemble de 16 supersymétries locales contient un sous-ensemble commun de huit supersymétries, ce qui fait que l'objet entier constitue une configuration $\frac{1}{4}$-BPS.

Il est naturel de s'attendre à ce que les themelia émergent comme la sous-structure fondamentale[1] des micro-états des trous noirs. Il y a trois raisons à cela. Premièrement, et de manière évidente, le themelion est nécessairement un état lié, car on ne peut pas séparer les charges fondamentales sans briser certaines des 16 supersymétries locales.

Deuxièmement, un système de N branes identiques qui préservent seize supersymétries *globalement* peut avoir une entropie au plus de l'ordre de $logN$. Cela signifie que la structure locale d'un themelion ne peut expliquer que des contributions de l'ordre de $logN$ à l'entropie. Cependant, la structure globale d'un themelion peut impliquer des excitations de ses modules, comme des modes de forme et des densités de branes, qui sont paramétrées par des fonctions continues arbitraires, et ces excitations peuvent porter une entropie proportionnelle à une puissance de N. Un themelion ne peut encoder une entropie aussi grande que dans sa structure globale, à grande échelle.

L'exemple le mieux étudié est probablement le système D1-D5. Ce système porte une entropie de l'ordre de $\sqrt{N_1 N_5}$. Pris isolément, il produit une géométrie de trou noir singulière avec un horizon à l'échelle de Planck. Cependant, ce n'est pas un themelion : il n'a que huit supercharges localement. Si l'on ajoute un monopôle de Kaluza-Klein (KKM) et un moment angulaire, il peut être transformé en supertube, une géométrie lisse, avec seize supercharges localement et huit globalement [14, 16, 18, 31]. Les états fondamentaux dégénérés qui donnent lieu à l'entropie peuvent alors être interprétés comme des modes de forme du supertube. En effet, cet exemple, ainsi que le système F1-P relié par dualité, ont conduit à la proposition originale du fuzzball.

Plus largement, il a été observé dans [29] que toutes les géométries de micro-états connues (et les solutions de micro-états [32]) sont en réalité basées sur des themelia : cela inclut les systèmes de branes sous-jacents aux solutions à bulles à trois charges [33–35], les superstrata [24, 30] et le supermaze [36].

La troisième raison pour laquelle les themelia doivent être considérés comme des constituants fondamentaux de la microstructure des trous noirs est qu'un themelion complètement rétro-réagi *ne peut jamais donner lieu à une solution classique de trou noir avec un horizon des événements.* En effet, la surface de l'horizon, en unités de Planck,

[1] Le mot grec ancien *themelion* ($\theta\epsilon\mu\acute{\epsilon}\lambda\iota\sigma\nu$) se traduit par *fondation*, ou *structure fondamentale*. Malheureusement, l'autre mot pour une structure indivisible, *atomon*, était déjà pris.

est invariante sous dualité [37], et reste donc identique dans *tous* les cadres de dualité. D'un autre côté, un themelion peut toujours être dualisé localement en un empilement de N monopôles de Kaluza-Klein, et cette solution est simplement un espace vide avec une singularité d'orbifold Z_N, ce qui constitue une configuration exacte, complètement rétro-réagi, sans horizon en théorie des cordes.

Indépendamment des considérations géométriques, la conjecture du themelion affirme que *les constituants fondamentaux de la microstructure des trous noirs doivent être des themelia.* De plus, comme un themelion porte son entropie dans sa structure à grande échelle, les solutions de supergravité correspondant à des collections cohérentes de themelia devraient pouvoir accéder précisément aux degrés de liberté qui portent cette entropie. Bien entendu, la supergravité ne peut pas décrire les phénomènes à l'échelle des cordes, mais on peut espérer qu'elle puisse décrire les limites classiques des themelia et les degrés de liberté qui portent leur entropie. Nous désignerons cette extension de la conjecture du themelion comme la *conjecture du themelion géométrique.*

La conjecture du themelion fournit ainsi une réalisation explicite de la proposition fuzzball en théorie des cordes, tandis que la conjecture du themelion géométrique offre un cadre précis pour réaliser les objectifs du programme des géométries de micro-états [23, 32].

On peut voir comment la conjecture du themelion peut se réaliser dans le trou noir M2-M5-P. L'entropie de ce système provient du fait que chaque brane M2 peut se fractionner en N_5 bandes qui peuvent transporter une impulsion indépendamment[2]. Étant donné que chacune des N_2N_5 bandes a quatre directions bosoniques, il n'est pas difficile de voir que l'entropie totale (y compris les fermions) correspond exactement à celle du trou noir associé, $S = 2\pi\sqrt{N_2N_5N_P}$. Lorsque l'on considère les interactions entre les branes, on trouve que les bandes M2 transportant l'impulsion tirent sur les branes M5 et les déforment. La caractéristique remarquable de cette configuration transportant l'impulsion, que nous appelons le supermaze, est qu'elle préserve globalement quatre supercharges, mais si l'on effectue un zoom sur n'importe quel point de celle-ci, elle préserve localement seize supercharges [36]. Ainsi, le supermaze M2-M5-P est une réalisation explicite d'un themelion qui porte toute l'entropie du trou noir.

Si l'on pouvait construire les solutions de supergravité correspondant à ce supermaze et montrer explicitement que ces solutions n'ont pas d'horizon, cela établirait la conjecture du themelion géométrique. Cependant, il existe plusieurs obstacles techniques à surmonter. Une grande partie de cette thèse est consacrée à aborder ces questions.

Organisation de la Thèse

Cette thèse est divisée en deux parties. Dans la première partie, nous étudions certains aspects clés de la proposition KKLT pour obtenir des vides de Sitter à quatre dimensions métastables en théorie des cordes. Dans la deuxième partie, nous présentons les

[2]Ce dénombrement est l'élévation en théorie M de celui du trou noir F1-NS5-P en type IIA [38].

développements récents du programme des géométries de micro-états pour les trous noirs supersymétriques à trois charges.

Un composant crucial de la construction KKLT est l'ajout d'une anti-D3 brane au bas d'une gorge de Klebanov-Strassler (KS), ce qui brise la supersymétrie et élève la constante cosmologique à une valeur positive. Dans toutes les constructions de type KKLT, l'anti-D3 brane est considérée comme une sonde, et seule la contribution positive au potentiel scalaire provenant de son action sur le volume du monde est prise en compte. Dans les chapitres 2 et 3, nous étudions la rétroaction des anti-D3 branes à l'extrémité d'une gorge KS et trouvons qu'elles génèrent également des flux à trois formes.

Dans le chapitre 2, nous montrons que ces flux donnent lieu à des termes non triviaux dans le superpotentiel lorsque la gorge est intégrée dans une compactification avec flux. Nous décrivons ces termes à la fois dans une perspective en dix dimensions et en quatre dimensions, et nous montrons qu'en incluant la stabilisation des modules de Kähler, le potentiel résultant admet des minima de Sitter. Notre construction proposée pour obtenir des vides de Sitter ne nécessite pas de flux $(0,3)$ supplémentaires brisant la supersymétrie et est donc plus minimaliste que la proposition KKLT.

Dans le chapitre 3, nous établissons un tableau détaillé de tous les composants (m,n) des flux brisant la supersymétrie générés par les anti-D3 branes et calculons leur effet sur la stabilisation des modules de Kähler via la condensation de gauginos sur les D7-branes. Cela nous permet d'obtenir une nouvelle contrainte sur la validité de ce mécanisme de stabilisation.

Dans la première étape de la construction KKLT, où l'on obtient un vide AdS_4 supersymétrique, on suppose que les modules de structure complexe sont fixés par les flux. Ensuite, pour tenir compte de l'effet non perturbatif de la condensation de gauginos sur les D7-branes enveloppant des cycles à quatre dimensions de la variété interne, nécessaire pour la stabilisation des modules de Kähler, il faut recourir à une théorie effective en quatre dimensions. Dans le chapitre 4, nous fournissons une description en dix dimensions des vides AdS_4 de KKLT. Nous utilisons d'abord le langage de la géométrie complexe généralisée pour dériver les équations de supersymétrie pour les vides AdS_4 de type II, incluant l'effet localisé de la condensation de gauginos sur les D-branes. Nous les résolvons ensuite pour les compactifications de type IIB avec des condensats de gauginos sur des D7-branes étalées et trouvons que cela conduit à une solution AdS_4 supersymétrique très similaire à celle de KKLT. De plus, nous trouvons qu'une séparation exponentielle entre les échelles AdS et KK est possible tant que les flux à trois formes ont une composante $(0,3)$ exponentiellement supprimée. Quant à la solution localisée, elle nécessite d'aller au-delà des variétés internes à structure SU(3). Néanmoins, nous montrons que l'action peut être évaluée à l'équilibre sans dépendre des détails d'une configuration aussi complexe.

Passant à la deuxième partie de cette thèse, dans le chapitre 5, nous étudions une limite problématique où les superstrata semblent développer un horizon, et nous montrons que cet horizon n'apparaît que parce que certains degrés de liberté essentiels dans cette limite de moment angulaire nul sont négligés. Nous intégrons certains de ces degrés de liberté en construisant, pour la première fois, des solutions avec une surface d'horizon nulle qui ont

les mêmes charges qu'un trou noir à trois charges F1-NS5-P en théorie des cordes de type IIA et qui préservent la symétrie sphérique du trou noir. L'impulsion de ces solutions est portée par des fluctuations de densité longitudinales D0-D4 le long de la direction commune F1-NS5. Nous soutenons que ces solutions doivent être interprétées comme la limite à gorge longue des superstrata. L'existence de ces géométries indique qu'un horizon de taille finie n'apparaît pas, même dans les coins singuliers de l'espace des modules des géométries de micro-états à trois charges.

Dans le chapitre 6, nous proposons une nouvelle approche pour rendre pleinement compte de l'entropie des trous noirs supersymétriques à trois charges en utilisant des géométries de micro-états. En particulier, nous étudions le trou noir à trois charges F1-NS5-P en théorie des cordes de type IIA, dont l'entropie provient de la fragmentation des N_1 cordes F1 en N_1N_5 petites cordes, qui deviennent des transporteurs d'impulsion indépendants. En théorie M, ce système a une signification géométrique claire, puisque les petites cordes se traduisent en bandes de branes M2 qui connectent des paires de branes M5 parallèles séparées le long de la direction de la théorie M. La rétroaction de ces bandes M2 se terminant sur des branes M5 est similaire aux pointes de Callan-Maldacena décrivant les cordes F1 rétro-réagies se terminant sur des branes D3 [39]. Pour des branes M5 et M2 multiples, on obtient une structure complexe ressemblant à un labyrinthe. L'ajout d'ondes d'impulsion aux bandes M2 donne lieu à une configuration de branes porteuses d'impulsion, que nous appelons le Supermaze. L'élément clé est que le Supermaze possède quatre supercharges globales, mais en préserve localement 16, et nous nous attendons donc à ce que sa rétroaction donne lieu à des solutions sans horizon.

Le projecteur de supersymétrie correspondant au supermaze montre qu'en plus des charges M2, M5 et P (ou des charges F1, NS5, P en type IIA), il faut six autres charges dipolaires, qui sont nécessaires pour former la « colle » transformant les branes individuelles en un état lié avec seize supersymétries localement. Inspirés par cela, dans le chapitre 7, nous introduisons les « themelia ». Ce sont des objets en théorie des cordes qui possèdent seize supersymétries localement, mais en ont moins lorsqu'on les considère globalement. Nous soutenons qu'ils sont les blocs de construction fondamentaux des micro-états des trous noirs. Nous montrons que toutes les géométries de micro-états lisses et sans horizon existantes peuvent être considérées comme des états liés de themelia, et nous conjecturons que tous ces états liés donneront lieu à des géométries de micro-états. Nous construisons également le themelion le plus général ayant une isométrie de trois-tore et montrons qu'il interpole entre les superstrata et le supermaze.

Dans le chapitre 8, nous faisons le premier pas vers le développement de la formulation en supergravité du supermaze, en étudiant les supermazes sans impulsion. Nous montrons que les solutions de supergravité pour des systèmes intersectants $\frac{1}{4}$-BPS de branes M2 et M5 sont entièrement caractérisées par une unique fonction de « maze » qui satisfait une équation non linéaire de « maze » semblable à l'équation de Monge-Ampère. Nous utilisons des branes M2 et M5 sondes flottantes pour explorer la structure de ces solutions et relions une classe de nos solutions aux réseaux de cordes (p, q) F1-D1. Résoudre l'équation du maze est généralement une tâche complexe, mais nous identifions deux méthodes pour

trouver des classes spécifiques de solutions. La première consiste à considérer un état lié infini M2-M5 à un certain angle et avec un certain ratio de densités M2 et M5. Cette solution est présentée dans l'appendice H et peut être démontrée comme satisfaisant exactement l'équation du maze. La seconde méthode consiste à considérer une limite proche de l'horizon. Nous considérons une telle limite et parvenons à relier nos solutions à une classe de solutions $AdS_3 \times S^3 \times S^3$ déformées sur une surface de Riemann construites dans [40], pour lesquelles les équations BPS se réduisent à un système linéaire. Enfin, nous explorons l'ajout d'une simple charge d'impulsion.

Dans le chapitre 9, nous abordons correctement le problème de l'ajout d'impulsion à un labyrinthe de bandes de branes M2 étirées entre des branes M5 pour construire des solutions $\frac{1}{8}$-BPS qui préservent seize supersymétries localement. Nous montrons qu'étant donné une solution de supergravité $\frac{1}{4}$-BPS décrivant le labyrinthe, il est possible d'ajouter des ondes d'impulsion sans modifier le fond M2-M5. Fait remarquable, ces excitations sont entièrement déterminées par un ensemble stratifié d'équations linéaires. Les champs responsables du transport de l'impulsion sont paramétrés par des fonctions arbitraires d'une direction nulle et ont exactement la même structure que dans les constructions sur le volume du monde des branes. Le fait que les excitations d'impulsion et de flux du système M2-M5-P soient régies par une structure linéaire nous rapproche de l'utilisation des solutions de supergravité pour capturer l'entropie des trous noirs supersymétriques.

Dans le chapitre 10, nous étudions en détail une classe particulière de solutions AdS_3 construites dans [40] et montrons qu'elles décrivent des intersections simples M2-M5, qui sont toutefois loin d'être sans caractéristiques. En particulier, elles décrivent ce qui apparaît depuis l'infini comme un seul empilement de branes M2 semi-infinies se terminant sur, et déformant, un seul empilement de branes M5. Cependant, lorsque l'on effectue un zoom sur l'intersection, les M2 et M5 se résolvent en pointes physiquement séparées (une « crête »), avec la distance entre chaque pointe contrôlée par le nombre de M2 et M5 formant chaque pointe. Nous expliquons pourquoi nous soupçonnons que toute limite proche des branes menant à un tel facteur AdS_3 est nécessairement limitée à une seule intersection, et nous commentons l'interprétation CFT de ces crêtes.

Chapter 1

Introduction

During the past century, it became possible to describe with remarkable precision phenomena involving small and large energies—or equivalently large and small distances—through the development of two extraordinary theories that now serve as the pillars of our understanding of the world. On one hand, it was understood that the microcosm is described by the principles of quantum physics, which introduced the shocking observation that our world is fundamentally probabilistic. Since the early 1900s, when Planck introduced the concept of quanta to explain blackbody radiation, quantum theory has evolved significantly, culminating in the creation of the Standard Model of Particle Physics. This model unifies all known elementary particles and three of the four fundamental forces, electromagnetism, the weak force, and the strong force, within a single framework. Although not yet entirely complete, this model has been tested with incredible precision and has made significant predictions, many of which have been confirmed much later, such as the Higgs boson, discovered at CERN 40 years after its prediction.

Moving now to large distances/low energies, the other remarkable discovery of the past century was Einstein's General Theory of Relativity, which proposes that gravity is a geometric phenomenon. Specifically, the gravitational attraction experienced between all bodies arises from the curvature of four-dimensional spacetime caused by the presence of mass and energy. This theory, too, has been experimentally tested and has led to extraordinary predictions, such as the deflection of light passing near a massive object, gravitational waves, and, of course, black holes. The existence of black holes was indirectly confirmed by the observation of gravitational waves from black hole mergers in 2016, 100 years after their theoretical prediction, and more recently, directly observed through the photograph of a black hole captured by the Event Horizon Telescope.

Unfortunately, despite the immense success of Quantum Mechanics and General Relativity, these theories are fundamentally incompatible with each other, and one of the greatest challenges in modern physics is the development of the framework that unifies them. The existence of such a theory of Quantum Gravity is not only pleasing on a philosophical level, but it is also necessary to describe extreme phenomena in the universe, such as the Big Bang and black holes, where neither gravity nor Quantum Mechanics can be ignored.

String Theory

Our best hope for a theory of Quantum Gravity is String Theory, which posits that the fundamental constituents of nature are not point-like particles but one-dimensional strings. Strings can vibrate at different frequencies, with the modes of vibration corresponding to the usual particles. A spin-2 massless field, the graviton, is always present in the spectrum; hence, gravity is naturally incorporated into String Theory. Moreover, Yang-Mills gauge theories and matter similar to that of the Standard Model can also be obtained. There are two types of strings: closed ones that have no endpoints and open ones that extend between higher dimensional objects, the D-branes. These are dynamic themselves and couple to fields that can be thought of as higher-dimensional analogues of the electromagnetic field.

Supersymmetry, a symmetry relating bosons and fermions, is one of the ideas that has not yet been experimentally observed, but which String Theory naturally incorporates. Unlike most theories, which do not predict their spacetime dimension, in its supersymmetric formulation internal consistency of String Theory requires that the number of spacetime dimensions be ten. It is possible to construct five different supersymmetric string theories in ten dimensions, which, though, are related to each other by dualities. Moreover, all of them are believed to descend from an eleven-dimensional theory called M-theory. In this thesis, we will mainly work in the low energy limits of string theories, which are supergravity theories that are extensions of General Relativity with the other fields in the zero mass string spectrum.

To make contact with the four-dimensional world we observe, we need to compactify String Theory down to four dimensions. To do that, we need to choose an internal six-dimensional manifold whose size is sufficiently small so that it has escaped detection. The choice of this manifold is important since the four-dimensional physics crucially depends on its topological properties. A torus is the easiest internal space to consider, but this leads to a lot of supersymmetry in four dimensions, which does not seem to match our experimental observations. For that reason, other spaces that lead to less supersymmetry, such as Calabi-Yau manifolds, are usually employed for phenomenologically relevant string compactifications. Another unrealistic feature of most compactifications is the presence of a typically large number of massless scalar fields called moduli. These lead to long-rage interactions which are not observed in nature, and hence, a significant challenge, known as the moduli stabilization problem, is to find a mechanism to provide these moduli with a potential that fixes their masses.

De Sitter Vacua

Around 25 years ago, it was discovered that in the present epoch, the universe is expanding at an accelerated rate [1, 2], and one of physics' biggest open questions is the nature of energy that drives this expansion. The simplest explanation for this "dark energy" is

that it comes from a cosmological constant, i.e. a constant vacuum energy density, that should be positive and extremely small (of the order 10^{-120} in Planck units). Currently, there is no dynamical explanation for why the cosmological constant has such a tiny value. However, given that string compactifications can give rise to an enormous number of four-dimensional vacua, the string theory landscape, one could resort to anthropic reasoning to address the cosmological constant problem since a much larger vacuum energy would not allow the formation of galaxies (and hence the development of intelligent life) [3]. It has been argued that there exists at least around 10^{500} four-dimensional vacua due to the vast number of Calabi-Yau manifolds and all the possible ways of putting flux on them, so it could indeed be the case that the value of the cosmological constant is environmental, determined by where we happen to be in this multiverse of vacua.

The multiverse paradigm might not be particularly satisfying, as one would hope that String Theory would point to a unique vacuum that would reproduce exactly the physics we observe. However, there is an even bigger issue since it turns out that it is extremely difficult to build de Sitter solutions in String Theory, and one could argue that there does not exist even a single fully rigorous four-dimensional de Sitter vacuum, let alone more than 10^{120} of them. Constructing, therefore, four-dimensional metastable de Sitter vacua continues to be a great challenge, and the twenty-year-old construction of Kachru, Kallosh, Linde, and Trivedi (KKLT) [4], although not uncontested, remains one of the prototypical examples.

The question of whether de Sitter space is attainable is String Theory has also been explored from the bottom-up perspective of the swampland program, which aims to determine the set of seemingly consistent low-energy field theories that cannot be coupled to quantum gravity. Motivated by the significant challenges in constructing a de Sitter vacuum in String Theory and by connections to other swampland conjectures, the de Sitter conjecture has been proposed [5, 6], which excludes (meta-)stable de Sitter vacua in String Theory. If true, this would mean that the nature of dark energy in our universe cannot be a cosmological constant.

Therefore, it is important to keep revisiting and scrutinizing the existing proposals for obtaining solutions with a positive cosmological constant in String Theory, as well as devise new, more solid ones. The work presented in the first part of the thesis contributes to these efforts.

Black Holes and their Puzzles

As we mentioned in the foreword, Quantum Mechanics and General Relativity are fundamentally incompatible. This clash is especially pronounced in the study of black holes, which serve, therefore, as an ideal arena to test any theory of quantum gravity.

Black holes are astrophysical objects that arise from the gravitational collapse of supermassive stars. They are classical solutions to the equations of motion of General Relativity and are only described by a few macroscopic parameters: their mass, charge and

angular momentum. They describe a region in spacetime where all mass is concentrated in a spacetime singularity, which is cloaked by an event horizon. This null hypersurface separates the exterior spacetime from the black hole interior, from which not even light can escape.

Another remarkable feature of black holes is that classically, they obey laws that bear a close resemblance to the laws of thermodynamics. A priori, this is just a formal analogy, but it turns out that when quantum effects are considered, black holes exhibit true thermodynamic properties, and hence a deep connection between black hole geometry, Quantum Mechanics and Thermodynamics is revealed. Already without invoking any quantum physics, considering that throwing a mass into a black hole should not lead to any loss of entropy, Bekenstein conjectured that black holes should have an entropy proportional to the area of their horizon [7]. Shortly after, Hawking verified this intuition by studying quantum fields near the horizon [8]. In particular, he showed that black holes emit thermal radiation at a temperature $T_H = \frac{\hbar c^3}{8\pi G M k_B}$, which, using the second law of thermodynamics, can be used to derive their entropy S :

$$S = \frac{k_B c^3 A}{4\hbar G}\,, \tag{1.1}$$

where A is the area of the black hole horizon.

The so-called Bekenstein-Hawking entropy is enormous, of the order of the square of the black hole's mass. For example, for the black hole at the center of the Milky Way, Sagittarius A*, this number is around 10^{90}. According to Boltzmann's entropy formula $S = log(N)$, this entropy should correspond to an even bigger number of microstates N with the same macroscopic properties. However, in General Relativity, the black hole uniqueness theorem tells us that $N = 1$, since for a given mass, charge and angular momentum, there is a single stationary black hole. The big puzzle, therefore, is where all these microstates are. General Relativity cannot answer this question.

Another profound puzzle is the information paradox, which appears when one considers the evaporation of a black hole through Hawking radiation. Imagine that a black hole is formed by the gravitational collapse of a star. This black hole will then radiate, slowly losing mass, and if we wait long enough, it will eventually evaporate completely, leaving behind only radiation. However, this radiation originates from the horizon region, and according to the black hole uniqueness theorem, it should be universal and cannot have information about what originally made the black hole. This process seems to lead to loss of information about the initial state, and hence it violates unitarity, one of the core principles of Quantum Mechanics.

The Fuzzball Proposal

The puzzle of the microscopic origin of the black-hole entropy and the information paradox point towards the realization that we need a Quantum Theory of Gravity to resolve them, and as we have already stated, String Theory is our best hope for doing that. Indeed, one

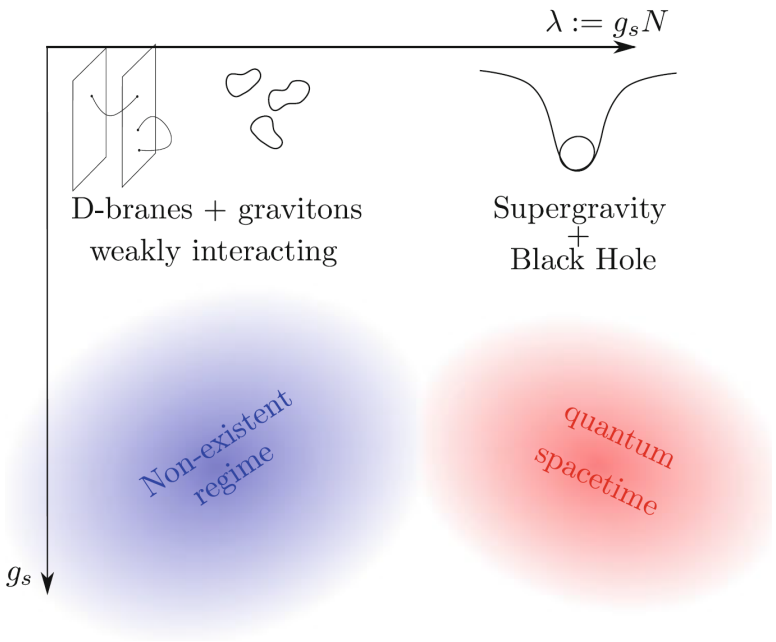

Figure 1.1: The regimes of parameters in String Theory. The Figure is taken from [9].

of the biggest achievements of String Theory is counting the degrees of freedom that give rise to the entropy of supersymmetric black holes in terms of bound states of strings and branes at the regime of parameters where gravitational interactions are turned off.

In String Theory, one can perform a perturbative expansion in two parameters: the string length l_s, which sets the scale at which stringy effects become important, and the string coupling g_s, which controls the strength of the interaction between strings. In terms of these parameters, the gravitational constant is expressed as $G_N \sim g_s^2 l_s^{d-2}$, with d the number of dimensions. When $g_s \ll 1$, we are in the (semi)classical regime, while for $g_s \sim 1$ we are in the quantum regime. In the presence of a bound state of N D-branes, the effective coupling between open and closed strings, which is also the coupling between open strings, is given by $g_s N$. At low $g_s N$, we can describe the system in terms of weakly coupled open strings on the background of the N D-branes since, in this regime, open and closed strings become decoupled and gravity can be neglected. At large $g_s N$, the D-branes backreact on the geometry and the system is described using Supergravity. These two regimes are depicted in Fig. 1.1. An important thing to note is that the Bekenstein-Hawking entropy is independent of the string coupling (and the string length), which means that we should be able to reproduce it by counting the supersymmetric states in the $g_s N \ll 1$ regime.

This was firstly achieved for the two-charge supersymmetric black hole by Sen in 1995 [10]. In the F1-P duality frame, where one has N fundamental strings with momentum P on them, the entropy of the system comes from the different ways the fundamental strings can carry the momentum, and in the vanishing coupling regime, the degeneracy of states can be computed using the Cardy formula within the underlying conformal field theory. Turning on g_s , the system backreacts and forms a black hole, which has classi-

cally a vanishing horizon area. However, it was shown in [11] that, taking into account stringy corrections, the black hole develops a small horizon, whose entropy matches Sen's calculation. This system is very particular, and one could doubt that a similar matching would hold for black holes with a macroscopic horizon, but one year after Sen's paper, Strominger and Vafa extended his result to the D1-D5-P black hole [12], showing that the CFT counting at vanishing coupling exactly matches the Bekenstein-Hawking entropy.

These results are remarkable, but they only show what are the microscopic degrees of freedom of supersymmetric black holes in a regime of parameters where the classical black hole solution does not exist, leaving open an important question that is still subject to debate: What happens to the black hole microstates as the gravitational coupling is turned on? Do they fall behind the horizon, or are they still visible through some new horizon-scale physics?

Since gravitational attraction is universal and gets stronger with the gravitational constant, ordinary matter compresses with increasing G_N. Only a black hole's horizon grows in size and, therefore, one would expect that as g_s increases, eventually a horizon will form, and the microstates that made up the entropy at vanishing coupling will be engulfed by it and become indistinguishable from the black hole. However, in String Theory this is not always the case, as there are brane configurations that actually expand and never form a horizon. Moreover, they increase in size at the same rate as the black hole horizon radius.

The fuzzball proposal [13] claims that this happens generically and not only for special examples. In particular, it claims that when we attempt to form a black hole in String Theory, we do not end up with the traditional black hole solution but with a horizon-scale horizonless object, a fuzzball. This object radiates from its surface like a normal body and hence there is no information paradox. A remarkable feature of the proposal is that quantum gravity effects become important and modify the geometry not at the Planck length scale but already at the scale of the horizon. A black hole should be seen, therefore, as an average description over fuzzball degrees of freedom, and horizons and singularities appear only when gravity is described using a theory that is not rich enough to capture the underlying physics.

Microstate Geometries

For the fuzzball proposal to be valid, there should be around e^S horizonless non-singular configurations for a given black hole of entropy S. For the two-charge black hole, this has been achieved since it has been shown that the BPS states of the CFT describing the low energy physics of the D1-D5 system are mapped to certain non-singular horizonless configurations, called supertubes, which have D1 and D5 electric charges and a Kaluza Klein monopole (KKM) dipole charge. Their supergravity solutions are parametrized by an arbitrary shape, and the quantization of their moduli space reproduces exactly the two-charge black hole entropy one gets from the vanishing coupling counting: $S = 2\pi\sqrt{2N_1N_5}$

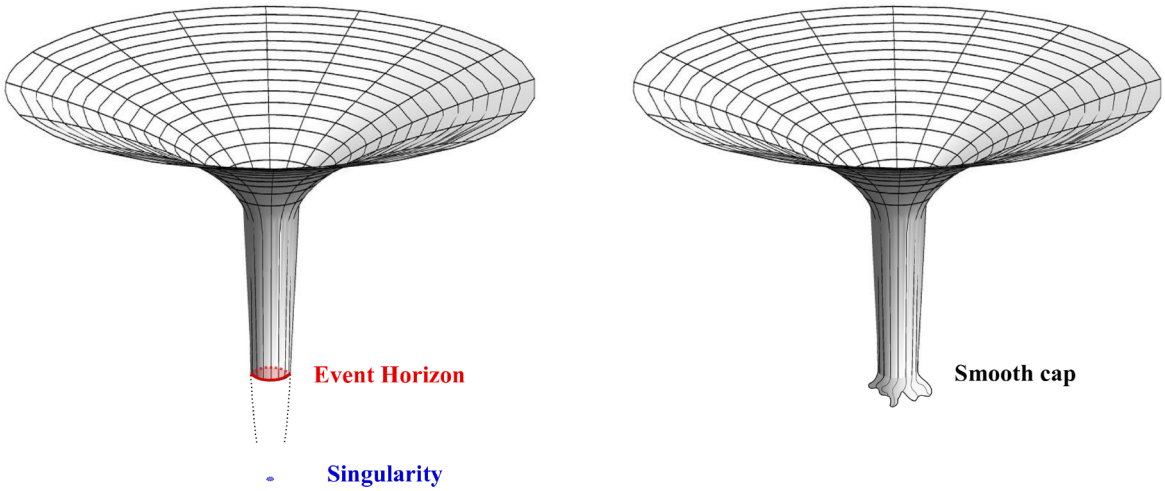

Figure 1.2: Schematic representation of a microstate geometry. To the left, the black-hole geometry ends in a singularity that is hidden behind the event horizon. To the right, the microstate geometry asymptotically looks exactly like the black-hole solution, but the throat caps off smoothly before the horizon. The Figure is taken from [21].

[14–20].

However, as we already pointed out, the two-charge system is a fairly special one, so to make progress with the fuzzball proposal we should consider black holes that have a macroscopic horizon. This naturally leads us to consider three-charge supersymmetric black holes. They, too, have a vanishing Hawking temperature, which means that they do not allow us to address the information paradox. However, it is very important to study them in order to understand the information storage problem.

Fuzzballs are the most general horizon-scale horizonless configurations with the same mass, charge and angular momentum as a given black hole and can be arbitrarily quantum and strongly curved. This means that, in practice, it is difficult to describe a generic fuzzball. Instead, one can try to construct microstate geometries, which are fuzzballs that can be described as smooth horizonless solutions in supergravity, see Fig. 1.2. Since there is an enormous number of quantum black-hole microstates, there should be a similarly enormous number of coherent expressions of those microstates, and the goal of the microstate geometries program (see [22, 23] for recent reviews), which started almost twenty years ago, is to build them.

A tremendous amount of geometries has been constructed for the three-charge supersymmetric black hole, and they have also been mapped to the dual CFT via precision holography. However, it has not been possible to construct states that account for the entire black hole entropy. In particular, the entropy of superstrata [24–26], which represent the largest family of D1-D5-P black hole microstate geometries, grows as $\sqrt{N_1 N_5} N_P^{1/4}$ [27, 28], which is parametrically smaller than the black hole entropy, $\sqrt{N_1 N_5 N_P}$. The reason for that is that superstrata are constructed in six-dimensional supergravity, which cannot resolve the brane fractionation that is essential for accessing the twisted sector of

the dual CFT, from which most of the black hole microstructure originates.

A great challenge, therefore, is to describe brane fractionation using supergravity in ten or eleven dimensions. In the second part of this thesis, we begin to address this problem by studying the M2-M5-P black hole, whose entropy comes from the fractionation of each M2-brane into momentum-carrying strips hanging between parallel M5-branes.

Themelia

In resolving the microstructure of black holes, one is naturally led to ask: what are the fundamental structures in String Theory? The simplest, and most naive answer is, of course, strings. However, the answer to this question must be duality invariant. The obvious solution is to include all objects that can be obtained by dualizing strings, like branes, KK monopoles and brane bound states that preserve sixteen supercharges.

One can then envision a further extension, to include objects that preserve sixteen supercharges *locally*, but preserve only a fraction (or possibly none) of these supercharges when the object is taken as a whole. Such objects were dubbed *themelia* in [29].

A simple example: a string carrying right-moving momentum is $\frac{1}{4}$-BPS, preserving eight supersymmetries. It is a themelion because, when one "zooms in" on the string, one only sees a boosted segment of a string, which preserves 16 supersymmetries. Another segment of the string also preserves 16 supersymmetries, but different ones: the supersymmetries depend on the orientation of the string segment [30]. However, each set of 16 local supersymmetries contains a common subset of eight supersymmetries, which make the whole object a $\frac{1}{4}$-BPS configuration.

It is natural to expect that themelia will emerge as the fundamental substructure[1] of black hole microstates. There are three reasons for this. First, and most obvious, the themelion is necessarily a bound state because one cannot separate the fundamental charges without breaking some of the 16 local supersymmetries.

Secondly, a system of N identical branes that preserve sixteen supercharges *globally* can have an entropy, at most, of order $logN$. This means that the local structure of a themelion can only account for $logN$ contributions to the entropy. However, the global structure of a themelion can involve excitations of its moduli, like shape modes and brane densities, that are parameterized by arbitrary continuous functions, and these can carry an entropy proportional to a power of N. A themelion can only encode such a large entropy in its large-scale, global structure.

The best-studied example is probably the D1-D5 system. This system carries an entropy of order $\sqrt{N_1 N_5}$. Taken by itself, it produces a singular black-hole geometry with a Planck-scale horizon. However, this is not a themelion: it only has eight supercharges locally. If one adds a KKM and angular momentum, it can be spun out into a supertube, a smooth geometry, with sixteen supercharges locally and eight globally [14, 16, 18, 31].

[1] The ancient Greek word *themelion* ($\theta\epsilon\mu\acute{\epsilon}\lambda\iota o\nu$) translates to *foundation*, or *fundamental structure*. Unfortunately, the other word for indivisible structure, *atomon*, was already taken.

The degenerate ground states that give rise to the entropy can now be seen as shape modes of the supertube. Indeed, this example, and the duality-related F1-P system, led to the original fuzzball proposal.

More broadly, it was observed in [29] that all known microstate geometries (and microstate solutions [32]) are actually based on themelia: this includes the brane systems underlying three-charge bubbling solutions [33–35], superstrata [24,30] and the supermaze [36].

The third reason why themelia should be thought of as fundamental constituents of microstate structure, is that a fully back-reacted themelion *can never give rise to a classical black hole solution with an event horizon.* This is because the horizon area, in Planck units, is duality invariant [37], and so is the same in *all* duality frames. On the other hand, a themelion can always be locally dualized into a stack of N Kaluza-Klein monopoles, and this solution is simply empty space with a Z_N orbifold singularity, which is an exact, fully-back-reacted, horizonless string background.

Independent of geometric considerations, the themelion conjecture states that *the fundamental constituents of black-hole microstructure must be themelia.* Moreover, because a themelion carries its entropy in its large-scale structure, the supergravity solutions corresponding to coherent collections of themelia should be able to access precisely the degrees of freedom that carry this entropy. Obviously, supergravity cannot describe string-scale phenomena, but one might hope that supergravity can describe the classical limits of themelia and the degrees of freedom that carry their entropy. We will refer to this extension of the themelion conjecture as the *geometric themelion conjecture.*

The themelion conjecture thus provides an explicit string-theory realization of the fuzzball proposal, while the geometric themelion conjecture provides a precise framework for realizing the goals of the Microstate Geometry programme [23, 32].

One can see how the themelion conjecture can be realized in the M2-M5-P black hole. The entropy of this system arises from the fact that each M2 brane can fractionate into N_5 strips that can carry momentum independently[2]. Since each of the N_2N_5 strips has four bosonic directions, it is not hard to see that the total entropy (including the fermions) is exactly that of the corresponding black hole, $S = 2\pi\sqrt{N_2N_5N_P}$. When one considers the brane-brane interactions one finds that the momentum-carrying M2 strips pull on, and deform, the M5 branes. The remarkable feature of this momentum-carrying configuration, that we call the supermaze, is that it preserves four supercharges globally, but if one zooms in at any location along it it preserves locally 16 supercharges. [36]. Thus, the M2-M5-P super-maze is an explicit realization of a themelion that carries all the black hole entropy.

If one could build the supergravity solutions corresponding to this super-maze and show explicitly that these solutions have no horizon, this would establish the geometric themelion conjecture. However, there are several technical hurdles to be overcome. A great part of this thesis is devoted to addressing these issues.

[2]This counting is the M-theory uplift of that of the Type IIA F1-NS5-P black hole [38].

Organization of the Thesis

This thesis is divided into two parts. In the first part, we study certain key aspects of the KKLT proposal for obtaining metastable four-dimensional de Sitter vacua in String Theory. In the second part, we present recent developments in the microstate geometries programme for three-charge supersymmetric black holes.

A crucial component of the KKLT construction is the addition of an anti-D3 brane at the bottom of a Klebanov-Strassler (KS) throat, which breaks supersymmetry and lifts the cosmological constant to a positive value. In all KKLT-like constructions the anti-D3 brane is considered a probe and one only takes into account the positive contribution to the scalar potential coming from its worldvolume action. In Chapters 2 and 3 we study the backreaction of anti-D3 branes at the tip of a KS throat and find that they also source three-form fluxes.

In Chapter 2, we show that these fluxes give rise to nontrivial terms in the superpotential when the throat is embedded in a flux compactification. We describe these terms both from a ten-dimensional and from a four-dimensional perspective and show that, upon including Kähler-moduli stabilization, the resulting potential admits de Sitter minima. Our proposed de Sitter construction does not require additional supersymmetry-breaking $(0,3)$ fluxes, and hence is more minimalist than the KKLT proposal.

In Chapter 3, we tabulate in detail all (m,n) components of the supersymmetry-breaking fluxes sourced by the anti-D3 branes, and calculate their effect on the stabilization of Kähler moduli via gaugino condensation on D7-branes. This allows us to obtain a new constraint on the validity of this stabilization mechanism.

In the first step of the KKLT construction, where one obtains a supersymmetric AdS_4 vacuum, complex structure moduli are assumed to be fixed by fluxes and then to account for the non-perturbative effect of gaugino condensation on D7 branes wrapping four-cycles of the internal manifold, which is necessary for the stabilization of the Kähler moduli, one needs to resort to an effective four-dimensional theory. In Chapter 4 we provide the ten-dimensional description of the KKLT AdS_4 vacua. We first use the language of Generalized Complex Geometry to derive the supersymmetry equations for type II AdS_4 vacua including the localized effect of gaugino condensation on D-branes. We then solve them for type IIB compactifications with gaugino condensates on smeared D7-branes and find that this leads to a supersymmetric AdS_4 solution, which is very similar to that of KKLT. Moreover, we find that exponential separation between the AdS and the KK scales is possible as long as the three-form fluxes are such that their $(0,3)$ component is exponentially suppressed. As for the localized solution, it requires going beyond SU(3)-structure internal manifolds. Nevertheless, we show that the action can be evaluated on-shell without relying on the details of such complicated configuration.

Moving to the second part of the thesis, in Chapter 5 we study a problematic limit where superstrata appear to develop a horizon and we show that the horizon only emerges due to the neglect of degrees of freedom that are essential in this vanishing angular momentum limit. We incorporate some of these degrees of freedom by constructing, for

the first time, solutions with zero horizon area that have the same charges as a three-charge F1-NS5-P Type-IIA black hole and preserve the black hole's spherical symmetry. The momentum of these solutions is carried by longitudinal D0-D4 density fluctuations along the common F1-NS5 direction. We argue that these solutions should be interpreted as the long-throat limit of superstrata. The existence of these geometries indicates that a finite-size horizon does not appear even in the singular corners of the moduli space of three-charge microstate geometries.

In Chapter 6, we propose a novel approach to fully account for the entropy of supersymmetric three-charge black holes using microstate geometries. In particular, we study the three-charge F1-NS5-P black hole in Type IIA string theory, whose entropy comes from the breaking of the N_1 F1 strings into N_1N_5 little strings, which become independent momentum carriers. In M theory, this system has a clear geometric meaning, since the little strings uplift to strips of M2 branes that connect pairs of parallel M5 branes separated along the M-theory direction. The backreaction of these M2 strips ending on M5 branes is similar to the Callan-Maldacena spikes describing backreacted F1 strings ending on D3 branes [39], and for multiple M5 and M2 branes, one gets a complicated maze-like structure. Adding momentum waves to the M2 strips gives rise to a momentum-carrying brane configuration, that we call the Supermaze. The important point is that the Supermaze has four global supercharges, but locally preserves 16, and hence we expect that its backreaction will give rise to horizonless solutions.

The supersymmetry projector corresponding to the supermaze shows that besides the M2, M5 and P charges (or the F1, NS5, P charges in type IIA) one needs six other dipolar charges, which are necessary to form the "glue" that transforms the individual branes into a bound state with sixteen supersymmetries locally. Inspired by this, in Chapter 7 we introduce "Themelia". These are objects in String Theory that have sixteen supersymmetries locally, but have fewer when considered globally, and we argue that they are the fundamental building blocks of black hole microstates. We show that all existing smooth horizonless microstate geometries can be seen as bound states of themelia, and we conjecture that all such bound states will give rise to microstate geometries. We also construct the most general themelion with a three-torus isometry and show that it interpolates between superstrata and the supermaze.

In Chapter 8, we take the first step towards developing the supergravity formulation of the supermaze, by studying momentum-free supermazes. We show that the supergravity solutions for $\frac{1}{4}$-BPS intersecting systems of M2 and M5 branes are completely characterized by a single "maze" function that satisfies a non-linear "maze" equation similar to the Monge-Ampère equation. We use floating probe M2 and M5 branes to explore the structure of these solutions and relate a class of our solutions to F1-D1 (p, q) string-webs. Solving the maze equation is generally a challenging task, but we identify two methods for finding specific classes of solutions. The first, is to consider an infinite M2-M5 bound state at a certain angle and with a certain ratio of M2 and M5 densities. This solution is presented in Appendix H and can be shown to satisfy exactly the maze equation. The second method to solve this equation is to consider some near-horizon limit. We consider

such a limit and we manage to relate our solutions to a class of the $AdS_3 \times S^3 \times S^3$ solutions warped over a Riemann surface constructed in [40], for which the BPS equations reduce to a linear system. Finally, we explore the addition of a simple momentum charge.

In Chapter 9, we properly tackle the problem of adding momentum to a maze of M2-brane strips stretched between M5 branes in order to construct $\frac{1}{8}$-BPS solutions that preserve sixteen supercharges locally. We show that given a $\frac{1}{4}$-BPS supergravity solution describing the maze, one can add momentum waves without modifying the M2-M5 background. Remarkably, these excitations are fully determined by a layered set of linear equations. The fields responsible for carrying the momentum are parameterized by arbitrary functions of a null direction, and have exactly the same structure as in brane world-volume constructions. The fact that the momentum and flux excitations of the M2-M5-P system are governed by a linear structure brings us one step closer to using supergravity solutions to capture the entropy of supersymmetric black-holes.

In Chapter 10, we study in detail a particular class of the AdS_3 solutions constructed in [40] and show that they describe single M2-M5 intersections, which are, however, far from featureless. In particular, they describe, what appears from infinity, to be a single stack of semi-infinite M2 branes ending on, and deforming, a single stack of M5 branes, but as one zooms into the intersection, the M2's and M5's resolve into physically separated spikes (a "mohawk") with the distance between each spike being controlled by the number of M2's and M5's making up each spike. We argue why we suspect that any near-brane limit that leads to such an AdS_3 factor is necessarily limited to a single intersection, and we comment on the CFT interpretation of these mohawks.

Part I

De Sitter Vacua in String Theory

Chapter 2

Bare-bones de Sitter

2.1 Introduction

The accelerated expansion of our Universe points towards the existence of a positive vacuum energy density, whose value is about 120 orders of magnitudes smaller than the value expected from field-theory estimates. On the other hand, there are by now several arguments [5] that stable de Sitter vacua cannot be constructed in controlled low-energy effective theories that are consistent with quantum gravity. This leaves only two open possibilities: either the accelerated expansion of our Universe comes from a time-dependent vacuum energy density, or there is a problem with the no-de-Sitter conjecture, which can be disproved by an explicit construction.

Unfortunately, constructing metastable de Sitter vacua is notoriously difficult in String Theory. Despite its intricate ingredients, short-comings and potential instabilities, the twenty-year-old construction of KKLT [4] still stands out as one of the very few generic proposals that has not been fully proven to be unstable. It is a three-step construction that combines fluxes, non-perturbative phenomena and anti-D3 branes in a warped Calabi-Yau compactification with a deformed conifold-type throat. In order to obtain a positive and small cosmological constant, the fluxes required in the first step need to break supersymmetry generating a very small superpotential $W_{0,\mathrm{KKLT}}$. This has been criticized on two counts: theory and practice. On the formal side, these supersymmetry-breaking runaway solutions are not protected against corrections, and it was argued in [41] that they are not a good ground onto which one can add the non-perturbative ingredients necessary in the second step to prevent the runaway and stabilize the volume moduli. On the practical side, it is very hard to obtain explicit solutions with a sufficiently small superpotential, although there has been recent progress in engineering this type of flux vacua [42–44].

In this Chapter, we take a step towards bridging the conflict between the no-de-Sitter swampland arguments [5] and what can be constructed explicitly and controllably in String Theory. We propose a new method to construct de Sitter vacua, which has one less ingredient than the KKLT construction, and hence is potentially plagued by less problems. More precisely, we show that one can construct de Sitter vacua with a small cosmological constant without the need of a flux superpotential $W_{0,\mathrm{KKLT}}$. Note

that this requires restricting to manifolds that can support supersymmetric flux vacua. Manifolds admitting supersymmetric flux vacua were conjectured to require a "geometric modularity" property [45]. While many Calabi-Yau manifolds seem to have the desired modularity property and admit supersymmetric vacua [46], a few of them were shown not to allow for such solutions (see [47] and references therein).

Our key observation is that the anti-D3-branes necessary to uplift the cosmological constant source fluxes that generate precisely a small superpotential. Therefore, in our "bare bones" de Sitter construction, only supersymmetric fluxes are needed in the first step, thus avoiding the problems mentioned above.

2.2 Fluxes generated by $\overline{\text{D3}}$ branes

A strongly warped region in a Calabi-Yau compactification can be engineered as a Klebanov-Strassler (KS) throat [48]. This is a cone over an $S^2 \times S^3$ base (see Fig. 2.1). The two-sphere of the base shrinks at the tip of the cone while the three-sphere has always finite size, parameterized by a modulus S. The base can be also thought as a $U(1)$ fibration over $S^2 \times S^2$. The symmetries of the geometry consist of two $SU(2)$ factors acting on the base two-spheres and a $\mathbb{Z}_2$ swapping them.

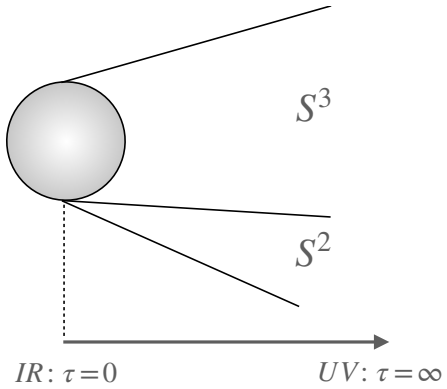

Figure 2.1: An artist's impression of the KS geometry.

The most general deformation of the conifold metric with fluxes preserving the $\mathrm{SU}(2)^2 \times \mathbb{Z}_2$ symmetry can be written in terms of eight functions of a radial coordinate $\{\Phi_i(r)\}$ [49]; this space of type-IIB supergravity solutions includes the Klebanov-Strassler [48], Maldacena-Nuñez [50], and baryonic branch solutions [51]. Here, we are interested in the deformation of the KS solution caused by the addition of $\overline{N}$ anti-D3 branes at the tip of the throat. In particular, we calculate how the anti-D3 branes affect the complexified three-form flux G_3, whose (p,q) components can be put in correspondence with various quantities in the effective four-dimensional low-energy theory describing the system[1].

Assuming that the backreaction of the anti-D3 branes on the geometry is small and

[1]For a more detailed review of the KS geometry and its $SU(2)^2 \times \mathbb{Z}_2$ symmetry-preserving deformation see Section 3.2.

can be studied in perturbation theory, the deformed geometry is given by

$$\Phi_i \;=\; \Phi_i^{KS} + \varepsilon\,\phi_i + O(\varepsilon^2)\,, \tag{2.1}$$

where the analytical dependence of the fluctuations ϕ_i has been computed in [52–54] and the small expansion parameter is:

$$\varepsilon = \frac{\overline{N}}{g_s M^2}\,, \tag{2.2}$$

where M is the integral of the Ramond-Ramond F_3-flux on the S^3. Usually, the number of anti-D3 branes is taken to be $\overline{N}=1$, since configurations with multiple anti-D3 branes have a tachyon [55], but we will keep track of it for completeness.

In the KS solution, the complexified three-form flux, G_3, is $(2,1)$ with respect to the choice of complex structure picked by supersymmetry [56]. When the anti-D3 branes are added at the tip of throat, the three-form flux also gets corrections, $G_3 = G_3^{\rm KS} + G_3^{\overline{\rm D3}}$ and, at the same time, the complex structure is rotated. This implies that in general G_3 is not of (2,1)-type anymore (and neither is imaginary-self-dual (ISD)) but it develops all other components: for example, the (0,3) component is

$$\begin{aligned} G_{(0,3)}^{\overline{\rm D3}} &= -\frac{4\pi^2}{g_s S}\frac{\partial_\tau\varphi(\tau)}{\sinh^2(\tau)}\,\overline{\Omega}_{\rm KS} + O(\epsilon^2)\,,\\ \varphi &= g_s\,\sinh(\tau)\,\phi_7 + \cosh\!\left(\tfrac{\tau}{2}\right)^2\phi_5 - \sinh\!\left(\tfrac{\tau}{2}\right)^2\phi_6\,, \end{aligned} \tag{2.3}$$

where $\Omega_{\rm KS}$ is the (3,0) form defined by the KS complex structure, S is the conifold modulus and $\phi_{5,6,7}$ are functions of the radius, whose UV and IR expansions are in [52], and whose full analytic expression can be found in [53].

Even though the solution is non-supersymmetric, one can analyse it using off-shell supersymmetry methods. Indeed, the non-supersymmetric back-reacted anti-D3-brane solution computed in [52–54] uses the Papadopoulos-Tseytlin ansatz which is based on the existence of an SU(3) structure (or analogously a globally-defined spinor). This is an algebraic property required to use off-shell supersymmetric methods, that the cone over $S^2\times S^3$ satisfies. On-shell supersymmetry then requires this spinor to be covariantly constant (with respect to some connection, which in the supersymmetric Klebanov-Strassler solution is just the Levi-Civita one, i.e., the manifold is Calabi-Yau). In the non-supersymmetric solution, there is no such simple condition, and one has instead to solve the second order equations. Nevertheless, the fact that there is an underlying off-shell supersymmetry due to the globally defined spinor, allows to attack this problem using off-shell $\mathcal{N}$=1 supersymmetry methods, in particular using the flux-induced superpotential. For the complex structure (or analogously, the globally defined spinor) of the Klebanov-Strassler zeroth order solution, such superpotential is nothing but the Gukov-Vafa-Witten (GVW) superpotential [57]:

$$W_{\overline{\rm D3}} \;=\; M_{pl}^8 \int G_3^{\overline{D3}}\wedge\Omega\,. \tag{2.4}$$

Given that the anti-D3-brane generates a (0,3) component of flux, it thus gives rise to a superpotential. Using (2.3), the integral can be performed explicitly, giving

$$W_{\overline{\rm D3}} \,=\, -34.2\, i\, \varepsilon M_{pl}^8\, \alpha'\, M\, S + O(\varepsilon^2)\,, \tag{2.5}$$

where the first-order term is obtained using $\Omega_{\rm KS}$. In this Chapter we will redefine the S field in the following way:

$$S = 512\pi^{12}\alpha' ||\Omega||^3 Z\,, \tag{2.6}$$

where the holomorphic 3-form on the warped geometry is normalized such that the integral of the unwarped Klebanov-Strassler 3-form Ω_{KS} over the S^3 at the bottom of the throat is equal to S. This gives $||\Omega||^2 = 3/\pi^4$. Moreover, we will perform the following Kähler transformation on the superpotential and Kähler potential:

$$\begin{aligned} W \quad &\to \quad e^{-\mathcal{F}}\, W\,, \\ \mathcal{K} \quad &\to \quad \mathcal{K} + \mathcal{F} + \overline{\mathcal{F}} \end{aligned} \tag{2.7}$$

with $e^{\mathcal{F}} = \left(4\pi^2\alpha' M_{pl}^8\right)\, 512\pi^{12}\alpha' ||\Omega||^3$. With these transformations (2.5) now becomes

$$W_{\overline{\rm D3}} \,=\, -0.87\, i\, \varepsilon\, M\, Z + O(\varepsilon^2)\,. \tag{2.8}$$

The anti-D3-brane not only generates this flux component, but also imaginary-anti-self-dual (IASD) pieces. These generate F-terms for the axio-dilaton and conifold moduli, given by

$$D_\tau W = -\frac{i\, g_s}{2}\int G_3^{*\overline{\rm D3}} \wedge \Omega_{KS}\,, \quad D_Z W = \int G_3^{\overline{\rm D3}} \wedge \chi\,, \tag{2.9}$$

where χ is a $(2,1)$-form (whose first-order expression in λ can be found in [58]). Such integrals can be numerically evaluated using the explicit form of $G_-^{\overline{\rm D3}}$ given in [59]:

$$\begin{aligned} D_Z W &= -1.5\, i\, \lambda\, M + O(\lambda^2)\,, \\ D_\tau W &= 0.6\, \lambda\, g_s M\, Z + O(\lambda^2)\,. \end{aligned} \tag{2.10}$$

This superpotential and F-terms, computed using the ten-dimensional solution, will be used in Section 2.4 to compute an effective potential for the Kähler modulus in a KKLT-like construction.

2.3 4d supergravity description

Before adding the $\overline{\rm D3}$ branes at the tip of the throat, the superpotential and Kähler potential describing the conifold-modulus dynamics in a warped compactification have been computed in [60–62] [2].:

$$\begin{aligned} W &= \frac{M}{2\pi i}\left(Z\log\frac{\Lambda_{\rm UV}^3}{Z} + Z + w_Z\right) + i\frac{K}{g_s}Z\,, \\ \mathcal{K} &= -3\log\left(\rho + \overline{\rho} - \frac{\xi}{3M_{pl}^2}|Z|^{2/3}\right) + \log\left(2\gamma^4\right)\,, \end{aligned} \tag{2.11}$$

[2]Here we assume that all the other complex structure moduli have been stabilized at a higher scale in a supersymmetric way and only consider the conifold modulus. Moreover, we have employed transformations (2.6) and (2.7) in the superpotential and Kähler potential of Appendix A in [60] using $\alpha' = \frac{V_w^{1/4}}{2\sqrt{2}\pi^{7/4}\sqrt{M_{pl}}}$ with V_w a fiducial six-dimensional volume

where $\gamma^2 = 16\sqrt{2}\pi^7 ||\Omega||^2$, $\xi = 9c' g_s M^2$ and $c' \approx 1.18$ is a numerical factor coming from the warping [63]. Notice that these expressions are obtained after performing (2.6) and (2.7), and that the Kähler potential for the Z modulus is known in a small-field expansion, and only the $Z^{2/3}$ term was worked-out explicitly. To avoid cumbersome expressions in what follows, we use the log form of the Kähler potential above (2.11), but it is understood that in the final results only the leading term in $Z^{2/3}$ is kept.

The supersymmetric Minkowksi vacuum is given by:

$$\partial_Z W|_{Z_{KS}} = 0 \quad \Rightarrow \quad Z_{KS} = \Lambda_{\rm UV}^3 \, e^{-\frac{2\pi K}{g_s M}} \,. \tag{2.12}$$

Since the KS scalar potential and superpotential have to be zero on-shell in a supersymmetric Minkowski vacuum, this fixes the constant w_Z in (2.11):

$$W_{\text{on-shell}} = 0 \quad \Rightarrow \quad w_Z = -\Lambda_{\rm UV}^3 \, e^{-\frac{2\pi K}{g_s M}} \,. \tag{2.13}$$

We can promote this to an off-shell superpotential for the axion-dilaton as well, given by

$$W_{\rm KS} = \frac{M}{2\pi i}\left[Z\left(\log\frac{\Lambda_{\rm UV}^3}{Z} + 1\right) - \Lambda_{\rm UV}^3 e^{\frac{2\pi i \tau K}{M}}\right] + K\tau Z \,. \tag{2.14}$$

This satisfies the supersymmetry condition in the axion-dilaton direction $D_\tau W|Z_{KS} = \partial_\tau W|_{Z_{KS}} = 0$.

We now add anti-D3 branes, whose backreaction can be captured in the language of the four-dimensional effective theory by:

- an uplift term in the scalar potential, breaking supersymmetry and shifting the conifold modulus vev from Z_{KS} to Z_0 (to be computed below).
- A $(0,3)$ flux giving rise to an additional superpotential $W_{\overline{D3}}(Z)$, whose off-shell dependence on the conifold and axion-dilaton moduli will be determined by requiring consistency with the ten-dimensional computation (2.5).

To compute the former, it is useful to describe the antibrane uplift potential in a manifestly supersymmetric way (more precisely in a non-linearly supersymmetric way) introducing a nilpotent chiral multiplet X [64, 65], with the following Kähler potential and superpotential [62] :

$$\begin{aligned} \mathcal{K} &= -3\log\left(\rho + \overline{\rho} - \frac{|X|^2}{3} - \frac{\xi}{3M_{pl}^2}|Z|^{\frac{2}{3}}\right) - \log\left(\frac{\text{Im}\tau}{\gamma^4}\right) \,, \\ W &= W_{KS} + \frac{M_{pl}}{M}\sqrt{\frac{c''\,\overline{N}}{\pi}} Z^{2/3}\tau X + Ae^{-a\rho} + W_{\overline{D3}} \,, \end{aligned} \tag{2.15}$$

where $c'' \approx 1.75$ is a numerical factor related to the anti D3 brane energy [60] and we have also included the non-perturbative contribution to the superpotential coming from gaugino condensation or D3-brane instantons. Moreover, note that $W_{\overline{D3}}$ is considered a function of the conifold modulus Z. The usual $\mathcal{N}$ =1 four-dimensional scalar potential

$$V = \frac{e^{\mathcal{K}}}{M_{pl}^2}\left\{ G^{a\bar{b}} D_a W D_{\bar{b}} \overline{W} - 3|W|^2 \right\} \tag{2.16}$$

can then be written as

$$V = \frac{\gamma^4 g_s}{M_{pl}^2 r^2}\left\{\frac{9M_{pl}^2}{\xi}|Z|^{4/3}|\partial_Z W|^2 + |\partial_X W|^2 + \frac{4}{g_s^2 r}|D_\tau W|^2\right\}$$
$$+\frac{\gamma^4 g_s}{M_{pl}^2 r^3}\left\{G^{\rho\bar{\rho}}\partial_\rho W \partial_{\bar{\rho}}\overline{W} - r(\partial_\rho W \overline{W} + \partial_{\bar{\rho}}\overline{W} W)\right\}\,, \tag{2.17}$$

where $r \equiv \rho + \overline{\rho} - \frac{\xi}{3M_{pl}^2}|Z|^{2/3}$ and where we used the on-shell axion-dilaton value $\mathrm{Im}\tau = g_s^{-1}$.

In deriving (2.17) we used the following no-scale relation:

$$G^{i\bar{j}}\partial_i \mathcal{K}\partial_{\bar{j}}\mathcal{K} = 3 + \mathcal{O}\left(\frac{\xi^2|Z|^{4/3}}{M_{pl}^4(\rho+\overline{\rho})^2}\right)\,, \tag{2.18}$$

together with

$$\begin{aligned} G^{z\bar{j}}\partial_{\bar{j}}\mathcal{K} &= G^{i\bar{z}}\partial_i \mathcal{K} = \mathcal{O}\left(\frac{\xi Z^{4/3}\overline{Z}^{1/3}}{M_{pl}^2(\rho+\overline{\rho})}\right) \\ G^{\rho\bar{j}}\partial_{\bar{j}}\mathcal{K} &= G^{i\overline{\rho}}\partial_j \mathcal{K} = -r + \mathcal{O}\left(\frac{\xi^2|Z|^{4/3}}{M_{pl}^4(\rho+\overline{\rho})}\right)\,. \end{aligned} \tag{2.19}$$

Moreover, we omitted the terms $G^{z\overline{\rho}}\partial_z W \partial_{\overline{\rho}}\overline{W}$ and $G^{\rho\bar{z}}\partial_\rho W \partial_{\bar{z}}\overline{W}$ as they are subleading. From now on we will also not take into account the $|D_\tau W|^2$ term as it scales like $\mathcal{O}(|Z|^2/r^3)$ and hence is subleading as well.

In the absence of the non-perturbative term (setting $A = 0$), the second line in (2.17) is zero and the scalar potential becomes

$$V = \frac{\gamma^4|Z|^{4/3}}{c' r^2}\left\{\left|\frac{1}{2\pi i}\log\frac{\Lambda_{\rm UV}^3}{Z} + \frac{iK}{g_s M} - 0.87 i\lambda\right|^2 + \frac{c'\,c''}{\pi}\lambda\right\}\,. \tag{2.20}$$

This is the KS + uplift scalar potential, which as a function of the conifold modulus Z has a minimum at

$$\begin{aligned} Z_0 =& \Lambda_{\rm UV}^3 e^{-\frac{2\pi K}{g_s M}} e^{-\frac{3}{4}\left(1-\sqrt{1-\frac{64\pi c' c'' \overline{N}}{9 g_s M^2}}\right)} e^{1.74\pi\lambda} \simeq \\ &\simeq \left(1 + \left(1.74\pi - \frac{8\pi c' c''}{3}\right)\lambda\right) Z_{KS} \equiv Z_{KS} + \delta Z\,, \end{aligned} \tag{2.21}$$

where we expanded to the first order in the $\overline{D3}$ uplift parameter λ, defined in (2.2), in order to compare to the 10d computation.

The on-shell value of the superpotential is then computed to first order

$$\begin{aligned} W(Z_0) &\simeq W_{KS}(Z_{KS}) + \partial_Z W_{KS}(Z_{KS})\delta Z + W_{\overline{D3}} \\ &= W_{\overline{D3}} = -0.87\, i\,\lambda\, M Z_0\,, \end{aligned} \tag{2.22}$$

where in the first line we used (2.12) and (2.13) and in the second line we inserted the 10d input (2.5).

The F-term of the conifold modulus can similarly be evaluated

$$\begin{aligned} &D_Z W(Z_0) = \partial_Z W(Z_0) + \mathcal{K}_Z W(Z_0) \simeq \\ &\partial_Z W_{\overline{D3}}(Z_{KS}) + \partial_Z^2 W_{KS}(Z_{KS})\delta Z + \mathcal{K}_Z W_{\overline{D3}} \simeq \\ &\frac{4c'c''}{3i} M\lambda \simeq -2.75\, i\lambda\, M\,, \end{aligned} \tag{2.23}$$

where in deriving the result we anticipated, using the explicit form of the Kähler potential in (2.15), that the term $\mathcal{K}_Z W_{\overline{D3}} \sim O(Z_0^{2/3})$ and is therefore subleading. This F-term has the same parametric dependence as its 10d counterpart (2.10), with a different numerical coefficient.

Finally, the F-term of the axion-dilaton is

$$\begin{aligned} D_\tau W(Z_0) &\simeq \partial_Z \partial_\tau W(Z_{KS})\delta Z + \partial_\tau W_{\overline{D3}} + \mathcal{K}_\tau W_{\overline{D3}} \\ &= \left(1.74\pi - \frac{8\pi c'c''}{3}\right) \lambda\, K\, Z_{KS} + \frac{0.435}{M} Z_{KS} + \partial_\tau W_{\overline{D3}} \quad . \end{aligned} \tag{2.24}$$

In order to obtain the correct parametric dependence of the ten-dimensional result (2.10) we impose

$$\partial_\tau W_{\overline{D3}} = -\left(1.74\pi - \frac{8\pi c'c''}{3}\right) \lambda\, K\, Z_{KS} \simeq -K(Z_0 - Z_{KS})\,, \tag{2.25}$$

and thus

$$D_\tau W(Z_0) = 0.435\, g_s M \lambda\, Z_{KS}\,. \tag{2.26}$$

The off-shell value of $W_{\overline{D3}}$ should therefore be considered as an expansion

$$W_{\overline{D3}}(Z,\tau) = W_{\overline{D3}}(Z,\tau_0) + \partial_\tau W_{\overline{D3}}(\tau_0)(\tau - \tau_0) + \cdots\,, \tag{2.27}$$

where we have determined the first two coefficients $W_{\overline{D3}}(\tau_0)$ and $\partial_\tau W_{\overline{D3}}(\tau_0)$ by consistency with the 10d results.

Let us stress that we do not expect exact numerical agreement between the ten and four-dimensional results, but we do get the same parametric dependence. One of the reasons that the numerical factors might not exactly match is that the four-dimensional theory misses the effects of massive but light modes of the compactification [61].

Before closing this Section, note that the complete scalar potential (2.17) has an approximately decoupled structure

$$V = V_{\text{KS+uplift}} + V_{\text{KKLT}}\,, \tag{2.28}$$

with

$$V_{\text{KKLT}} = \frac{\gamma^4 g_s}{M_{pl}^2 r^3} \left\{ G^{\rho\bar{\rho}} \partial_\rho W \partial_{\bar{\rho}} \overline{W} - r(\partial_\rho W \overline{W} + \partial_{\bar{\rho}} \overline{W} W) \right\}. \tag{2.29}$$

Noting that $r \simeq \rho + \overline{\rho}$, (2.29) is the usual AdS KKLT potential for $W = W_{0,KKLT} + Ae^{-a\rho}$, where the KKLT small superpotential constant W_0 is given in our construction by the on-shell value of the ρ-independent term in the superpotential of (2.15)

$$W_{0,KKLT} = W(Z_0)|_{A=0} \simeq W_{\overline{D3}}\,, \tag{2.30}$$

where as usual, we kept terms up to order λ.

2.4 Bare-Bones de Sitter

In this Section, we show that for certain choices of the parameters, the potential:

$$V = e^{\mathcal{K}} \left(G^{i\bar{j}} D_i W \overline{D_j W} - 3|W|^2 \right) \tag{2.31}$$

leads to de Sitter vacua. The potential is computed using the 10d input $D_i W$, $W = W_{\overline{\text{D3}}} + A e^{-a\rho}$ and Kähler potential as in (2.15).

In Fig. 2.2 we plot the potential for a particular choice of parameters. This choice is not unique: we have performed a partial scan of the parameters and we are able to find several other de Sitter vacua.

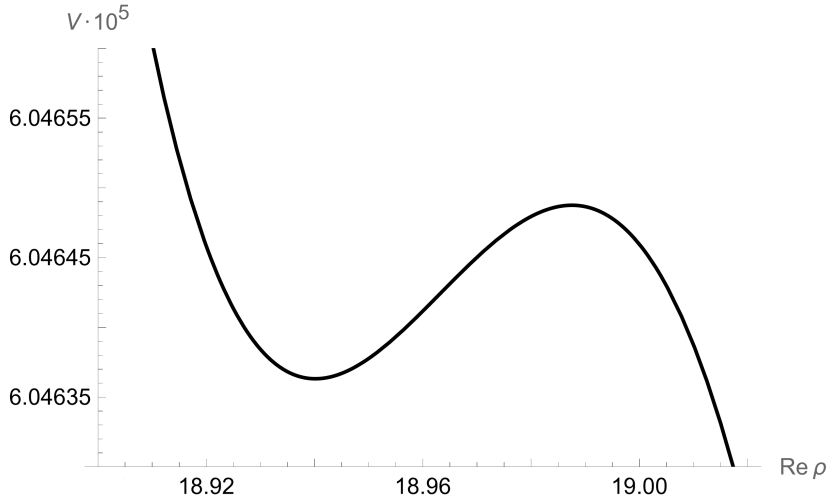

Figure 2.2: The potential for the choice of parameters $a = \frac{\pi}{3}$, $g_s = 0.22$, $A = 2550$, $K = 21$, $M = 80$. This gives $Z_0 \approx 5 \times 10^{-4}$.

For our de Sitter minimum the hierarchy between the bottom of the KS throat and the UV scale is of order $\frac{2\pi K}{g_s M} \approx 7.5$. For other de Sitter constructions without a large warping, see [66].

In the future, it would be important (but rather non-trivial) to check if the existence of this minimum survives higher order corrections in λ and Z, as well as quantum corrections.

2.5 Conclusions

A non-vanishing on-shell Gukov-Vafa-Witten superpotential is crucial in a KKLT-like construction of de Sitter vacua. In this Chapter, we have shown that a small GVW superpotential, dubbed $W_{\overline{D3}}$ above, is generated by $\overline{D3}$ branes at the tip of a KS throat. This superpotential, together with the anti D3-brane-generated F-terms provide all that is needed to obtain a compactification with a positive cosmological constant.

As we explained above, our proposal for constructing de Sitter solutions is more bare-bones and hence more robust than the KKLT one, because it has one less ingredient. Of course, as in all phenomenological constructions, adding more ingredients gives one

more freedom to tune the resulting physical parameters. Hence, one can argue that our proposal, though more robust, is less accommodating that the KKLT construction for obtaining a parametrically small cosmological constant. However, the aim of this work is not phenomenological, bur rather to understand which ingredients are absolutely necessary to construct de Sitter, and which are optional, with an ultimate purpose of achieving a robust construction that may provide a way to escape the no-go arguments of [5]. We believe our result represents a step in that direction.

Another interesting result of the calculation presented in this Chapter is the parametric agreement between the first-principle, ten-dimensional computation of the effective potential (in Section 2.2) and the four-dimensional-supergravity computation (in Section 2.3). To our knowledge, this is the first confirmation of the validity of the off-shell four-dimensional warped effective action [63] and the analysis of [60].

Last, but not least, our proposal does not avoid some of the known constraints on KKLT-like models. It would be interesting to explore whether the problems underlined in [67] also apply to our model. Furthermore, the minimum we found requires the contribution to the D3 tadpole of the fluxes in the KS throat to be of order $KM \approx 2 \cdot 10^4$. In [68] it was conjectured that such throats cannot be embedded in a flux compactification with stabilized moduli. It would be interesting to use our procedure to search for vacua where this tadpole contribution is smaller.

Chapter 3

$\overline{\text{D3}}$-branes and gaugino condensation

3.1 Introduction

Many proposals to construct de Sitter vacua in String Theory involve uplifting the negative cosmological constant that one typically obtains in flux compactifications after fixing the moduli. The original and most popular uplifting ingredient are anti-D3 branes placed in long warped throats within the compactification manifold [4]. They are argued to give a tunably small uplift energy, which would make the cosmological constant positive without perturbing the stabilization of the other moduli.

The prototypical example of such a warped throat is the Klebanov-Strassler (KS) geometry, obtained by adding fluxes to the deformed conifold [48]. There is by now an extensive body of work investigating the physics of anti-D3 branes in the KS geometry, in several regimes of parameters. Many of the results of these calculation point towards the existence of pathologies and instabilities when multiple anti-D3 branes are placed at the bottom of the KS geometry [52,54,55,61,69]. Furthermore, if the flux on the three-cycle of the deformed conifold is not large, even a single anti-D3 brane appears to have the power to cause a runaway behavior in the conifold deformation modulus [60–62, 70], collapsing the whole KS geometry into the singular Klebanov-Tseytlin one [71] and annihilating against the singularity.[1] A similar behavior is found when considering black holes in the KS geometry[73, 74]. Hence, the only corner of parameter space where KS antibranes have any chance of being metastable is when there is a single antibrane and the flux on the three-cycle of the deformed conifold is large.

However, even a single anti-brane has a significant back-reaction, and is capable of significantly affecting the other ingredients of the de Sitter construction. The purpose of this Chapter is to calculate the strength of the interactions between this single antibrane at the bottom of a KS solution and other ingredients that are used in the KKLT proposal [4] to construct de Sitter vacua with stabilized moduli in String Theory.

If we start from a supersymmetric solution in which a KS throat is glued to a CY geometry, the complex structure of the KS throat will match the complex structure of the

[1] For a recent argument against this scenario see [72].

bulk compact CY. Hence, the fluxes sourced by the anti-D3 branes can be decomposed according to the complex-structure of the KS throat and, as expected, have all possible components. The values of the field strength fluxes at the top of the KS geometry, where it is glued to the compactification manifold, are expected to be of the same order as the values of these fluxes in the rest of this manifold, away from the throat, and they determine the magnitude of the effect of antibranes on the other ingredients needed in de Sitter construction proposals.

As we have shown in Chapter 2, the $(0,3)$ component of the fluxes sourced by the anti-D3 branes gives rise to a nontrivial constant term in the superpotential. This avoids the need of one of the ingredients of the KKLT proposal, namely a finite but very small constant term in the superpotential, introduced ad hoc by turning on (0,3) fluxes. Hence, taking the interactions between antibranes and the rest of the flux-compactification ingredients fully into account can result in simplified "bare-bones" de Sitter proposals [75], which use one less ingredient than KKLT.

Another possible consequence of the antibrane fluxes is to affect gaugino condensation on D7 branes wrapping certain divisors of the CY geometry. In the absence of D7 branes, the volumes of these divisors (which correspond to Kähler moduli of the compactification) are flat directions. The low-energy physics of the D7 branes wrapping a holomorphic divisor is an $\mathcal{N}=1$ Super-Yang-Mills theory, which confines in the infrared. The non-perturbative Affleck-Dine-Seiberg superpotential [76] of this confining theory depends nontrivially on the Kähler moduli, and gives rise to a term in the potential that is responsible for stabilizing the size of the divisors [4].

The fields sourced by the anti-D3 brane can in principle interfere with this sensitive mechanism of Kähler-moduli stabilization. Indeed, as shown in [77–79], both the (1,2) and the (0,3) components of the complex three-form field strength give rise to mass terms for the fermions on the D7 brane. These mass terms break the supersymmetry of the $\mathcal{N}=1$ theory on the D7 branes, and can modify the RG flow and the gaugino-condensation scale. More precisely, they can affect the Affleck-Dine-Seiberg superpotential and can introduce extra terms in the potential for the Kähler moduli, potentially ruining their stabilization.

In this Chapter we use the expression of the supersymmetry-breaking fluxes sourced by the anti-D3 branes [53, 54] to calculate precisely their effect on the stabilization of Kähler moduli via D7-brane gaugino condensation. We obtain a new bound relating various parameters of compactification with long warped throats, which must be satisfied in order to be able to stabilize Kähler moduli via D7-brane gaugino condensation. We combine this bound with other constraints appearing in vanilla-type KKLT compactifications, and find that it is generically satisfied. We leave the exploration of the importance of this bound on de Sitter proposals that do involve large warping[2] to future exploration.

Beside their effect on the gaugino condensation on D7 branes, the extra fluxes and

[2]Such as the LVS proposals in [66, 80]. Note though that for large warping both KKLT and LVS were argued to suffer from control issues, the former by the so-called singular bulk problem [67], and the latter by large α' corrections [81]. Here we we are assuming a constant warp factor in the bulk, such that the singular bulk problem does not arise.

fields sourced by the antibranes can also affect the number of fermion zero modes on the D3 instantons that also give rise to non-perturbative terms in the superpotential [82] that can stabilize other Kähler moduli, possibly switching off these terms. This is a subtle effect [83,84][3], which potentially can be more drastic than the effect on D7 gaugino condensation: even the tiniest "wrong fluxes" sourced by the antibranes are enough to uplift fermion zero modes and ruin the stabilization of certain Kähler moduli. We leave its investigation for future work.

As a byproduct of our calculation, we decode some aspects of the holographic dictionary corresponding to anti-D3 branes in the Klebanov-Strassler geometry. If a single anti-D3 brane in the KS geometry with large three-form flux on the S^3 of the deformed conifold is indeed metastable, the resulting solution would be holographically dual to a metastable vacuum of the quiver gauge theory dual to the KS geometry. The structure of vacua of this theory is quite rich [91], and the existence of a metastable vacuum at strong coupling would be a nontrivial prediction of holography. It would be very interesting to try construct this putative vacuum directly in field theory, using for example ISS methods [92] (see [93] for the dual of a similar suspersymmetry-breaking vacuum). The fact that this vacuum can only exist in a very restricted region of parameter space may also explain why earlier attempts at finding it have not been successful [94].

Our analysis gives several clear holographic indications as to what the physics of this vacuum is. In particular, the fall-offs of the three-form fluxes with the radius can be used to show that certain dimension-three operators corresponding to fermion bilinears and certain dimension-seven operators corresponding to fermion bilinears multiplied by $F_{\mu\nu}F^{\mu\nu}$ acquire non-trivial vacuum expectation values. Furthermore, the $(1,2)$ fluxes sourced by the antibranes fall off as $1/r^4$, and hence give rise to a nontrivial vacuum expectation value of a dimension-4 operator corresponding to a marginal deformation of the superpotential [95]. Since the dictionary between the bulk three-form fields and the fermion bilinears is well understood [96, 97], we believe this information will be useful in searching for the holographic dual of the putative KS metastable vacuum.

The Chapter is organized as follows: In Section 3.2 we review the Klebanov-Strassler geometry, as well as the most general deformation preserving its $SU(2) \times SU(2) \times \mathbb{Z}_2$ symmetry and describe how the solution corresponding to anti-D3 branes smeared at the tip of the throat is obtained. In Section 3.3 we write the analytic expression, as well as the UV expansion, of all G_3 flux components that are generated by the addition of the anti-D3 branes and comment on their holographic duals. In Section 3.4 we compute the D7-brane gaugino mass induced by the $G_{(0,3)}$ flux sourced by the anti-D3 branes and compare it with a four-dimensional supergravity description of supersymmetry-breaking gaugino masses finding parametric agreement. Moreover, we derive a bound that all KKLT-like constructions should satisfy in order for the Kähler moduli stabilization via gaugino condensation to work, and argue that it is easily satisfied by the existing constructions.

[3] See also [85–90].

3.2 $\overline{\text{D3}}$formed KS geometry

3.2.1 Review of the KS solution and its non-supersymmetric deformations

A long warped Klebanov-Strassler-like throat, at the bottom of which anti-D3 branes (denoted as $\overline{\text{D3}}$-branes in the following) can sit, is a key element in the KKLT proposal for constructing de Sitter vacua in String Theory [4]. In this Section we review the supersymmetric Klebanov-Strassler (KS) geometry [48], as well as the ansatz that describes the most general deformation (with vanishing RR axion C_0) that preserves its $SU(2)\times SU(2)\times\mathbb{Z}_2$ symmetry [49]. The ten-dimensional spacetime consists of a warped product of four-dimensional Minkowski space and the deformed conifold :

$$\mathrm{d}s_{10}^2 \,=\, e^{2A+2W-X}\mathrm{d}s_{1,3}^2 + e^{-6W-X}\mathrm{d}\tau^2 + e^{X+Y}(g_1^2+g_2^2) + e^{X-Y}(g_3^2+g_4^2) + e^{-6W-X}g_5^2\,, \quad (3.1)$$

where $\{A, W, X, Y\}$ are functions of the radial coordinate, τ, and the one-forms g_i are:

$$\begin{aligned} g_1 \,&=\, -\frac{1}{\sqrt{2}}\,\mathrm{Im}(w_1+w_2)\,, \quad g_2 \,=\, \frac{1}{\sqrt{2}}\,\mathrm{Re}(w_1-w_2)\,,\\ g_3 \,&=\, -\frac{1}{\sqrt{2}}\,\mathrm{Im}(w_1-w_2)\,, \quad g_4 \,=\, \frac{1}{\sqrt{2}}\,\mathrm{Re}(w_1+w_2)\,,\\ g_5 \,&=\, \mathrm{d}\psi + \sum_{i=1}^{2}\cos\theta_i\mathrm{d}\phi_i\,, \quad g_6 \,=\, \mathrm{d}\tau\,, \end{aligned} \quad (3.2)$$

with $0\le\psi\le 4\pi$, $0\le\theta_i\le\pi$, $0\le\phi_i\le 2\pi$. Here we introduced the forms $w_1 \equiv \mathrm{d}\theta_1 + i\sin\theta_1\,\mathrm{d}\phi_1$ and $e^{i\psi}w_2 \equiv \mathrm{d}\theta_2 + i\sin\theta_2\,\mathrm{d}\phi_2$, with $\mathbb{Z}_2$ exchanging the two S^2's defined by w_i [49].

The NSNS and RR forms, H_3, F_3 and F_5, are all non-vanishing and their form is fixed by Bianchi identities and isometries:

$$\begin{aligned} H_3 \,&=\, \frac{1}{2}(k-f)g_5\wedge(g_1\wedge g_3+g_2\wedge g_4) \,+\, \mathrm{d}\tau\wedge(f'\,g_1\wedge g_2 \,+\, k'\,g_3\wedge g_4)\,,\\ F_3 \,&=\, F\,g_1\wedge g_2\wedge g_5 \,+\, (2P-F)\,g_3\wedge g_4\wedge g_5 \,+\, F'\,\mathrm{d}\tau\wedge(g_1\wedge g_3+g_2\wedge g_4)\,,\\ F_5 \,&=\, \left[\frac{\pi\,Q}{4}+(k-f)F+2P\,f\right](1+\star_{10})\,g_1\wedge g_2\wedge g_3\wedge g_4\wedge g_5\,,\\ \Phi \,&=\, \Phi(\tau)\,, \quad C_0 \,=\, 0 \end{aligned} \quad (3.3)$$

with Q a constant and $\{k, f, F\}$ functions of τ.

The radial dependence of the functions appearing in the KS metric is:

$$\begin{aligned} e^{X_{KS}} \,&=\, \frac{1}{4}h(\tau)^{1/2}\left(\frac{1}{2}\sinh(2\tau)-\tau\right)^{1/3}\,, \quad e^{6A_{KS}} \,=\, S^2\frac{\sinh(\tau)^2}{3\cdot 2^5}e^{2X_{KS}}\,,\\ e^{6W_{KS}} \,&=\, \frac{24}{h(\tau)\sinh(\tau)^2}\left(\frac{1}{2}\sinh(2\tau)-\tau\right)^{1/3}\,, \quad e^{Y_{KS}} \,=\, \tanh(\tau/2)\,, \end{aligned} \quad (3.4)$$

where S is a complex-structure modulus and $h(\tau)$ is the solution that vanishes at infinity to the following differential equation:

$$\frac{\mathrm{d}h}{\mathrm{d}\tau} \;=\; 32\,P^2\,g_s\,\frac{\tau\coth\tau-1}{\sinh(\tau)^2}\left(\frac{1}{2}\sinh(2\tau)-\tau\right)^{1/3}\,, \tag{3.5}$$

with $P=\frac{1}{4}\alpha' M$ and M the number of units of F_3 flux on the large S^3 of the warped deformed conifold (also known as the compact A-cycle). To simplify the expressions, it is useful to define the constants $h_0\equiv h(\tau=0)$ and $\mathcal{I}_0\equiv\frac{h_0}{32P^2g_s}$.

Moreover, the functions $\{f,k,F\}$ appearing in the fluxes are given by:

$$\begin{aligned} f_{KS} \;&=\; -g_s\,P\,\frac{(\tau\coth(\tau)-1)(\cosh(\tau)-1)}{\sinh(\tau)}\,,\\ k_{KS} \;&=\; -g_s\,P\,\frac{(\tau\coth(\tau)-1)(\cosh(\tau)+1)}{\sinh(\tau)}\,,\\ F_{KS} \;&=\; P\,\frac{\sinh(\tau)-\tau}{\sinh(\tau)}\,, \end{aligned} \tag{3.6}$$

and, when there are not mobile D3 branes, Q is zero.

It is worth noting that in the KS solution the complexified three-form, G_3, satisfies the ISD condition, $(i+\star_6)G_3=0$. Furthermore, G_3 has only $(2,1)$ components with respect to the choice of holomorphic vielbeins picked by supersymmetry :

$$\begin{aligned} h_1 \;&=\; E_1+i\,(\cos\omega E_2+\sin\omega\,E_4)\,,\\ h_2 \;&=\; E_3+i\,(\sin\omega E_2-\cos\omega\,E_4)\,,\\ h_3 \;&=\; E_5+i\,E_6\,, \end{aligned} \tag{3.7}$$

where $\sin\omega=-\tanh Y$ and:

$$\begin{aligned} E_1 \;&=\; \frac{e^{X/2}}{\sqrt{2\cosh(Y)}}(g_2+g_4)\,,\quad E_2 \;=\; \frac{e^{X/2}}{\sqrt{2\cosh(Y)}}(g_1+g_3)\,,\\ E_3 \;&=\; \frac{e^{X/2}\sqrt{\cosh(Y)}}{\sqrt{2}}(g_4-g_2-(g_2+g_4)\tanh Y)\,,\\ E_4 \;&=\; \frac{e^{X/2}\sqrt{\cosh(Y)}}{\sqrt{2}}(g_3-g_1-(g_1+g_3)\tanh Y)\,,\\ E_5 \;&=\; e^{-X/2-3W}\mathrm{d}\tau\,,\quad E_6 \;=\; e^{-X/2-3W}g_5\,. \end{aligned} \tag{3.8}$$

We will denote the holomorphic 3-form on the *warped* geometry as $\Omega\equiv n\,h_1\wedge h_2\wedge h_3$, where the normalization constant, n, is such that Ω^{KS}, the unwarped Klebanov-Strassler 3-form, satisfies:

$$\int_A\Omega^{\mathrm{KS}} \;=\; \int_A H^{-3/4}\Omega=S \quad\Rightarrow\quad n=-\frac{\sqrt{6}}{4\pi^2}\,, \tag{3.9}$$

where $H=e^{-4A-4W+2x}$ is the warp factor[4]. The explicit form of the normalized Ω^{KS} in terms of the set of $\{g_i\}$ is the following:

$$\Omega^{\mathrm{KS}}=-\frac{S}{16\pi^2}\sinh\tau\Big(\tanh\Big(\tfrac{\tau}{2}\Big)g_1\wedge g_2-\coth\Big(\tfrac{\tau}{2}\Big)g_3\wedge g_4+ig_1\wedge g_3+ig_2\wedge g_4\Big)\wedge(g_5-ig_6)\,. \tag{3.10}$$

[4]The KS metric (3.1) can be written in terms of H as $ds^2=H^{-1/2}ds_4^2+H^{1/2}ds_6^2$.

Note that with this normalization constant, $\Omega \wedge \overline{\Omega} = \frac{3i}{\pi^4}\text{vol}_6$, instead of $\Omega \wedge \overline{\Omega} = 8i\text{vol}_6$, which is the usual convention in the literature[5].

3.2.2 Adding $\overline{\text{D3}}$-branes

Anti-D3 branes have a charge that is opposite to that of the Klebanov-Strassler geometry and, in the probe approximation, fall to the S^3 tip of the throat. When the antibranes are localized on the S^3, the fields they source have a complicated dependence on τ and the S^3 coordinates, and are hard to compute analytically. However, if we are interested in the solution away from the tip, one can assume the antibranes to be smeared, and then the solution will have $SU(2) \times SU(2) \times \mathbb{Z}_2$ symmetry. Its metric and fluxes will then be described by the eight functions of τ appearing in the Papadopoulos-Tseytlin ansatz (3.1)-(3.3):

$$\{\Phi^i\} \,=\, \{X - 2W - 5A,\, Y,\, X + 3W,\, X - 2W - 2A,\, f,\, k,\, F,\, \Phi\}\,, \tag{3.11}$$

where we performed the above redefinition for convenience.

When the number of the anti-D3 branes, $\overline{N}$, is small one can describe their solution as a small perturbation around the KS geometry [53, 54, 98, 99]:

$$\Phi^i \,=\, \Phi^i_{\text{KS}} \,+\, \varepsilon\, \varphi^i \,+\, O(\varepsilon^2) \tag{3.12}$$

where ε is an expansion parameter that can be taken to be:

$$\varepsilon = \frac{\overline{N}}{g_s M^2}\,. \tag{3.13}$$

We then require the equations of motion of type-IIB supergravity to be satisfied at leading order in ε. Plugging the particular ansatz (3.1)-(3.3) in the type IIB supergravity action, one gets an action for the fields $\{\Phi^i\}$ that can be cast in the following form [49]:

$$\mathcal{L} \,=\, -\frac{1}{2}\text{G}_{ij}\left(\frac{\text{d}\Phi^i}{\text{d}\tau} - \frac{1}{2}\text{G}^{ik}\frac{\partial W}{\partial \Phi^k}\right)\left(\frac{\text{d}\Phi^j}{\text{d}\tau} - \frac{1}{2}\text{G}^{jl}\frac{\partial W}{\partial \Phi^l}\right) - \frac{1}{2}\frac{\partial W}{\partial \tau}\,, \tag{3.14}$$

where G and W are respectively a Φ-dependent metric and superpotential whose exact functional dependence is not relevant in the following. To study perturbations around a supersymmetric solution governed by this action [100] it is useful to introduce the set of functions, $\{\xi^i\}$, conjugate to the perturbations, $\{\varphi^i\}$. They are defined as:

$$\xi_i \,\equiv\, \text{G}_{ij}(\Phi_{\text{KS}})\left(\frac{\text{d}\varphi^j}{\text{d}\tau} - \text{M}^j{}_k\,(\Phi_{\text{KS}})\,\varphi^k\right)\,, \quad \text{M}^j{}_k \,\equiv\, \frac{1}{2}\frac{\partial}{\partial\Phi^k}\left(\text{G}^{jl}\frac{\partial W}{\partial \Phi^l}\right)\,. \tag{3.15}$$

The supersymmetric KS background corresponds to $\xi_i = 0$ for all i. Our goal is to find other solutions to the equations of motion:[6]

$$\begin{aligned} \frac{\text{d}\xi_i}{\text{d}\tau} \,+\, \xi_j \text{M}^j{}_i(\Phi_{\text{KS}}) \,&=\, 0\,, \\ \frac{\text{d}\varphi^i}{\text{d}\tau} - \text{M}^i{}_j(\Phi_{\text{KS}})\varphi^j \,&=\, \text{G}^{ij}\xi_j\,. \end{aligned} \tag{3.16}$$

[5] Remember that vol_6 is the volume of the six-dimensional internal space including the warp factor.

[6] These equations are actually supplemented by the zero-energy condition $\xi_i \frac{\text{d}\Phi^i_{\text{KS}}}{\text{d}\tau} = 0$.

An analytical form for the most general perturbation can be found and it involves various nested integrals [53]. Nevertheless, such integrals can be evaluated both as series expansions in the UV or IR limits, or numerically throughout the whole solution. The numerical evaluation allows one to match the parameters of the UV and IR expansions. The simplest example of this matching is the evaluation of the "momentum" ξ_1, which controls the force on a probe D3-brane:

$$F_{\rm D3} = \frac{2\varepsilon}{3} e^{-2X_{\rm KS}} \xi_1 \,, \quad \xi_1 \,=\, X_1\, h(\tau)\,, \tag{3.17}$$

where $X_1 = \frac{3\pi}{8\mathcal{I}_0}\frac{S^{4/3}}{h_0}$ is an integration constant. As we have already observed, the function $h(\tau)$ can be expressed as a definite integral, and its value at an arbitrary τ can only be evaluated numerically. However, its asymptotic IR and UV expansions can be evaluated straightforwardly:

$$h_{\mathbb{R}} = h_0 - \frac{16}{3}\left(\frac{2}{3}\right)^{\frac{1}{3}} g_s P^2\, \tau^2 \,+\, O(\tau^4)\,,\; h_{\rm UV} = 12\times 2^{\frac{1}{3}} g_s P^2 (4\tau-1) e^{-4\tau/3} \,+\, O(e^{-10\tau/3}). \tag{3.18}$$

The expressions for the other perturbations and momenta are considerably more involved and can be found in [54].

3.3 The flux zoo

When the KS throat is deformed because of the presence of anti-D3 branes, the G_3 flux takes the most general form:

$$G_3 \,=\, G_{(3,0)} \,+\, G_{(0,3)} \,+\, G_{(1,2)} \,+\, G_{(2,1)}\,. \tag{3.19}$$

The first three components, which break supersymmetry, are sourced by the anti-D3 branes and appear at $O(\varepsilon)$. This happens because the fluxes H_3 and F_3, defined in (3.3), do not combine anymore into a $(2,1)$ form (with respect to the complex structure (3.7) of the zeroth order KS solution) for a generic choice of the functions Φ^i.

Using the complex structure (3.7), we can extract the various components of G_3. For example, the $(0,3)$ component of G_3 for an arbitrary set of Φ^i is:

$$\begin{aligned} G_{(0,3)} \,&=\, -\frac{1}{8}\,\gamma_{(0,3)}\,\overline{h}_1\wedge\overline{h}_2\wedge\overline{h}_3\,,\\ \gamma_{(0,3)} \,&=\, e^{3W-\phi-X/2}\left(2e^{\phi}\left(e^{Y}P-\cosh Y\, F - F'\right)+e^{Y}k'-e^{-Y}f'+k-f\right)\,. \end{aligned} \tag{3.20}$$

This expression holds at any order in ε. The function $\gamma_{(0,3)}$ vanishes in the KS limit, while its first-order term in the ε expansion is:

$$\gamma_{(0,3)} = -\frac{8\sqrt{6}\, g_s^{-1}}{h^{\frac{3}{4}}\sinh(\tau)^2}\partial_\tau\left(g_s\sinh\tau\,\varphi_7+\cosh\left(\tfrac{\tau}{2}\right)^2\varphi_5-\sinh\left(\tfrac{\tau}{2}\right)^2\varphi_6\right)+O(\varepsilon^2)\,. \tag{3.21}$$

Let us stress that in (3.20) the vielbeins, $\overline{h}_i$, can be taken to be the Klebanov-Strassler ones, since any correction to them would come at order $O(\varepsilon^2)$. Thus, the first correction to $G_{(0,3)}$ is:

$$G_{(0,3)} = -\frac{4\pi^2}{g_s S \sinh(\tau)^2}\partial_\tau\Big(g_s \sinh\tau\,\varphi_7 + \cosh\Big(\tfrac{\tau}{2}\Big)^2\varphi_5 - \sinh\Big(\tfrac{\tau}{2}\Big)^2\varphi_6\Big)\,\overline{\Omega}^{\rm KS} + O(\varepsilon^2) \quad (3.22)$$

with Ω^{KS} normalized as in (3.9). Following the same procedure, we obtain the expressions at order $O(\varepsilon)$ for the other components of G_3. The $(3,0)$ component is given by:

$$G_{(3,0)} = -\frac{8\pi^2\, h^{1/4}}{S^{4/3}\sinh(\tau)^2}\,\partial_\tau(\sinh\tau\,\xi_6 - \tau\xi_5)\,\Omega^{\rm KS} + O(\varepsilon^2)\,, \quad (3.23)$$

and the $(1,2)$ component by:

$$\begin{aligned} G_{(1,2)} \;=\; & -\frac{2\sqrt{6}h^{1/4}}{\sinh(\tau)^2}\Bigg[\Big(\xi_5 - \mathrm{sech}(\tau)\xi_6\Big)\Big(h_1\wedge\overline{h}_2\wedge\overline{h}_3 + h_2\wedge\overline{h}_1\wedge\overline{h}_3 \\ & + \sinh(\tau)\Big(h_1\wedge\overline{h}_1\wedge\overline{h}_3 - h_2\wedge\overline{h}_2\wedge\overline{h}_3\Big)\Big) + (-\xi_5 + \tau\partial_\tau\xi_5 \\ & + \cosh(\tau)\xi_6 - \sinh(\tau)\partial_\tau\xi_6\,)\,h_3\wedge\overline{h}_1\wedge\overline{h}_2\Bigg] + O(\varepsilon^2)\,. \end{aligned} \quad (3.24)$$

Finally, as we have already noted, the $(2,1)$ component is the only one that has a non-vanishing term at zeroth order in ε, given by:

$$\begin{aligned} G^0_{(2,1)} \;=\; & \frac{2\sqrt{6}}{h^{3/4}}P\mathrm{csch}(\tau)\mathrm{sech}(\tau)\Big(2\coth(\tau)\,(-1+\tau\,\coth(\tau))\,h_1\wedge h_2\wedge\overline{h}_3 + \Big(\cosh(\tau) \\ & - \tau\,\mathrm{csch}(\tau)\Big)\Big(h_1\wedge h_3\wedge\overline{h}_1 + \mathrm{csch}(\tau)(h_1\wedge h_3\wedge\overline{h}_2 + h_2\wedge h_3\wedge\overline{h}_1) - h_2\wedge h_3\wedge\overline{h}_2\Big)\Big)\,, \end{aligned} \quad (3.25)$$

whereas, at first-order in ε, the non-vanishing $G_{(2,1)}$ components, $G^1_{ij\bar{k}}h_i\wedge h_j\wedge\overline{h}_k$, are:

$$\begin{aligned} G^1_{12\bar{3}} = & \frac{\sqrt{3}\,\mathrm{csch}(\tau)}{5\sqrt{2}g_s h^{3/4}}\Big(5\varphi_5 + \mathrm{csch}(\tau)(4g_sP\,(-1+\tau\coth(\tau))\,(6\varphi_1+4\varphi_3-5(3\varphi_4+\varphi_8)) \\ & - 5(\varphi_5'+\varphi_6')) - 5(\varphi_6 + \coth(\tau)\,(2g_s\varphi_7 + \varphi_5' - \varphi_6') - 2g_s\varphi_7')\,, \end{aligned} \quad (3.26)$$

$$\begin{aligned} G^1_{13\bar{1}} = -G_{23\bar{2}} = & \frac{\sqrt{6}\mathrm{csch}(\tau)}{5h^{3/4}S^{4/3}}\Big(10h(\xi_5 - \xi_6(\mathrm{sech}(\tau)) \\ & + S^{4/3}\big(P\,(6(1-\tau\mathrm{csch}(\tau)\mathrm{sech}(\tau))\varphi_1 \\ & + 10\tau\,\mathrm{sech}(\tau)\tanh(\tau)\varphi_2 - (-1+\tau\mathrm{csch}(\tau)\mathrm{sech}(\tau))(4\varphi_3 - 15\varphi_4\Big) + 10\mathrm{sech}(\tau)\varphi_7)\Big)\,, \end{aligned} \quad (3.27)$$

$$\begin{aligned} G^1_{13\bar{2}} = G_{23\bar{1}} = & \frac{2\sqrt{6}\mathrm{csch}(\tau)\mathrm{csch}(2\tau)}{5h^{3/4}S^{4/3}}\Big(10h(\xi_6 - \xi_5\cosh(\tau)) \\ & + S^{4/3}\big(-6P(\cosh(\tau) - \tau\mathrm{csch}(\tau))\varphi_1(\tau) + 5P(1+\cosh(2\tau) - 4\tau\coth(2\tau))\varphi_2(\tau) \\ & - P(\cosh(\tau) - \tau\mathrm{csch}(\tau))(4\varphi_3(\tau) - 15\varphi_4(\tau)) - 10\varphi_7(\tau)\big)\Big)\,. \end{aligned} \quad (3.28)$$

Note that the (2,1) flux remains primitive at first order: $G^1_{(2,1)} \wedge J = 0$, where the Kähler form is:

$$J = \frac{1}{2} i \left(h_1 \wedge \overline{h}_1 + h_2 \wedge \overline{h}_2 + h_3 \wedge \overline{h}_3 \right) . \tag{3.29}$$

The behavior in the UV of all components of G_3 can be obtained using the UV expansion of the functions φ_i and ξ_i of [52]. The $(0,3)$ component is given by:

$$G^{UV}_{(0,3)} = \left(\frac{2}{3}\right)^{3/4} \frac{81\pi\,\varepsilon}{5\,\mathcal{I}_0} \frac{1}{\sqrt{\alpha' M} g_s^{3/4}} \log\left(r^3_{UV}/|S|\right)^{5/4} \left(\frac{|S|}{r^3_{UV}}\right)^{7/3} \overline{h}_1 \wedge \overline{h}_2 \wedge \overline{h}_3 \, + \, O\left(\varepsilon^2\right) , \tag{3.30}$$

where we introduced a new radial coordinate, r:

$$r \equiv \frac{3^{1/2}}{2^{5/6}} |S|^{1/3} e^{\tau/3} , \tag{3.31}$$

such that for large values of τ, the six-dimensional metric of the deformed conifold approaches the conifold metric: $dr^2 + r^2 ds^2_{T^{11}}$.

Note that $G_{(0,3)}$ falls down as r^{-7} in the UV and is dual to an operator of dimension $\Delta = 7$. Such operator is a fermion bilinear of the (schematic) form $F_{\mu\nu}F^{\mu\nu}\lambda\lambda$ where λ is the gaugino and $F_{\mu\nu}$ the field strength.

In the same way, we can compute the asymptotic behavior of the $(3,0)$ component of G_3:

$$G^{UV}_{(3,0)} \, = \, \left(\frac{3}{2}\right)^{29/4} \frac{2\pi\,\varepsilon}{5\mathcal{I}_0^2} \frac{1}{\sqrt{\alpha' M} g_s^{3/4}} \log\left(r^3_{UV}/|S|\right)^{5/4} \left(\frac{|S|}{r^3_{UV}}\right)^{11/3} h_1 \wedge h_2 \wedge h_3 + O(\varepsilon^2) \, . \tag{3.32}$$

The asymptotic decay of $G_{(3,0)}$ indicates that it is dual to an operator of dimension $\Delta = 11$ that is again a combination of a fermion bilinear and the field strength of the gauge field of the (schematic) form $(F_{\mu\nu}F^{\mu\nu})^2\lambda\lambda$. In a similar way, using the asymptotic expansion of the more involved $G_{(1,2)}$ component, we find that the leading term is primitive (as one could also see from (3.24)) and is given by:

$$G^{UV}_{(1,2)} = \left(\frac{3}{2}\right)^{7/4} \frac{2\pi\varepsilon}{\mathcal{I}_0} \frac{1}{\sqrt{\alpha' M} g_s^{3/4}} \log\left(\frac{r^3_{UV}}{|S|}\right)^{1/4} \left(\frac{|S|}{r^3_{UV}}\right)^{4/3} \left(h_1 \wedge \overline{h}_1 \wedge \overline{h}_3 - h_2 \wedge \overline{h}_2 \wedge \overline{h}_3\right) + O(\varepsilon^2), \tag{3.33}$$

which means that this must be holographically dual to the expectation value of an operator of dimension $\Delta = 4$, which corresponds to a marginal deformation of the superpotential [95].

Finally, the leading asymptotic terms in the (2,1) component at zeroth order in ε is given by:

$$G^{0\ UV}_{(2,1)} = \left(\frac{2}{3}\right)^{1/4} \frac{1}{\sqrt{\alpha' M} g_s^{3/4}} \log\left(\frac{r^3_{UV}}{|S|}\right)^{-3/4} \left(h_1 \wedge h_3 \wedge \overline{h}_1 - h_2 \wedge h_3 \wedge \overline{h}_2\right) , \tag{3.34}$$

whereas the leading asymptotic behavior of the (2,1) component at first order in ε is

$$G^{1\ UV}_{(2,1)} = \frac{24\varepsilon}{\sqrt{\alpha' M} g_s^{3/4}} \log\left(\frac{r^3_{UV}}{|S|}\right)^{-7/4} \left(h_1 \wedge h_3 \wedge \overline{h}_1 - h_2 \wedge h_3 \wedge \overline{h}_2\right) . \tag{3.35}$$

3.4 Fermion masses

The presence of new components of the fluxes can strongly affect the worldvolume dynamics of D7-branes in the UV. In fact, any component of G_3 that is not $(2,1)$ generates fermion masses, possibly breaking supersymmetry on the brane. For instance, a non-trivial $G_{(0,3)}$ component is responsible for a non-vanishing gaugino mass $m_\lambda \neq 0$ [77–79]. A gaugino mass that is larger than the gaugino condensation scale, $\Lambda_{\rm YM}$, signals a breakdown of the $\mathcal{N}=1$ supersymmetric dynamics at this scale, and affects the expression of the ADS superpotential. Hence, in order for the KKLT *"moduli stabilization via gaugino condensation"* scenario to apply we need $\frac{m_\lambda}{\Lambda_{\rm YM}} \ll 1$. Our purpose is to calculate this ratio.

The mass of the canonically normalized gaugino is given by [79]:

$$m_\lambda = \left(-\frac{4\pi^2}{\sqrt{6}}\right)\frac{1}{4}\frac{\int \delta^{(0)}_\Sigma\, e^{\phi/2} G_3\wedge\Omega}{\int_\Sigma \frac{1}{2}J\wedge J}\,, \tag{3.36}$$

where we work in Einstein frame and $\delta^{(0)}_\Sigma$ localizes the integral on the cycle Σ wrapped by the seven-branes. The three-form, Ω, is again normalized such that $\Omega\wedge\overline{\Omega} = \frac{3i}{\pi^4}\text{vol}_6$ and the two-form J such that $\frac{1}{2}J\wedge J = \text{vol}_4$. Here vol_6 is the volume form of the warped Calabi-Yau threefold and vol_4 is the volume of the 4-cycle wrapped by the D7-branes. The $(0,3)$ fluxes (3.30) then generate the D7 worldvolume gaugino mass[7]:

$$m_\lambda = (-i)\left(\frac{2}{3}\right)^{3/4}\frac{162\,\pi\,\varepsilon}{5\,\mathcal{I}_0}\frac{g_s^{-1/4}}{\sqrt{\alpha' M}}\log\!\left(r^3_{\rm UV}/|S|\right)^{5/4}\left(\frac{|S|}{r^3_{\rm UV}}\right)^{7/3}\,, \tag{3.37}$$

where $r_{\rm UV}$ is the radial cut-off, whose value can be determined if we require the warping to be of order one in the UV[8].

We now compare this with a four-dimensional supergravity computation of the supersymmetry breaking gaugino masses. In order to compare correctly, we should use the Gukov-Vafa-Witten superpotential, without including the non-perturbative superpotential coming from gaugino condensation on the D7-branes, since the computation of the $\overline{\text{D3}}$ brane induced fluxes is performed without it. The general form of Majorana gaugino masses in four-dimensional supergravity is given, up to an irrelevant phase, by

$$m_\lambda = \frac{1}{2Ref}\mathcal{K}^{i\bar{\jmath}}e^{\frac{\mathcal{K}}{2}}\overline{D_{\bar{\jmath}}W}\frac{\partial f}{\partial z^i}\,, \tag{3.38}$$

where $\mathcal{K}$ is the Kähler potential, $D_iW = \partial_i W + (\partial_i\mathcal{K})W$ is the Kähler covariant derivative of the superpotential W, $f(z^i)$ is the gauge kinetic function and z^i denote the complex scalars in the chiral multiplets.

The relevant quantities in the 4d SUGRA Lagrangian for a single Kähler modulus are[9]

$$\mathcal{K} = -3\log r - \log(2/g_s) - \log\left(\frac{|\Omega|^2 V_w^2}{\kappa_4^{12}}\right)\,,\; W = \frac{1}{\kappa_4^8}\int_M G_3\wedge\Omega\,,\; f_{D7} = T\,, \tag{3.39}$$

[7]Note that this is the fall-off corresponding to an operator of dimension 7 in the holographic theory dual to the KS solution, and not to an operator of dimension 3, which would correspond to a gaugino mass in this theory.

[8]This is the natural assumption if the Calabi-Yau manifold is weakly warped.

[9]For more details of this particular form of the Kähler potential and superpotential see [101].

where

$$r = T + \overline{T} - \frac{3c' g_s (\alpha' M)^2}{\pi |\Omega|^2 V_w} |S|^{2/3} \,. \tag{3.40}$$

Here V_w is a fiducial volume that we take to be equal to one, $\kappa_4 = M_{pl}^{-2}$, $c' = 1.18$ is a numerical factor coming from taking into account warping effects in the effective field theory [63] and Ω has the usual normalization: $|\Omega|^2 = 8$. From (3.39) one can easily see that

$$D_T W = -\frac{3}{\kappa_4^8 r} \int G_3 \wedge \Omega \,. \tag{3.41}$$

Combining all the above relations, the gaugino mass (3.38) is

$$m_\lambda = -\frac{\sqrt{g_s}}{4\kappa_4^8 (T+\overline{T}) r^{1/2}} \int G_3 \wedge \Omega \,. \tag{3.42}$$

In order to compare this expression with (3.37) we should note that in Einstein frame, $T = \frac{\text{vol}_4}{2\pi\alpha'^2}$ and that for a single Kähler modulus $\text{vol}_6 = \frac{\sqrt{2}}{3} T^{3/2}$. Taking into account the $\delta_\Sigma^{(0)}$ localization factor in (3.36), it is not hard to see that, in the regime where we can neglect the conifold contribution in (3.40), the two results agree parametrically.[10]

3.4.1 Gaugino mass and gaugino condensation

As already mentioned, the component $G_{(0,3)}$ is non-vanishing and gives rise to a mass for the world-volume gaugino of the D7-branes. Since this mass is generated by the addition of $\overline{\text{D3}}$ branes in the IR throat, we can think of it as the manifestation of a $\overline{\text{D3}}$-D7 interaction. In order to see whether and how this mass can affect the dynamics of the gaugino condensation responsible for Kähler-moduli stabilization in the KKLT scenario, we need to compute the various energy scales of our system. In the following, we will mostly follow the same conventions as in [60, 74]. First let us recall that:

$$M = \frac{1}{4\pi^2\alpha'} \int_A F_3 \,, \quad K = \frac{1}{4\pi^2\alpha'} \int_B H_3 \,, \tag{3.43}$$

where the A-cycle is the S^3 at the bottom of the throat. The B-cycle is a bit more subtle, extending to the brim of the KS throat and into the Calabi-Yau compactification manifold. Here we approximate K with the integral of H_3 over the part of this cycle inside the throat, ignoring the contribution from the rest of the compactification manifold.

If we call τ_{UV} the distance from the tip of the KS throat to the region where the throat merges with the CY[11], then

$$K = \frac{1}{4\pi^2\alpha'} \int_0^{\tau_{UV}} \text{d}\tau \int_{\text{S}^2} H_3 \,, \tag{3.44}$$

[10] An independent check of the agreement between the 10d versus the 4d description would be a ten-dimensional computation of the gravitino mass, along the lines of [102], taking into account the backreaction effects from the antibrane.

[11] In KS holography this corresponds to the UV cutoff, Λ_{UV} .

where the two-sphere is taken at $\psi = 0$, $\theta_1 = -\theta_2$, $\phi_1 = -\phi_2$. Using the form (3.3) for the fluxes and working at zeroth order in ε, we can compute the units of NSNS-flux as:

$$K = -\frac{2}{\pi\alpha'} f(\tau)\Big|_0^{\tau_{UV}} \approx \frac{g_s M}{2\pi}\,\tau_{UV}\,, \tag{3.45}$$

where in the last expression we evaluated $f(\tau)$ assuming τ_{UV} to be large. This gives the radial cutoff of the throat and its associated energy scale :

$$r_{UV}^3 = \Lambda_{UV}^3 \;=\; \frac{3^{3/2}}{2^{5/2}}\,|S|\,e^{\frac{2\pi K}{g_s M}}\,, \tag{3.46}$$

where we used the relation between τ and r given in (3.31). Using holographic KS terminology, one can also define an infrared energy scale, which can be taken to coincide with the value of r at the bottom of the throat ($\tau = 0$). We can thus introduce a parameter, η, measuring the hierarchy between the ultraviolet and infrared scales:

$$\eta \;=\; 3\ln\frac{\Lambda_{UV}}{\Lambda_{IR}} \;=\; \frac{2\pi K}{g_s M}\,. \tag{3.47}$$

Even if we do not know the full metric and fluxes of the Calabi-Yau compactification, it is reasonable to assume that, when the size of the compactification manifold is not very large, the fields at the location of the $N_{\rm D7}$ seven-branes wrapping a four-cycle Σ are of the same order as the fields at the brim of the KS throat, at $r_{UV} = \Lambda_{UV}$.

In the absence of a gaugino mass, the low-energy world-volume theory of D7 branes at a non-singular locus is 8-dimensional $SU(N_{\rm D7})$ SYM theory, which one further compactifies on Σ[12]. The coupling constant of the resulting $\mathcal{N} = 1$ four-dimensional gauge theory runs logarithmically with the energy and the theory confines in the infrared at a scale

$$\Lambda_{\rm YM} \;\approx\; \mu_0 e^{-\frac{2\pi\,{\rm Re}\,T}{3N_{D7}}}\,, \tag{3.48}$$

where μ_0 is the "UV scale" that depends on (stabilized) complex-structure moduli and will be assumed to be of order one (in Planck units). If the world-volume theory has a more general gauge group, G, the exponent in (3.48) must be replaced by $-2\pi\,{\rm Re}\,T/(3\,\#_C(G))$, with $\#_C(G)$ the dual Coxeter number of G. Furthermore, in the confined phase the gaugino condenses, giving rise to a nontrivial contribution to the superpotential that depends on the coupling constant of the four-dimensional $\mathcal{N} = 1$ theory, and hence on the volume of the four-cycle wrapped by the D7 branes.

In the presence of gaugino mass, m_λ, induced by the three-form fields sourced by the antibranes, this scenario can change. In particular, when m_λ is larger than $\Lambda_{\rm YM}$, the theory will confine at an energy scale proportional m_λ, and the resulting potential will be independent of the four-cycle volume, thus ruining the Kähler moduli stabilization. Hence, gaugino condensation can only stabilize the Kähler moduli when:

$$\frac{m_\lambda}{\Lambda_{\rm YM}} \ll 1\,. \tag{3.49}$$

[12]When the D7 branes are on top of an O7-plane, the gauge group can be orthogonal or symplectic.

To estimate this ratio one can consider a KKLT-like scenario, in which the value of the potential at the AdS minimum is proportional to the square of the non-perturbative superpotential, while the contribution to the scalar potential from the anti-D3 branes (which sit at the tip of the throat, where their energy is minimized) is proportional to H^{-1}. In a realistic de Sitter compactification, where we want the cosmological constant to be as small as possible, these two quantities should have approximately the same magnitude, which means that the following relation should hold[13]

$$V_{\overline{D3}} \approx V_{\rm AdS} \to \frac{|S|^{4/3}}{h_0} \approx e^{-\frac{4\pi}{N_c}\,{\rm Re}(T)}\,. \tag{3.51}$$

In our conventions the hierarchy is given by $e^{-\eta}$ and we note that $\tau_{\rm UV} \approx \eta$. We also require that the warping is $O(1)$ in the UV. All these give a relation between the complex-structure modulus, S, and the flux-induced D3 charge of the throat, $Q_{\rm D3}^{\rm Throat} = KM$:

$$H \;=\; \frac{h(\tau)}{|S|^{4/3}} \approx 1 \quad \to \quad |S|^{4/3} \approx h(\tau_{UV}) \;\approx\; 6\,\pi\cdot 2^{1/3}(\alpha')^2 e^{-\frac{4\eta}{3}}\,Q_{\rm D3}^{\rm Throat}\,. \tag{3.52}$$

Combining (3.51) (more precisely (3.50)) and (3.52), we can estimate the value of the stabilized Kähler modulus

$${\rm Re}\,T \sim \frac{2N_cK}{3g_sM} \;=\; \frac{N_c}{3\pi}\eta\,, \tag{3.53}$$

where we have ignored logarithmic corrections coming from the non-exponential terms in (3.50).

Using this approximation, we can evaluate the ratio between the gaugino mass and the condensation scale in the KKLT scenario:

$$\frac{m_\lambda}{\Lambda_{\rm YM}} \approx 10^2\overline{N}M^{-5/2}g_s^{-5/4}\eta^{5/4}e^{-\frac{19}{9}\eta}\,. \tag{3.54}$$

Our calculation indicates that this ratio must be smaller than one in all flux compactifications where Kähler moduli are stabilized via D7 gaugino condensation and where the cosmological constant is uplifted using anti-D3 branes in warped Klebanov-Strassler-like throats. It is not hard to see that for the range of parameters one uses in "vanilla" KKLT scenarios this bound will be satisfied. For example for the de Sitter minimum of [61], where $M = K = 70$ and $g_s = 1/2$ we find this ratio to be:

$$\frac{m_\lambda}{\Lambda_{\rm YM}} \sim 10^{-13}\,. \tag{3.55}$$

[13] If one takes into account the explicit expression for both $V_{\overline{D3}}$ [62] and V_{AdS}, one finds using (3.52) a more precise expression

$$e^{-\frac{2\pi\,{\rm Re}\,T}{3N_c}} \approx \left(\frac{N_c}{A}\right)^{1/3}\left(\frac{\eta}{{\rm Re}\,T}\right)^{1/6} e^{-2\eta/9}\,, \tag{3.50}$$

where A is the Pfaffian factor that appears in the non-perturbative superpotential. Since we assume both A and N_c to be of order one, the difference between the results obtained with (3.50) and those obtained with (3.51) is negligible.

Hence, in these scenarios, the stabilization of the Kähler moduli via D7 gaugino condensation is not affected by the fluxes produced by the anti-D3 branes.

It would be interesting to try to span larger families of possible flux compactifications and other de Sitter scenarios which use a smaller hierarchy (such as those of [66,80]) to see whether this bound may become harder to satisfy and may result in nontrivial constraints on the parameters of the compactification.

Chapter 4

Smearing and Unsmearing KKLT AdS Vacua

4.1 Introduction

Gaugino condensation on D-branes wrapping internal cycles of string compactifications provides a mechanism for stabilizing their associated moduli. Indeed, the gauge coupling, appearing in the superpotential, depends on the corresponding volumes. This is particularly handy in type IIB compactifications on Calabi-Yau manifolds. The three-form fluxes threading the internal three-cycles are routinely included, and provide a potential for their sizes, parameterised by the complex structure moduli. On the other hand, Kähler moduli, which define the sizes of the even cycles, are unfixed at the perturbative level, hence the non-perturbative contributions coming from gaugino condensates on D-branes are crucial. For type IIB compactifications with three-form fluxes and O3/O7 planes, such as the ones considered in this Chapter, the supersymmetric branes are D7-branes wrapped on calibrated four-cycles Σ_4.

As we have already seen, this proposal for supersymmetric compactifications with fully stabilized moduli was put forward by Kachru, Kallosh, Linde and Trivedi in [4]. More explicitly, complex structure moduli are assumed to be fixed by fluxes[1], and at a lower energy scale one uses effective field theory to study Kähler moduli. The corresponding F-term conditions then lead to a supersymmetric AdS_4 solution. As long as the (0,3) fluxes can be fine tuned to give a very small contribution to the superpotential, comparable to the non-perturbative one, the resulting cosmological constant is exponentially small, while the Kähler moduli are fixed at a large value. This is a prominent example of scale separation, which violates the Swampland conjecture formulated in [103]. Importantly, a family of explicit examples were constructed recently in [42, 43, 104, 105].

In this Chapter we provide the ten-dimensional description of these supersymmetric AdS_4 vacua with fluxes and gaugino condensates captured by the EFT of [4]. For

[1]This mechanism was conjectured not to work for a large number of moduli because of the tadpole cancellation condition [68].

that, we first derive the supersymmetry equations for AdS_4 compactifications in the presence of gaugino condensates, combining different elements that appeared in the literature [101, 106–109] and bringing them together into a consistent picture. We work within the framework of Generalized Complex Geometry (GCG) [106]. This is necessary since, as shown in [101, 108, 110], the backreaction of the gaugino condensate breaks the SU(3) structure of Calabi-Yau manifolds down to a more general so-called "dynamic SU(2) structure", best understood in terms of generalized complex structures. Requiring $\mathcal{N}$=1 supersymmetry gives three equations, involving the generalizations of the complex structure and the complexified Kähler structure. The first two of these conditions were shown to be equivalent to the F-flatness conditions for the Kähler and complex structure moduli, while the third one corresponds to a D-flatness condition [111] of the effective theory of compactifications on generalized geometries [106, 112]. In the presence of gaugino condensates, these equations get modified. While the modification of the first supersymmetry condition was understood in [107, 108] in terms of the backreaction on the geometry itself, that of the third equation, which involves the RR fluxes, is more subtle. This was considered first in [108, 109] under some approximations. Here we take an alternative route and find the generalized geometry extension for gaugino condensation in any type II branes wrapping a calibrated cycle. We do so by building on the analysis of gaugino mass terms presented in [79]. Furthermore, we argue for self-consistency of the whole set of equations, and consistency with the four-dimensional effective theory[2].

We then solve these modified supersymmetry equations for type IIB AdS_4 compactifications with gaugino condensates on *smeared* D7-branes. We find that the solution is surprisingly simple, and shares many features with its Minkowski counterpart without gauginos. More precisely, we find that the internal manifold is still (conformal) Calabi-Yau, and three-form fluxes are still imaginary self-dual. Nevertheless, they contain an additional (0,3) piece, which turns out to be proportional to the non-vanishing cosmological constant, whose value is in turn dictated by the vacuum expectation value (VEV) of the gaugino bilinear. These features of the ten-dimensional solution reproduce the expectations from the four-dimensional effective field theory analysis in [4] not only qualitatively but also quantitatively. We take this as strong evidence confirming both our modified supersymmetry equations and also the applicability of the EFT for finding supersymmetric vacua.

We further analyze scale separation (see e.g. [113] and references therein) in the smeared solution, finding two relevant scales, the dilaton and the volume. We show that exponential scale separation can be achieved as long as the gaugino vev is very small, which happens at weak coupling in the gauge theory, and as long as one can cook up fluxes giving rise to an equally small (0,3) component.

The equations for gaugino condensates on localised D7-branes are, not surprisingly, much harder to solve. We leave the study of the complete solution for future work, and only comment on some of the key features of the partial solutions obtained in [108, 109].

[2]At this level, our results are consistent with the discussion of [109], see their Appendix A in the latest version.

Nevertheless, we consider in detail the on-shell value of the bulk plus brane action. Since some components of the flux, as well some derivatives of the pure spinors that encode the generalized complex geometry contain delta functions that localize them on the Σ_4 cycle, one might worry whether such on-shell action is divergent (i.e. whether it has terms involving squares of delta functions). This question was raised recently and discussed in several papers [109, 114–118], without reaching a common conclusion. We show that it is possible to compute the on-shell action without knowing the details of the solution, assuming it solves the modified supersymmetry conditions. More precisely, we compute the on-shell action up to two-fermion terms using the results obtained in [79] for the relevant terms of the D-brane action, as well as the expression for the bulk ten-dimensional supergravity Lagrangian for generalized geometry compactifications in terms of fluxes and derivatives of the pure spinors, obtained in [119]. We find that the action is indeed divergent, and compute the coefficients of the terms involving one and two delta functions. The former should be cancelled by four-fermion terms in the D-brane action, while the latter indicate that a counterterm must be included as well.

The Chapter is organized as follows. In Section 4.2 we review the supersymmetry equations without gaugino condensates, their equivalence with supersymmetry conditions of the four-dimensional description, their self-consistency and the four-dimensional Minkowski solutions. In Section 4.3 we present the supersymmetry equations with gaugino condensates and the arguments that lead to them, including self-consistency of the equations. In Section 4.4 we construct the solution for smeared branes, compare with the effective four-dimensional theory and discuss scale separation. In Section 4.5 we discuss the main features of the localised solution, and the divergence of the on-shell action. Finally, we discuss our results in Section 4.6.

4.2 Supersymmetry conditions for type II AdS_4 vacua from 10D

In this Section we review how type II superstring theory $Mink_4$ and AdS_4 vacua with classical sources (such as D-branes or O-planes) are described from the ten-dimensional point of view using the language of generalized complex geometry. We also establish the conventions that we will use throughout this Chapter, following [111, 120].

4.2.1 Supersymmetric AdS_4 vacua without gaugino condensates

The GCG conditions for type II string flux compactifications to four-dimensional flat and AdS vacua preserving $\mathcal{N} = 1$ supersymmetry were found originally in [106]. They are written in terms of two polyforms, denoted $\Psi_\pm$, which characterize the internal geometry.

For type IIB these conditions read

$$d_H\left(e^{3A-\phi}\Psi_-\right) = 2i\mu e^{2A-\phi}\mathrm{Im}\,\Psi_+ \tag{4.1a}$$

$$d_H\left(e^{2A-\phi}\mathrm{Im}\,\Psi_+\right) = 0 \tag{4.1b}$$

$$d_H\left(e^{4A-\phi}\mathrm{Re}\,\Psi_+\right) = 3e^{3A-\phi}\mathrm{Re}\,[\overline{\mu}\,\Psi_-] + e^{4A}\ast_6\alpha(F)\,, \tag{4.1c}$$

while for type IIA one just has to interchange Ψ_+ with Ψ_-. In Eqs. (4.1) ϕ is the dilaton, while A is the warp factor, such that, in the string frame, the 10D metric splits as follows:

$$ds_{10}^2 = e^{2A(y)}g_{\mu\nu}(x)dx^\mu dx^\nu + h_{mn}(y)dy^m dy^n\ , \tag{4.2}$$

where $g_{\mu\nu}$ describes the extended $\mathrm{AdS}_4/\mathrm{Mink}_4$ directions. Moreover, μ is related to the cosmological constant by

$$\Lambda = -3|\mu|^2\,, \tag{4.3}$$

and

$$d_H \equiv d + H\wedge \tag{4.4}$$

is the H-twisted exterior derivative. The polyforms or pure spinors $\Psi_\pm$ are defined as

$$\Psi_\pm \equiv -\frac{8i}{||\eta||^2}\sum_p \frac{1}{p!}\eta_\pm^{2\dagger}\gamma_{m_1\ldots m_p}\eta_+^1\, dy^{m_1}\wedge\cdots\wedge dy^{m_p}\ , \tag{4.5}$$

where η^1 and η^2 are two globally defined spinors on the internal manifold, that can become parallel at certain loci, and whose norm is related to the warp factor as $||\eta^1||^2 = ||\eta^2||^2 = e^A$. By using properties of spinor bilinears in six dimensions it is easy to see that Ψ_- and Ψ_+ are sums of odd and even p-forms, respectively, and satisfy the self-duality condition

$$\ast_6\alpha(\Psi_\pm) = i\Psi_\pm\,, \quad \alpha(\omega_q) = (-1)^{\frac{q(q-1)}{2}}\omega_q\,. \tag{4.6}$$

Finally, the polyform F accounts for the RR fluxes on the internal manifold, which are related to those with external legs by self-duality. More explicitly, the total[3] RR flux $\widehat{F}$ is

$$\widehat{F} = F + e^{4A}\mathrm{vol}_4\wedge\widetilde{F}, \tag{4.7}$$

such that

$$\widetilde{F} = \ast_6\,\alpha(F)\ . \tag{4.8}$$

As discussed in [79], the third supersymmetry condition, namely Eq. (4.1c), can be understood in terms of the generalized flux

$$G \equiv F + ie^{-4A}d_H\left(e^{4A-\phi}\mathrm{Re}\,\Psi_+\right) \tag{4.9}$$

as follows:

$$(1 - i\ast_6\alpha)G = 3ie^{-A-\phi}\overline{\mu}\Psi_-\,. \tag{4.10}$$

[3]Here we use the democratic formulation [121], with the polyform notation, where $F = \sum F_q$ with $q = 1,3,5,7,9$ ($q = 0,2,4,6,8,10$) for type IIB (IIA).

Upon restricting to internal manifolds with a well-defined SU(3) structure and compactifications with $\mu = 0$, this reduces to the usual imaginary-self-duality (ISD) condition on the three-form flux

$$G_3 = F_3 + ie^{-\phi} H \,. \tag{4.11}$$

In this sense, any AdS_4 solution to the (classical) supersymmetry conditions (4.1) must include some IASD contributions to the generalized flux G.

A supersymmetric configuration is a solution to the equations of motion iff Eqs. (4.1) are satisfied and all fluxes satisfy the corresponding Bianchi identities

$$dH = 0 \,, \quad d_H F = dF + H \wedge F = \delta_{\rm Dp} \,, \tag{4.12}$$

where the possible sources encoded in $\delta_{\rm Dp}$ are either D-branes or O-planes. Indeed, the EOM for the fluxes follow directly from the supersymmetry conditions. In the polyform language, they read

$$d_H \left[e^{4A} *_6 \alpha(F) \right] = 0 \,, \tag{4.13}$$

as can be seen by applying d_H to Eq. (4.1c) and using that $d_H^2 = 0$, together with (4.1a). Although the EOM for H is more cumbersome in the GCG language, it was shown in [122] that it follows from the hodge-dual of the three-form component of Eq. (4.1c). We will come back to this later on.

4.2.2 Supersymmetry conditions from the 4D EFT and superpotential

The conditions in Eq. (4.1) are equivalent to requiring that the supersymmetry variations of the gravitino and the dilatino vanish. Importantly, it was shown in [107, 111, 112, 123–125] that they can also be understood as D- and F-flatness conditions in the four-dimensional effective action for the scalars in vector and chiral multiplets. In type IIB, the former come from deformations of the complex structure, while the latter are combinations of the RR axions and the Kähler deformations. In the language of GCG, the complex structure is encoded in Ψ_-, while the Kähler moduli are contained in $\mathrm{Re}\,\Psi_+$. One therefore defines the holomorphic fields

$$Z = e^B e^{3A-\phi} \Psi_- \,, \qquad T = e^B (C + ie^{-\phi}\, \mathrm{Re}\,\Psi_+) \,, \tag{4.14}$$

where C are the RR gauge potentials, i.e. $d_H C = F$. These are precisely the combinations whose exterior derivatives appear in Eqs. (4.1a) and (4.1c), respectively. The argument of the derivative in (4.1b) can be formally thought of as a function of Z and T [112]. In order to build the low-energy effective action one would need to specify the (a priori massless) deformations of these geometric objects, which contain all relevant information about the internal metric, the warp factor A, the dilaton ϕ and the B-field. Here however what one does is to build a superpotential in terms of the full pure spinors, which involves

an infinite number of fields, including all the Kaluza-Klein modes. In this sense, we can define a ten-dimensional superpotential, which is given by [110, 112, 123, 124]

$$W_{\rm GCG} = \pi \int_{M_6} \langle Z, d\,T \rangle = \pi \int_{M_6} \langle e^{-B} Z, G \rangle \ , \tag{4.15}$$

where G was defined in (4.9). The brackets in Eq. (4.15) correspond to the so-called Mukai pairing,

$$\langle A, B \rangle \equiv [A \wedge \alpha(B)]_6 \ , \tag{4.16}$$

where one only includes the 6-form component. As discussed below, the variations of $W_{\rm GCG}$ as function of Z and T then vanish iff Eqs. (4.1) are satisfied.

4.2.3 Kähler potential, cosmological constant, and self-consistency

Having defined the generalized superpotential in Eq. (4.15), we now turn to the Kähler potential. This can be understood in terms of

$$\mathcal{N} = 4\pi \int_{M_6} e^{2A-2\phi} {\rm vol}_6 \, , \tag{4.17}$$

which is the constant appearing in front of the Einstein-Hilbert term of the effective four-dimensional action, thus setting the corresponding Planck scale. This defines the Kähler potential in the (Einstein frame) 4D supergravity language [111]

$$\mathcal{K} = -3 \log \mathcal{N} . \tag{4.18}$$

By using the pure spinor normalizations

$$\langle \Psi_+, \overline{\Psi}_+ \rangle = \langle \Psi_-, \overline{\Psi}_- \rangle = -8i {\rm vol}_6 \, , \tag{4.19}$$

the Kähler potential can be expressed as

$$\mathcal{K} = -2 \log i \int_{M_6} e^{2A} \langle t, \bar{t} \rangle - \log i \int_{M_6} e^{-4A} \langle z, \bar{z} \rangle - 3 \log \frac{\pi}{2} \, , \tag{4.20}$$

with $t = e^{-\phi} \Psi_+$ and $z = e^{3A-\phi} \Psi_-$. This allows one to interpret Eqs. (4.1a) and (4.1c) as the F-flatness conditions associated to the variations of $W_{\rm GCG}$ with respect to T and Z, respectively. The remaining condition (4.1b) (which is automatically satisfied for compactifications with non-zero μ) can similarly be interpreted as a D-term condition.

For this interpretation to hold, and for Eqs. (4.1c) to give a self-consistent system of equations in terms of $W_{\rm GCG}$, the cosmological constant as denoted by μ must correspond to the on-shell value of the superpotential. More precisely, we should have

$$\langle W_{\rm GCG} \rangle = \mu \, \mathcal{N} \, . \tag{4.21}$$

We now review how this is derived. Let us split the contributions to the on-shell superpotential (4.15) as follows:

$$\langle W_{\rm GCG} \rangle = \pi \int_{M_6} \langle e^{3A-\phi} \Psi_-, F \rangle + \pi \int_{M_6} \langle e^{3A-\phi} \Psi_-, i d_H [e^{-\phi} {\rm Re} \Psi_+] \rangle \, . \tag{4.22}$$

In order to relate the term proportional to F with Eq. (4.1a) we use that the Mukai pairing satisfies $\langle \Psi, \Phi \rangle = \langle *_6\alpha(\Psi), *_6\alpha(\Phi) \rangle$ for generic polyforms Ψ, Φ. Since, the pure spinors are ISD (see Eq. (4.6)), by using Eq. (4.1c) we have

$$\langle e^{3A-\phi}\Psi_-, F\rangle = i\langle e^{3A-\phi}\Psi_-, \widetilde{F}\rangle = i\langle e^{3A-\phi}\Psi_-, e^{-4A}d_H\left(e^{4A-\phi}\mathrm{Re}\,\Psi_+\right) - 3e^{-A-\phi}\mathrm{Re}\,[\overline{\mu}\,\Psi_-]\rangle. \tag{4.23}$$

Moreover, the following compatibility conditions hold:

$$\langle \Psi_\pm, dy^m \wedge \Psi_\mp\rangle = \langle \Psi_\pm, \iota_m \Psi_\mp\rangle = 0\,. \tag{4.24}$$

This allows us to take the warp factor out of the derivative in the first term on the RHS of (4.23), which then combines with the second term in (4.22). We are then left with

$$\begin{aligned}\langle W_{\rm GCG}\rangle &= 2\pi i\int_{M_6}\langle e^{3A-\phi}\Psi_-, d_H\left(e^{-\phi}\mathrm{Re}\,\Psi_+\right)\rangle - \frac{3\pi i}{2}\mu\int_{M_6} e^{2A-2\phi}\langle\Psi_-, \overline{\Psi}_-\rangle \\ &= (16-12)\,\pi\mu\int_{M_6} e^{2A-2\phi}\mathrm{vol}_6 = \mu\,\mathcal{N},\end{aligned} \tag{4.25}$$

where in the first line we have integrated the first term by parts and used (4.1a) together with (4.19).

For later reference, we note that, using properties of the Mukai pairing, we can actually compute the first term in (4.25) exactly as above but without the need to integrate by parts, i.e. directly at the level of the integrand. This is because[4]

$$\langle e^{3A-\phi}\Psi_-, i d_H[e^{-\phi}\mathrm{Re}\Psi_+]\rangle = \langle d_H[e^{3A-\phi}\Psi_-], ie^{-\phi}\mathrm{Re}\Psi_+\rangle\,. \tag{4.27}$$

We conclude that the integrand in (4.15) can be evaluated on-shell, giving

$$\left\langle e^{3A-\phi}\Psi_-, F + i\,d_H\left(e^{-\phi}\mathrm{Re}\,\Psi_+\right)\right\rangle = 4\mu e^{2A-2\phi}\mathrm{vol}_6\,. \tag{4.28}$$

This will be useful in Section 4.5 below.

4.2.4 SU(3) structure and Minkowski solutions

Configurations where η^1 and η^2 are parallel everywhere on the internal manifold up to a constant phase correspond to SU(3) $\subset$ O(6) structure compactifications. In these solutions the pure spinors reduce to[5]

$$\Psi_- = \Omega\,, \quad \Psi_+ = \exp(iJ)\,, \tag{4.29}$$

[4]Due to the compatibility condition (4.24) and the fact that $\langle e^B\Psi_-, e^B\Psi_+\rangle = \langle\Psi_-, \Psi_+\rangle$ it is enough to consider the exterior derivative without the twisting by H, and without dilaton and warp factors. Then, we see that

$$\langle\Psi_-, d\Psi_+\rangle - \langle d\Psi_-, \Psi_+\rangle = -d[\Psi_-|_1\wedge\Psi_+|_4 - \Psi_-|_3\wedge\Psi_+|_2 + \Psi_-|_5\wedge\Psi_+|_0] = 0\,. \tag{4.26}$$

Here we have used that from the compatibility condition (4.24) the five-form being differentiated on the LHS vanishes when it is wedged with any one-form and also when it is contracted with any vector, so it must be zero. This implies (4.27).

[5]There is actually an overall phase in both pure spinors, given by the relative phase between the internal spinors: $\eta^1_+ = ie^{i\theta}\eta^2_\mp$. The relevant sypersymmetry we use throughout this Chapter is the one compatible with O3- and O7-planes, namely $\theta = 0$ [126].

where J and Ω are a real (1,1)-form and a holomorphic (3,0)-form, respectively. The conditions in Eqs. (4.24) and (4.19) then read

$$J \wedge \Omega = 0\,, \qquad \frac{1}{6} J \wedge J \wedge J = -\frac{i}{8} \Omega \wedge \overline{\Omega} = \text{vol}_6\,. \tag{4.30}$$

Consequently, the superpotential (4.15) reduces to the usual Gukov-Vafa-Witten (GVW) expression [57]

$$W_{\text{GVW}} = \pi \int_{M_6} e^{3A-\phi} \Omega \wedge G_3\,. \tag{4.31}$$

It is not hard to see that, in this context, the supersymmetry equations reduce to the well-known type IIB supersymmetric Mink_4 solutions compactified on warped Calabi-Yau manifolds [56]. Indeed, due to the absence of a 1-form component in Ψ_-, the 2-form component of Eq.(4.1a) implies $\mu = 0$, while the corresponding 4-form equation and the 3-form component of (4.1b) read

$$d\left(e^{3A-\phi}\Omega\right) = d\left(e^{2A-\phi}J\right) = 0. \tag{4.32}$$

Moreover, from the three-form components of (4.1a) and (4.1c) one also finds

$$H \wedge \Omega = 0\,, \qquad e^{-\phi} H - \widetilde{F_3} = 0\,, \tag{4.33}$$

so that G_3 must be ISD and its (0,3) component must vanish. The remaining equations give

$$d\left(4A - \phi\right) = e^{\phi} \star_6 F_5\,, \qquad d\phi \wedge J \wedge J = -2 e^{\phi} \star_6 F_1\,. \tag{4.34}$$

By defining the relevant 5-form flux and the axio-dilaton as

$$F_5 = (1 + *_{10})\, \text{vol}_4 \wedge d\alpha\,, \qquad \tau = C_0 + i e^{-\phi}\,, \tag{4.35}$$

with $\alpha = \alpha(y)$, the conditions in (4.34) can be written as

$$d\left(4A - \phi - \alpha\right) = 0\,, \quad d\tau \wedge \Omega = 0\,. \tag{4.36}$$

Hence, one can have a non-trivial warp factor, related to the 5-form flux, while τ must be holomorphic.

4.3 Revisiting the effect of the gaugino condensate

In this Section we focus on the situation where one includes a stack of D-branes undergoing gaugino condensation, and discuss how such non-perturbative effects can be encoded in a set of modified supersymmetry conditions. In doing so, we combine the different elements considered originally in [108, 110] and more recently in [101, 109], bringing them together into a consistent picture.

4.3.1 Supersymmetry conditions with localized terms

We focus on the D7-brane case for concreteness, and because it is what we will be interested in in the following Sections. The set of modified supersymmetry conditions we propose reads as follows:

$$d_H\left(e^{3A-\phi}\Psi_-\right) = 2i\mu e^{2A-\phi}\mathrm{Im}\,\Psi_+ - 2i\langle S\rangle\delta^{(2)}\left[\Sigma_4\right]\,, \tag{4.37a}$$

$$d_H\left(e^{2A-\phi}\mathrm{Im}\,\Psi_+\right) = 0\,, \tag{4.37b}$$

$$d_H\left(e^{4A-\phi}\mathrm{Re}\,\Psi_+\right) = 3e^{3A-\phi}\mathrm{Re}\left[\overline{\mu}\,\Psi_-\right] + e^{4A}*_6\,\alpha(F) - e^{A}\delta^{(0)}\left[\Sigma_4\right]\mathrm{Re}\left[\overline{\langle S\rangle}\Psi_-\right]\,. \tag{4.37c}$$

Here $\delta^{(2)}\left[\Sigma_4\right]$ is the localized 2-form Poincaré dual to the four-cycle wrapped by the branes, namely for any closed 4-form ω_4 one has

$$\int_{M_6}\omega_4\wedge\delta^{(2)}\left[\Sigma_4\right] = \int_{\Sigma_4}\omega_4\,, \tag{4.38}$$

while $\langle S\rangle$ is the VEV of the usual condensate superfield, related to the gaugino bilinear by

$$\langle S\rangle = \frac{1}{16\pi^2}\langle\lambda\lambda\rangle\,. \tag{4.39}$$

Moreover, $\delta^{(0)}[\Sigma_4]$ is the scalar version of the delta function, defined as [79]

$$\delta^{(0)}[\Sigma_4] = (\mathrm{Im}\,\Psi_+)^{(2)}\cdot\delta^{(2)}[\Sigma_4] \quad\Rightarrow\quad \delta^{(0)}[\Sigma_4]\,\mathrm{vol}_6 = \langle\mathrm{Re}\,\Psi_+,\delta^{(2)}[\Sigma_4]\rangle\,. \tag{4.40}$$

The analysis for other types of branes and for the type IIA case is analogous. For gaugino condensates on other type IIB Dp-branes wrapping $p-3$ cycles, one replaces $\delta^{(2)}(\Sigma_4)$ by $\delta^{(9-p)}(\Sigma_{p-3})$. For the type IIA cases one further exchanges Ψ_+ with Ψ_-.

4.3.2 Motivation

We now explain how this proposal comes about. Let us start with the modification to the first supersymmetry equation, namely Eq. (4.37a). In the ten-dimensional language, this should come from the F-term condition associated with the variation of the superpotential with respect to the superfield T, defined in (4.14). As advocated in [108,111] and further discussed in [101], assuming a non-trivial gaugino condensate on a stack of calibrated D7-branes leads to an extra contribution to the F-term. Indeed, in the 4D $\mathcal{N}=1$ superspace description of the Yang-Mills (YM) theory living on the branes one must include a chiral contribution to the effective Lagrangian of the form

$$\frac{i}{8\pi}\int d^2\theta\,\tau\,\mathrm{Tr}\left[W^\alpha W_\alpha\right]\,, \tag{4.41}$$

where τ is the complexified gauge coupling[6] and W_α is the usual chiral superfield, i.e.

$$\tau = i\frac{4\pi}{g^2_{\mathrm{YM}}} + \frac{\theta_{\mathrm{YM}}}{2\pi}\,, \qquad W_\alpha = -i\lambda_\alpha + \cdots\,. \tag{4.42}$$

[6]We use the same notation as for the axio-dilaton defined in Eq. (4.35). The distinction should be clear from the context.

The non-perturbative effects that generate a non-trivial expectation value for the condensate superfield

$$S = \frac{1}{16\pi^2}\,\mathrm{Tr}\,\lambda^\alpha\lambda_\alpha \tag{4.43}$$

are then captured by the Veneziano-Yankielowicz (VY) superpotential[7] [127]

$$W_{\rm VY} = W_0 + 2\pi i\tau S + NS\left[1 - \log\left(S/\mu_0^3\right)\right] , \tag{4.44}$$

where μ_0 is the scale at which τ is defined, and W_0 is taken to be independent of S.

As the effective four-dimensional YM coupling comes from integrating over Σ_4, it depends on its volume, and also on the RR potentials involved. More precisely, we have

$$\tau = \int_{\Sigma_4}\left(C + ie^{-\phi}\mathrm{Re}\,\Psi_+\right)|_{\Sigma_4} = \int_{M_6}\langle T, -\delta^{(2)}(\Sigma_4)\rangle\,, \tag{4.45}$$

where we have used that T is the calibration form on the holomorphic cycle Σ_4, which defines the associated volume form and Chern-Simons coupling. Therefore, τ must be seen as a function of the chiral field T. The corresponding F-term condition then picks up an extra contribution given by the last term on the RHS of (4.37a). The exterior derivative of the resulting condition still gives (4.37b), so it is not modified. Note that upon integrating out S in Eq. (4.44) one finds the VEV and effective superpotential

$$\langle S\rangle = \mu_0^3\exp\left(\frac{2\pi i\tau}{N}\right) , \quad W_{\rm eff} = W_0 + N\langle S\rangle\,, \tag{4.46}$$

used in the 4D EFT analysis of [4].

On the other hand, the argument for the third supersymmetry condition in Eq. (4.37c) is more delicate. Indeed, even in the absence of a gaugino condensate it is not straightforward to see that this equation is equivalent to the F-term condition for the chiral field Z, as it was discussed in [111].

Consider the DBI action describing the D7-brane theory. As it was shown recently in [79] (see also [119]), for a generic internal manifold in a GCG compactification, the quadratic terms in the gaugino action can be written as

$$S_{\lambda\lambda} = \int d^4x\,\left(\frac{i}{2}f\,\overline{\lambda}_+\gamma^\mu\nabla_\mu\lambda_+ + \frac{1}{2}m_\lambda\,\overline{\lambda}_-\lambda_+ + c.c.\right) , \tag{4.47}$$

with $\overline{\lambda}_-\lambda_+ = i16\pi^2\overline{S}$, and where[8]

$$m_\lambda = -\frac{i}{8\pi}\int_{M_6}\delta^{(0)}[\Sigma_4]\,e^A\Big\langle\Psi_-, F + i\,d_H\left(e^{-\phi}\mathrm{Re}\,\Psi_+\right)\Big\rangle\,. \tag{4.48}$$

Note that the integrand is precisely that of the superpotential, Eq. (4.15)[9]. Focusing on the RR flux contribution to the gaugino mass, we have

[7] Here we take the gauge group to be SU(N) for simplicity. When considering, say, D7-branes coincident with O7-planes such that the charges are cancelled locally, it should be taken to be SO(8) instead. This introduces only minor modifications.

[8] Here we have included a warp factor missing in the original version of [79].

[9] Although this holds for the D7 case, for other D-branes one must be more careful when considering the contribution of the NSNS 3-form flux [79]. This is in agreement with the results of [108].

$$S_{\lambda\lambda,F} = 2\pi \int_{M_6} e^A \delta^{(0)}\left[\Sigma_4\right] \langle \mathrm{Re}\left[\overline{\langle S\rangle}\Psi_-\right], F\rangle\,. \tag{4.49}$$

This additional term in the bulk action provides a new source in the equations of motion for the RR fluxes. More explicitely, Eq. (4.13) is modified as follows:

$$d_H\left[e^{4A} *_6 \alpha(F)\right] = d_H\left[e^A \delta^{(0)}\left[\Sigma_4\right] \mathrm{Re}\left(\overline{\langle S\rangle}\Psi_-\right)\right]\,. \tag{4.50}$$

As discussed in Sec. 4.2 above, we expect this to follow from the derivative of the third supersymmetry condition. We find that the localized term introduced in Eq. (4.37c) ensures that this is indeed the case.

Importantly, Eq. (4.37c) should also account for an electric source for H as implied by the corresponding contribution to the mass term in (4.48). Since $*_\alpha\Psi_- = i\Psi_-$, by acting with $*_\alpha$ on (4.37c) we see that the new term becomes proportional to Im $\left[\overline{\langle S\rangle}\Psi_-\right]$. Further multiplying by $e^{-\phi}$ and taking the exterior derivative we find that the proposed non-perturbative correction is consistent with the coupling between H and the gaugino condensate in Eq. (4.48).

A localized term similar to the one introduced in (4.37c) was also discussed originally in [108] and more recently in [109]. The authors of [108] consider the rigid, decompactified limit where $\mu = 0$, and argue that the supersymmetry conditions are "more fundamental" when written in terms of the dual field $\widetilde{F}_3 = d\widetilde{C}_2$, where $\widetilde{C}_2$ is the Lagrange multiplier enforcing the Bianchi identity for F_3, whose expression is modified when the gaugino condensate acquires a non-zero expectation value. Relatedly, in (the revised version of) [109] the presence of the additional localized term in (4.37c) was motivated from compatibility with the 3-form flux Bianchi identities. However, in both cases a small deviation from SU(3) structure was assumed, and, as a result, the final term in (4.37c) contained Ω instead of Ψ_-. Here we have shown that no such approximation is needed to motivate Eq. (4.37c) in generalized geometry compactifications involving non-perturbative sources. Moreover, the presence of the full Ψ_- in the localized contribution to (4.37c) will be crucial in our analysis of the effective potential carried out in Sec. (4.5) below.

4.3.3 Self-consistency and interpretation

We now show that the system of equations given in (4.37) is self-consistent, and argue that the GCG superpotential encodes all ingredients relevant to the effective action, including non-perturbative terms.

Given a solution to the modified supersymmetry conditions (4.37), we can compute the on-shell value of the GCG superpotential defined in (4.15). The procedure is analogous to what we described in Sec. 4.2.3, except that we now get two additional contributions coming from the localized terms present in the first and third supersymmetry conditions. One comes from inserting the on-shell value of $\widetilde{F}$ as given by (4.37c), similarly to (4.23), while the other comes from the integration by parts and the use of (4.37a), as was done

in (4.25). These additional contributions are given by

$$\langle W^{\rm loc}_{\rm GCG}\rangle = -4\int_{M_6}\langle\langle S\rangle\delta^{(2)}\left[\Sigma_4\right], e^{-\phi}{\rm Re}\,\Psi_+\rangle + i\int_{M_6}\langle e^{3A-\phi}\Psi_-, e^{-3A}\delta^{(0)}\left[\Sigma_4\right]{\rm Re}\left[\overline{\langle S\rangle}\Psi_-\right]\rangle\,, \tag{4.51}$$

where we have used (4.40). Taking into account the definition of the scalar delta function in (4.40), we find that the two terms in Eq. (4.51) precisely cancel each other, namely

$$\langle W^{\rm loc}_{\rm GCG}\rangle = 0\ . \tag{4.52}$$

Although this cancellation was recently obtained in an extended version of appendix A in [109], we believe that its origin has not been fully clarified. We stress that from the point of view adopted in the previous Sections it is surprising to learn that the constant μ appearing in the supersymmetry equations corresponds to the on-shell value of the GCG superpotential (4.15) *even in the presence of the gaugino condensate*. In other words, the *explicit* contributions associated with the non-zero VEV of the gaugino bilinear vanish. There are, however, *implicit* contributions since the on-shell values of the different fields – and in particular that of the cosmological constant – are indeed affected by the presence of the condensate. This is in contrast to the naive expectation according to which one should have $W\sim W_0+W_{\rm np}$, where W_0, i.e. the "flux superpotential", would correspond to $W_{\rm GCG}$ evaluated on-shell, while $W_{\rm np}$ would in turn be associated to the VEV of a putative additional non-perturbative term in the "full superpotential".

This further agrees with what one finds both in the heterotic context [128–130] and (very similarly) in type I theories, although of course in these cases the gaugino condensate is not localised. Nevertheless, it would be reassuring to understand exactly how $W_{\rm GCG}$ as defined in (4.15) is able to fully capture the backreaction associated to gaugino condensation on the localized D7-branes. In other words, we would like to understand how the non-perturbative terms in $W_{\rm VY}$ are generated, see Eq. (4.44). Although we have not been able to show this fully explicitly, we suggest a possible mechanism for how this might happen.

Let us first recall how open string degrees of freedom are captured by $W_{\rm GCG}$ in GCG compactifications, as it was discussed in Section 3.3 of [111]. Including D-branes (or O-planes) in a given setting induces a localized source term $\delta_{\rm Dp}$ in the Bianchi identities for the RR fluxes, see Eq. (4.12). Locally, we can write $\delta_{\rm Dp}=d_H\theta_{\rm Dp}$ for some $\theta_{\rm Dp}$. Then, we can formally split the physical RR fluxes according to $F=F_0+\theta_{\rm Dp}$. This distinguishes two contributions to the superpotential, namely

$$W_{\rm GCG}=\int_{M_6}\langle e^{-B}Z,G\rangle=\int_{M_6}\langle e^{-B}Z,G_0\rangle+\int_{M_6}\langle e^{-B}Z,\theta_{\rm Dp}\rangle=W_0+W_{\rm op}\,, \tag{4.53}$$

where G was defined in (4.9), while G_0 is defined analogously with the replacement $F\to F_0$. One finds that $W_{\rm op}$ computes the open-string superpotential of [131]. Conversely, W_0 is interpreted as the closed-string superpotential. We see that both of them come from $W_{\rm GCG}$.

We propose that a similar phenomenon occurs when the gaugino bilinear on a stack of D-branes acquires a non-zero expectation value. Similarly to the D-branes themselves

sourcing bulk RR fluxes, it was argued in [108] that gaugino condensates constitute sources for the geometry itself. More precisely, they source the degrees of freedom contained in the holomorphic variable Z. This is because, as reviewed above, the periods of T define the effective coupling of the gauge theory on stacks of space-filling D-branes wrapping calibrated internal cycles [120]. For instance, a generic Mink_4 vacuum involving such non-perturbative contributions should satisfy a supersymmetry condition of the form $d_H\left(e^{-B}Z\right) = \delta_{\rm np}$, where $\delta_{\rm np}$ is the localized non-perturbative current proportional to the gaugino condensate. Hence, at least locally, we can define some $\theta_{\rm np}$ for which $d_H\theta_{\rm np} = \delta_{\rm np}$. We interpret this as capturing the backreaction of the geometry, and split $e^{-B}Z = e^{-B}Z_0 + \theta_{\rm np}$. Combining this with the discussion above, the superpotential reads

$$W_{\rm GCG} = \int_{M_6} \langle e^{-B}Z, G\rangle = W_0 + W_{\rm np}\,, \tag{4.54}$$

where now $W_{\rm np}$ contains all terms proportional to the condensate, while the remaining ones are packed into W_0. The former contains two contributions, $W_{\rm np} = W_{\rm np,1} + W_{\rm np,2}$, the first of which is given by

$$W_{\rm np,1} = \int_{M_6} \langle \theta_{\rm np}, G_0\rangle = \int_{M_6} \langle d_H\theta_{\rm np}, C_0 + ie^{-\phi}\text{Re}\,\Psi_+\rangle = 2\pi i\tau S\,. \tag{4.55}$$

where in the second equality we have integrated by parts. Hence, $W_{\rm np,1}$ gives precisely the second term in the VY superpotential (4.44). We conclude that at least part of the non-perturbative terms in the superpotential are indeed generated upon evaluating $W_{\rm GCG}$ on-shell, and propose that the rest of $W_{\rm VY}$ is generated as well, arising from the combination of the two effects we have just described. Indeed, the second contribution comes from implementing the replacement $e^{-B}Z \to e^{-B}Z_0 + \theta_{\rm np}$ *inside* the open string superpotential $W_{\rm op}$, i.e. the final term in (4.53). This leads to

$$W_{\rm np,2} = \int_{M_6} \langle \theta_{\rm np}, \theta_{\rm Dp}\rangle\,. \tag{4.56}$$

Although we have not been able to evaluate this explicitly, we note that it must be proportional to both the number of branes N and the condensate S. This matches our expectation for the final term in $W_{\rm VY}$ as defined in Eq. (4.44). However, it would be nice to understand exactly how the $\log S$ factor appears.

Our proposal is further motivated by the well-studied case of geometric transitions in conifolds, which can be described in the GCG language applied to the SU(3) structure case. Consider, for concreteness, N D5-branes wrapping the compact two-cycle $\Sigma_2 = S^2$ located down the throat of the resolved conifold. At large N, one has a geometric transition where the 2-cycle shrinks to zero size, and a 3-cycle opens up, thus leading to the deformed conifold geometry [132–134]. The original D5-branes disappear, and we are left with fluxes together with a modified geometry. After the transition, we can evaluate the superpotential as

$$W = \int_{M_6} \Omega\wedge(F_3 + ie^{-\phi}dJ) = \int_{S^3}\Omega\int_{B_3}(F_3 + ie^{-\phi}dJ) - \int_{B_3}\Omega\int_{S^3}(F_3 + ie^{-\phi}dJ)\,, \tag{4.57}$$

where B_3 is the non-compact 3-cycle dual to the A-cycle S^3. Now, the integral of Ω on the resulting S_3 is set by $\langle S \rangle$, while B_3 can be thought to have a boundary given by an S_c^2 at a radial cutoff scale Λ_c. Hence, the first term on the RHS of (4.57) gives the second term in $W_{\rm VY}$, namely

$$\int_{S^3} \Omega \int_{B_3} (F_3 + ie^{-\phi} dJ) \sim S \int_{S_c^2} (C_2 + ie^{-\phi} J) = 2\pi i \tau S \,, \tag{4.58}$$

up to an overall constant, where τ corresponds to the running YM coupling. On the other hand, evaluating the second term with the help of the explicit solution presented in [50], and analogously to what was done in [132] (see also [134]) one gets

$$-\int_{B_3} \Omega \int_{S^3} (F_3 + ie^{-\phi} dJ) \sim NS \left[1 - \log\left(S/\Lambda_c^3\right)\right] , \tag{4.59}$$

which, together with (4.58) reproduces the full VY superpotential, as expected. Conversely, it was proposed in [108] that one can consider the same computation *before* the geometric transition (or more generally at smaller values of N such that the transition is not induced), so that the S^3 cycle is trivial in homology but the S^2 is not. Including the effect of gaugino condensation in an SU(3) structure background one has[10]

$$d\Omega = 2i\langle S \rangle \delta^{(4)}[\Sigma_2] \,, \quad dF_3 = -N\delta^{(4)}[\Sigma_2] \,, \tag{4.60}$$

where we have set $H = 0$. The evaluation of the GCG superpotential in this context then ammounts to a computation very similar to what we have described above in Eqs. (4.55) and (4.56). Since we expect to find the same result, namely $W_{\rm VY}$, we consider this as an example of the general mechanism proposed there.

4.4 Smearing the condensate: KKLT as a proof of concept

The modified supersymmetry conditions (4.37) imply that for localised sources a 10D description of the KKLT solution can not have SU(3) structure. For instance, this can be deduced from the 2-form component of (4.37a) [101, 107, 108]. One thus needs to consider internal manifolds with what is known as a dynamical SU(2) structure group. However, explicit models of this type are hard to construct in practice (see for instance [135]).

There are (at least) two ways of evading these difficulties. On the one hand, one could study these solutions as small perturbations (in $\langle S \rangle$, or equivalently, in the deviation from SU(3) structure) on top of the flat solution. This was attempted in [108, 109]. On the other hand, as is often done in the context of string compactifications, one can try to simplify the problem by *smearing* the source. This possibility was suggested in [107], although at the time the modified version of the third supersymmetry equation (4.37c) was not available. In this Section we reconsider this proposal. By carefully carrying out the

[10] The first equation is simply the flat limit of (4.37a) with constant warp factor and dilaton.

smearing procedure for the gaugino condensate, we find that the modified supersymmetry equations given in (4.37) lead to a remarkably simple solution. The latter is such that SU(3) structure is maintained, and turns out to be in perfect agreement with the original effective four-dimensional analysis by KKLT [4].

Let us see how this works. So far we have implicitly assumed that the gauge fluxes $\mathcal{F}$ on the worldvolume of the D7-branes vanish, which allowed us to think of the source in (4.37a) as a two-form. (Otherwise we would have needed to include higher degree forms coming from $\delta^{(2)} \wedge e^{\mathcal{F}}$). This was done also because $\mathcal{F}$ was explicitly set to zero when computing the different contributions to the gaugino mass terms in [79], which motivated our modification of the other supersymmetry condition. The appropriate smearing is given by the replacement

$$\delta^{(2)}[\Sigma_4] \to \gamma e^{2A-\phi} J \,, \qquad \gamma = -\frac{4\pi\sigma_4}{3\mathcal{N}} \,, \tag{4.61}$$

where $\mathcal{N}$ was defined in (4.17), while σ_4 keeps track of the volume of Σ_4. The numerical constant γ is fixed by requiring that the integral of the localized source and that of its smeared counterpart give the same result, namely

$$\sigma_4 = \int_{M_6} \langle e^{-\phi} \mathrm{Re}\, \Psi_+, -\delta^{(2)}[\Sigma_4] \rangle = -\int_{M_6} \langle e^{-\phi} \mathrm{Re}\, \Psi_+, \gamma e^{2A-\phi} J \rangle = -\frac{3\gamma\mathcal{N}}{4\pi} \,, \tag{4.62}$$

where we have used (4.19). The same can be done for the scalar delta function. We set

$$\delta^{(0)}[\Sigma_4] \to 3\gamma e^{2A-\phi} \tag{4.63}$$

so that, using (4.40), we get

$$\sigma_4 = -\int_{M_6} \delta^{(0)}[\Sigma_4]\, e^{-\phi} \mathrm{vol}_6 = -\frac{3\gamma\mathcal{N}}{4\pi} \,, \tag{4.64}$$

as expected. The fact that the coefficient appearing in the smearing of the scalar delta function is three times that of the localized 2-form delta is consistent with the identity [136]

$$\frac{1}{2} J \wedge J \wedge \delta^{(2)} = \frac{1}{6} J \wedge J \wedge J \delta^{(0)} \,. \tag{4.65}$$

Inserting (4.61) into Eq. (4.37a), we find that, as anticipated above, we do not need to consider an internal manifold with a more general structure group than SU(3). Indeed, the problematic two-form component now reads

$$d(e^{3A-\phi}\Psi_-|_1) = 2i(\mu - \gamma\langle S \rangle) e^{2A-\phi} J \,, \tag{4.66}$$

which is satisfied when Ψ_- has no 1-form component provided

$$\mu = \gamma \langle S \rangle \,. \tag{4.67}$$

Moreover, we get

$$d\left(e^{3A-\phi}\Omega\right) = d\left(e^{2A-\phi} J\right) = 0 \,. \tag{4.68}$$

Although this is starting to sound very similar to the configuration described in Sec. 4.2.4, there are some crucial differences. First, the extended part of the solution is now AdS_4. The presence of μ generates a non-trivial contribution in the RHS of the 6-form component of Eq. (4.37a). This reads

$$H \wedge \Omega = \frac{\mu}{3} e^{-A} J \wedge J \wedge J = -\frac{\mu}{4} e^{-A} \overline{\Omega} \wedge \Omega \,. \tag{4.69}$$

Hence, we find that an additional (0,3) component in the 3-form flux is needed.

Notably the condition (4.69) is the only place where the terms proportional to the cosmological constant in the system of equations (4.37a) do not cancel with those coming from the smeared gaugino condensate sources. Indeed, the replacement of (4.63), including the crucial factor of 3, implies that the first and third terms on the RHS of the polyform equation (4.37c) cancel exactly upon imposing (4.67). Consequently, the ISD condition on the G_3 fluxes is preserved! From (4.69) we get

$$H_{(0,3)} = -\frac{1}{2} e^{-A} \, \mathrm{Re}(\overline{\mu}\Omega) \,, \qquad F_{(0,3)} = -\frac{1}{2} e^{-\phi - A} \mathrm{Im}(\overline{\mu}\Omega) \,. \tag{4.70}$$

Note that the phase of the gaugino condensate sets the phase of the cosmological constant, which then fixes the phase of these flux terms relative to Ω. This suggests that the cycles dual to the NSNS and RR three-form fluxes are Special Lagrangian.

By using (4.68), we find that the Bianchi identities for these fluxes are satisfied iff

$$d(4A - \phi) = 0 \,, \qquad d\tau \wedge \Omega = 0 \,. \tag{4.71}$$

As the supersymmetry equations involving the relevant RR fluxes are the same as in Section 4.2.4, holomorphicity of the axio-dilaton is consistent with the 5-form component of Eq. (4.37c) in the smeared approximation. On the other hand, the corresponding 1-form implies that in order to satisfy (4.71) we must have $F_5 = 0$. The Bianchi identity for F_5 then reads

$$H_3 \wedge F_3 = \delta_{\mathrm{D3}} \,, \tag{4.72}$$

where δ_{D3} stands for any source with D3-charge, implying that these must be smeared as well. This Bianchi identity then turns into the tadpole cancellation condition.

4.4.1 Summary and effective theory

In summary, we see that not much has changed as compared to the supersymmetric Mink_4 solutions described in Section 4.2.4. Upon including the gaugino condensate sources as in (4.37) and smearing them according to Eqs. (4.61) and (4.63), we have constructed supersymmetric AdS_4 solutions which have the following characteristics:

- the internal manifold is still Kähler with an SU(3) structure group, and for constant dilaton and warp factor it is still CY,
- the axio-dilaton is still holomorphic,

- the 3-form flux G_3 is still ISD, and its primitive (2,1) component sets the mass scale for complex structure and axio-dilaton deformations,

- the 5-form flux F_5 must now vanish, which also sets $4A = \phi + \text{const}$, i.e. the Einstein frame warp factor $A_{\rm E}$ is constant,

- the value of the cosmological constant, encoded in μ, is fixed by that of the gaugino condensate $\langle S \rangle$ as in Eq. (4.67), where the coefficient γ is fixed by the consistency of the smearing approximation, and

- the 3-form flux G_3 now acquires a (0,3) piece proportional to the cosmological constant, see (4.70).

We now compare with the effective theory discussed in [4]. In terms of the corresponding on-shell superpotential, the relation between the curvature scale μ appearing in the supersymmetry conditions and the gaugino condensate derived in (4.67) becomes

$$\langle W_{\rm 4D} \rangle = \mu \mathcal{N} = -\frac{4\pi\sigma_4}{3}\langle S \rangle = -\frac{4\pi\sigma_4}{3N}\langle W_{\rm np} \rangle \,, \tag{4.73}$$

where we have used Eq. (4.61) together with $\langle W_{\rm np} \rangle = N \langle S \rangle$. This precisely reproduces the KKLT results [4].

The exact matching between our ten-dimensional smeared solution and the effective theory we have obtained is, in some sense, not entirely surprising. Indeed, it is consistent with the expectation that the latter captures the physics of the zero-modes on the internal manifold. This is exactly the sector of the theory we have restricted to when carrying out the smearing procedure. This is similar to what happens in the DGKT case in type IIA [137–139]. As in that case, we also find that a specific combination of the warp factor and the dilaton must be constant in the smeared limit.

Moreover, we also confirm the interpretation of [4]: the non-vanishing cosmological constant originates from the presence of ISD supersymmetry-breaking fluxes and non-perturbative physics captured by gaugino condensation. In our construction, their precise balance is showcased in Eq. (4.69).

On the other hand, note that by looking at the on-shell value of the (0,3) fluxes given in (4.70) we *can not* isolate a term independent of the Kähler modulus σ_4 contributing to the superpotential (this was denoted W_0 in [4]). Indeed, the condensate itself is expected to source (0,3) 3-form flux. This was shown in [108, 136], where this component was found to be completely localized on Σ_4. Upon smearing, this becomes an extra contribution to the total $G_{(0,3)}$. In this sense, one should not think about the supersymmetric AdS KKLT vacua as a two-step procedure, the first involving susy-breaking fluxes and the second introducing the gaugino condensate. These two ingredients come hand in hand in order to produce a stable supersymmetric solution.

4.4.2 Scale separation

Here we discuss whether the smeared solution allows for scale separation. For that, we consider the scalings of the various fields that leave the (smeared) supersymmetry equations invariant. There are two variables in the game: $g_s = e^{\phi}$ and R, the characteristic scale of the compactification, assuming there is only one such scale. Under these assumptions, the p-form components of the pure spinors scale as $\sim R^p$, namely

$$\Omega \sim R^3\,, \quad J \sim R^2\,, \quad \Rightarrow \quad \sigma_4 \sim \frac{R^4}{g_s}\,. \tag{4.74}$$

The coefficient γ defined in (4.61), which relates the condensate to the cosmological constant by (4.67), scales as

$$\gamma \sim \frac{\sigma_4}{\mathcal{N}} \sim \frac{g_s}{R^2}\,, \tag{4.75}$$

hence the cosmological constant scales as

$$\mu \sim \langle S \rangle \frac{g_s}{R^2}\,. \tag{4.76}$$

From the ISD condition we have $e^{-\phi} H = \widetilde{F}_3 \sim F_3$. On the other hand, (4.70) implies that the (0,3) component of H scales as

$$H_{(0,3)} \sim \mu R^3 \sim \langle S \rangle g_s R \quad \Rightarrow \quad F_{(0,3)} \sim \langle S \rangle R\,, \tag{4.77}$$

where we have assumed that $e^A \sim 1$. The (2,1) components are on the contrary not related to the gaugino condensate expectation value, so that the full G_3 flux scales as

$$G_3 = G_{(2,1)} + G_{(0,3)} \sim G_{(2,1)} + \langle S \rangle R. \tag{4.78}$$

The tadpole cancellation condition then works as follows

$$\begin{aligned} \frac{1}{24}\chi\left(X_4\right) &= N_{\mathrm{D3}} + \int_{M_6} H \wedge F_3 \\ &= N_{\mathrm{D3}} - 2ig_s \int_{M_6} G_{(2,1)} \wedge \overline{G}_{(2,1)} - 2ig_s \int_{M_6} G_{(0,3)} \wedge \overline{G}_{(0,3)} \\ &\sim N_{\mathrm{D3}} + g_s\, G_{(2,1)}^2 + g_s \langle S \rangle^2 R^2\,. \end{aligned} \tag{4.79}$$

Here $\chi(X_4)$ is the Euler characteristic of the elliptic CY 4-fold of the associated F-theory compactification, which can take values from $\mathcal{O}(100)$ to $\mathcal{O}(10^6)$ [140, 141]. One might think that by flux quantization, both contributions to the tadpole coming from the fluxes have to be of a similar order, but recall that flux quantization applies to real cycles, while these cycles are complex. In other words the split of the integer value of the flux induced charge into the two terms in (4.79) depends on the complex structure moduli.

The question is what sets the value of the gaugino condensate, which is related to the cosmological constant via (4.67). Once this relation is plugged in, the terms involving the condensate cancel with the cosmological constant ones. Consequently, geometric quantities do not rescale with $\langle S \rangle$. Such a relation comes only from the non-perturbative

superpotential, namely the relevant terms in Eq. (4.44). On-shell, this leads to an exponential behaviour of the type

$$|S| \sim e^{-\frac{1}{g_s}R^4} \ . \tag{4.80}$$

Plugging this back into the tadpole cancellation condition, we find that there is no apparent contradiction. If one can attain the regime of large R and small g_s, the contribution from the (0,3) piece is much smaller than the one from the (2,1), the latter giving the main contribution to the tadpole. Everything then is consistent with the following scalings

$$\mu \sim \frac{g_s}{R^2}\, e^{-\frac{1}{g_s}R^4} \ , \quad H_{(0,3)} \sim R\, e^{-\frac{1}{g_s}R^4} \ , \quad H_{(2,1)} \sim R^0 \ , \quad \Omega \sim R^3 \ , \quad J \sim R^2 \ , \tag{4.81}$$

which imply

$$\frac{\ell_{KK}}{\ell_{AdS}} = \mu R \sim \frac{g_s}{R}\, e^{-\frac{1}{g_s}R^4} \ . \tag{4.82}$$

Hence, at least in the smeared solution, the AdS and KK scales are exponentially separated. This can be achieved if one can find quantized fluxes such that W_0 is very small. This was achieved recently in a family of explicit examples described in [42], where the authors provide flux configurations where the (0,3) pieces vanish in the limit where the prepotential has only polynomial terms, but they are non-trivial when the corresponding exponentially small corrections are included[11].

To be precise, Eq. (4.80) is not derived from ten dimensions since the VY type superpotential (4.44) is motivated from IR physics of the 4d EFT on the D7-branes. We can only conclude that, under this assumption, there seems to be no obstruction to scale separation in our smeared solution to the ten-dimensional supersymmetry conditions, as long as an exponentially small W_0 can be realized.

4.5 Features of the localized solution

We finish by providing some insights on the main features of any putative solution to the supersymmetry conditions (4.37) with localized sources, leaving the construction of the full configuration for future work. We also settle the issue of divergences and four-fermion terms analyzed in [109, 114, 115, 117, 118].

4.5.1 Dynamic SU(2) structure and IASD fluxes

As stated in [101, 111], the modified conditions (4.37) imply that in order to find supersymmetric AdS_4 solutions sourced by a gaugino condensate on a stack of D7-branes one needs to leave the realm of SU(3) structure compactifications[12]. Nevertheless, construct-

[11] Note, however, that such construction has been criticised in [142].

[12] This is easy to see from the two-form piece of (4.37a). For SU(3) structure, Ψ_- is a three-form, therefore the left-hand side has no two-form piece, while both terms on the right hand side do. For the smeared solution these two terms cancel each other, but in the localised one this is no longer possible. Thus, a solution to this equation would require Ψ_- to contain a one-form piece as well.

ing explicit solutions with so-called "dynamic SU(2) structure" (where the alignment of the spinors η^1 and η^2 in the pure spinors (4.5) depends on the position) constitutes a considerable challenge.

Some steps in this direction were given in [108, 109, 135], see also [136]. In [135] the authors attempted to construct a solution of this type, and although the localized sources were not included explicitly, they managed to describe the region of the geometry close to the D7-branes wrapping the four-cycle at the bottom of a resolved $\mathbb{P}^2$ cone. On the other hand, [108] and [109] considered an expansion in powers of the (absolute value of the) gaugino condensate, and studied the solution at first order. In this regime, also the cosmological constant and the angle parameterising the deviation from SU(3) structure can be considered small. This approximation is expected to work best far away from the localized sources. It was argued in [101] that Kähler moduli stabilization can be understood from a consistent matching of both regimes of the solution.

As expected, the gaugino condensate not only backreacts on the geometry, but it also affects the three-form fluxes. More precisely, and consistent with our discussion around Eq. (4.10), both the non-perturbative dynamics on the D7-branes and the non-zero cosmological constant can be seen as sourcing imaginary anti-self-dual components of G_3, namely contributions that are (1,2) and (3,0) in terms of the original almost complex structure. Away from the smeared limit considered in the previous Sections, these additional components do not vanish. Furthermore, some of them diverge when approaching Σ_4. Moreover, one also obtains new localized contributions to the ISD component of type (0,3).

Although we do not construct the localized solution in this work, in the following Section we evaluate the action on-shell in such configuration, in order to compute the effective four-dimensional potential. In particular, we focus on the possible divergences arising from the corresponding terms involving the new flux and pure spinor components discussed above.

4.5.2 Cancellation of divergences

Given the presence of various terms that diverge at the location of the four-cycle Σ_4, one might worry that evaluating the full ten-dimensional supergravity action (including the D7-brane action) on the actual solution may lead to a divergent result. This issue was raised recently in [109, 114–118], without reaching a common conclusion about whether certain counterterms must be included or not. We now show that this question can be settled even without knowing the details of the localized solution. We will only assume that such solution exists, and that it satisfies the supersymmetry conditions given in Eqs. (4.37).

Let us first present the issue at hand more explicitly. Consider, for instance, the localized contribution to the (0,3) component of the G_3 flux obtained in [108]. In terms of the first order approximation considered there, we can write $G_3^{(0,3)} \sim \langle S \rangle \delta^{(0)}[\Sigma_4]\overline{\Omega}$. Upon evaluating the flux kinetic term in the supergravity action on-shell, one picks up a

contribution to the effective four dimensional potential of the form

$$\int_{M_6} G_3 \wedge \star_6 \overline{G}_3 \sim \int_{M_6} |S|^2 \left(\delta^{(0)}[\Sigma_4]\right)^2 \mathrm{vol}_6 + \cdots \,, \tag{4.83}$$

which is clearly divergent, and is furthermore difficult to interpret. Of course, this is not the only divergent term, and moreover, this is not the only type of divergence we can have: although the (1,2) component of G_3 given in [108] is not localized, it still diverges at Σ_4. It was argued recently in [118] that the different divergent terms coming from the fluxes do not cancel out. This problem must be resolved if we expect to have a consistent picture. The authors of [114, 115] have argued that this should be understood in terms of an admixture between the conjectured "perfect square" structure of the higher-order D7-brane action [117] and a *local* renormalization procedure put forward in [118]. This is in contradiction with the analysis provided in the appendix C of [109], where it was argued that no counterterms were necessary.

We resolve this conundrum by computing the on-shell action. For that, we use the expression for the four-dimensional action in generic GCG compactifications derived in [119]. For the ten-dimensional metric ansatz (4.2) the effective four-dimensional action is

$$S_{\text{eff}} = \int_{X_4} d^4x \sqrt{-g} \left(\frac{1}{2}\mathcal{N} R_4 - 2\pi V_{\text{eff}}\right) \,, \tag{4.84}$$

where R_4 is the four-dimensional scalar curvature, and the effective potential is given by the following expression

$$\begin{aligned} V_{\text{eff}} = & -\frac{1}{2}\int_{M_6} \mathrm{vol}_6 e^{4A} [\widetilde{F} - e^{-4A} d_H(e^{4A-\Phi}\mathrm{Re}\,\Psi_+)]^2 \\ & + \frac{1}{2}\int_{M_6} \mathrm{vol}_6 [d_H(e^{2A-\Phi}\mathrm{Im}\,\Psi_+)]^2 + \frac{1}{2}\int_{M_6} \mathrm{vol}_6 e^{-2A} |d_H(e^{3A-\Phi}\Psi_-)|^2 \\ & - \frac{1}{4}\int_{M_6} e^{-2A} \left(\frac{|\langle \Psi_+, d_H(e^{3A-\Phi}\Psi_-)\rangle|^2}{\mathrm{vol}_6} + \frac{|\langle \overline{\Psi}_+, d_H(e^{3A-\Phi}\Psi_-)\rangle|^2}{\mathrm{vol}_6}\right) \\ & + \sum_{i \in loc.sources} \tau_i \int_{M_6} e^{4A-\Phi} \left(\mathrm{vol}_6 \rho_i^{\text{loc}} - \langle \mathrm{Re}\,\Psi_+, j_i\rangle\right) \\ & - 4\int_{M_6} \langle e^{4A-\Phi}\mathrm{Re}\,\Psi_+ - C^{el}, d_H F + j_{\text{tot}}\rangle \,. \end{aligned} \tag{4.85}$$

Here, for a given polyform A we have $[A]^2\,\mathrm{vol}_6 = A \wedge *_6 A$ and $|A|^2\,\mathrm{vol}_6 = A \wedge *_6 \overline{A}$. On the other hand, for the expressions in the third line one should first compute the 6-form given by the Mukai pairing, and then square only the coefficient in front of the volume form. We consider supersymmetric solutions for which the Bianchi Identities are satisfied and the relevant cycles are calibrated. Hence, the last two lines in Eq. (4.85) vanish identically.

Let us briefly compute this action on-shell in the absence of gaugino condensates, and verify that by using the supersymmetry conditions (4.1), one obtains the expected cosmological constant term. Upon using (4.1c) in the first term of (4.85), the integrand becomes

$$\begin{aligned} e^{4A}[\widetilde{F} - e^{-4A} d_H(e^{4A-\Phi}\mathrm{Re}\,\Psi_+)]^2 \mathrm{vol}_6 &= -\frac{1}{2} e^{4A} \left[-3e^{-A-\phi}\mathrm{Re}\,[\overline{\mu}\,\Psi_-]\right]^2 \mathrm{vol}_6 \\ &= 18\, e^{2A-2\phi} |\mu|^2 \mathrm{vol}_6 \,, \end{aligned} \tag{4.86}$$

where we used the self-duality and normalization of the pure spinors, given respectively in Eqs. (4.6) and (4.19). For the second line of (4.85), the first term vanishes due to (4.1a), whereas using (4.1b) the second one gives

$$e^{-2A}|d_H(e^{3A-\Phi}\Psi_-)|^2\,\mathrm{vol}_6 = \frac{1}{2}e^{-2A}|2i\mu e^{2A-\phi}\mathrm{Im}\,\Psi_+|^2 = 8e^{2A-2\phi}|\mu|^2\mathrm{vol}_6\,. \tag{4.87}$$

Finally, it is not hard to see that, employing (4.1a), the third line contributes

$$-\frac{1}{4}e^{-2A}\left(\frac{|\langle\Psi_+, 2ie^{2A-\phi}\mathrm{Im}\,\Psi_+\rangle|^2}{\mathrm{vol}_6} + \frac{|\langle\overline{\Psi}_+, 2ie^{2A-\phi}\mathrm{Im}\,\Psi_+\rangle|^2}{\mathrm{vol}_6}\right) = -32|\mu|^2e^{2A-2\phi}\mathrm{vol}_6\,. \tag{4.88}$$

Putting everything together, we get

$$V_{\rm eff} = -6|\mu|^2\int_{M_6} e^{2A-2\phi}\mathrm{vol}_6 \quad\Rightarrow\quad 2\pi V_{\rm eff} = \Lambda\mathcal{N} \tag{4.89}$$

as expected.

We now include the effect of the localized gaugino condensate. Besides the same three terms proportional to $|\mu|^2$, using the modified supersymmetry conditions (4.37) in the same way as above, new terms proportional to either $\delta^{(0)}$ or $(\delta^{(0)})^2$ will be generated. More explicitly, the on-shell value of the contributions to the effective potential contained in Eq. (4.85) now gives

$$\begin{aligned} V_{\rm eff}^{\rm bulk} = &-\frac{1}{2}\int_{M_6}\mathrm{vol}_6\left[-3e^{-A-\phi}\mathrm{Re}\,(\overline{\mu}\Psi_-) + e^{-3A}\delta^{(0)}\,[\Sigma_4]\,\mathrm{Re}\,\left[\overline{\langle S\rangle}\Psi_-\right]\right]^2 \\ &+\frac{1}{2}\int_{M_6}\mathrm{vol}_6 e^{-2A}\left|2i\mu e^{2A-\phi}\mathrm{Im}\,\Psi_+ - 2i\langle S\rangle\delta^{(2)}\,[\Sigma_4]\right|^2 \\ &-\frac{1}{4}\int_{M_6}e^{-2A}\left(\frac{|\langle\Psi_+, 2i\mu e^{2A-\phi}\mathrm{Im}\,\Psi_+ - 2i\langle S\rangle\delta^{(2)}\,[\Sigma_4]\rangle|^2}{\mathrm{vol}_6}\right. \\ &\qquad\left.+\frac{|\langle\overline{\Psi}_+, 2i\mu e^{2A-\phi}\mathrm{Im}\,\Psi_+ - 2i\langle S\rangle\delta^{(2)}\,[\Sigma_4]\rangle|^2}{\mathrm{vol}_6}\right). \end{aligned} \tag{4.90}$$

This expression can be evaluated using the properties given in Eqs. (4.19), (4.6), (4.24), together with the definitions (4.38) and (4.40). The contributions to the different type of terms we obtain for the integrand of (4.90) are summarised in Table 4.1. There, "1st",

	$\lvert\mu\rvert^2e^{2A-2\phi}\mathrm{vol}_6$	$\delta^{(0)}\,[\Sigma_4]\,\mathrm{Re}\,[\overline{\mu}S]\,e^{-\phi}\mathrm{vol}_6$	$\left(\delta^{(0)}\,[\Sigma_4]\right)^2\lvert S\rvert^2e^{-2A}\mathrm{vol}_6$
1st	18	-12	2
2nd	8	-4	2/3
3rd	-32	16	-2
Total	**-6**	**0**	**2/3**

Table 4.1: The different contributions to the bulk on-shell action of the terms in the first three lines of (4.90).

"2nd", and "3rd" indicate the contributions from the first, second, and third lines on the RHS of Eq. (4.90), respectively, while the coefficients in each column give the contributions to each of the different types of terms. For instance, the numbers 18, 8, and -32 in the first column are precisely the original contributions obtained in Eqs. (4.86)-(4.88).

Hence, we find that, in the on-shell bulk action, the terms proportional to $\delta^{(0)}\left[\Sigma_4\right]$ cancel out. However, this does not happen with the divergent contributions, i.e. those that come with a factor $\left(\delta^{(0)}\left[\Sigma_4\right]\right)^2$. These are both unexpected results in some sense. The cancellation of terms with a single delta function in the bulk action is unexpected as one should also consider the brane action when the gaugino condensate acquires a non-trivial expectation value, which evaluated on-shell gives a localised contribution with a single delta. This should somehow be cancelled in order to get the desired result. On the other hand, we will see that, at least at quadratic level in the gauginos, the D-brane action does not contain terms with a square of delta functions, which can only be cancelled by counterterms, as put forward in [118]. We now discuss these two issues separately.

The brane action contains the gaugino mass-term, whose off-shell form was computed in [79], and is given in Eqs. (4.47) and (4.48). We now evaluate this on-shell. As we already noted, the integrand in (4.48) is proportional to that of the superpotential (4.15). Hence, we can use directly Eq. (4.28). This holds even when using the modified supersymmetry conditions (4.37) instead of the original ones in Eq. (4.1) because the localized contributions cancel each other, see the discussion around (4.51). The gaugino mass contribution to the effective potential is therefore

$$V_{\text{eff}}^{\lambda\lambda} = -\frac{1}{4\pi}\left(m_\lambda \overline{\lambda}_- \lambda_+ + c.c.\right) = -4\int_{M_6} \delta^{(0)}\left[\Sigma_4\right] e^{-\phi}\text{Re}\left[\mu\overline{\langle S\rangle}\right]\text{vol}_6\,, \tag{4.91}$$

where we used that $\overline{\lambda}_-\lambda_+ = i16\pi^2\overline{S}$. Note that having a non-zero mass for the gaugino does not contradict the fact that the solution is supersymmetric since, in this context, the gaugino bilinear itself has acquired a non-trivial expectation value[13].

The D-brane action also contains higher-order terms such as terms quartic in the gauginos. These are, however, much more difficult to obtain in general, see for instance the recent computation in [143] of four-fermion terms in the M2 action. Moreover, there are possible counterterms. Here we will be agnostic about how all these terms look like off-shell. Nevertheless, we note that consistency of the overall procedure demands that adding up all contributions to the on-shell action gives only the correct cosmological constant term, as in Eq. (4.89).

Combining our results given in Eq. (4.91) and in Table 4.1, we conclude that all terms not included in our analysis above must provide two types of contributions. We find that a divergent contribution coming from the aforementioned counterterms must be included in order to cancel the terms proportional to $\left(\delta^{(0)}\left[\Sigma_4\right]\right)^2$ in the third column of Table

[13] In the limit where $\langle S\rangle = 0$ we recover solutions with $\mu = 0$, for which the mass term indeed vanishes, as expected. Higher order terms in the action would be necessary to compute the effective mass of the fermion fluctuations around the KKLT-AdS vacuum. As discussed in the main text, for the D7-brane these are difficult to compute.

4.1. Finally, four-fermion terms in the D7-brane action (and possibly finite contributions coming from the counterterms) should add up to

$$V_{\text{eff}}^{\lambda^4+\text{c.t.}} = \frac{\gamma}{64\pi^4}\int_{M_6}\delta^{(0)}\left[\Sigma_4\right]e^{-\phi}|\lambda\lambda|^2\text{vol}_6\,, \tag{4.92}$$

which, using (4.67), cancels exactly (4.91). We note here that this term is somewhat similar to the four-fermion term considered in [109].

Putting everything together, the effective potential in (4.84) should be

$$V_{\text{eff}}^{\text{bulk}} + V_{\text{eff}}^{\lambda\lambda} + \frac{\gamma}{64\pi^4}\int_{M_6}\delta^{(0)}\left[\Sigma_4\right]e^{-\phi}|\lambda\lambda|^2\text{vol}_6 - \frac{2}{3}\int_{M_6}e^{-2A}|\langle S\rangle|^2(\delta^{(0)}\left[\Sigma_4\right])^2\text{vol}_6\,, \tag{4.93}$$

where $V_{\text{eff}}^{\text{bulk}}$ is given by the "Total" row in Table 1, and $V_{\text{eff}}^{\lambda\lambda}$ is given in (4.91). In particular, the numerical coefficients in (4.93) are such that no "perfect square" structure arises.

4.6 Conclusions

In this Chapter we considered the ten-dimensional description of KKLT-AdS vacua. For this, we argued that the set of supersymmetry conditions in Eqs. (4.37) describes $\mathcal{N}=1$ generalized complex geometry compactifications of type II superstring theories, including the effects of gaugino condensates on stacks of D-branes wrapping calibrated cycles of the internal manifold. In the type IIB setting, such non-perturbative contributions provide a mechanism for the stabilization of Kähler moduli, while the complex structure and axio-dilaton moduli acquire masses generated by 3-form fluxes[14].

The gaugino condensate terms in Eqs. (4.37) combine several ingredients discussed in the literature in one form or another. Eq. (4.37a) was put forward in [108, 111] and later discussed in [101]. It can be understood as an F-flatness condition for the (complexified) volume of the cycle wrapped by the D-branes undergoing gaugino condensation, if one takes into account the dependence of the Veneziano-Yankielowicz superpotential (4.44) on this modulus, which sets the value of the corresponding effective gauge coupling. On the other hand, the localized contribution in Eq. (4.37c) constitutes a generalization of the proposals of [108, 109]. We have shown that it generates the correct additional term in the flux equations of motion arising when the gaugino bilinear on the branes has a non-trivial expectation value. The coupling comes from the gaugino mass term, whose precise form was obtained in [79].

As established in [101, 108, 111], a localized source with a gaugino condensate requires going beyond internal manifolds with SU(3) structure. Appropriate configurations with a more general structure group are, however, difficult to construct in practice. We have by-passed this issue by smearing the D7-branes along the internal directions. In this way, we focused on zero modes on the internal manifold, which provide the relevant ingredients for the low-energy effective four-dimensional theory.

[14] The expectation that fluxes can give masses to a large number of complex structure moduli has been challenged though by the so-called Tadpole conjecture [68].

We have provided an explicit ten-dimensional solution in the smeared approximation, where the extended directions span an AdS_4 space, while the internal manifold remains (conformally) CY. Moreover, the three-form flux is still imaginary self-dual, but it contains a crucial contribution of type (0,3), proportional to the cosmological constant. We have also shown that the latter is set by the expectation value of the gaugino condensate and the stabilized four-cycle volume. This precisely reproduces the results of [4]. Importantly, we emphasize that given that the gaugino condensate generates (0,3) fluxes (together with the cosmological constant) while keeping supersymmetry, one should not think of the AdS vacuum as the result of a two-step procedure, the first involving supersymmetry-breaking fluxes in a Minkowski solution, and the second one adding the gaugino condensate. Clearing this misconception furthermore avoids the criticism of [41] regarding adding non-perturbative effects on top of a supersymmetry-breaking, rolling solution. This perspective was also advocated in [142].

We have also considered the issue of scale separation in this context. At least at the level of our smeared solution, we have found no obstruction for an exponentially small cosmological constant generated by the non-perturbative effects, while retaining a large internal volume. This holds as long as the fluxes can be combined in such a way that they result in an exponentially small (0,3) component. Explicit examples were provided recently in [42, 43, 104, 105]. These examples were however questioned in [142], where the authors argue that the cycles dual to the corresponding fluxes can not have a Special Lagrangian representative, and thus no dual brane domain-wall interpretation. We found, in the smeared limit, that the (0,3) fluxes are given by (4.69), suggesting that their dual cycles are indeed Special Lagrangian.

Finally, we have discussed the localized solution, focusing in particular on the issue of divergences arising in the on-shell evaluation of the ten-dimensional action that gives the effective potential of the four-dimensional theory. We have shown that this can be evaluated *without knowing the details of the localized solution*. Indeed, assuming that such localized solution exists, we have evaluated the expression for the effective potential in terms of derivatives of the pure spinors given in [119], using only the supersymmetry conditions with gaugino condensates. We find that no "perfect square" structure is present, contrary to the expectation in [114, 115, 117], based on four-dimensional supergravity, as well as on heterotic and type I actions. Furthermore, divergences coming from squared delta functions do arise, indicating the need for a local counterterm. In this sense, our results suggest a structure similar to what was discussed recently in [118], as opposed to the conclusions of [109]. Although we can precisely establish what the counterterm gives on-shell, its off-shell form remains an open question. It would be very interesting to figure out what kind of off-shell terms in the brane action would contribute to the on-shell expression we found.

Part II

Black Hole Microstates in String Theory

Chapter 5

Resolving Black-Hole Microstructure with New Momentum Carriers

5.1 Introduction

One of the remarkable achievements of string theory is that it can provide a microscopic description of black-hole entropy. It was found that, at vanishing string coupling, different string/brane configurations could reproduce the Bekenstein-Hawking entropy of the corresponding black hole [10, 12]. The black-hole geometry, and its horizon, then emerge as the string coupling, and hence Newton's constant, G_N, becomes finite. Indeed, the horizon grows with G_N [144–146], but because gravity generically compresses matter, it was believed that all the perturbative string states would collapse behind a horizon. Thus the perturbative microstates, whose counting gives the black-hole entropy, would not be visible once gravity takes effect.

Insights from brane physics show that this picture is too naïve. The tension of D-branes and NS-branes decreases as the coupling increases, and so adding momentum excitations causes them to spread in directions transverse to their world-volume. Indeed, it was noted in [147] that three-charge brane configurations carrying momentum would grow with G_N at the same rate as the black-hole horizon. It was then found that three-charge horizonless geometries supported by topological fluxes have the same behavior [33, 34, 148]. Thus was born the Microstate Geometry (MG) Programme in which one constructs *smooth, horizonless geometries* that approximate the classical black-hole solution everywhere except at the horizon scale, where MG's end in a smooth, horizonless cap.

Microstate Geometries are part of a larger framework, known as the *Fuzzball Programme*. The defining ideal of this programme is that individual black-hole microstates, generically referred to as fuzzballs, must be horizonless because horizons imply entropy and give rise to information loss [149, 150]. Fuzzballs have the same mass, charge and angular momentum as a given black hole and can be arbitrarily quantum and arbitrarily strongly curved. They describe pure states of the black hole and, if a holographic description is available, are dual to pure states of the CFT that can be used to account for the black-hole entropy. Microstate Geometries fit in this paradigm as the string-theory

fuzzballs that are sufficiently coherent as to become well approximated by smooth solutions of supergravity.

There also exist fuzzballs that are not smooth supergravity solutions but can be described using other well-defined limits of string theory. Indeed, this led to the definition of a *Microstate Solution*, [32], which is a horizonless solution of supergravity, or a horizonless, physical limit of a supergravity solution, that has the same mass, charge and angular momentum as a given black hole. Microstate solutions are allowed to have singularities that either correspond to brane sources, or can be patch-wise dualized into a smooth solution. In this Chapter we will refine this classification further to distinguish microstate solutions corresponding to pure states from *Degenerate Microstate Solutions*, which correspond to a limited family of microstates.

It is important to emphasize that Fuzzballs are all, by definition, horizonless, regardless of whether they can be described within supergravity. In this paradigm, horizons arise only as a consequence of averaging over microstates and are thus necessarily related to ensembles of such states. This is what leads to the entropy-area relation. But if pure states correspond to horizonless microstates, then a solution with a horizon should not describe the physics of *any* pure state of the system and should not be holographically related to any pure state of the dual CFT.[1]

The purpose of this Chapter is to make some steps towards the resolution of what appears to be a counterexample to the Fuzzball paradigm: the possibility that some pure CFT states are dual to a supergravity solution with a horizon. The putative counterexample comes from a singular limit of a class of Microstate Geometries known as *superstrata.*

Superstrata are horizonless solutions that have the same charges as a D1-D5-P supersymmetric black hole. They are, perhaps, the most analyzed and well-studied of all MG's [24–26, 152–168], and the holographic dictionary for these geometries is now well-established [20, 169–176]. The corresponding black holes have an infinitely-long AdS_2 throat, but in superstrata, this throat is capped off at a large but finite depth, which is inversely proportional to a parameter, a, that controls the angular momentum, and the spatial extent of the configuration. The momentum charge of a superstratum is carried by flux excitations whose Fourier amplitudes give an additional set of parameters, b_n. The problematic limit, and putative counterexample, arises as one takes $a \to 0$.

These parameters have a well-understood interpretation in the dual D1-D5 CFT [173]. The CFT states dual to superstrata are constructed starting from RR-ground states that are usually described as having $(+,+)$ strands and $(0,0)$ strands.[2] The former carry angular momentum but no momentum, and their number is proportional to a^2. The $(0,0)$ strands have vanishing angular momentum but, in the superstratum, carry momentum excitations with a quantum number, n. The number of such excited strands is proportional

[1] This has only been shown so far for (0+1)-dimensional CFT's dual to asymptotically-AdS_2 spacetimes [151].

[2] For explanation of this notation, see, for example, [24, 177].

to b_n^2 and the total momentum charge is given by:

$$Q_P \;\sim\; \sum_{n=1}^{\infty} n\, b_n^2 \,. \tag{5.1}$$

Requiring the superstrata to be smooth and free of closed time-like curves imposes a constraint of the schematic form:

$$\frac{Q_1 Q_5}{R_y^2} \;=\; a^2 \;+\; \frac{1}{2}\sum_{n=1}^{\infty} b_n^2 \,, \tag{5.2}$$

where Q_1 and Q_5 are the supergravity D1 and D5-brane charges and R_y is the asymptotic radius of the common D1-D5 direction. The important point is that adding more momentum-carrying modes (by increasing the b_n's) makes a smaller, so the AdS_2 throat becomes longer, capping off at higher and higher red-shifts. In the $a \to 0$ limit, the cap moves to infinite redshift and the superstratum solution appears to become identical to the classical extremal D1-D5-P black hole.

From the perspective of the dictionary to the dual CFT, this limit appears well-defined and corresponds to a pure state with only $(0,0)$ strands. Thus it appears that as one moves in the space of CFT states dual to superstrata, one encounters some pure states whose bulk dual has a horizon. This violates the basic principle of the Fuzzball/MG programme: Pure states should not be dual to a configuration that has a horizon.

As we discuss in Section 5.2, the appearance of a horizon is explained by noting that in the D1-D5-P frame, the standard superstratum construction not only restricts the momentum-carrying excitations, but also involves a smearing operation. This smearing preserves the details of the microstructure only when $a \neq 0$, while in the $a \to 0$ limit it averages over distinct momentum-carrying configurations and this gives rise to a solution with a horizon. If one avoids this smearing, and takes into account the degrees of freedom this smearing erases, the geometry remains horizonless even as $a \to 0$.

In this Chapter we show how this can be achieved by constructing a new class of three-charge solutions with vanishing horizon area that go beyond the standard superstratum construction by incorporating additional momentum-carrying excitations. We do this by working in the Type IIA F1-NS5-P duality frame, and the new momentum carriers that can resolve the microstructure are D0-brane and D4-brane charge densities that vary along the common F1-NS5 direction. These excitations have the important property that, unlike all other microstate geometries, they carry momentum *without* expanding the branes in directions transverse to their world-volume. Hence, one can think of them as giving rise to a longitudinally polarized momentum wave on branes that remain localized at a single point in the transverse directions, and do not break the rotational $SO(4)$ symmetry of the black-hole solution.

Since duality transformations preserve degrees of freedom while encoding them in different ways, our Type IIA F1-NS5-P supergravity solutions must have counterparts in the D1-D5-P frame. However, to get from one frame to the other, one must perform a T-duality along the common F1-NS5 direction, and the solutions we construct depend

explicitly on this direction. As a result, our Type IIA supergravity solutions become configurations involving a coherent set of higher Kaluza-Klein modes, and thus cannot be described as D1-D5-P solutions in Type IIB supergravity.[3]

The main result of this Chapter is the solution given in equation (5.14): It represents a family of three-charge F1-NS5-P solutions with D0 and D4 densities and no macroscopic horizon. Globally, this solution preserves the four supercharges of the corresponding three-charge black hole. However, if we zoom in at a fixed location along the F1 and NS5-branes, we find that the configuration *locally* preserves eight supercharges. In this limit, the local D0 and D4 densities are approximately constant and the solution preserves eight Killing spinors, four of which are identical to those of the F1-NS5-P black hole. Hence, near the brane sources the solution behaves locally like a two-charge system with a vanishing horizon area.

It is important to emphasize that the solution presented here is a singular brane configuration with vanishing horizon area, and its role as a fuzzball needs clarification. As originally conceived, a *Microstate Solution* is a horizonless, but singular, brane configuration that corresponds to a black-hole microstate that can be fully resolved in string theory. We need to broaden this idea to include *Degenerate Microstate Solutions*. Such an object is defined to be a singular supergravity solution with the following properties:

- It must have vanishing horizon area.
- The source must correspond to a well-defined family of branes.
- The microstructure of the brane source can be revealed, and counted, through standard string theory methods.
- There must be geometric deformations, or transitions, that can resolve the solution into microstate solutions or microstate geometries.

One of the features of microstate solutions, and microstate geometries, is that if one zooms into their cores, the underlying geometric elements are "locally primitive," which means that they locally preserve 16 supercharges (this observation will lead us to introduce *Themelia* in Chapter 7). Taken as a whole, though, the complete solution preserves only a subset of these supercharges. By contrast, the cores of degenerate microstate solutions will typically preserve only 8 supercharges. This is too much supersymmetry for the configuration to generate a horizon, and so the underlying structure can still be accessed and probed by string theory. However, the reduction from 16 supercharges to 8 supercharges reflects the fact that such solutions still correspond to a family of individual microstates, but this family is too small to generate a horizon in supergravity.

In the past, the configurations we are classifying as degenerate microstate solutions have sometimes been said to have "small" (string-scale) horizons because they represent

[3]It is also interesting to note that the exact same phenomenon happens when one tries to dualize D1-D5-P superstrata that depend on the common D1-D5 direction to the IIA F1-NS5-P duality frame we consider: the smooth geometries are dualized into microstate solutions that contain excited towers of KK modes and are not describable in supergravity.

stringy ensembles of states. We prefer the defining ideas of degenerate microstate solutions because they accentuate the accessibility of the microstructure to stringy analysis and geometric resolutions, while the cloaking of such things in horizons is, once again, just code for ensemble averaging of microstructure.

The archetype of a degenerate microstate solution is, of course, the pure D1-D5 solution, whose microstructure has been throughly understood in string theory [16, 18, 178]. As we will discuss, the degenerate microstate solutions that we will construct in this Chapter are, at their core, equivalent to D1-D5 degenerate microstate solutions. In subsequent work we plan to explore geometric transitions that will resolve these degenerate microstate solutions into microstate solutions and microstate geometries.

In Section 5.2 we describe the general features of the standard superstratum construction and how it neglects some degrees of freedom and necessarily results in smearing in the $a \to 0$ limit. We also discuss the supersymmetries preserved by the solution. In Section 5.3 we describe the construction of the eight-supercharge NS5 solution with D0-D4 charges that carry momentum without transverse fluctuations. We then add coherent F1-string excitations to this system, and obtain the complete supergravity description. It is this microstate solution that provides the resolution of the $a \to 0$ limit: a solution with black-hole charges, vanishing horizon area, and SO(4) symmetry.

In Section 5.4 we analyze this new geometry and compare it to the three-charge black-hole solution. Section 5.5 contains a discussion of our results and an outline of possible future research. Some of the details of the construction that are omitted in Section 5.3 are presented in Appendix A. In Appendix B we collect some of the conventions used throughout this Chapter.

5.2 Momentum carriers on superstrata

In five dimensions, a BPS black hole only has a finite-sized horizon if it has three charges and thus preserves four supercharges ($\frac{1}{8}$-BPS). The corresponding microstate geometries and microstate solutions must globally preserve the same supercharges, however their *cores* can have more supersymmetries *locally.* Indeed, their fundamental building blocks are locally *primitive* and have 16 supercharges [30], but have fewer supersymmetries when considered globally because their shapes and dipolar charge distributions break the supercharges down to the universal subset that is common to the entire configuration.

Since microstate geometries and microstate solutions are supported by sources that have locally more supersymmetries than the black hole, they do not have in general an event horizon. Indeed, the existence of superstrata was originally conjectured based on a double-bubbled geometric transition of the D1-D5 system [30]. Specifically, if one starts with a stack of D1-branes and adds a momentum wave, then the configuration is globally $\frac{1}{4}$-BPS but locally $\frac{1}{2}$-BPS. If one then combines a D1-brane with a profile carrying a momentum wave with a D5-brane with the same profile, the system is globally $\frac{1}{8}$-BPS but locally $\frac{1}{4}$-BPS. By adding angular momentum and a KKM dipole charge, one can make

a geometric transition to a momentum carrying object that is globally $\frac{1}{8}$-BPS but locally $\frac{1}{2}$-BPS. The result is a superstratum [24].

To make a smooth geometry, the "special direction" of the KKM must coincide with the common D1-D5 direction, which we parameterize with the coordinate v.[4] However, the standard Kaluza-Klein Monopole (KKM) geometry must be v-independent,[5] and this conflicts with the addition of momentum excitations, which necessarily depend on v. Indeed, the v-circle pinches off at the KKM location, and so one cannot source v-dependent fluctuations on the KKM locus without creating a singularity.

This difficulty was resolved in [179] and is best understood by starting from the standard, maximally-spinning supertube [14, 180]. One takes the D1-D5 system and adds a KKM dipole and angular momentum so that the supertube wraps a circle in an $\mathbb{R}^2$ of the $\mathbb{R}^4$ transverse space. The angle along this circle is denoted by ϕ, and the solution is independent of (ϕ, v). This describes the maximally-spinning $\frac{1}{4}$-BPS supertube and it corresponds to a coherent superposition of RR ground states in the CFT consisting of only $(+,+)$ strands. One can now allow the density of D1- and D5-branes to vary *along the ϕ direction of the supertube*. In terms of the standard mode numbers inherent in superstrata, (k, m, n), this density fluctuation corresponds to a $(k, 0, 0)$ excitation. The result is still a $\frac{1}{4}$-BPS supertube, and it is still v-independent, but it is now a mixture of $(+,+)$ and $(0,0)$ strands (of length k). The numbers of such strands is determined by Fourier coefficients, a and $b_{k,m=0,n=0}$.

In superstrata one can think of the $(0,0)$ strands (or the ϕ-dependent density fluctuations in the $(k,0,0)$ solution) as the "medium" that carries the momentum, and the solutions where these modes are excited have generic values of (k, m, n). One necessarily has $k > 0$ because the momentum is being carried by the density fluctuations around ϕ. As discussed in detail in [179], the v-dependent fluctuations are not, and cannot be, sourced on the original supertube locus: these fluctuations are delocalized in the fluxes and geometry of the topologically-non-trivial three-cycles of the D1-D5-KKM solution.

The $a \to 0$ limit of superstrata is motivated by the desire to construct solutions with vanishing angular momentum that resemble a black hole with arbitrary precision.[6] In view of the previous discussion it is now evident just how pathological this limit is for standard superstrata. Namely, by keeping the UV unchanged and taking $a \to 0$, one is collapsing

[4] To be more precise, the common D1-D5 direction is described by a periodic coordinate y, while v is a null coordinate: see equation (5.5). Supersymmetry requires the solution to be independent of the other null coordinate, u, and one can think of the latter as describing "time" while v denotes the "spatial" coordinate (see also [152] for a more careful discussion).

[5] One can obviate this difficulty by allowing higher Kaluza-Klein modes in the monopole, but this takes us outside of Type-IIB supergravity.

[6] As explained in [151], there are two such limits. In the first limit, one keeps finite the energy of asymptotic observers and the asymptotic structure of spacetime, and the AdS_2 throat becomes longer and longer and its cap becomes deeper and deeper, approaching the infinite throat of the supersymmetric black hole. In the second limit, one keeps finite the energy of an observer in the cap, and in this limit the cap remains fixed, while the asymptotic structure of the solution becomes AdS_2 times a compact space. This discussion is about the first limit.

both the supertube that defines the momentum carriers and the topological bubble that supports the momentum-carrying fluxes. The end result is to push the KKM locus and the center of the $\mathbb{R}^4$ base-space of the solution to a point, while keeping the momentum fixed. Since the KKM forces v-independence, the momentum charge only survives in this limit because the momentum carriers are smeared along the v-circle and as a result the geometry develops a horizon. Hence, the standard superstratum momentum carriers, which are v-dependent and have polarizations in the $\mathbb{R}^4$ directions are crushed to a point in the transverse space and smeared along the v-direction in the $a \to 0$ limit.

In the dual CFT picture, the $a \to 0$ limit of various superstratum solutions corresponds to various states that only have $(0,0)$ but no $(+,+)$ strands, and hence have no angular momentum. Hence, these pure states appear naively to be dual to a bulk solution with a horizon. Furthermore, the bulk information that distinguishes these pure states from one another appears to vanish in this limit. Thus in the limit of vanishing angular momentum, the superstratum holographic dictionary appears to break down. In order to solve this puzzle, and the apparent loss of information in the holographic dictionary, we need to consider all possible momentum carriers of the system, and, in particular, find the modes that carry momentum and have vanishing angular momentum in the space-time. The simplest duality frame in which one can build these modes is the Type IIA frame in which the three charges of the black hole correspond to F1 strings, NS5-branes and momentum.[7]

One can relate this frame very easily to the normal IIB D1-D5-P frame by an S-duality to a Type IIB F1-NS5-P system, followed by a T-duality. In this duality frame, the NS5-brane can carry momentum along the common F1-NS5 direction by the excitation of the internal scalar field of the Type IIA NS5-brane. This corresponds in supergravity to turning on fluctuating Ramond-Ramond fields C_1 and C_3, that can be thought of as coming from D0- and D4-brane density fluctuations inside the NS5-brane. These density fluctuations can be chosen to integrate to zero, so that the total solution only has F1, NS5 and P charge. These momentum-carrying excitations have vanishing angular momentum in the transverse $\mathbb{R}^4$ space and are well-defined even in the $a \to 0$ limit.

The fact that adding D0-D4 dipole charges to the F1-NS5 system is natural is perhaps best understood by going to the M-theory frame. Consider Type IIA theory on $\mathbb{R}^{1,4} \times S^1(v) \times T^4$ and denote the M-theory circle by $S^1(x_{10})$. The F1-NS5 system lifts to a configuration of M5 and M2-branes, where the M5-branes wrap $T^4 \times S^1(v)$ and the M2-branes wrap $S^1(x_{10}) \times S^1(v)$ (see Fig. 5.1). The D0-D4 densities carry momentum as a longitudinal wave along the common direction in the F1-NS5 system. In M-theory the NS5-D0-D4-P subsystem uplifts to a momentum-carrying wave on the M5-brane, whose transverse polarization is strictly in the M-theory direction. This M5-brane has 8 supersymmetries, but if one zooms near the profile at a specific location one finds an M5-brane with orthogonal momentum, which preservers 16 supercharges. When one

[7] It is also possible to add such fluctuations in the D1-D5-P duality frame, but these correspond to fluctuations of brane and string densities that wrap partially the T^4 compact space, and hence break the isotropy of the torus. The advantage of the IIA F1-NS5-P frame is that these modes preserve the T^4 isotropy.

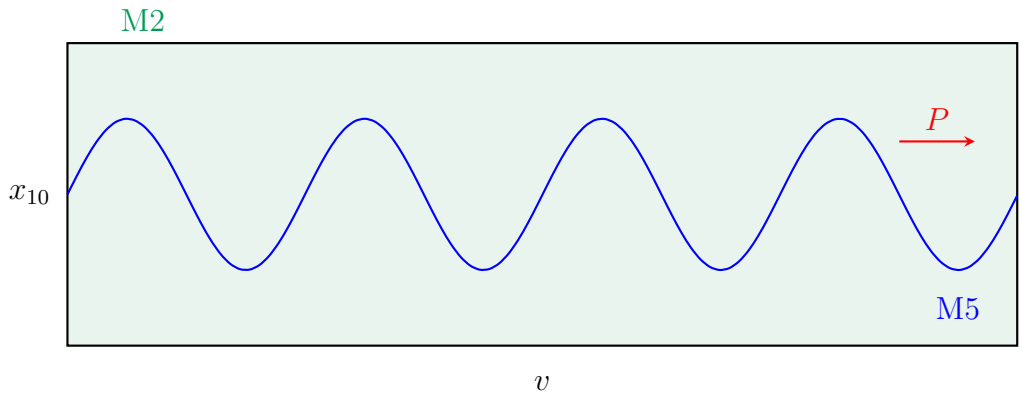

Figure 5.1: Initial configuration in the M-theory frame: M2-branes (green) are wrapping the $S^1(v) \times S^1(x_{10})$ circles, while the M5-branes (blue) wrap the $S^1(v) \times T^4$ (T^4 is not pictured) and have a wave carrying a momentum, P, along v. The M5-branes with a momentum wave have a non-trivial profile in the $S^1(v) \times S^1(x_{10})$ plane, and hence have locally non-zero M5 charges parallel to the x_{10} direction, as well as non-trivial momentum along x_{10}. When one compactifies this M-theory solution to Type IIA along x_{10}, these charge components become D4 and D0 charge densities respectively.

reduces this configuration along the x_{10} direction to ten-dimensional Type IIA theory, the momentum and M5-charge polarized along the x_{10} become D0 and D4 charge densities.

This leads to the starting point of our analysis: Our aim is to construct three-charge Type IIA supergravity solutions with F1-NS5-P charges, where the momentum is carried by fluctuating D0-D4 density waves. In contrast to all the three-charge horizonless solutions constructed so far, our solutions are $SO(4)$ singlets under rotations on the $\mathbb{R}^4$ base space, exactly as the black hole. Furthermore, these solutions are $\frac{1}{8}$-BPS (4 supercharges) globally, but $\frac{1}{4}$-BPS (8 supercharges) locally, and hence have a vanishing horizon area. But as we explained earlier, the result of our analysis will be a new family of degenerate microstate solutions.

5.3 Construction of the new three-charge solution

Our construction starts from the well-known solution for the F1-P system in Type IIB supergravity in ten dimensions. We then use a series of S-dualities and T-dualities (whose details are presented in Appendix A) to arrive at the geometry corresponding to the two-charge NS5-P system with local D0-D4 charges. We then add a fundamental string charge to this system. We do this by applying an S-duality and then a T-duality to the initial frame which results in a system with D5 and P charges. In that duality frame one can add a D1 charge in a straightforward manner. After we add the D1 charge, reversing the last duality chain takes us to the solution we are seeking: One which carries F1-NS5-P charges, has SO(4) spherical symmetry and vanishing horizon area.

5.3.1 Generating an NS5-P solution with local D0-D4 charges

Starting point: the F1-P solution with a non-trivial T^4 profile

The solution in D spacetime dimensions sourced by a fundamental string carrying momentum lies entirely in the NS sector of the theory, and is given by [181, 182]:

$$ds^2 = -\frac{2}{H}\,dv\left[du - \frac{\dot{F}^2(v)}{2}\,(H-1)\,dv + \dot{F}_M(v)\,(H-1)\,dx^M\right] + \delta_{MN}dx^M\,dx^N\,, \quad (5.3a)$$

$$B = -\left(1-\frac{1}{H}\right)\left[du\wedge dv + \dot{F}_M(v)\,dv\wedge dx^M\right]\,, \qquad e^{2\phi} = \frac{1}{H}\,, \quad (5.3b)$$

with all other fields vanishing. The coordinates u and v define the light-cone directions along the world-sheet of the string. The remaining transverse directions are parameterized by Cartesian coordinates, x_M, with $M = 1, \ldots D-2$. The shape of the string is given by profile functions, $F_M(v)$, with the dot denoting the derivative with respect to v. The string sources a warp factor which is a harmonic function, H, in the $D-2$ dimensional transverse space:

$$H \equiv 1 + \frac{Q}{|x_M - F_M(v)|^{D-4}}\,, \quad (5.4)$$

where Q is the supergravity charge associated to the fundamental string and is proportional to the ADM mass per unit length [182].

We take the space-time to be ten-dimensional with the topology $\mathbb{R}_t \times \mathbb{R}^4 \times S^1(y) \times T^4$. We will refer to the $\mathbb{R}^4$ as the base space, and it will be parameterized by x_i, with $i = 1, 2, 3, 4$, while the T^4 will be parameterized by z_a with $a = 6, 7, 8, 9$. We take the radius of the circle $S^1(y)$ to be given by R_y, and the coordinate y is periodically identified with $y \sim y + 2\pi\,R_y$. The null coordinates appearing in (5.3) are related to the usual spacetime coordinates through:[8]

$$v = \frac{t+y}{\sqrt{2}}\,, \qquad u = \frac{t-y}{\sqrt{2}}\,. \quad (5.5)$$

We choose the momentum-carrying string to wrap the compact y direction and to be localized at the origin of $\mathbb{R}^4$. For simplicity, we take the string to oscillate along one of the directions of the torus, z_9. Since we are interested in a solution that is isotropic along the torus, we smear the string source along the full T^4. The corresponding profile function is

$$F_M(v) = \delta_{Ma}\,c_a + \delta_{M9}\,F(v)\,, \quad (5.6)$$

where $F(v)$ is an arbitrary periodic function of period $\sqrt{2}\pi R_y$ and we include constants c_a which are integrated over in the process of smearing. The solution after smearing on

[8] Note that compared to [181, 182], we have rescaled u and v by a factor of $\sqrt{2}$.

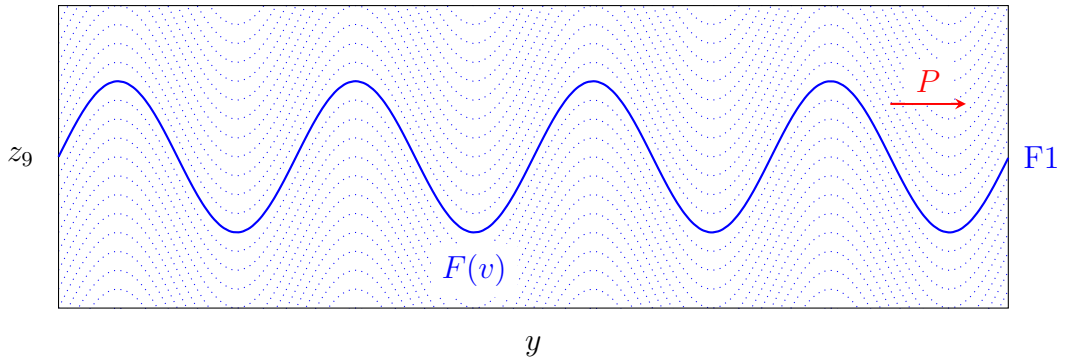

Figure 5.2: The shape of the fundamental string in the $y - z_9$ plane at a fixed time t. The string is wrapping the y-circle while its profile in the z_9 direction is given by an arbitrary periodic function $F(v)$. The system has a global F1 charge and a global momentum charge, denoted by P. Finally, the profile is smeared on the $S(z_9)$ circle, the smearing process being here depicted with the dotted lines. The non-trivial profile results in local variations of the charges in the z_9 and y directions.

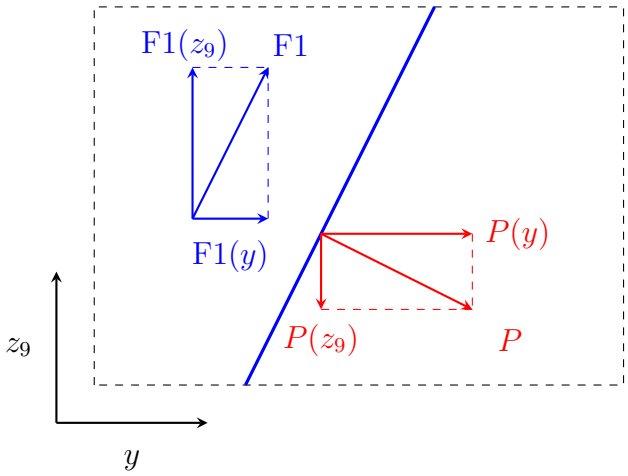

Figure 5.3: Zoom in on a local piece of the fundamental string presented in Fig. 5.2. We decompose the string charge F1 (directed along the string direction) and momentum P (directed transverse to the string) into components along the y and z_9 directions: They source the metric and B-field along these directions. Different charge components transform into different objects upon S and T-dualization.

the torus (see also Fig. 5.2) is

$$ds^2 = -\frac{2}{H_5}\, dv \left[du - \frac{\dot{F}^2(v)}{2}\,(H_5 - 1)\, dv + \dot{F}(v)\,(H_5 - 1)\, dz^9\right] + dx^i\, dx^i + dz^a\, dz^a\,, \tag{5.7a}$$

$$B = -\left(1 - \frac{1}{H_5}\right)\left[du \wedge dv + \dot{F}(v)\, dv \wedge dz^9\right], \qquad e^{2\phi} = \frac{1}{H_5}\,, \tag{5.7b}$$

where the harmonic function (5.4) is now given by[9]

$$H_5(r) = 1 + \frac{Q_5}{r^2}\,, \qquad r^2 = x_i\, x_i\,. \tag{5.8}$$

The profile of the momentum-carrying wave, $F(v)$, is arbitrary in the $y - z_9$ plane, so the system has locally varying F1 and momentum charge densities, which generically source the metric and B-fields with components both along the y-direction and along the z_9-direction. We denote these configurations as F1(y), P(y), and F1(z_9), P(z_9), respectively (see Fig. 5.3). Since the string does not wind around the z_9 direction, the total value of the P(z_9) and F1(z_9) charges is zero. Only F1(y) and P(y) correspond to charges measured at infinity.

NS5-P solution with local D0-D4 charges

We now perform a series of S-dualities and T-dualities that take us to a solution with global NS5-P charges and local D0-D4 charges. We give here only the duality chain and the explicit expression for the final solution, leaving the solutions obtained at intermediate steps to Appendix A.

The duality chain starts from the type-IIB solution in Equation (5.7):

$$\begin{pmatrix} \mathrm{F1}(y) \\ P(y) \\ \mathrm{F1}(z_9) \\ P(z_9) \end{pmatrix}_{\mathrm{IIB}} \overset{\mathrm{S}}{\longleftrightarrow} \begin{pmatrix} \mathrm{D1}(y) \\ P(y) \\ \mathrm{D1}(z_9) \\ P(z_9) \end{pmatrix}_{\mathrm{IIB}} \overset{\mathrm{T}(z_9)}{\longleftrightarrow} \begin{pmatrix} \mathrm{D2}(y, z_9) \\ P(y) \\ \mathrm{D0} \\ \mathrm{F1}(z_9) \end{pmatrix}_{\mathrm{IIA}} \overset{\mathrm{T}(z_8,z_7,z_6)}{\longleftrightarrow} \begin{pmatrix} \mathrm{D5}(y, T^4) \\ P(y) \\ \mathrm{D3}(z_6, z_7, z_8) \\ \mathrm{F1}(z_9) \end{pmatrix}_{\mathrm{IIB}}$$
$$\overset{\mathrm{S}}{\longleftrightarrow} \begin{pmatrix} \mathrm{NS5}(y, T^4) \\ P(y) \\ \mathrm{D3}(z_8, z_7, z_6) \\ \mathrm{D1}(z_9) \end{pmatrix}_{\mathrm{IIB}} \overset{\mathrm{T}(z_9)}{\longleftrightarrow} \begin{pmatrix} \mathrm{NS5}(y, T^4) \\ P(y) \\ \mathrm{D4}(T^4) \\ \mathrm{D0} \end{pmatrix}_{\mathrm{IIA}} . \tag{5.9}$$

The columns depict the objects appearing in each of the solutions, with the upper two entries denoting the charges that can be seen at infinity while the lower entries denote the local charges (which are the duals of the F1(z_9) and $P(z_9)$ local charges in the solution (5.7)). Above the double-headed arrows we write the duality that connects the two solutions, and show the direction along which we T-dualize. The subscripts of the parentheses denote the theory in which the solution exists.

At the end of the chain we obtain a solution corresponding to NS5-branes that wrap all five compact directions, momentum P along the y direction, as well as D4-branes wrapping the T^4 and D0-branes. Note that the solution has arbitrary and equal D0 and D4 charge densities, which can either integrate to finite values or to zero. Since we are trying to construct microstate geometries for the F1-NS5-P black hole, we choose an $F(v)$ profile that does not wind along the z_9 direction, and which gives a solution in which the total D0 and D4 charges vanish.

[9]The label is added to the harmonic function and to the charge for future convenience.

Following the rules of S-dualities and T-dualities (summarized in Appendix B, together with the democratic formalism [121] that we use to present the solution), we find that fields associated with the NS5-P solution with D0-D4 charges are given by

$$ds^2 = -2dv\left[du - \frac{\dot{F}(v)^2}{2}\left(1-\frac{1}{H_5}\right)dv\right] + H_5\, dx^i\, dx^i + dz^a\, dz^a\,, \tag{5.10a}$$

$$B_2 = \gamma\,, \qquad e^{2\phi} = H_5\,, \tag{5.10b}$$

$$C_1 = -\dot{F}(v)\left(1-\frac{1}{H_5}\right)dv\,, \tag{5.10c}$$

$$C_3 = -\dot{F}(v)\,\gamma\wedge dv\,, \tag{5.10d}$$

$$C_5 = -\dot{F}(v)\left(1-\frac{1}{H_5}\right)dv\wedge\widehat{\text{vol}}_4 = C_1\wedge\widehat{\text{vol}}_4\,, \tag{5.10e}$$

$$C_7 = -\dot{F}(v)\,\gamma\wedge dv\wedge\widehat{\text{vol}}_4 = C_3\wedge\widehat{\text{vol}}_4\,, \tag{5.10f}$$

where the two-form γ is defined by

$$d\gamma \equiv *_4 dH_5\,, \tag{5.11}$$

and $\widehat{\text{vol}}_4$ denotes the volume form of the torus. One should note that even though we started with a F1-P profile that was not isotropic along the T^4, through the chain of dualities (5.9) we arrive at (5.10) where the torus only appears through its volume form.

It is useful to note that our solution exhibits the expected features. The harmonic function H_5 appears in the solution in the way one expects for an NS5-brane: it multiplies the part of the metric that is transverse to the brane, it shows up in the expression for the dilaton (which diverges as one approaches the NS5-brane), and it determines the NS-NS two form which is sourced magnetically by the NS5-brane (see (5.11)). The solution also has non-vanishing momentum, which can be read off from the g_{vv} component of the metric. This momentum arises from the non-trivial profile function, $F(v)$, which also enters in the expression of the Ramond-Ramond gauge fields. Since the local contribution to the momentum of the solution is proportional to $\dot{F}(v)^2$, the total momentum is always positive for any non-constant profile function.

When $F(v)$ is a constant, the solution reduces to that of a stack of NS5-branes at the origin of $\mathbb{R}^4$. When the profile function is linear in v, the solution describes an NS5-brane with constant D0, D4, and momentum charges. The D0-branes source C_1 electrically and C_7 magnetically, while the D4-branes source C_3 electrically and C_5 magnetically. These gauge fields have the structure $C_{p+4} = C_p\wedge\widehat{\text{vol}}_4$, which is a consequence of the fact that in our solution the D0 and D4 charges are locked and is related to the enhanced supersymmetry one observes when $\dot{F}(v)$ is constant.

It is interesting to observe that the solution with a non-trivial $F(v)$ profile can be written in a much simpler fashion by redefining $\widetilde{v} \equiv F(v)$. Since $F(v)$ is periodic, and not monotonic, this re-definition is only locally well-defined, but it allows one to transform (5.10) into a solution in which all the fields and metric components except $g_{u\widetilde{v}}$ are independent of the choice of profile. Hence, the only difference between the solution with

a linear $F(v)$ profile and the v-dependent solution with an arbitrary profile comes from multiplying g_{uv} with an arbitrary function of v. The fact that this multiplication transforms a solution into another solution points to the possible existence of a simple method to add null waves on certain solutions, which we plan to further explore in future work.

5.3.2 Generating the F1-NS5-P solution with local D0-D4 charges

The solution (5.10) with a periodic $F(v)$ only has global NS5 and P charges and can be thought of as describing a microstate of the two-charge system. To add a third charge, we add a stack of fundamental strings on top of the NS5-P-D0-D4 solution. These strings will wrap the $S^1(y)$ circle along which the momentum is oriented, and will be smeared along the four-torus. To add this F1 charge we perform a duality chain on the solution in (5.10), we transform it to a certain class of D1-D5-P supersymmetric solutions [183], add an extra charge, and dualize back.

The most obvious way to dualize from the Type IIA F1-NS5-P frame to the D1-D5-P frame is to do a T-duality along the y direction, followed by an S-duality. However, this supergravity duality cannot be performed on (5.14), except upon smearing the profile $F(v)$, which results in a trivial solution with no v dependence. To preserve the non-trivial v-dependent information, one needs to T-dualize along another isometry direction.

We will use instead an isometry of the transverse space: Rewrite the flat metric on $\mathbb{R}^4$ in the Gibbons-Hawking form [184]

$$dx^i\, dx^i = \frac{1}{V}(d\psi + A)^2 + V\, ds_3^2\,, \tag{5.12}$$

where ψ is the Gibbons-Hawking fiber, ds_3^2 is the line-element of flat $\mathbb{R}^3$, V is a scalar function and A a one-form on this three-dimensional space, satisfying the relation $*_3 dA = dV$. Since the Gibbons-Hawking fiber is periodic, one can T-dualize along it without losing information about the local charges along the $S^1(y)$ circle, but at the cost of destroying the asymptotic structure of the solution. However, this does not cause any problems, since we only use this duality as a tool for introducing the F1 charge: The asymptotic behavior is restored after we dualize back to the original frame. Hence the chain of dualities we consider is

$$\left(\begin{array}{c} \mathrm{NS5}(y,T^4) \\ P(y) \\ \mathrm{D4}(T^4) \\ \hline \mathrm{D0} \\ \mathrm{F1}(y) \end{array}\right)_{\mathrm{IIA}} \overset{\mathrm{T}(\psi)}{\longleftrightarrow} \left(\begin{array}{c} \mathrm{KKM}(y,T^4;\psi) \\ P(y) \\ \mathrm{D5}(T^4,\psi) \\ \hline \mathrm{D1}(\psi) \\ \mathrm{F1}(y) \end{array}\right)_{\mathrm{IIB}} \overset{\mathrm{S}}{\longleftrightarrow} \left(\begin{array}{c} \mathrm{KKM}(y,T^4;\psi) \\ P(y) \\ \mathrm{NS5}(T^4,\psi) \\ \hline \mathrm{F1}(\psi) \\ \mathrm{D1}(y) \end{array}\right)_{\mathrm{IIB}}, \tag{5.13}$$

where the $\mathrm{KKM}(y,T^4;\psi)$ denotes a KKM charge with special direction ψ that is distributed along the $S^1(y)$ circle and the torus. Note that the interpretations of these charges is heuristic, since the NS5-brane sits at a fixed point of the isometry of the T-duality along ψ, and the asymptotic structure is singular. Below the line we describe

the duality chain for the fundamental string that we want to add to (5.10). In the final frame (which is often called the D1-D5 frame and is commonly used in the superstrata constructions) this corresponds to adding a D1-brane wrapped along the y circle. Since all the torus-independent supersymmetric solutions in this frame are perfectly understood [183], we know the precise way in which to add such a D1-brane to the dual of our initial two-charge configuration, and we present the details of the calculation in Appendix A.

After adding the D1-brane in the D1-D5 frame (5.13) and performing the duality transformations backwards (from right to left), we obtain the following solution describing an F1-NS5-P system with non-trivial D0-D4 density wave, localized at the origin of the flat $\mathbb{R}^4$ base (see also Fig. 5.4):

$$ds^2 = -\frac{2}{H_1} dv \left[du - \frac{\dot{F}(v)^2}{2} \left(1 - \frac{1}{H_5}\right) dv \right] + H_5\, dx^i\, dx^i + dz^a\, dz^a\,, \tag{5.14a}$$

$$B_2 = -\frac{1}{H_1}\, du \wedge dv + \gamma\,, \qquad e^{2\phi} = \frac{H_5}{H_1}\,, \tag{5.14b}$$

$$C_1 = -\dot{F}(v) \left(1 - \frac{1}{H_5}\right) dv\,, \tag{5.14c}$$

$$C_3 = -\dot{F}(v)\, \gamma \wedge dv\,, \tag{5.14d}$$

$$C_5 = -\dot{F}(v) \left(1 - \frac{1}{H_5}\right) dv \wedge \widehat{\text{vol}}_4 = C_1 \wedge \widehat{\text{vol}}_4\,, \tag{5.14e}$$

$$C_7 = -\dot{F}(v)\, \gamma \wedge dv \wedge \widehat{\text{vol}}_4 = C_3 \wedge \widehat{\text{vol}}_4\,, \tag{5.14f}$$

where we have introduced a new harmonic function associated with the F1 charge

$$H_1(r) = 1 + \frac{Q_1}{r^2}\,, \tag{5.15}$$

and the two-form γ is defined through (5.11). This solution is the main result of our construction. Note that this solution can be simplified locally in the same way as (5.10), by redefining the v coordinate as $\widetilde{v} = F(v)$ and seeing that all the non-trivial fluctuations along the null direction can be absorbed into a fluctuation of $g_{u\widetilde{v}}$.

In the next Section we perform a detailed analysis of the this solution and compare it to the three-charge F1-NS5-P black-hole solution.

5.4 Analysis and comparison

In this Section we compare the newly obtained three-charge solution (5.14) to the three-charge F1-NS5-P black-hole that has a finite-size horizon. We begin by reviewing this black hole, focusing on the behavior of the solution near the horizon. We then perform a similar analysis on the solution constructed above, and compare and contrast the results. We find that, while the two solutions asymptotically look alike, they differ drastically in the near-horizon region. In the black-hole solution the singular source appearing in the harmonic function associated with the momentum is responsible for stabilizing the y-circle thus giving rise to an event horizon with a finite area. This does not happen in

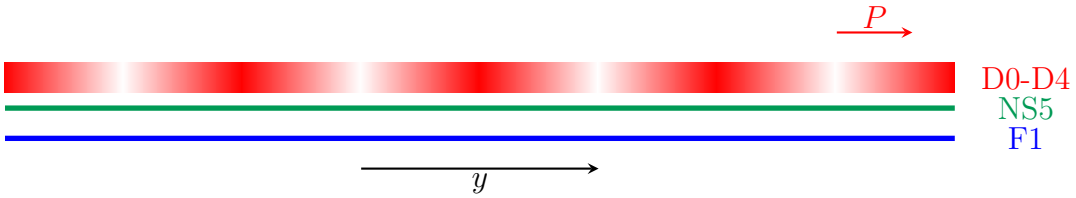

Figure 5.4: A constant-time snapshot of the periodic y direction at the origin of $\mathbb{R}^4$. We have fundamental strings (F1, blue) and NS5-branes (green) wrapping the y circle with momentum-carrying D0-D4 charges densities (red density plot) living on the world-volume of the NS5-brane. The D0 and D4 charges have the same y (or v) dependence, given by the profile function $F(v)$, which is necessary for the configuration to be supersymmetric.

the new solution (5.14), where the momentum is produced by the fluctuations of the local D0 and D4 charges, whose corresponding function remains finite at the location of the F1 and NS5-brane sources. As a consequence, the y-circle pinches off and the horizon area vanishes. The existence of our solution indicates that if one considers all the degrees of freedom of the system, an event horizon does not form even when the system has no transverse fluctuations.

5.4.1 The F1-NS5-P three-charge black hole

The F1-NS5-P three-charge black hole is obtained by superimposing a stack of NS5-branes (wrapping $S^1(y) \times T^4$) and a stack of F1-strings (wrapping $S^1(y)$), both of which are located at the origin of $\mathbb{R}^4$, and allowing for additional momentum charge in the y direction [185]. This yields the solution:[10]

$$ds^2 = -\frac{2}{H_1}\, dv \left(du + \frac{\mathcal{F}}{2}\, dv\right) + H_5\, dx^i\, dx^i + dz^a\, dz^a\,, \tag{5.16a}$$

$$B_2 = -\frac{1}{H_1}\, du \wedge dv + \gamma\,, \qquad e^{2\phi} = \frac{H_5}{H_1}\,, \tag{5.16b}$$

with all other fields vanishing.

The harmonic functions associated to the NS5-branes and F1-strings, H_5 and H_1, are given by the expressions (5.8) and (5.15). Furthermore, the magnetic component of B_2, which is sourced by the NS5-branes is given by the expression (5.11). The harmonic function associated to the momentum, $\mathcal{F}$, has a δ-function source at the origin of $\mathbb{R}^4$, whose strength is proportional to the momentum charge as measured at spatial infinity, Q_P:

$$\mathcal{F} = -\frac{2\,Q_P}{r^2}\,. \tag{5.17}$$

In the backreacted solution, there is an event horizon at $r = 0$. To calculate its area one needs to look at the size of the orthogonal dimensions as one approaches it. One can

[10] Throughout Section 5.4 we are working with string-frame metrics, unless explicitly stated otherwise.

show that the radius of the $S^1(y)$ circle at an arbitrary value of r is

$$R_y(r) = \sqrt{\frac{Q_P + r^2}{Q_1 + r^2}}\, R_y\,, \tag{5.18}$$

where, as before, R_y denotes the value of this radius at infinity. We can see that the y-circle remains finite in size as we approach the horizon at $r = 0$. Combining this with the finite size of the S^3 of the $\mathbb{R}^4$, we find that (5.16) has a non-zero horizon area. This is a direct consequence of the stabilization of the $S^1(y)$ circle at the location of the horizon, caused by the balancing between the effect of the momentum, which exerts a centrifugal force towards a large radius, and the tension of the branes wrapping the circle, which try to shrink it. In the absence of momentum ($Q_P = 0$), one can see from (5.18) that the $S^1(y)$ circle wrapped by the NS5-branes and F1-strings pinches off as $r \to 0$ and thus the horizon area vanishes.

Finally, we note that the metric is actually smooth at the horizon, and it can be smoothly continued across it. As one would expect, the curvature invariants remain finite:

$$R = -20\frac{Q_1 - Q_5}{Q_1\, Q_5^2}\, r^2 + \mathcal{O}\left(r^3\right)\,, \tag{5.19a}$$

$$R_{\mu\nu}\, R^{\mu\nu} = \frac{24}{Q_5^2} + \mathcal{O}\left(r^2\right)\,, \tag{5.19b}$$

$$R_{\mu\nu\rho\sigma}\, R^{\mu\nu\rho\sigma} = \frac{24}{Q_5^2} + \mathcal{O}\left(r^2\right)\,. \tag{5.19c}$$

5.4.2 The new three-charge solution with local D0-D4 charges

We can write the metric of our new solution (5.14) as

$$ds^2 = -\frac{2}{H_1} dv\left[du - \frac{\dot{F}(v)^2}{2}\left(1 - \frac{1}{H_5}\right) dv\right] + H_5\, dx^i\, dx^i + dz^a\, dz^a\,, \tag{5.20a}$$

$$= \frac{1}{H_1}\left[-dt^2 + dy^2 + \frac{\dot{F}(v)^2}{2}\left(1 - \frac{1}{H_5}\right)(dt + dy)^2\right] + H_5\, dx^i\, dx^i + dz^a\, dz^a\,, \tag{5.20b}$$

where we used (5.5) to obtain the second line. If the harmonic functions H_1 and H_5 contain a constant, the geometry is asymptotically flat $\mathbb{R}^{4,1} \times S_y \times T^4$. The main difference with the black hole comes from the behavior of the g_{vv} component of the metric, which contains the information about the momentum of the system. In contrast to (5.16), this metric does not contain a freely choosable harmonic function, $\mathcal{F}$, with an independent charge Q_P. Rather, the momentum is encoded in the profile $F(v)$ and the combination $(1 - H_5^{-1})$, which, as already mentioned, is finite everywhere in the base space. This is because the momentum is carried in a fundamentally different way compared to the black-hole solution. The finiteness of $(1 - H_5^{-1})$ suggests an absence of a localized source for the momentum. This is in conflict with the naive "NS5 world-volume intuition," according to which the momentum is sourced by longitudinal fluctuations of the D0 and

D4 densities inside the NS5-brane world-volume, and hence it should also be sourced at the location of the NS5-brane. Of course, the NS5 world-volume intuition ignores back-reaction, so it is not the appropriate intuition for the the full supergravity solution. But it is rather puzzling that other aspects of this world-volume intuition are described correctly in supergravity, while this particular aspect is not.

The asymptotics

Despite the absence of a singular source, one can calculate the value of the momentum along the y direction in this solution from the asymptotic expansion [157, 186]:

$$g_{vv} \approx \frac{1}{r^2}\left(2Q_P + \textit{oscillating terms}\right) + \mathcal{O}\left(r^{-3}\right) . \tag{5.21}$$

Thus we can read off

$$g_{vv} = \frac{\dot{F}(v)^2}{H_1}\left(1 - \frac{1}{H_5}\right) \approx \frac{Q_5\,\dot{F}(v)^2}{r^2} + \mathcal{O}\left(r^{-3}\right) , \tag{5.22}$$

from which we extract the non-oscillating part by averaging over the y-circle:

$$Q_P = \frac{Q_5}{2}\,\frac{1}{\sqrt{2}\pi R_y}\int_0^{\sqrt{2}\pi R_y} \dot{F}(v)^2\, dv\,. \tag{5.23}$$

Note that if the profile function admits a decomposition as a Fourier sum

$$F(v) = R_y\, a_0 + R_y \sum_{n=1}^{\infty}\left[\frac{a_n}{n}\cos\left(\frac{\sqrt{2}nv}{R_y}\right) + \frac{b_n}{n}\sin\left(\frac{\sqrt{2}nv}{R_y}\right)\right] , \tag{5.24}$$

then one can evaluate the integral in (5.23) and obtain

$$Q_P = \frac{Q_5}{2}\sum_{n=1}^{\infty}\left(a_n^2 + b_n^2\right) . \tag{5.25}$$

Thus, different solutions in the family we constructed (5.14), parameterized by different profile functions $F(v)$, have the same asymptotic momentum charge, Q_P, as the black hole (5.23). However, while the g_{vv} component of the black-hole solution only contains a harmonic function proportional to Q_P

$$g_{vv}^{\rm BH} = \frac{1}{H_1}\frac{2\,Q_P}{r^2} , \tag{5.26}$$

the metric of our solutions deviate from that of the black hole at higher order in the asymptotic expansion in r, because of the $(1 - H_5^{-1})$ term in g_{vv} (5.22):

$$g_{vv}(v) = \frac{\dot{F}(v)^2}{H_1}\left(\frac{Q_5}{r^2} - \frac{Q_5^2}{r^4} + \mathcal{O}((r^{-6})\right) . \tag{5.27}$$

Averaging (5.27) over v suggests that the higher multipoles of our solutions may be different from those of the black hole:

$$\langle g_{vv}\rangle_v \equiv \frac{1}{\sqrt{2}\pi R_y}\int_0^{\sqrt{2}\pi R_y} g_{vv}(v)\,dv = \frac{1}{H_1}\left(\frac{2\,Q_P}{r^2} - \frac{2\,Q_5\,Q_P}{r^4} + \mathcal{O}(r^{-6})\right). \tag{5.28}$$

Hence, our solution deviates from the black-hole metric via $\frac{Q_5 Q_P}{r^4}$ and higher terms in g_{vv}, which indicates that the momentum wave of the microstructure in the backreacted solution develops a finite size. This will be further confirmed in Section 5.4.2.

The vanishing-area horizon

Much like in the two-charge F1-NS5 solution, one finds that g_{tt} goes to zero at $r = 0$, the location of the pole of the brane harmonic functions. Furthermore, the curvature invariants are finite at this point and are equal to those of the F1-NS5 two-charge solution[11] and those of the F1-NS5-P three-charge black hole (5.19). The crucial difference comes from behavior of the length of the y-circle near the brane sources, which we calculate using (5.20)

$$L_y = \sqrt{\frac{2}{H_1}}\int_0^{\sqrt{2}\pi R_y}\sqrt{1+\frac{\dot{F}(v)^2}{2}\left(1-\frac{1}{H_5}\right)}\,dv \approx r\sqrt{\frac{2}{Q_1}}\int_0^{\sqrt{2}\pi R_y}\sqrt{1+\frac{\dot{F}(v)^2}{2}}\,dv\,, \tag{5.29}$$

where we have expanded around $r = 0$. Since the integrand is a strictly positive function, we find that near the origin the y-circle pinches off, despite the fact that the solution has a non-trivial momentum along that direction. One can show that, as $r \to 0$, all other dimensions are finite in size.[12] Therefore, (5.14) has a singularity that can be thought of as a zero-area horizon. This is the same type of singularity as in the F1-NS5 or D1-D5 two-charge solutions. Our new solution is thus very peculiar: For a non-trivial profile $F(v)$, we can see from (5.23) that it contains momentum along with F1 and NS5 charges, making it a three-charge solution. On the other hand, one can see from (5.29) that the y-circle shrinks at the origin, which gives rise to a singularity of the type present in two-charge solutions.

The near-horizon behavior - a first pass

There exist two ways to analyze the near-horizon behavior of the solution. One can, as we discuss in this subsection, focus on the region where

$$r^2 \ll Q_1, Q_5\,. \tag{5.30}$$

[11] One should remember that the near-brane limit of the two-charge solution is, locally, like Poincaré $AdS_3 \times S^3$, and so the curvature invariants are all well-behaved. What makes the solution singular is the fact that the S^1 pinches off in the $r \to 0$ limit, where g_{tt} also vanishes.

[12] One can show that the three-sphere which appears in the base space has an area of $\text{Area}(S^3) = 2\pi^2\left(r^2\,H_5\right)^{\frac{3}{2}} \approx 2\pi^2 Q_5^{\frac{3}{2}}$, where we have expanded near $r = 0$. Furthermore, the volume of the T^4 is independent of r and is taken to be finite. Then the string-frame area of the would-be horizon is $A_H = L_y\,\text{Area}(S^3)\,\text{Vol}(T^4)$, which vanishes as one approaches the brane sources because of the pinching of the y-circle.

By expanding (5.14) in small r, one can probe the solution in the vicinity of the brane sources. The expansion of the metric is, up to order $\mathcal{O}(r^2)$, given by:

$$ds^2 = \sqrt{\frac{Q_5}{Q_1}}\left[-\frac{2\,r^2}{\sqrt{Q_1\,Q_5}}\,dv\left(du-\frac{\dot{F}^2(v)}{2}dv\right)+\frac{\sqrt{Q_1\,Q_5}}{r^2}\,dr^2+\sqrt{Q_1\,Q_5}\,d\Omega_3^2\right]+d\hat{s}_4^2\,, \tag{5.31}$$

which is locally $\mathrm{AdS}_3\times S^3\times T^4$, as can be seen more explicitly by introducing a new coordinate

$$w\equiv u-\int\frac{\dot{F}(v)^2}{2}\,dv\,,\qquad dw=du-\frac{\dot{F}(v)^2}{2}\,dv\,. \tag{5.32}$$

Thus, near the brane sources, the solution is locally simply empty AdS. The transformation (5.32) removes the metric component $g_{vv}\propto\dot{F}^2(v)\,r^2$, which is the only term in the near-horizon region sensitive to $\dot{F}^2(v)$. This metric component vanishes at $r\to 0$, but grows as r^2 with increasing radius. Therefore, it does not vanish at the boundary of AdS_3 ($r\to\infty$), but corresponds to a non-trivial deformation of the boundary metric.

The growing behavior of g_{vv} as one is increasing the radius implies that the momentum is not localized in the interior of the AdS region. Since the asymptotically-flat solution (5.14) contains non-vanishing momentum charge, the momentum wave must be located in the transition zone between the AdS_3 near-horizon region and the flat space region. This explains why our new solution has a momentum that can be measured at infinity (5.23), despite the absence of a no momentum-charge source at $r=0$. Indeed, as can be seen from Fig. 5.5, which depicts the g_{vv} for arbitrary values of r, (5.31) captures only the leading near-horizon behavior but fails to capture the asymptotic fall-off. Furthermore, in the string frame the maximum of g_{vv} is located at $r^2=\sqrt{Q_1\,Q_5}$, providing further evidence that the momentum wave is localized in the transition region between AdS_3 and flat space.

Finally, let us note that the metric (5.31) does not correspond to the results from the heuristic method of taking a near-horizon limit by "dropping the 1" in the harmonic functions. This method gives a metric which has an additional term:

$$ds^2 = \sqrt{\frac{Q_5}{Q_1}}\left[-\frac{2\,r^2}{\sqrt{Q_1\,Q_5}}\,dv\left(dw+\frac{\dot{F}^2(v)\,r^2}{2\,Q_5}dv\right)+\frac{\sqrt{Q_1\,Q_5}}{r^2}\,dr^2+\sqrt{Q_1\,Q_5}\,d\Omega_3^2\right]+d\hat{s}_4^2\,, \tag{5.33}$$

where we have used the shifted coordinate (5.32). This metric corresponds holographically to a deformation of $\mathrm{AdS}_3\times S^3\times T^4$ with a non-normalizable mode corresponding to an irrelevant operator of the dual CFT. Furthermore, the metric is no longer locally AdS: the additional term in g_{vv} that scales as r^4 and diverges at the boundary of AdS cannot be reabsorbed by a coordinate transformation.

This deformation of the metric is accompanied by a non-vanishing deformation of the RR gauge fields:

$$C_1=\left(1-\frac{r^2}{Q_5}\right)\dot{F}(v)\,dv\,,\qquad C_3=-Q_5\,\dot{F}(v)\,\gamma'\wedge dv\,, \tag{5.34}$$

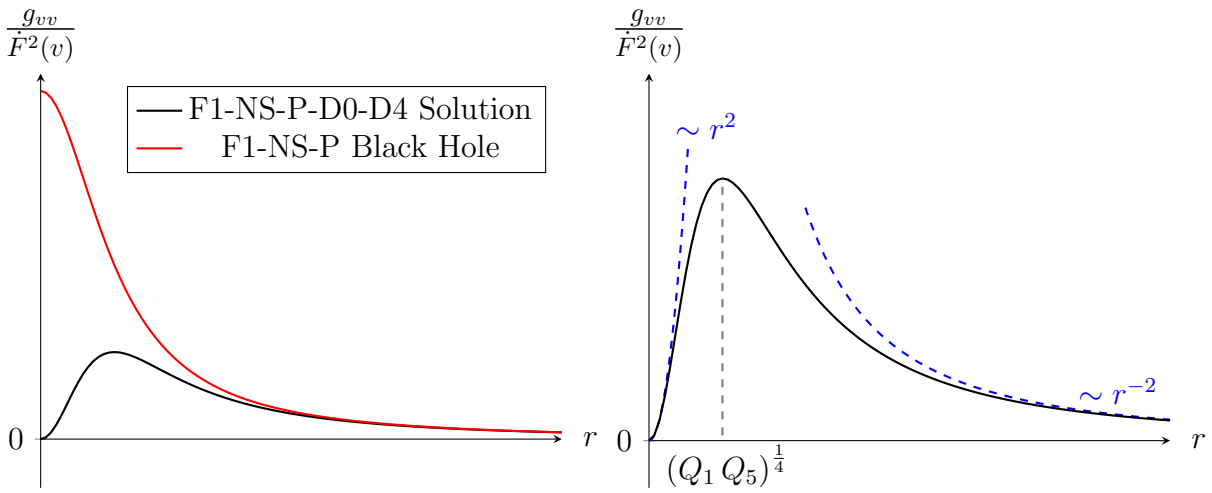

Figure 5.5: The schematic behavior of the metric component g_{vv} as a function of the radial coordinate. On the left is the plot of the exact expression (modulo the $\dot{F}^2(v)$ function) for the new F1-NS5-P-D0-D4 solution (5.22) (black) and the F1-NS5-P black hole (red). The momentum charge of the latter is taken to be such that the asymptotic behavior of the two solutions match. In the bulk the two solutions differ significantly: At $r = 0$ the black hole has a finite value for g_{vv} which is related to the finite size of the horizon, while in the new solution this metric component vanishes and the $S^1(y)$ circle pinches off. On the right, we have a close-up of the solution with local D0-D4 charges, superposed with the asymptotic and near-brane behavior in blue. The momentum is localized away from the brane sources, with the maximum at $r^2 = \sqrt{Q_1\,Q_5}$.

and all higher order forms can be obtained by using the self-duality conditions (B.3). In C_3 we have used the fact that when writing $\mathbb{R}^4$ in spherical coordinates, $d\gamma = *_4 dH_5 = 2Q_5\,\mathrm{vol}\,(S^3)$. Thus it is convenient to define a new, "bare", two-form γ' such that $d\gamma' \equiv 2\,\mathrm{vol}\,(S^3)$. It then naturally follows that C_3 remains unchanged in the near-horizon expansion, since it is independent of the radial coordinate. Finally, the NS-NS gauge field is the same as in the standard decoupling limit and the corresponding field strength supports the $\mathrm{AdS}_3 \times S^3$ structure.

The near-horizon behavior - a second pass

Another way of decoupling the near-horizon region from the asymptotically flat region and obtain a background that is holographically dual to the low-energy physics of a brane system is to take a double-scaling limit [187] involving α' and the transverse radial direction. To do this we need to first express the charges appearing in the supergravity solution, Q_1 and Q_5, in terms of the moduli and the quantized numbers of F1 strings, N_1, and NS5-branes, N_5:

$$Q_1 = \frac{g_s^2\,\alpha'^3}{V_4}\,N_1\,, \qquad Q_5 = \alpha'\,N_5\,, \tag{5.35}$$

where g_s is the string coupling constant, α' is the Regge slope, and V_4 is the coordinate volume of the four-torus divided by $(2\pi)^4$. The double scaling limit is [187]

$$\alpha' \to 0\,, \qquad U \equiv \frac{r}{\alpha'} = \text{fixed}\,, \qquad v_4 \equiv \frac{V_4}{\alpha'^2} = \text{fixed}\,, \qquad g_6 \equiv \frac{g_s}{\sqrt{v_4}} = \text{fixed}\,, \tag{5.36}$$

and it yields the ten-dimensional string frame metric:

$$\frac{ds^2}{\alpha'} = N_5 \left[-\frac{2\,U^2}{g_6^2\,N_1\,N_5}\,dv\left(du - \frac{\dot{F}^2(v)}{2}dv\right) + \frac{dU^2}{U^2}\,dU^2 + d\Omega_3^2\right] + dz^a\,dz^a\,. \tag{5.37}$$

This result is consistent with the near-brane expansion of the metric (5.31), provided one makes the substitutions $Q_1 \to g_6^2\,N_1$ and $Q_5 \to N_5$. Thus, as before, the metric in the decoupling limit corresponds to locally empty AdS, with a deformation that is non-trivial at the asymptotic boundary. Performing the same scaling on the gauge fields in the solution (5.14), one finds that the NS-NS two-form becomes such that the corresponding field strength is comprised of a part proportional to the volume form of AdS_3 and a part proportional to the volume form of S^3. On the other hand, the RR gauge fields C_p are such that all field strengths, F_{p+1}, vanish in this limit.

It is important to note that the double scaling limit (5.36) and the near-brane expansion considered in (5.31) lose all information about the harmonic function H_5 appearing in g_{vv} and about the nontrivial RR fields of the solution. It is interesting to try to construct a decoupling limit which does not erase this information. It is not hard to see that such a limit combines (5.36) with a scaling of the null coordinates defined in (5.32), while keeping fixed

$$d\widetilde{v} \equiv \sqrt{\alpha'}dv = \text{fixed}\,, \qquad d\widetilde{w} \equiv \frac{dw}{\sqrt{\alpha'}} = \text{fixed}\,. \tag{5.38}$$

This results in a metric[13]

$$\frac{ds^2}{\alpha'} = N_5 \left[-\frac{2\,U^2}{g_6^2\,N_1\,N_5}\,d\widetilde{v}\left(d\widetilde{w} + \frac{\dot{F}^2(\widetilde{v})\,U^2}{2\,N_5}d\widetilde{v}\right) + \frac{dU^2}{U^2} + d\Omega_3^2\right] + dz^a\,dz^a\,, \tag{5.39}$$

corresponding to a non-trivial deformation of $\text{AdS}_3 \times S^3 \times T^4$. We also find the non-trivial RR gauge fields

$$C_1 = -\frac{U^2}{N_5}\,\dot{F}(\widetilde{v})\,d\widetilde{v}\,, \qquad C_3 = -N_5\,\dot{F}(\widetilde{v})\,\gamma' \wedge d\widetilde{v}\,, \tag{5.40}$$

where in writing the latter expression we again used the two-form γ', as defined in (5.34). All higher-order forms can be obtained from these by using the democratic formalism. It is interesting to observe that despite the non-trivial scaling of the coordinates $\widetilde{w}$ and $\widetilde{v}$, the final result matches the one obtained by simply "dropping the 1" in the harmonic functions (5.33), if one appropriately identifies coordinates and moduli of the two solutions.

[13]Note that despite the scaling (5.38) we keep $\dot{F}(v)$ fixed. This can be achieved by scaling $F(v)$ in a way which cancels out the scaling of v coming from the differentiation.

Finally, let us note that the same results can be obtained by another scaling limit which is more commonly used in the F1-NS5-P system [188–190]. Begin by defining dimensionless coordinates $\widetilde{u} \equiv u/R_y$ and $\widetilde{v} \equiv v/R_y$. Then one takes the AdS_3 decoupling limit[14] by scaling $g_s \to 0$ and $R_y \to \infty$, while keeping fixed the supergravity charges, Q_1 and Q_5, the coordinates $\widetilde{u}$, $\widetilde{v}$, and r/g_s, and the remaining string moduli. In practice, we can implement this limit by making the replacements [189]

$$r \to \epsilon\, r\,, \qquad R_y \to \frac{R_y}{\epsilon}\,, \tag{5.41}$$

followed by sending $\epsilon \to 0$.[15] One finds that the resulting metric is exactly equal to (5.31), obtained by the near-brane expansion of the full asymptotically flat geometry. If, on the other hand, one first performs the transformation (5.32), defines $\widetilde{w} \equiv w/R_y$, and, in addition to (5.41), scales

$$\widetilde{w} \to \epsilon\, \widetilde{w}\,, \qquad \widetilde{v} \to \frac{\widetilde{v}}{\epsilon}\,, \tag{5.42}$$

then the $\epsilon \to 0$ limit yields the solution obtained by "dropping the 1" in the Harmonic functions (5.39).

5.4.3 Supersymmetries and singularities

Since our NS5-P-D0-D4 solution is a dual of the F1-P string, it must have eight supersymmetries, which are identical to the common supersymmetries preserved by NS5-branes and a momentum wave. Moreover, if one zooms in locally, the function, $F(v)$, becomes approximately linear in v, and the resulting solution has 16 supersymmetries. One can also confirm this by directly calculating the brane projectors, like in [30]. Alternatively, this can be seen by noting that such a linear solution comes from dualizing a tilted fundamental string boosted orthogonally, or equivalently, by uplifting to 11 dimensions, where the linear system becomes an M5-brane with orthogonal momentum, as depicted in Fig. 5.1. Both such configurations preserve 16 supersymmetries.

It is natural to ask how the NS5-P-D0-D4 solution can preserve the same supersymmetries as the NS5-P system, despite the presence of D0 and D4 densities. This is achieved because the D0 and D4 densities have the same distribution on the $S^1(y)$-circle, which makes their joint contribution to the supersymmetry projector compatible with the Killing spinors preserved by NS5-branes and momentum. This phenomenon was observed in the construction of the magnetube [192], and it is not hard to see that if one T-dualizes our solution twice along the D4-brane world-volume, one obtains an NS5-D2-D2-P brane configuration that uplifts to the M5-M2-M2-P magnetube of [192].

[14] For the F1-NS5-P system there exists an additional linear-dilaton region [191] which is obtained by taking only $g_s \to 0$ while keeping the ratio r/g_s fixed. As can be seen from (5.35), this limit focuses on the region of spacetime where $Q_1 \ll r^2 \ll Q_5$. We are interested in the scaling which accesses the region (5.30), which is achieved by the scaling described in the main text. We would like to thank David Turton and Soumangsu Chakraborty for helpful discussions on this point.

[15] Again we keep $\dot{F}(v)$ fixed in this scaling.

Upon adding F1-strings to the NS5-P-D0-D4 solution, the supersymmetry is reduced to half. Thus, the resulting solution has globally four supercharges, but if one zooms near the source (or considers a solution with a linear $F(v)$) the number of supercharges is enhanced to eight. This is consistent with the fact that the singularity in this solution is the same as that of a two-charge single-center solution.

5.5 Conclusion and discussion

The Fuzzball and Microstate Geometry Programmes exist precisely because string theory and supergravity have a rich variety of degrees of freedom that can be used to evade the formation of horizons. A recent, but illustrative example is the long-term trapping [193] near evanescent ergosurfaces which was believed to lead to Aichelburg-Sexl shockwaves and horizon formation. However, a more detailed analysis showed that this would actually result in scrambling into more and more typical modes of the solution [194]. Furthermore, the extremely long-term trapping needed to create singularities requires sub-stringy wavelengths for the modes [160]. In short, the stringy degrees of freedom are activated before horizons develop and one must explore the full range of supergravity and stringy phase space or one risks mimicking the limitations of General Relativity and concluding that horizons are inevitable.

In this work we examined another manifestation of this phenomenon: In the D1-D5 frame, a family of smooth, three-charge Microstate Geometries (the *superstrata* family) appears to develop a horizon in the limit of vanishing angular momentum ($a \to 0$). We have now given strong evidence that *the horizon only emerges because one has neglected degrees of freedom that are essential in the* $a \to 0$ *limit*. Indeed, we incorporated some of these degrees of freedom by introducing D0- and D4-brane densities in the Type IIA F1-NS5 frame and showed that these resulted in a solution that has a vanishing horizon area.

We have also understood that reason behind the failure of the naïve intuition according to which $a \to 0$ D1-D5-P superstrata appear to collapse into a black hole. The momentum of these superstrata is only carried by D1 and D5 dipole-charge distributions [24,179] that are compressed to zero size in the $a \to 0$ limit.[16] If one takes into account all possible momentum carriers, no such collapse happens.

Indeed, the D1-D5 configuration on which one builds the microstate geometries comes from dualizing an F1-string with momentum, and since the F1-string only carries momentum waves that are transversely polarized [16], this configuration has finite size. By contrast, we find that NS5-branes can carry momentum also through longitudinal fluctuations, via a non-trivial profile of world-volume fluxes corresponding to D0- and D4-brane densities. It is this fact that allows us to construct 3-charge zero-horizon-area solutions, despite the NS5-branes being localized at a single point in the $\mathbb{R}^4$ base space. Hence, our

[16]Furthermore, in bubbling solutions [33,34] the momentum charge comes from the non-trivial dipole fluxes, which also vanish when $a \to 0$.

solutions are $SO(4)$ singlets under rotations on the $\mathbb{R}^4$, exactly as the usual three-charge black hole solution.

An interesting observation, which only emerges from analyzing the full supergravity solution, is that the momentum "carried" by the D0 and D4 charge densities inside the NS5 world-volume is *not* localized near the NS5-brane source, but resides in the transition region between the near-horizon $\text{AdS}_3 \times S^3$ and the asymptotically flat region. As such, this momentum cannot prevent the $S^1(y)$ wrapped by the F1-strings and the NS5-branes from collapsing at the location of the brane sources, which in turn causes the horizon area to vanish.

As we remarked earlier, there is an important distinction between microstate solutions and degenerate microstate solutions. Both have vanishing horizon area, but the former represent pure states, whereas the latter encode a large number of microstates. The singularities of two-charge solutions, like the F1-NS5 singularity, or the D1-D5 singularity, and the singular core of our F1-NS5-P-D0-D4 solution are, in this sense, degenerate microstate solutions, and their cores represent ensembles of microstates that have neither the charges nor the degrees of freedom to create a macroscopic horizon.

Degenerate microstate solutions are also required to have microstructure that can be understood using string theory. Resolving the microstructure of the singular D1-D5 system was the focus of the original fuzzball program [16, 18]. More recently, our understanding of the microstructure of the F1-NS5 system has been greatly advanced using world-sheet methods [188–190, 195, 196].

Our work has enriched the "landscape" of superstrata by expanding the range of momentum carriers on the branes. As we have seen, the addition of the D0-D4 excitations reveals how the fuzzball paradigm works even in the singular corners [197–199] of the moduli space. This also suggests several interesting areas for further investigation: we expect that there are whole new classes of microstate geometries that come from the geometric transition of our degenerate microstate solutions. Another intriguing question is whether there are such transitions that only involve the T^4, and achieve this in a way that preserves the space-time $SO(4)$ invariance and the vanishing angular momentum.

It would also be interesting to see, in detail, how the solutions obtained in this Chapter emerge as a limit of smooth microstate geometries. In particular, one should be able to construct superstrata, with $a > 0$, that contain both "standard" momentum carriers and D0-D4 momentum carriers. In such a generalized superstratum with $a > 0$, the y-circle should pinch off smoothly, making a smooth cap at the bottom of a long BTZ-like throat. It would be interesting to construct this Type-IIA superstratum with F1-NS5-P charges, and to explore its $a \to 0$ limit and the relation of this limit to the solutions we construct in this Chapter.

In particular, if there exist Type IIA superstrata that limit to our solutions, there is then the question of what happens to the long BTZ throat. Do our solutions emerge in the center of a cap at the bottom of a long throat, or does the throat become much shallower? Indeed, this is directly related to the results presented in Section 5.4.2, where we showed that in the full supergravity solution, the momentum charge comes from modes localized

in the junction between the near-horizon $AdS_3 \times S^3$ region and the asymptotic flat space. In a generalized superstratum, with D0-D4 momentum carriers and with $a > 0$, we would still expect that, like in the original superstrata, all the momentum waves should localize in a band that creates the transition between the horizonless cap and the long $AdS_2 \times S^1$ region of the BTZ throat. It would be very interesting to see whether and how the location of the momentum waves shifts in the $a \to 0$ limit of the generalized superstratum.

Even though our solutions have the same spherical symmetry as a single-center black hole with the same charges, their asymptotic expansions are different. This happens because the momentum is carried by null waves located at the top of the $AdS_3 \times S^3$ throat, and hence there is no limit of our solutions where they approach those of the black-hole solution to arbitrary precision. This makes them different from the usual microstate geometries which have a "scaling" parameter controlling the depth of the throat, that can be tuned so that their metric and the gravitational multipoles approach those of the black hole [200, 201]. Our new solutions do not have such a parameter and hence we expect them to have a metric whose asymptotics differs from that of the black-hole solution at higher orders in the radial distance. Furthermore, although the extra fields in our solutions fluctuate along a null coordinate, they all contribute to the metric with the same sign. Hence, even if one considers an ensemble of our new solutions with D0-D4 modes, these features will not average to zero, and the $1/r$-expansion will still differ from that of the black hole.

The location of the momentum also presents a puzzle in terms of the dual CFT picture. As discussed in the introduction, we expect that, in the $a \to 0$ limit, the state dual to the superstratum consists of momentum-carrying $(0, 0)$ strands and no $(+, +)$ strands. However, in our solution taking the standard decoupling limit results in a locally $AdS_3 \times S^3 \times T^4$ spacetime, (5.37) with a deformation to the metric at the boundary of the spacetime. Furthermore, performing an alternative scaling, one can obtain an $AdS_3 \times S^3 \times T^4$ solution deformed with an non-normalizable momentum-carrying mode dual to an irrelevant deformation of the CFT. If, as mentioned above, in a generalized superstratum one were to find some microstructure at the center of a smooth cap, then there should exists an equivalent description in the dual CFT. Establishing the precise holographic dictionary for both the new microstate solution and potential generalized superstrata, is thus of great interest.

From a technical point of view, constructing generalized superstrata requires solving a new set of non-trivial BPS equations. From the perspective of six-dimensional supergravity, the ten-dimensional fields sourced by the D0 and D4 charge densities are encoded in a U(1) gauge field. Furthermore, the equations governing six-dimensional supersymmetric solutions with tensor and vector gauge fields were derived in [202]. The further generalisation to an arbitrary number of vector and tensor multiplets was carried out in [203]. It is important to remember that the construction of the original superstrata relied on the hidden linear structure of the BPS equations of six-dimensional supergravity with tensor fields, but no gauge fields [24, 204]. In [205] was shown that such a linear structure persists when one adds U(1) gauge fields. This should alleviate some technical issues in

the path of constructing smooth geometries in the F1-NS5-P frame.

Finally, in our analysis, we focused only on momentum-carrying modes that preserve the isometry of the T^4. It would be interesting to consider momentum-carrying waves coming from fluctuations of branes along some of the torus directions, and which break this isometry. These fluctuations give rise to U(1) vector fields even in the D1-D5-P duality frame. Furthermore, one can obtain examples of such solutions by performing a 9-11 flip on our solutions with D0-D4 density modes. Thus, the solutions we have constructed provide a simple way to access dynamics of compactification tori, while also preserving the isotropy of the T^4. We therefore expect the D0-D4 fluctuations to provide qualitatively similar results to analyzing more complicated excitations on the T^4 of IIA or IIB supergravity [20, 206, 207].

Chapter 6

The (amazing) Super-Maze

6.1 Introduction

String Theory is famous for its ability to count the degrees of freedom that give rise to the entropy of supersymmetric black holes, but this counting is always done in a regime of parameters where the interactions are weak and the classical black-hole solution does not exist [12, 38, 208]. This leaves open the question of how these microscopic degrees of freedom look like in the regime of parameters where the classical black hole solution exists. This question is hard to answer, because it is difficult to track these degrees as one moves to this regime of parameters, and also because the black-hole microscopic degrees of freedom look different in different duality frames.[1]

Historically, the quest for understanding the black hole degrees of freedom has been pursued from the opposite direction: people have first constructed solutions with black-hole charges that do not have a horizon and that exist in the same regime of parameters as the classical black hole solution [24–26, 33, 34, 152–154, 156–162, 164, 167, 168, 204, 209–221]. By construction, these solutions (known as microstate geometries) describe *some* of the black-hole microstates. The second step was to use holographic tools to relate some of them to the corresponding states in the CFT that counts the black-hole entropy [20, 155, 169–176]. This endeavor has been very successful, and has produced some of the finest checks of the power of holography to date. However, despite the tremendous amount of geometries constructed[2], it has not been possible to construct geometries dual to the states that account for the total black-hole entropy.

In this Chapter, we take the opposite approach: We start from a weakly-coupled system whose degrees of freedom count the entropy of the black hole, and attempt to track these degrees of freedom to the regime of parameters where the classical black-hole solution exists. Our starting point is the F1-NS5-P black hole in Type IIA string theory, whose entropy comes from the fractionation of each of the N_1 fundamental strings into N_5

[1] For example, the entropy of the D1-D5-P black hole for example comes from 1-5 strings carrying fractional momentum quanta, while the entropy of the U-dual IIA F1-NS5-P black hole comes from fractionated little strings carrying integer momenta.

[2] Of order $e^{\sqrt{N_1 N_5 N_p^{1/2}}}$ for the D1-D5 system [27, 28].

little strings living in the worldvolume of the NS5-branes [191,222]. The resulting $N_1 \times N_5$ little strings wrap the common F1-NS5 direction and can carry momentum along this direction by transverse oscillations in the other four internal directions of the NS5 branes [38][3]. It is not hard to see that in the Cardy limit the entropy of these oscillations and of their fermionic superpartners is $S_{\text{little strings}} = 2\pi\sqrt{(4+2)\frac{N_1 N_5 N_p}{6}}$, reproducing precisely the entropy of the F1-NS5-P black hole.

The M-theory uplift of this system makes the little strings less mysterious: One obtains N_5 M5 branes wrapping the common 1-5 direction (that we will henceforth call y) and that are located at different points of the M-theory circle. One fundamental string uplifts to an M2 brane wrapping y and the M-theory circle, x^{11}, and this M2 brane can break into N_5 "strips" stretching between two adjacent M5 branes. As one can see from Fig. 6.1, these M2 strips can move independently along the other internal directions of the M5 branes. Hence, the fractionation of an F1 string into N_5 little strings has a clear geometric picture in M-theory, as the breaking of an M2 brane into N_5 strips.

The purpose of this Chapter is to begin tracking the fractionated little strings, from the "zero backreaction" regime, where their counting reproduces the the F1-NS5-P black-hole entropy, to the regime of parameters where their backreaction becomes important. We will show that the momentum-carrying fractionated strings coalesce into 4-supercharge brane bound-states that have locally 16 supersymmetries.

The first step in our endeavor is to understand the backreaction of the M2 strips ending on a single M5 brane. We show that their behavior is similar to that of the *Callan-Maldacena spikes* describing backreacted F1 strings ending on D3 branes [39]. Since the M5 branes and the M2 branes extend along a common direction, the M2 branes will now form "furrows" on the M5 brane worldvolume, whose transverse section will look like a Callan-Maldacena spike. A key feature of these bound-states is that they preserve 8 supersymmetries, but if one zooms on a piece of the spike or of the furrow, one finds that locally there are 16 preserved supersymmetries, as a result of the presence of extra "dipolar" charges.

Besides the infinite M5-M2 brane furrow, one can consider more complicated bound state of multiple M5 branes and multiple M2 strips stretching between them (like the system in Fig. 6.1). This will result in a complicated maze of furrows, that connect these M5 branes. This super-maze preserves the same supersymmetries and the M5 branes and M2 branes whose charges it carries, but if one zooms in on a piece of maze, one expects that the supersymmetry will be locally enhanced from 8 to 16 supercharges.

Note that each of the $N_1 N_5$ M2 brane strips whose pull on the M5 branes gives the

[3]In the rest of this Chapter, we refer to these microstates as "Dijkgraaf-Verlinde-Verlinde (DVV) microstates" or "little-string microstates." It is important to note that the DVV microscopic counting is different in spirit from the Strominger-Vafa/D1-D5 counting: here the momentum is carried by $N_1 N_5$ fractionated strings carrying integer momenta, while in the D1-D5 CFT we have a single long effective string with modes with momentum quantized in units of $1/N_1 N_5$. Hence, the entropy of the DVV microstates comes from fractionating the F1 strings, while the Strominger-Vafa entropy comes from fractionating the momentum carriers.

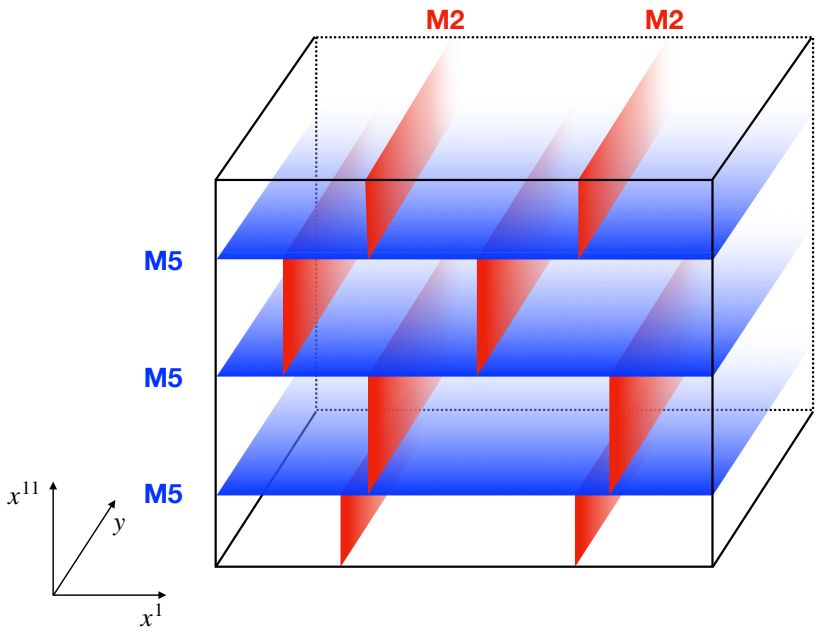

Figure 6.1: Cross-section of $N_1 = 2$ M2 branes splitting into strips between $N_5 = 3$ M5 branes. The vertical axis is the M-theory direction, and the horizontal axis represents one of the internal directions of the M5 branes, x^1. The strips can carry momentum along the y-circle, which is common to the M2 and M5 branes.

super-maze can be located at an arbitrary position inside the T^4 or $K3$ wrapped by the M5 branes. Therefore, the dimension of the moduli space of super-mazes is $4N_1N_5$. This matches, as expected, the dimension of the moduli space of the D1-D5 (F1-NS5) system deformations that preserve rotational invariance in the transverse space [15, 19, 223]

The second step in our endeavour is to add momentum to the super-maze, in order to construct a brane bound-state configuration that has 16 supercharges locally and that carries the charges of a black hole with a macroscopically-large event horizon. To do this, we will first construct the two-charge bound states formed by M2 branes and momentum, and by M5 branes and momentum. The former is the M-theory uplift of the F1-P system, whose solutions have been described in supergravity in [182]. The momentum is carried by the transverse oscillations of the M2 branes and, if one zooms in near a piece of the momentum-carrying M2 brane one finds that the supersymmetry is enhanced to 16 supercharges.

Similarly, the M5 branes can carry momentum by transverse fluctuations, that we can restrict to be oriented only along the M-theory direction, so that the resulting solution is

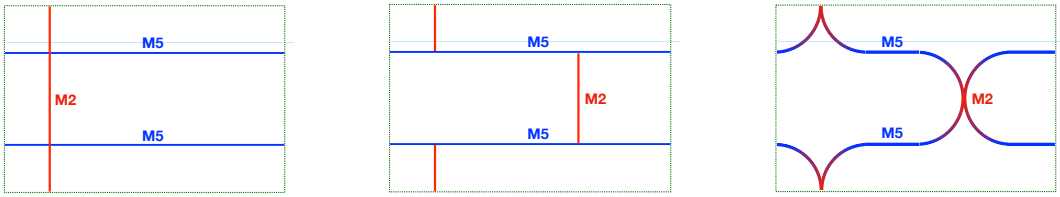

Figure 6.2: The fractionation of M2 branes into strips and the super-maze: Before the fractionation (left panel) the M2 brane does not interact with the M5 branes, and can be freely taken away. After the fractionation, each strip of the M2 branes can move independently, giving the naïve configuration in the middle panel. However, the M2 strips pull on the M5 brane, creating the super-maze depicted in the right panel.

spherically symmetric in the non-compact spacetime directions. This system is the uplift of the NS5-P-D0-D4 solution found in [224]. This solution also preserves 8 supersymmetries, but locally the supersymmetry is enhanced to 16. For both the M2-P and the M5-P system, this is ensured by the presence of dipolar charges, which can be thought of as the "glue" needed to construct the bound states of two-charge system. Of course, for the M5-P system one can consider other types of glue, coming for example from 2 species of M2 branes inside the M5-brane worldvolume. The resulting configuration is called a magnetube, and its supergravity solution was constructed in [192, 225].

The main result of this Chapter is to identify the ingredients needed to construct the bound states of the NS5-F1-P Type IIA system and of its M-theory M2-M5-P uplift. These bound states describe the DVV little strings carrying momentum in the regime of parameters where the brane interactions are taken into account. We show that there exists a supersymmetry projector corresponding to a brane configuration that has 16-supersymmetries locally and 4 globally, and which describes the zooming in on a piece of the momentum-carrying M2-M5 maze. Besides the M2, M5 and P charges of the black hole, this system has 6 other dipolar charges, which are necessary to form the glue that transforms these branes into a bound state.

The entropy of the DVV little strings carrying momentum reproduces (upon taking into account all bosonic and fermionic polarizations) the entropy of the F1-NS5-P black hole [38], and our result shows that the microstates carrying this entropy correspond (upon taking brane interactions into account) to a momentum-carrying super-maze whose supersymmetry is enhanced everywhere to 16 supercharges locally.

It is important to emphasize that the local enhancement of supersymmetry to 16 supercharges is the hallmark of the existence in certain duality frames of smooth supergravity solutions that result from the backreaction of these configurations and, more generally, of the absence of event horizons. We will explain the connection between local enhancement of supersymmetry and smooth horizonless solutions in more detail in Section 6.5. Confirming that the entropy of this black hole comes from horizonless super-mazes would

constitute a proof of the fuzzball proposal for three-charge supersymmetric black holes in String Theory, and we are looking forward to the construction of the fully-backreacted solution corresponding to the brane microstates we have discovered.

Our result points towards a change of strategy in the fuzzball/microstate geometry programme of constructing horizonless solutions dual to microstates of string-theory black holes. Until now, the strategy of this programme has been to "blow up" the delta-function source of the harmonic functions of the branes making up the black hole, and replace it by an extended source in the *non-compact* spatial dimensions. This has resulted in a huge plethora of solutions [24–26, 33, 34, 152–154, 156–162, 164, 167, 168, 204, 209–221], all of which break the spherical symmetry of the black-hole horizon. However, the connection between these solutions and the microstates that give rise to the black-hole entropy at weak coupling is difficult to establish, and has only been worked out for superstrata, whose entropy is parametrically smaller than that of the black hole [27, 28]. Furthermore, all the known superstrata have at least one unit of angular momentum in one of the non-compact angular directions in which supersymmetric black holes cannot rotate[4].

Our work points out a new route for constructing microstate geometries that solves these two challenges at the same time: the momentum-carrying super-maze preserves the same spacetime spherical symmetry as the black-hole solution, and it is directly connected to DVV fractionated strings that give rise to the entropy of the F1-NS5-P black-hole in Type IIA String Theory. Furthermore, as we will explain in Section 6.5 the fact that locally the supersymmetry is enhanced to 16 supersymmetries indicates that the fully-backreacted super-mazes will give rise to smooth horizonless black hole microstate geometries, and will not have an event horizon.

In Section 6.2 we review the construction of two-charge bound states and the role of branes that act as "glue" and transform singular configurations of branes into bound states preserving locally 16 supercharges. In Section 6.3 we describe the construction of the new three-charge bound state, which preserves 16 supercharges locally and is a piece of the super-maze coming from the backreaction of DVV black-hole microstates. In Section 6.4 we explain the link between the projector and the local orientation of the branes that make up the super-maze, and confirm our construction by showing that the energy of the super-maze saturates the BPS bound. In Section 6.5 we discuss the relation between smooth horizonless supergravity solutions and brane configurations preserving locally 16 supercharges, and argue that the backreaction of the super-maze will give rise to bubbling horizonless solutions. In Appendix C we collect the projectors corresponding to branes, strings, KK Monopoles and momentum in String and M Theory.

Note on nomenclature: Throughout this Chapter we will refer to two- and three-charge systems as systems of two or three sets of branes that preserve 8 respectively 4 common supersymmetries and that exert no force on each other. Thus, a system of D5 branes and parallel D1 branes can be properly called a two-charge system, but a system of D3 branes and parallel D1 branes is not: the D1 branes are attracted to the D3 branes

[4]The five-dimensional supersymmetric three-charge black holes can have finite J_L, but their J_R must be zero. In contrast superstrata always have $J_R \neq 0$.

and form a bound state that has 16 supercharges everywhere and is T-dual to a single oblique stack of parallel D2 branes. Similarly a D7 brane and a parallel D1 brane do not constitute a two-charge system, because the D1 branes run away from the D7 branes.

6.2 Making two-charge bound states out of strings and branes

The vacuum of Type II String Theory preserves 32 supersymmetries. Adding excitations such as strings or branes decreases the number of preserved supersymmetries. Indeed, one can derive using the BPS equations that the presence of branes imposes a constraint on the Killing spinor ϵ:

$$P\,\epsilon \;=\; -\,\epsilon\,, \quad \text{or equivalently} \quad \Pi\,\epsilon \;\equiv\; \frac{1}{2}(1+P)\,\epsilon \;=\; 0\,, \tag{6.1}$$

where P is a traceless *involution* ($P^2 = 1$), typically a product of gamma matrices, that depend on the exact type and orientation of the object considered. Thus Π is a projector, verifying $\Pi^2 = \Pi$. A list of the involutions corresponding to branes, strings, solitons and momentum waves is given in Appendix C. The constraint (6.1) divides the number of preserved global supersymmetries by two.

If one considers configurations with several types of branes whose supersymmetries are compatible, the constraints add up. For example, for a two-charge system, the Killing spinor must respect

$$\Pi_1\,\epsilon \;=\; 0\,, \quad \text{and} \quad \Pi_2\,\epsilon \;=\; 0\,. \tag{6.2}$$

In other words, the Killing spinor must lie in the intersection of the kernels of Π_1 and Π_2. The dimension of this intersection is the number of preserved global supersymmetries (8).

The number of states of a two-charge system is however much larger than one can surmise by considering the individual motion of its component branes. Indeed, the branes can form bound states[5], which contain more fields than those of the naïve multi-brane solution. These fields can be thought of as coming from the dipolar branes that act as the "glue" needed to form the bound state, and which also give rise to a local enhancement of the number of preserved supersymmetries to 16.

For a general bound state, the Killing spinor satisfies

$$\widehat{\Pi}\,\epsilon \;\equiv\; \frac{1}{2}(1+\alpha_1 P_1+\cdots+\alpha_n P_n)\,\epsilon \;=\; 0\,, \tag{6.3}$$

where P_i are the traceless involutions associated to the branes whose charges the bound state has and where, for each species of brane, i, the coefficient α_i is the ratio between the

[5]In the D0-D4 system for example, the individual motion of the branes corresponds to the Coulomb branch, where the branes do not form a bound state. However, the large degeneracy of the system comes from the Higgs branch, which describes bound states of D0 branes inside the D4 branes.

charge density corresponding to this brane, Q_i,[6] and the mass density of the full bound state, M:

$$\alpha_i \equiv \frac{Q_i}{M}\,. \tag{6.4}$$

Hence, the projector can be written as

$$\widehat{\Pi} \;\equiv\; \frac{1}{2M}(M + Q_1 P_1 + \cdots + Q_n P_n)\,. \tag{6.5}$$

The number of preserved supersymmetries is now the dimension of the kernel of $\widehat{\Pi}$. This operator is in general not a projector, but when it is, the configuration preserves 16 global supersymmetries.

It is thus possible to reveal the extra dipole charges needed to construct the bound states of a two- or three-charge system by finding involutions corresponding to suitable branes and tuning their charges to make $\widehat{\Pi}$ a projector. For a given bound state, the solution for α_i is often not unique: There often exists a whole moduli space of values of the charges that make $\widehat{\Pi}$ a projector. One can then imagine varying these charge densities along the internal dimensions of the bound state, so that the constraint becomes:

$$\widehat{\Pi}(\boldsymbol{x})\,\epsilon(\boldsymbol{x}) \;\equiv\; \frac{1}{2}\Big[1 + \alpha_1(\boldsymbol{x})P_1 + \cdots + \alpha_n(\boldsymbol{x})P_n\Big]\epsilon(\boldsymbol{x}) \;=\; 0\,, \tag{6.6}$$

where $\boldsymbol{x}$ denotes the internal dimensions of the bound state. Doing so, the number of *local* preserved supersymmetries is still 16. However, the number of *global* supersymmetries can be much less: it is the dimension of the common kernel to the projectors at all possible values of $\boldsymbol{x}$. The global Killing spinor does not depend on the position $\boldsymbol{x}$, and it must satisfy

$$\forall\,\boldsymbol{x}\,, \quad \widehat{\Pi}(\boldsymbol{x})\,\epsilon \;=\; 0\,, \tag{6.7}$$

where ϵ must be constant.

A common way to ensure that at least some amount of supersymmetry is preserved globally is to rewrite the projectors as

$$\widehat{\Pi}(\boldsymbol{x}) \;=\; f_1(\boldsymbol{x})\Pi_1 + \cdots + f_k(\boldsymbol{x})\Pi_k \tag{6.8}$$

where $\Pi_1, \ldots, \Pi_k$ are commuting projectors, and $f_1, \ldots, f_k$ can be any matrix-valued functions. Then, satisfying (6.7) is equivalent to

$$\Pi_1\,\epsilon \;=\; \ldots \;=\; \Pi_k\,\epsilon \;=\; 0\,, \tag{6.9}$$

so the number of preserved global supersymmetries is the dimension of the intersection of the kernels of $\Pi_1, \ldots, \Pi_k$.

When constructing bound states, one typically starts with the set of global charges and their projectors, $\Pi_1, \ldots, \Pi_k$. Combining (6.6) with (6.8) then leads to constraints on the charges of each constituent, Q_i, and hence on α_i.

[6] Note that the dependence in the string coupling, g_s, enters in the Q_i's.

The distinction between local and global supersymmetries is important, and is at the core of the results of this work. As we explained in the Introduction, by constructing two- and three-charge bound states preserving 16 local supersymmetries, we ensure that we construct microstates of these two- or three-charge systems and that furthermore their backreaction will not give rise to an event horizon.

This bound-state making philosophy was first used to conjecture the existence of superstrata [30], but the method presented here is a generalisation of that of [30], where an orthogonal momentum, $\mathrm{P}(\psi)$, was imposed to be one of the dipoles. In the following subsection, we will first illustrate the bound-state making philosophy with several examples of two-charge bound states.

6.2.1 The F1-P bound state

Consider an F1-P system where the strings wrap a compact direction, y, and momentum is also along y direction. The involutions and projectors associated to them are (see Appendix C):

$$\begin{aligned} P_{\mathrm{F1}(y)} &= \Gamma^{0y}\sigma_3\,, \qquad \Pi_{\mathrm{F1}(y)} = \frac{1}{2}(1+P_{\mathrm{F1}(y)})\,,\\ P_{\mathrm{P}(y)} &= \Gamma^{0y}\,, \qquad \Pi_{\mathrm{P}(y)} = \frac{1}{2}(1+P_{\mathrm{P}(y)})\,. \end{aligned} \tag{6.10}$$

When the F1 and P do not form a bound state, the constraints on the Killing spinor add up

$$\Pi_{\mathrm{F1}(y)}\epsilon = \Pi_{\mathrm{P}(y)}\epsilon = 0\,. \tag{6.11}$$

and the system preserves 8 supersymmetries everywhere.

It is possible to form a bound state possessing the same global charges as this system, but preserving locally 16 supersymmetries. In order to do so, one needs to add dipolar transverse strings and momentum which we choose to be along a single transverse direction inside the T^4, that we call x_1 (more complicated choices are also possible but not illustrative for our purpose here):

$$\begin{aligned} P_{\mathrm{F1}(1)} &= \Gamma^{01}\sigma_3\,, \qquad \Pi_{\mathrm{F1}(1)} = \frac{1}{2}(1+P_{\mathrm{F1}(1)})\,,\\ P_{\mathrm{P}(1)} &= \Gamma^{01}\,, \qquad \Pi_{\mathrm{P}(1)} = \frac{1}{2}(1+P_{\mathrm{P}(1)})\,. \end{aligned} \tag{6.12}$$

The objective is to construct a local projector, $\Pi_{\text{F1-P bound}}$, that can be written in two ways:

$$\Pi_{\text{F1-P bound}} = \frac{1}{2}\Big(1+\alpha_1 P_{\mathrm{F1}(y)}+\alpha_2 P_{\mathrm{P}(y)}+\alpha_3 P_{\mathrm{F1}(1)}+\alpha_4 P_{\mathrm{P}(1)}\Big) \tag{6.13}$$

$$= f_1\Pi_{\mathrm{F1}(y)}+f_2\Pi_{\mathrm{P}(y)} \tag{6.14}$$

where $\alpha_1,\ldots,\alpha_4$ are real numbers, and f_1, f_2 are matrices.

The equation $\Pi^2_{\text{F1-P bound}} = \Pi_{\text{F1-P bound}}$ first leads to

$$\alpha_1^2+\alpha_2^2+\alpha_3^2+\alpha_4^2 = 1\,, \qquad \alpha_1\alpha_4+\alpha_2\alpha_3 = 0\,, \tag{6.15}$$

while equalizing (6.13) and (6.14) leads to

$$\begin{aligned} \alpha_3 + \alpha_4 &= 0\,, \qquad \alpha_1 + \alpha_2 &= 1\,, \\ f_1 &= \alpha_1 - \alpha_4 \Gamma^{y1}\sigma_3\,, \qquad f_2 &= \alpha_2 - \alpha_3 \Gamma^{y1}\sigma_3\,. \end{aligned} \tag{6.16}$$

The solution given here for f_1 and f_2 is not unique.

Solving these equations is straightforward, the solution depends on the choice of an arbitrary angle, θ:

$$\begin{aligned} \Pi_{\text{F1-P bound}} &= \frac{1}{2}\Big[1 + c^2 P_{\text{F1}(y)} + s^2 P_{\text{P}(y)} + cs P_{\text{F1}(1)} - cs P_{\text{P}(1)}\Big] \\ &= c\Big(c + s\,\Gamma^{y1}\sigma_3\Big)\Pi_{\text{F1}(y)} \;+\; s\Big(s - c\,\Gamma^{y1}\sigma_3\Big)\Pi_{\text{P}(y)}\,, \end{aligned} \tag{6.17}$$

where $c \equiv \cos\theta$ and $s \equiv \sin\theta$.

Geometrically, the angle θ corresponds to the inclination of the string in the (y, x_1) plane. If θ is constant, the configuration is a straight string tilted in the (y, x_1)-plane, with transverse momentum. This transversely boosted F1 string preserves 16 supersymmetries.[7] In the limit $\theta = 0$, this is a pure F1 string along y, and when $\theta = \pi/2$ this is a pure momentum wave along y.

One can bend the string by allowing θ to vary along it. The resulting configuration still preserves 16 supersymmetries locally, but only 8 globally.

6.2.2 The NS5-P bound state

The same exercise can be done for the NS5-P system in type IIA. We start with NS5 branes extending along the directions $y, x_1, \ldots, x_4$, and momentum along y. The involutions associated to them are:

$$P_{\text{NS5}(y1234)} = \Gamma^{0y1234}\,, \qquad P_{\text{P}(y)} = \Gamma^{0y}\,. \tag{6.18}$$

Once again, if these constituents do not form a bound state the configuration preserves 8 supersymmetries. They can also form bound states that preserve locally 16 supersymmetries. Contrary to the fundamental string, the NS5-brane does not need to bend in the transverse directions to carry momentum. To make the bound state, one possibility is to use internal dipolar D4-branes (extending along the directions $x_1, \ldots, x_4$) and D0-branes [224]:

$$P_{\text{D4}(1234)} = \Gamma^{01234} i\sigma_2\,, \qquad P_{\text{D0}} = \Gamma^{0} i\sigma_2\,. \tag{6.19}$$

Note that this is not the only possible choice of dipoles. We can also form an F1-NS5 bound state by adding as "glue" two orthogonal sets of D2 branes. This system can be obtained from the one we have by two T-dualities along the NS5 internal directions that are not wrapped by the F1 strings. Its M-theory uplift is know as the magnetube [192, 225].

[7] For an illustration, see Fig. 2 and Fig. 3 in [224].

Another possibility to construct bound states with P and NS5 charges is to put a momentum-carrying transverse wave on the NS5 brane. This configuration can easily be obtained by dualizing the F1 strings with a transverse momentum wave described above and its "glue" consists of a dipolar NS5 charge and angular momentum. This solution breaks the spherical symmetry of the black-hole solution. Since in this Chapter we are interested in constructing bound states that respect this spherical symmetry and can describe locally the backreaction of the DVV microstates, we will describe in detail the brane bound states created using D0-D4 glue.

One needs to construct a projector satisfying

$$\begin{aligned} \Pi_{\text{NS5-P bound}} &= \frac{1}{2}\Big(1+\alpha_1 P_{\text{NS5}(y1234)}+\alpha_2 P_{\text{P}(y)}+\alpha_3 P_{\text{D0}}+\alpha_4 P_{\text{D4}(1234)}\Big) && (6.20)\\ &= f_1\Pi_{\text{NS5}(y1234)}+f_2\Pi_{\text{P}(y)} && (6.21)\end{aligned}$$

as well as the usual condition on projectors $\Pi^2_{\text{NS5-P bound}} = \Pi_{\text{NS5-P bound}}$, for some real numbers $\alpha_1,\ldots,\alpha_4$ and matrices f_1, f_2.[8]

The solution to this system is:

$$\begin{aligned} \Pi_{\text{NS5-P bound}} &= \frac{1}{2}\Big[1+c^2 P_{\text{NS5}(y1234)}+s^2 P_{\text{P}(y)}+csP_{\text{D0}}-csP_{\text{D4}(1234)}\Big]\\ &= c(c+s\,\Gamma^y i\sigma_2)\Pi_{\text{NS5}(y1234)} \;+\; s(s-c\,\Gamma^y i\sigma_2)\Pi_{\text{P}(y)}\,,\end{aligned} \tag{6.22}$$

where again $c\equiv\cos\theta$ and $s\equiv\sin\theta$.

6.2.3 The NS5-F1 bound state

One can form an NS5-F1 bound state in type IIA using a similar procedure. Consider an NS5-F1 system where the NS5 extends along the directions $y, x_1, \ldots, x_4$, and the string is along y. The involutions associated to them are

$$P_{\text{NS5}(y1234)} = \Gamma^{0y1234}\,, \qquad P_{\text{F1}(y)} = \Gamma^{0y}\sigma_3\,. \tag{6.23}$$

The bound state can be obtained from the NS5-P system by performing two T-dualities along the directions y and x_1. Again, the choice of x_1 among the four torus directions is at this point arbitrary.

The dipole charges needed to form it are D4-branes extending along the directions $y, x_2\ldots, x_4$, and D2-branes along the direction y and x_1:

$$P_{\text{D4}(y234)} = \Gamma^{0y234}i\sigma_2\,, \qquad P_{\text{D2}(y1)} = \Gamma^{0y1}\sigma_1\,. \tag{6.24}$$

The projector of this bound state is

$$\begin{aligned} \Pi_{\text{NS5-F1 bound}} &= \frac{1}{2}\Big[1+c^2 P_{\text{NS5}(y1234)}+s^2 P_{\text{F1}(y)}+csP_{\text{D2}(y1)}+csP_{\text{D4}(y234)}\Big]\\ &= c\Big(c+s\,\Gamma^1 i\sigma_2\Big)\Pi_{\text{NS5}(y1234)} \;+\; s\Big(s-c\,\Gamma^1 i\sigma_2\Big)\Pi_{\text{F1}(y)}\,.\end{aligned} \tag{6.25}$$

[8] It is not necessary to do this computation again. One can find the result by dualizing the F1-P system (if the directions are not compact, a T-duality can be seen as a solution-generating technique rather than a proper duality). The duality chain is $T_1 - S - T_{1234} - S - T_1$.

where again $c \equiv \cos\theta$ and $s \equiv \sin\theta$, and the angle θ is a function of the coordinates $y, x_1, \ldots, x_4$.

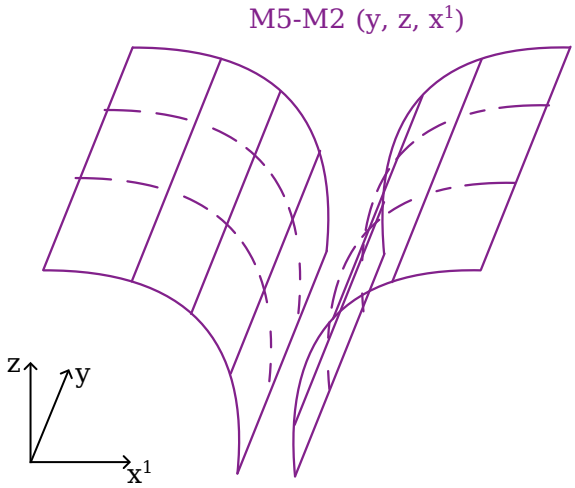

Figure 6.3: The backreaction of the M5-M2 bound state, projected onto the space (y, x_1, z). The M2-branes pull the M5-branes, forming a furrow. The mechanism is similar to the formation of a Callan-Madacena spike in the D3-F1 brane system.

The angle θ and the form of the projector have a clear geometric interpretation for the F1-P bound state (as the tilt of the string). For the NS5-F1 bound state, the interpretation is more complicated: one needs first to uplift the configuration to M-theory. The projector is then given by:

$$\Pi_{\mathrm{M5-M2}} = \frac{1}{2}\Big[1 + c^2 P_{\mathrm{M5}(y1234)} + s^2 P_{\mathrm{M2}(y\,z)} - csP_{\mathrm{M5}(y234\,z)} + csP_{\mathrm{M2}(y1)}\Big]\,. \tag{6.26}$$

The brane system then consists of M5-branes and M2-branes sharing one common direction, y. The M2-branes are also extended along the M-theory circle, denoted by z. It is easy to see that M2 branes terminating on the M5 branes will pull them along the (previously orthogonal) M-theory direction. This mechanism is similar to the formation of a Callan-Maldacena spike (see Fig. 6.3). At each location on the M5-brane, the angle θ corresponds to the tilt of the brane in the z direction. Of course, for a generic spike, the pull of the M2 brane will affect all the 4 directions of the NS5 brane, (x_1, x_2, x_3, x_4), and the spike will be described by a complicated function of all these four variables. To obtain the bound state depicted in Fig. 6.3, corresponding to the projector (6.25), we can either smear the M2 branes along the directions (x_2, x_3, x_4) or one can zoom in at a location of the spike where the tangent to the spike is orthogonal to x_1.

Another (more familiar) possibility to construct bound states with F1 and NS5 charges is to add a dipolar KKM charge (extending in the space transverse to the NS5 worldvolume and with the special direction along the F1-NS5 common direction) as well as angular momentum, J. This gives rise to a F1-NS5 supertube with KKM-J dipole charge, and

its supergravity solution is the S-dual of the well-known Lunin-Mathur geometry [16, 18]. Much like its better known supertube cousins [14, 180], the KKM can wrap an arbitrary curve in the four dimensions transverse to the NS5 branes, and the solution preserves 8 supercharges. As reviewed in [30], when one zooms near the supertube profile this configuration preserves locally 16 supercharges and this enhancement of supersymmetry comes from the presence of the KKM and angular-momentum "glue", and is equivalent to the fact that the supergravity solution corresponding to the F1-NS5-KKM-J supertube is smooth [226].

Starting from this two-charge bound state one can also add momentum, and build three-charge superstrata: bound states that have the same charges as an F1-NS5-P black hole and give rise to a smooth supergravity solution [24]. However, since our purpose in this Chapter is to build three-charge brane bound states that have the same charges as a black hole but that do not break the rotational symmetry of the black-hole horizon, we will not use the "KKM-angular momentum glue", and focus instead on the "D4-D2 glue".

6.2.4 The relation between the M5-M2 furrow and the Callan-Maldacena spike

There are two ways to relate the M2-M5 furrow whose Type-IIA reduction gives rise to the NS5-F1 bound state to the better known F-string and D-string spikes constructed in the D3 brane worldvolume by Callan and Maldacena [39, 227].

The first is to start with a D4-brane in the directions 1234, and an F1-string along the direction y, ending on the D4-brane. This picture is valid when $g_s \ll 1$. As one increases g_s or the number of F1 strings, these strings pull on the D4 brane and give rise to a spike. Much like the D3-F1 spike, this D4-F1 spike can be constructed as a solution to the D4-brane DBI action.

The M5-M2 bound state we consider is dual to the D4-F1 spike, after 11-dimensional uplift along z, and a flip in the coordinates (y, z):

$$\begin{pmatrix} \text{D4}(x^1x^2x^3x^4) \\ \text{F1}(y) \end{pmatrix}_{\text{IIA}} \xrightarrow{\text{uplift on } z} \begin{pmatrix} \text{M5}(z, x^1x^2x^3x^4) \\ \text{M2}(z, y) \end{pmatrix}_{\text{M}} \xrightarrow{(z,y)\text{-flip}} \begin{pmatrix} \text{M5}(y, x^1x^2x^3x^4) \\ \text{M2}(y, z) \end{pmatrix}_{\text{M}}. \tag{6.27}$$

Another way to obtain an M2-M5 furrow – but this time smeared over one of the internal directions – is to construct the furrow corresponding to a D2 along the directions $0, y, z$ that ends on a D4 brane extended along $0, y, 1, 2, 3$. From the perspective of the D4 brane DBI action, this smeared furrow has exactly the same solution as a D1-D3 spike [227]. This furrow can also be constructed using the non-Abelian DBI action of the D2 brane; the D2 non-commuting worldvolume fields are the same as the D6 brane fields describing a D6 brane ending on a D8 brane [228]. Upon uplifting the D2-D4 furrow to 11 dimensions, one obtains a solution smeared along this direction, which is precisely the same as an M2-M5 furrow smeared along one of the M5-brane worldvolume directions:

$$\begin{pmatrix} \text{D3}(x^1x^2x^3) \\ \text{D1}(z) \end{pmatrix}_{\text{IIB}} \xrightarrow{\text{T}_y} \begin{pmatrix} \text{D4}(y, x^1x^2x^3) \\ \text{D2}(y, z) \end{pmatrix}_{\text{IIA}} \xrightarrow{\text{uplift on } x^4} \begin{pmatrix} \text{M5}(y, x^1x^2x^3\widetilde{x^4}) \\ \text{M2}(y, z) \end{pmatrix}_{\text{M}}. \tag{6.28}$$

6.3 The three-charge NS5-F1-P bound state

This Section is devoted to the construction of the bound states of the three-charge system. As explained in the Introduction, we expect the bound state to have both the three charges of the NS5-F1-P system, but also several dipolar charges, which constitute the glue needed to construct a bound state that has locally 16 supercharges.

6.3.1 Constructing the projector

We consider the Type IIA three-charge system with NS5-branes extending along the directions $y, x_1, \ldots, x_4$, as well as F1 strings and momentum along the direction y. The involutions that enter in the construction of their corresponding projectors are:

$$P_{\text{NS5}(y1234)} = \Gamma^{0y1234}, \qquad P_{\text{F1}(y)} = \Gamma^{0y}\sigma_3, \qquad P_{\text{P}(y)} = \Gamma^{0y}. \tag{6.29}$$

In order to form a bound state, one needs to find the dipole charges that bind these branes into a configuration with 16 supersymmetries locally. In Section 6.2 we explained how to construct two-charge bound states for the F1-P, NS5-F1 and NS5-P systems: For each system, we found several pairs of dipole charges acting as a glue between the constituents to form bound states. However, upon demanding that these bound states preserve the rotational invariance of the black-hole horizon, only a limited choice of dipole-brane glue remained. The intuitive first attempt at constructing the NS5-F1-P three-charge bound state is to add all the six dipole charges that enter in the construction of the rotationally-invariant two-charge bound states (summarized in Table 6.1), and to try to construct a projector. We can easily find that this only works if the dipole charges of the F1-P bound state are oriented along the same direction, x_1, as the dipole charges of the NS5-F1 bound state.

NS5(y1234)	F1(y)	P(y)	D4(y234)	D2(y1)	D4(1234)	D0	F(1)	P(1)
$\otimes$	$\otimes$		$\times$	$\times$				
$\otimes$		$\otimes$			$\times$	$\times$		
	$\otimes$	$\otimes$					$\times$	$\times$

Table 6.1: Each line describes a two-charge bound state whose charges are two of the three charges of the NS5-F1-P brane systems (denoted by $\otimes$). Each bound state contains two more dipole charges, denoted by $\times$. We attempt to construct a three-charge bound state with NS5-F1-P and all six dipole charges.

Constructing the projector for this bound state follows the same rules as for the two-charge systems. One needs to determine the local charges, α_i, and the matrices, f_j, such that the expression:

$$\begin{aligned}\Pi_{\text{NS5-F1-P bound}} &= \frac{1}{2}\Big[1+\alpha_1 P_{\text{NS5}(y1234)}+\alpha_2 P_{\text{F1}(y)}+\alpha_3 P_{\text{P}(y)}+\alpha_4 P_{\text{D4}(y234)} \\ &\qquad +\alpha_5 P_{\text{D2}(y1)}+\alpha_6 P_{\text{P}(1)}+\alpha_7 P_{\text{F1}(1)}+\alpha_8 P_{\text{D4}(1234)}+\alpha_9 P_{\text{D0}}\Big]\,. \qquad (6.30)\\ &= f_1\Pi_{\text{NS5}(y1234)}+f_2\Pi_{\text{F1}(y)}+f_3\Pi_{\text{P}(y)}\,, \qquad (6.31)\end{aligned}$$

is a projector ($\Pi^2_{\text{NS5-F1-P bound}}=\Pi_{\text{NS5-F1-P bound}}$) and moreover, as the second line illustrates, is compatible everywhere with the supersymmetries of the NS5-F1-P system.

From (6.30) and (6.31) we find:

$$\begin{gathered}\alpha_1+\alpha_2+\alpha_3=1\,,\quad \alpha_4-\alpha_5=0\,,\quad \alpha_6+\alpha_7=0\,,\quad \alpha_8+\alpha_9=0\,,\\ \begin{aligned} f_1 &= \alpha_1+\alpha_4\,\Gamma^1 i\sigma_2-\alpha_8\,\Gamma^y i\sigma_2\,,\\ f_2 &= \alpha_2-\alpha_5\,\Gamma^1 i\sigma_2-\alpha_6\,\Gamma^{y1}\sigma_3\,,\\ f_3 &= \alpha_3-\alpha_9\,\Gamma^y i\sigma_2-\alpha_7\,\Gamma^{y1}\sigma_3\,.\end{aligned}\end{gathered} \qquad (6.32)$$

Here again the values of the functions f_j are not unique. The equation $\Pi^2_{\text{NS5-F1-P bound}}=\Pi_{\text{NS5-F1-P bound}}$ leads to:

$$\sum_{i=1}^{9}\alpha_i^2=1\,, \qquad (6.33)$$

$$\alpha_2\alpha_3+\alpha_6\alpha_7=0\,,\qquad \alpha_3\alpha_5+\alpha_7\alpha_9=0\,,\qquad \alpha_2\alpha_9-\alpha_5\alpha_6=0\,, \qquad (6.34)$$

$$\alpha_3\alpha_4+\alpha_6\alpha_8=0\,,\qquad \alpha_1\alpha_3+\alpha_8\alpha_9=0\,,\qquad \alpha_1\alpha_2-\alpha_4\alpha_5=0\,, \qquad (6.35)$$

$$\alpha_1\alpha_6-\alpha_4\alpha_9=0\,,\qquad \alpha_1\alpha_7-\alpha_5\alpha_8=0\,,\qquad \alpha_2\alpha_8-\alpha_4\alpha_7=0\,. \qquad (6.36)$$

The solutions to this system can be expressed in terms of three real numbers (a,b,c) satisfying $a^2+b^2+c^2=1$:

$$\alpha_1=a^2\,,\qquad \alpha_2=b^2\,,\qquad \alpha_3=c^2\,, \qquad (6.37a)$$

$$\alpha_4=ab\,,\qquad \alpha_5=ab\,,\qquad \alpha_6=bc\,, \qquad (6.37b)$$

$$\alpha_7=-bc\,,\qquad \alpha_8=-ac\,,\qquad \alpha_9=ac\,. \qquad (6.37c)$$

Then the projector is:

$$\begin{aligned}\Pi_{\text{NS5-F1-P bound}} &= \frac{1}{2}\Big[1+a^2 P_{\text{NS5}(y1234)}+b^2 P_{\text{F1}(y)}+c^2 P_{\text{P}(y)}+ab\left(P_{\text{D4}(y234)}+P_{\text{D2}(y1)}\right)\\ &\qquad +bc\left(P_{\text{P}(1)}-P_{\text{F1}(1)}\right)-ac\left(P_{\text{D4}(1234)}-P_{\text{D0}}\right)\Big]\,.\end{aligned} \qquad (6.38)$$

This projector preserves locally 16 supersymmetries. We now allows the parameters a, b, c to be functions of the coordinates $y, x_1, \ldots, x_4, z$. The supersymmetries rotate, but the projector still preserves the 4 global supercharges of the NS5-F1-P brane system:

$$\begin{aligned}\Pi_{\text{NS5-F1-P bound}} &= a\,(a + b\,\Gamma^1 i\sigma_2 + c\,\Gamma^y i\sigma_2)\;\Pi_{\text{NS5}(y1234)} \\ &+\; b\,(b - a\,\Gamma^1 i\sigma_2 - c\,\Gamma^{y1}\sigma_3)\;\Pi_{\text{F1}(y)} \\ &+\; c\,(c - a\,\Gamma^y i\sigma_2 + b\,\Gamma^{y1}\sigma_3)\;\Pi_{\text{P}(y)}\,.\end{aligned} \tag{6.39}$$

We represent the relative densities of the branes whose charges enter in this projector in Fig. 6.4.

Of course, in order for the projector (6.38) to correspond to a physical brane configuration the densities of branes wrapping a certain direction should not be functions of this direction. Since these densities are related to the coefficients in the projector via equation (6.4) this puts certain constraints on the parameters a, b and c. These constraints will be further explained in Section 6.4.

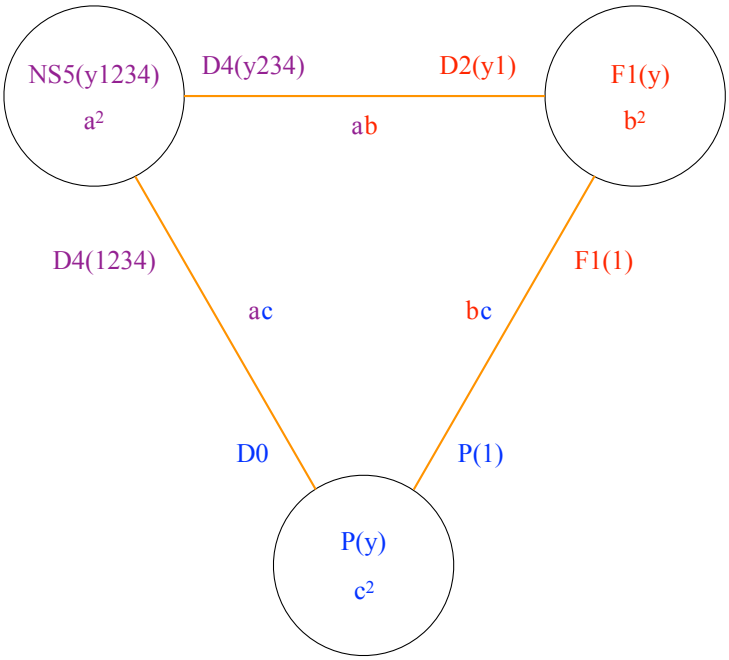

Figure 6.4: Schematic representation of the three-charge NS5-F1-P bound state. The nodes represent the three charges of the bound state. Every combination of two nodes and the orange line joining them corresponds to a two-charge bound state, and the dipole charges and their coefficients in the projector are indicated next to the line.

6.3.2 The M5-M2-P triality

It is also possible to uplift the three-charge bound state to M-theory, and argue that it is related to the local structure of DVV black-hole microstates.

The charges and dipole charges of the bound state have a clear M-theory origin. For simplicity we can rename the M-theory direction $x_{11} \equiv z$. As we explained in Section 6.2.3, the two-charge bound state of F1 strings and NS5 branes can be interpreted in M-theory as the near-brane limit of the furrow created by the backreaction of M2 branes that end on M5 branes. From the perspective of the M5 brane worldvolume theory, this furrow can be constructed similarly to the Callan-Maldacena spike describing the F1 strings terminating on D3 branes.

From the M-theory perspective, the dipole branes which form the glue of the M2-M5-P bound state are also M2 and M5 branes and momentum, oriented differently. The NS5-brane along $(y1234)$ becomes an M5 brane along the same directions, and the F1 string along (y) becomes an M2 brane along (y, z). The gluing dipole branes correspond to M5 branes along $(1234z)$ and along $(y234z)$, M2 branes along $(y1)$ and along $(1z)$, and momentum along 1 and along z. Fig. 6.5 reveals this triality.

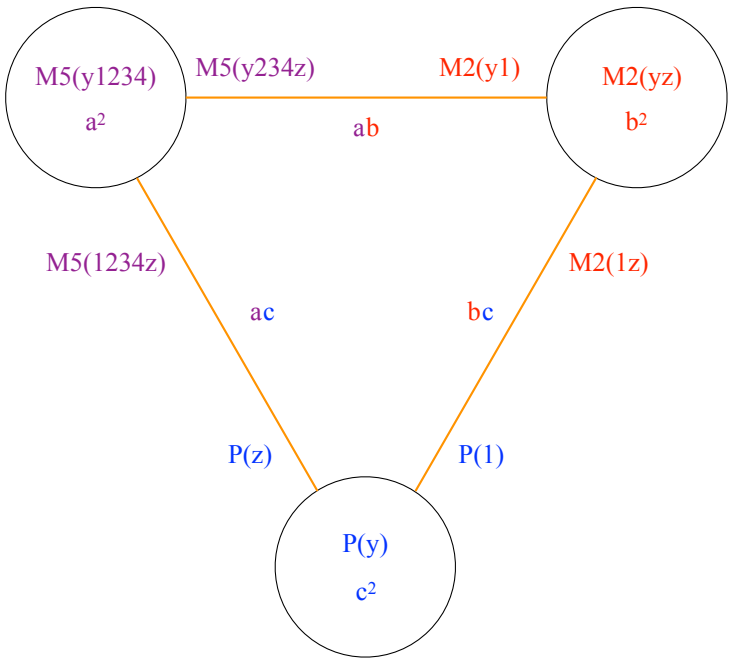

Figure 6.5: The M-theory uplift of the NS5-F1-P bound state. The nodes represent the three charges of the bound state. Every combination of two nodes and the orange line joining them corresponds to a two-charge bound state, and the dipole charges and their coefficients in the projector are indicated next to the line.

In terms of M-theory ingredients, the projector is written as:

$$\Pi_{\text{NS5-F1-P}} = \frac{1}{2}\left[1 + a\widehat{P}_{\text{M5}} + b\widehat{P}_{\text{M2}} + c\widehat{P}_{\text{P}}\right], \tag{6.40}$$

where

$$\widehat{P}_{\text{M5}} \equiv aP_{\text{M5}(y1234)} - bP_{\text{M5}(y234\,z)} + cP_{\text{M5}(1234\,z)}\,, \tag{6.41}$$
$$\widehat{P}_{\text{M2}} \equiv aP_{\text{M2}(y1)} + bP_{\text{M2}(y\,z)} - cP_{\text{M2}(1\,z)}\,, \tag{6.42}$$
$$\widehat{P}_{\text{P}} \equiv -aP_{\text{P}(z)} + bP_{\text{P}(1)} + cP_{\text{P}(y)}\,, \tag{6.43}$$

and the brane involutions are all of the following form:

$$P_{\text{M5}(y1234)} = \Gamma^{0y1234} \tag{6.44}$$
$$P_{\text{M2}(y1)} = \Gamma^{0y1} \tag{6.45}$$
$$P_{\text{P}(z)} = \Gamma^{0\,z}\,. \tag{6.46}$$

6.4 The Brane Content of the Super-Maze

Equations (6.41), (6.42) and (6.43), together with Fig. 6.5, reveal to us the microscopic physics of the M-theory super-maze. As we explained in Section 6.2.3, to understand the local physics of the super-maze surface it is best to work in the $(y, 1, z)$ space, in which both the M5 branes and the M2 branes wrap nontrivial two-surfaces, and 1 denotes a torus direction orthogonal to the original M2 brane. One can see for example that equation (6.41) implies that at every location along the super-maze, the local M5 charge density in the $(y, 1)$ direction (proportional to the projection of the surface of the super-maze along the $(y, 1)$-plane) is equal to a times the mass density of the full configuration. We recall that the parameters a, b, c have been promoted to functions of the position on the brane bound state. One can also see that equation (6.42) implies that the local M2 charge in the direction (y, z) (again proportional to the projection of the M2 charge of the super-maze in the (y, z)-plane) is equal to b times the mass density.[9]

We can span the $(y, 1, z)$ space using orthonormal vectors (u_y, u_1, u_z). Let $u^{\perp}_{\text{M5}}$ be the unit vector orthogonal to the two-dimensional M5-brane surface in the $(y, 1, z)$ space. Let $u^{\perp}_{\text{M2}}$ be its equivalent for the M2-brane, and u_{P} the unit vector along the direction of the momentum P. Then, by choosing the orientation signs appropriately, one can show that the equations (6.41), (6.42) and (6.43) imply successively

$$a = u^{\perp}_{\text{M5}} \cdot u_z\,, \qquad b = u^{\perp}_{\text{M5}} \cdot u_1\,, \qquad c = u^{\perp}_{\text{M5}} \cdot u_y\,, \tag{6.47}$$
$$a = u^{\perp}_{\text{M2}} \cdot u_z\,, \qquad b = u^{\perp}_{\text{M2}} \cdot u_1\,, \qquad c = u^{\perp}_{\text{M2}} \cdot u_y\,, \tag{6.48}$$
$$a = u_{\text{P}} \cdot u_z\,, \qquad b = u_{\text{P}} \cdot u_1\,, \qquad c = u_{\text{P}} \cdot u_y\,. \tag{6.49}$$

[9] Strictly speaking, the value is $\pm b$, where the choice of $\pm$ depends on which one of the two unit vectors orthogonal to the M5-brane surface we choose.

Hence, these equations simply imply that:

$$u^{\perp}_{\rm M5} = u^{\perp}_{\rm M2} = u_{\rm P}\,. \tag{6.50}$$

Thus, even though the super-maze has several M5 and M2 local charges pointing in different directions, when one zooms in on any particular location one finds a tilted M5 brane with parallel M2 charge dissolved in it and orthogonal momentum, which is a configuration preserving 16 supercharges. Of course, these 16 supercharges vary as one moves to a different location of the super-maze, and only 4 of them remain unchanged - the supercharges corresponding to the F1-NS5-P system whose microstates we are constructing.

Our projector also makes it clear how the energy density of the super-maze is distributed among its constituents. Before adding momentum ($c = 0$), we have a static y-independent maze, that contains M5 and M2 branes wrapping y. If one concentrates on a single furrow in the maze, the surface can de described by an equation $z = f(x_1)$. One can then parametrize a and b by an angle, β, that depends on x_1:

$$a \;=\; \cos\beta\,, \qquad b \;=\; \sin\beta\,. \tag{6.51}$$

This angle β corresponds locally to the bending of the surface of the momentum-less maze in the (y, z) plane: $\tan\beta = f'(x_1)$.

We can now compute the energy density of the momentum-less maze from its M5- and M2-brane constituent charges. Using (6.4), one finds

$$Q^{M5}_{(y1234)} \;=\; M\cos^2\beta\,, \qquad Q^{M5}_{(y234z)} \;=\; -\,M\cos\beta\sin\beta\,, \tag{6.52}$$

$$Q^{M2}_{(y1)} \;=\; M\cos\beta\sin\beta\,, \qquad Q^{M2}_{(yz)} \;=\; M\sin^2\beta\,, \tag{6.53}$$

where M is the mass density. As usual, the square of the energy density is equal to the sum of the squares of all the charges

$$M^2 \;=\; \sum_I (Q_I)^2\,. \tag{6.54}$$

However, since the ratio of the M5 and M2 charges is the same as the angle of the furrow, the mass simplifies to the usual BPS mass of a two-charge system:

$$M \;=\; Q^{M5}_{(y1234)} + Q^{M2}_{(yz)}\,. \tag{6.55}$$

If one now adds momentum, the super-maze oscillates along y. The furrow can now be described by a generic function of two variables (see Fig. 6.6.), and the bending angle, β, can also become y-dependent.

Moreover. we also need to introduce an additional "wiggling" angle, α, corresponding to the slope of the furrow waves carrying momentum along the y direction. This angle can also depend on both y and x_1. The parameters a, b and c can now be expressed in terms of these angles as

$$a = \cos\alpha\cos\beta = c_\alpha c_\beta\,, \qquad b = \cos\alpha\sin\beta = c_\alpha s_\beta\,, \qquad c = \sin\alpha = s_\alpha\,. \tag{6.56}$$

The energy density of the momentum-carrying furrow is distributed between the branes and the momentum:

$$Q^{M5}_{(y1234)} = Mc_\alpha^2 c_\beta^2\,, \qquad Q^{M5}_{(y234z)} = -Mc_\alpha^2 c_\beta s_\beta\,, \qquad Q^{M5}_{(1234z)} = Mc_\alpha s_\alpha c_\beta\,, \tag{6.57}$$

$$Q^{M2}_{(y1)} = Mc_\alpha^2 c_\beta s_\beta\,, \qquad Q^{M2}_{(yz)} = Mc_\alpha^2 s_\beta^2\,, \qquad Q^{M2}_{(1z)} = -Mc_\alpha s_\alpha s_\beta\,, \tag{6.58}$$

$$Q^{P}_{(1)} = -Mc_\alpha s_\alpha s_\beta\,, \qquad Q^{P}_{(z)} = Mc_\alpha s_\alpha c_\beta\,, \qquad Q^{P}_{(y)} = Ms_\alpha^2\,, \tag{6.59}$$

and once again, this leads to the BPS condition for the three-charge system

$$M = Q^{M5}_{(y1234)} + Q^{M2}_{(yz)} + Q^{P}_{y}\,. \tag{6.60}$$

Note that as one moves in the $(y, 1)$ plane, the projection of the M5 charge in this plane remains constant. Indeed, the original five-brane wraps the $y, 1$ plane, and its charge density cannot therefore depend on y or x_1. This appears to be in conflict with equation (6.57), but we have to realize that M is the mass density of the furrow in the $(y, 1)$ plane, which changes as one moves along the furrow. Hence, $Q^{M5}_{(y1234)}$ is independent on α and β, but M depends on them:

$$M(y, x_1) = \frac{Q^{M5}_{(y1234)}}{\cos^2\alpha(y, x_1)\cos^2\beta(y, x_1)}\,. \tag{6.61}$$

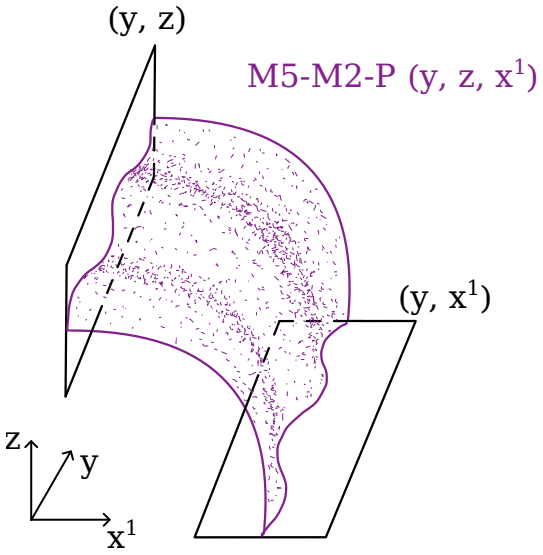

Figure 6.6: Wiggling half-furrow.

6.5 In lieu of a Conclusion: Some thoughts on Super-Maze backreaction

One key question about the super-maze we discovered is whether it gives rise to a horizonless and possibly smooth solution in the regime of parameters where the classical

black-hole solution exists. Naïvely one may argue that, since the super-maze contains N_1N_5 M2 brane strips crammed into a very small torus, its backreaction will give rise to a solution whose curvature is too large to be reliably described by supergravity. However, this intuition fails to take into account the fact that when branes backreact they can blow up the size of the transverse spacetime.

The key feature of the super-maze that makes us confident that its backreaction will be smooth and horizonless is the local enhancement of the supersymmetry to 16 supercharges. This is the smoking gun of the construction of the brane bound states that account for the entropy of the two-charge system. This is perhaps best known from the physics of supertubes [14, 180]: A supertube can have arbitrary shape and, if one zooms in at a certain location along this shape, one finds a brane system that preserves 16 supersymmetries. Moreover, as one moves along the supertube these supersymmetries rotate, and only a subset of 8 of them is preserved by the full configuration. When the supertube is dualized to the D1-D5 (or F1-NS5) duality frame and its two charges correspond to D1 and D5 (or F1 and NS5) branes [16, 18], the presence of 16 supercharges locally is equivalent to the existence of a smooth horizonless supergravity solution [226]. Another examples of a two-charge brane bound states is the F1 string carrying longitudinal momentum [182], reviewed in Section 6.2. This solution has again 8 supercharges, but if one zooms in near the location of the momentum-carrying string one finds a solution with 16 supercharges. These supercharges rotate as one moves along the string profile, and only 8 of them remain invariant and are preserved by the whole configuration. A similar bound state can be made from any brane carrying longitudinal momentum.

A third, slightly less known illustration of a two-charge bound state that has 16 supercharges locally is the magnetube, which has again two charges, corresponding to an M5 brane and longitudinal momentum, which are bound together by the presence of M2 brane dipole charges [192, 225]. Finally, a fourth illustration of this phenomenon is the NS5-P bound state recently constructed in [224], where the supersymmetry is enhanced locally to 16 supercharges because of the presence of dipolar D0 and D4 charges on the NS5 worldvolume.

There also exist brane configurations that have the same charges as those of a three-charge black hole, and again have 16 supercharges locally and only 4 globally. When the brane configurations correspond to multi-center solutions [229] whose centers are fluxed D6 branes (which preserve locally 16 supercharges), the solutions uplift [35] to the smooth horizonless bubbling solutions in eleven dimensions constructed in [33, 34]. Another three-charge brane configuration that has locally 16 supercharges is the superstratum conjectured in [30], which served as inspiration for the building of superstratum supergravity solutions [24].

Note that in all these systems, in the absence of the dipolar branes providing the "glue" and in the absence of the local enhancement of the supersymmetry to 16 supercharges, one obtains singular solutions or solutions with a horizon, which do not describe microscopic degrees of freedom of these systems, but rather ensemble averages. Thus the local enhancement of the supersymmetry is the key indication that the backreaction of

the brane bound state will result in a horizonless solution that describes a pure state of the system.

It is important to remark that the local enhancement of supersymmetry and the absence of a horizon are duality-frame-invariant phenomena. Of course, in some duality frames a smooth solution can become a singular solution, but a solution with an event horizon can never be dualized to a solution without one [37] and viceversa.

One can also speculate on how the supergravity solution corresponding to a super-maze may look. In Fig. 6.7 we illustrate the shape of a super-maze corresponding to two M5 branes extending along x_1 and a single fractionated M2 brane extended along z (the M-Theory direction) and smeared over three of the M5-brane worldvolume directions, x_{234}. Before the fractionation, the M2 brane does not pull on the M5 branes; this is depicted in the left panel. Once the M2 brane gets fractionated, its components start pulling on the M5 brane. However, since the M2 brane strips have been smeared along x_{234}, they end on a codimension-one surface inside the M5 branes. Therefore, the pull of a fractionated M2 brane does not give rise to a spike, but rather to a wedge.[10]

As one can see from the middle panel of Fig. 6.7, when the distance between the two M5 branes is large, the configuration consists of several M5 branes wedges with dissolved M2 charge, pulled by M2 branes extended along z. However, the bent M5 branes can move freely along the z direction, and when two opposite M5 wedges become close they can transform into the brane web depicted in the right panel, which contains also un-fluxed coincident M5 branes. In general, a more complicated super-maze smeared over three of the M5-brane worldvolume directions will correspond to a brane web in the (x_1, z)-plane which has the all the three ingredients of the web in the right panel of Fig. 6.7.

If the M2 branes are not smeared, the resulting maze does not have any "bare" M2 lines, but will be everywhere a fluxed M5 brane.[11] One can then ask how the supergravity solution corresponding to this M5 super-maze will look. First, the M5 branes source a magnetic four-form whose flux on a four-sphere is constant. When the M5 branes backreact, there will be a geometric transition: this four-sphere becomes large and topologically nontrivial, while the nontrivial maze surface wrapped by the M5 branes will shrink to zero size. Thus, the maze of M5 branes will transform into a maze of bubbles with fluxes.

As we have discussed in the Introduction, the existence of super-mazes and the possibility that their supergravity solution might be smooth, represents a paradigm shift for the microstate geometry programme and for the fuzzball conjecture in general. The starting point of this conjecture is the idea that collapsing matter do not form horizons in nature, but rather transition into horizonless "fuzzball" solutions of string theory. Stan-

[10] Remember that the Callan-Maldacena spike corresponds to a string ending on a codimension-three defect inside the D3 brane, and the profile of the pulled D3 brane is similar to the harmonic function in three dimensions, $1/r$. Here, the M2 branes end on a codimension-one defect, so the profile of the pulled M5 brane has the shape of the harmonic function in one dimension, $|x_1|$, and looks like a wedge.

[11] Even when the M2 branes are smeared, one can argue that because the distance between the M5 branes on the M-theory circle is small, the maze components will be mostly fluxed and unfluxed M5 branes.

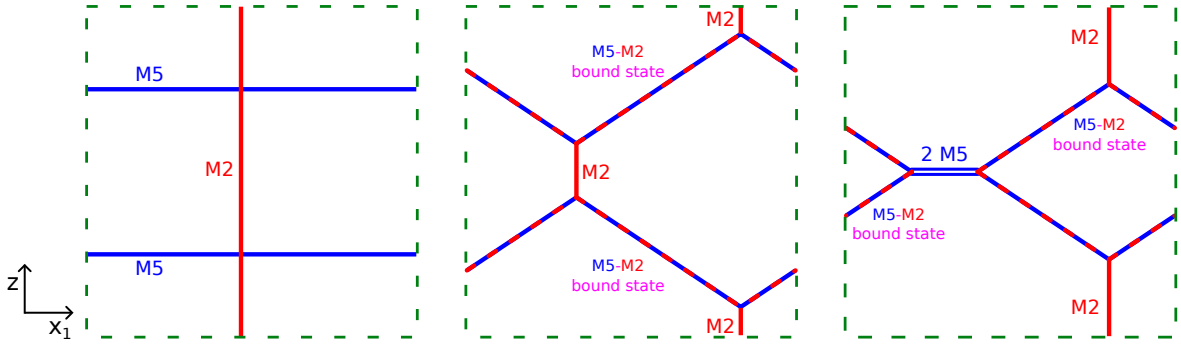

Figure 6.7: A super-maze made of 2 M5 branes and a single M2 brane which is smeared along three of the M5 brane worldvolume directions. Before the fractionation the M2 brane does not pull on the M5 branes, and can be freely taken away. After the fractionation (middle panel), each strip of the M2 branes deforms the M5 brane in its vicinity. As the branes move, the web depicted in the middle panel can also transform in the web depicted in the right panel, which has regions of coincident un-fluxed M5 branes.

dard black holes are then seen as average descriptions of the space of microstates that the stringy fuzzball matter can reach. One also expects on general grounds that some of these fuzzball solutions will have a classical limit, and will be describable purely using low-energy supergravity, as microstate geometries.

Despite the extraordinary success of the microstate geometry programme, the entropy of the solutions constructed so far, of order $\sqrt{N_1 N_5} N_P^{1/4}$ is parametrically smaller than the entropy of the three-charge black hole, $\sqrt{N_1 N_5 N_P}$. Furthermore, all the solutions that have been constructed break the spacetime spherical symmetry of the black-hole horizon, while we expect $\sqrt{5/6}$ of the black hole entropy to come from configurations that do not break this symmetry [223].[12]

The super-maze promises to solve both these problems at the same time. On one hand, we have constructed the super-maze using the types of "glue" that preserve the rotational invariance of the black hole. Furthermore, the DVV microstates that we have argued to backreact into super-maze configuration correspond to momentum carriers that are purely bosonic. Hence, we expect the super-maze and its corresponding supergravity solutions to have an entropy of order $2\pi\sqrt{\frac{4}{6} N_1 N_5 N_P}$.[13] Furthermore, since two of the fermionic zero modes also preserve the rotational symmetry of the black-hole horizon, and the super-maze is the most general brane bound state with black-hole charges that preserves this symmetry, it is possible that the super-maze could even have an entropy of order $2\pi\sqrt{\frac{5}{6} N_1 N_5 N_P}$.

Our construction also allows us to speculate how we may try to capture the remaining part of the black-hole entropy, which comes from fermion momentum carriers that break

[12] For other extremal black holes there are arguments that most of the entropy comes from such microstates [230].

[13] See also [231], expecting that disentangled microstates [232] – and therefore microstates without smooth horizons – to account for at least a finite fraction of the black-hole entropy.

the rotational symmetry of the black-hole horizon [223]: Instead of using the super-maze glue, we could could try to use the other types of glue, and construct generalizations of the super-maze that break this rotational symmetry.

It would be very interesting to construct the fully backreacted super-maze solutions, and to understand how this entropy is realized in supergravity. It would be also interesting to apply the "making bound states with glue" philosophy we used in this Chapter to reveal the microscopic structure of black holes in other duality frames, where microstate counting has not been done.

Chapter 7

Themelia: the irreducible microstructure of black holes

7.1 Introduction

Whether you describe it in General Relativity or think of it as a strongly-coupled quantum object, a black hole must necessarily reduce matter to its most fundamental constituents. From the perspective of string theory, this is usually interpreted as meaning strings and branes, but we will argue that the full range of fundamental constituents must include more general species of objects that we will call *themelia*. A themelion is defined to be any object in string theory that *locally preserves* 16 supercharges. This certainly includes fundamental strings and branes, but a themelion can carry multiple charges and preserve less supersymmetry when taken as a whole. A themelion will typically have varying charge densities along a non-trivial profile, but the defining idea is that when one "zooms in" on a small segment of the themelion, the localized part preserves sixteen supersymmetries and those supersymmetries will generically depend on their location on the themelion.

Our purpose here is not only to characterize some large families of themelia, but also to show that they play the central role in the description of black-hole microstructure, and that they are necessarily the irreducible constituents of a supersymmetric fuzzball. As we will describe, themelia not only include all known supersymmetric microstate geometries, but also greatly extend their range. Indeed, a central result of this Chapter will be to exhibit themelia that embed the microstate geometries known as superstrata [24–26] into highly fractionated brane configurations that include the super-maze [36].

The fuzzball paradigm [23, 233] seeks a gravitational and quantum description of black holes, and their microstructure, in terms of horizonless objects in string theory. The idea is that, because individual microstates have no entropy, they cannot have a horizon, and that horizons only arise through ensemble averaging. Fuzzballs are supposed to represent a new phase that emerges when matter is compressed to black-hole densities, and this new phase prevents the formation of a horizon or singularity.

The challenge has been to formulate fuzzballs more precisely [32] and this has been done largely through the construction of huge families of examples: In particular, mi-

crostate geometries are realizations of the fuzzball paradigm in terms of smooth solutions to supergravity. What is perhaps most startling about this program is the extent to which it can be realized. (For recent reviews, see [23,234].) This extensive body of work has also led to a much deeper understanding of the new phase of matter that underlies fuzzballs, and hence our proposal that their fundamental constituents should be themelia.

Fundamental constituents must themselves be horizonless. But this is not sufficient: there are "horizonless" string configurations, like the unadorned D1-D5 solution, that still have microstructure. While the classical horizon of such an object has vanishing area, it can be argued to have a "Planck-scale horizon" that accounts for the entropy of its microstructure [10]. On the other hand, the sixteen supersymmetries of the themelion not only preclude it from having a horizon, even at the Planck scale, but also makes it a fundamental bound state, an indivisible "atomic object" of string theory – hence the building block of fuzzballs.

Objects with 16 supersymmetries can always be dualized to a system consisting of a single species of brane, such as a stack of F1's, or the empty space of a KKM. A generic themelion is, however, highly non-trivial: It only has 16 supersymmetries *locally*, and so the "trivializing" duality transformation depends on the location on the themelion profile. In any fixed duality frame, a themelion can carry a huge range of charges that *vary* with location. Some of these will average to zero over the themelion, and some will average to non-zero values. We will refer to these as *dipolar* and *global* charges respectively. The global charges determine the overall supersymmetry preserved by the themelion.

The important point about themelia is that, individually, each one has essentially no microstructure and, upon dualizations, can be characterized locally using string theory (as an F1) or geometry (as a KKM). However, globally, themelia can have huge moduli spaces, expressed in terms of shapes and charge densities, and so they can encode a vast number of microstates within their configuration spaces. Conversely, because of the 16 supersymmetries, the moduli space of a themelion cannot *ipso facto* contain any black holes, or give rise to horizons.

Superstrata were originally conjectured to exist [30] entirely based on the underlying principle of themelia: namely, 16 supersymmetries locally. Five years later, large families of superstratum supergravity solutions were explicitly constructed [24–26] but their connection with the themelion of [30] was not clear.

In this Chapter we exhibit the themelion structure of the superstratum solution, and show that the supergravity constraints imposed by smoothness are equivalent to requiring that themelia have 16 local supercharges. We also reveal a similar structure in the recently constructed "vector superstrata" [235].

In addition to superstrata, one should recall that there is another huge family of smooth horizonless microstate geometries: the bubbling solutions constructed from ambipolar Gibbons-Hawking (GH) geometries [33, 34, 212]. Upon reduction to 10 dimensions along the GH fiber, one obtains a multi-center solution [229] where each center has 16 supercharges [35] (and hence is a themelion).

Based on our observations, we conjecture a relation between bound states of themelia

and smooth horizonless supergravity solutions:

All smooth horizonless solutions come from bound states of themelia with KKM charge. All bound states of such themelia give rise to a smooth supergravity solution.

As we remarked above, each themelion can have a large moduli space. Furthermore, combining different themelia can lead to an enhancement of the moduli space. As we will show, the superstratum solution is a combination of two themelia, each of which involves a function of one variable and yet, the generic superstratum solution is expected to be parameterized by arbitrary functions of three variables [156]. Therefore, our conjecture does not imply that a choice of component themelia leads to a unique smooth horizonless solution.

7.2 Themelia

To pin down the structure of a particular themelion, one must first specify its global charges, and the amount of supersymmetry it will preserve overall. One then chooses dipolar charges as "glue" that will bind the global object into a bound state with 16 supersymmetries locally [36]. There are typically multiple choices for such glue and, as we will see, one can often combine different types of glue to create an even larger themelion moduli space. The choice of these dipole charges is also motivated by the underlying physics of the themelion.

The construction, of course, depends on the duality frame and the charges we want the themelion to carry. Here we will work exclusively in the Type IIA/M-theory frame and focus on themelia that have the F1, NS5 and P charges of a supersymmetric black hole. We can uplift everything to M-theory, where the supersymmetries, $\mathcal{Q}$, are 32-component spinors and the themelion building blocks are M2 and M5 branes, momentum, P, and KKM charge. The supersymmetries of the themelion are then defined by projectors involving gamma matrices.

$$\Pi\mathcal{Q} \;=\; 0, \qquad \Pi = \tfrac{1}{2}\,(1 \;+\; P), \tag{7.1}$$

where the matrices, P, are given by [30]:

$$\begin{aligned} &P_{\mathrm{M2}(12)} = \Gamma^{012}\,, \qquad P_{\mathrm{M5}(12345)} = \Gamma^{012345} \\ &P_{\mathrm{P}(1)} = \Gamma^{01}\,, \quad P_{\mathrm{KKM}(123456;7)} = \Gamma^{0123456} = \Gamma^{789\,10}\,. \end{aligned}$$

Here the indices indicate the directions along which the branes extend. For the KKM the last entry denotes the "special direction" of the fibration.

We will also focus on the $\mathbb{T}^4$ compactification of IIA supergravity to six dimensions and will denote the M-theory circle by z and the torus directions as $1, 2, 3, 4$. We will also introduce two other circles: an $S^1(y)$ corresponding to the common direction of the F1 strings and NS5 branes that give global charges, and a "space-time" ψ-circle transverse to the $\mathbb{T}^4 \times S^1(y)$. If the ψ direction is non-compact then charges corresponding to branes wrapping this direction are necessarily dipolar. We will also find it useful to use the

standard IIA nomenclature: NS5, F1, D2 , D4 and D6 to encode the way in which the M-theory objects wrap the z-circle.

An archetypical example of the relation between themelia and supergravity solution comes from the Lunin-Mathur 8-supercharge solution [16]. This is a smooth horizonless solution, which can be thought of as a supertube [14] with F1(y) and NS5($1234y$) charges and a KKM($1234\psi z; y$) dipole charge. The global supersymmetries are defined by the vectors, ξ, satisfying:

$$\tfrac{1}{2}(1 \,+\, \Gamma^{0yz})\,\xi \;=\; 0\,, \quad \tfrac{1}{2}(1 \,+\, \Gamma^{01234y})\,\xi \;=\; 0\,. \tag{7.2}$$

This solution is made of two themelia. The first themelion is at the "supertube locus" and has F1 and NS5 charges, as well as a glue coming from the angular momentum P(ψ) along the supertube direction, ψ, and the KKM($1234\psi z; y$). Its projector has [30]:

$$P \;=\; \lambda_1\Gamma^{0yz} \,+\, \lambda_2\Gamma^{01234y} \,+\, \lambda_3\Gamma^{0\psi} \,+\, \lambda_4\Gamma^{01234\psi z}\,. \tag{7.3}$$

If one takes $\lambda_1 = \cos^2\phi$, $\lambda_2 = \sin^2\phi$ and $\lambda_3 = -\lambda_4 = \sin\phi\cos\phi$, then one has:

$$P^2 \;=\; 1\,, \qquad \Pi\,\xi \;=\; \tfrac{1}{2}(1+P)\,\xi \;=\; 0\,. \tag{7.4}$$

The identity $\Pi^2 = \Pi$ means that Π only has eigenvalues 0 or 1 and, combined with the fact that the products of gamma matrices are traceless, it means that Π must have sixteen null vectors, preserving 16 supersymmetries. However eight of those supersymmetries depend upon the parameter, ϕ, and eight are independent of ϕ and are determined by the global F1 and NS5 charges as in (7.2).

The second themelion is a bit less obvious when the supertube is in $\mathbb{R}^4$, but can be seen easily if one embeds the Lunin-Mathur geometry in Taub-NUT [236, 237]: The "center-of-space" themelion is a KKM wrapping the ($y1234z$) directions and with a special direction ψ. This reflects a more general principle: to reveal the themelion sources of a solution one should write it as a fibration over a spatial $\mathbb{R}^3$. The themelia are located where the fibers degenerate.

Supergravity superstrata of [24–26] are built by adding momentum waves along y to a generalized supertube solution. These momentum waves cannot be sourced on the themelion at the supertube locus, where the y-circle degenerates. Instead, they are sourced at the center of space, promoting the simple KKM themelion to a much more complicated momentum-carrying themelion.

To recast the original supergravity superstrata [24–26] in our IIA/M-theory frame, we perform an S-duality and a T-duality along one direction of the $\mathbb{T}^4$, which we can choose to be x_1. By writing the superstratum solution as circle fibrations over an $\mathbb{R}^3$ base, one can easily read off all the themelion charges from the singularities in the fluxes and metric functions. In particular, there are warp factors that diverge at the supertube location. These correspond to the global F1 (M2(yz)) and NS5 (M5($y1234$)) charges, and equal amounts of dipolar M2($1y$) and M5($z234y$) charges. At the center of space there are also singularities corresponding to the same set of branes wrapped on the ψ direction:

M2(ψz), M5($\psi 1234$) and equal amounts of M2($\psi 1$) and M5($\psi 234z$). These branes are dipolar. There is also the KKM with special direction ψ at the center of space.

In this Chapter, we will focus on three-charge themelia (with four global supercharges) carrying the charges F1(y), NS5($1234y$) and P(y) in Type IIA/M-theory. The global supersymmetries are given by:

$$\begin{aligned} &\tfrac{1}{2}(1 + \Gamma^{0yz})\,\xi = 0\,, \quad \tfrac{1}{2}(1 + \Gamma^{01234y})\,\xi = 0\,, \\ &\tfrac{1}{2}(1 + \Gamma^{0y})\,\xi = 0\,. \end{aligned} \tag{7.5}$$

The most general themelion projector with these charges and the dipole charges corresponding to the superstrata considered above is:

$$\begin{aligned} P = &(\alpha_1\Gamma^{0yz} + \alpha_2\Gamma^{0y1234} + \alpha_3\Gamma^{0y} + \alpha_4\Gamma^{0y1234z}) \\ &+ (\alpha_5\Gamma^{0\psi z} + \alpha_6\Gamma^{0\psi 1234} + \alpha_7\Gamma^{0\psi} + \alpha_8\Gamma^{0\psi 1234z}) \\ &+ (\alpha_9\Gamma^{0y1} + \alpha_{10}\Gamma^{0y234z}) + (\alpha_{11}\Gamma^{0\psi 1} + \alpha_{12}\Gamma^{0\psi 234z})\,, \end{aligned} \tag{7.6}$$

where the α_j can be interpreted as local charge densities divided by the mass density.

The global supercharge condition (7.5) leads to the following linear constraints:

$$\alpha_1 + \alpha_2 + \alpha_3 + \alpha_4 = 1\,, \tag{7.7}$$

$$\alpha_5 + \alpha_6 + \alpha_7 + \alpha_8 = 0\,, \tag{7.8}$$

$$\alpha_{10} = -\alpha_9\,, \quad \alpha_{11} = -\alpha_{12}\,, \tag{7.9}$$

and the projector condition $P^2 = 1$ in (7.4), leads to several quadratic conditions, which include, for example:

$$(\alpha_1\alpha_2 + \alpha_3\alpha_4 - \alpha_9^2) + (\alpha_5\alpha_6 + \alpha_7\alpha_8 - \alpha_{11}^2) = 0\,. \tag{7.10}$$

The complete solution to the *themelion constraints*, obtained using (7.6) in equations (7.4) and (7.5) is given by (D.1) and (D.2) with $\theta_2 = \frac{\pi}{2}$, $\varphi_2 = 0$.

Our first result is that: *All existing microstate geometries - both bubbling solutions and superstrata - are bound states of multiple themelia defined by* (7.6).

We find that all the themelion constraints have counterparts in the supergravity solutions. However, the relation is subtle. First, the themelion analysis is done for a non-backreacted brane probe in flat space. Thus, to link the supergravity charges to the α_i we have to arrange that themelion's environment be that of empty space: in particular one must perform large gauge transformations to eliminate all the Wilson lines along the themelion. Secondly, the themelion wraps several compact directions, whose radii affect the charge densities and hence the α_i. Since these radii typically vary across spacetime, some of the themelion constraints impose conditions on the location of the themelion itself.

The simplest themelion constraint to interpret is (7.7), which reflects the fact that the mass density of the themelion is the sum of its global charge densities: $M = Q_1 + Q_2 + Q_3 + Q_4$. The parameters in the second constraint, (7.8), depend on distinct powers or

Object	Coefficient	
F1(y)	α_1	x_1
NS5(y1234)	α_2	y_1
P(y)	α_3	z_1
KKm(y1234;ψ)	α_4	
D2(y1)	α_9	u_1
D4(y234)	$\alpha_{10} = -\alpha_9$	
D0	α_{13}	v_1
D4(1234)	$\alpha_{14} = -\alpha_{13}$	
F1(1)	α_{17}	w_1
P(1)	$\alpha_{18} = -\alpha_{17}$	

Object	Coefficient	
F1(ψ)	α_5	x_2
NS5(ψ1234)	α_6	y_2
P(ψ)	α_7	z_2
KKm(ψ1234;y)	α_8	
D2(ψ1)	α_{11}	u_2
D4(ψ234)	$\alpha_{12} = -\alpha_{11}$	
D2(yψ)	α_{15}	v_2
D6(yψ1234)	$\alpha_{16} = -\alpha_{15}$	
NS5(yψ234)	α_{19}	w_2
KKm(yψ234; 1)	$\alpha_{20} = -\alpha_{19}$	

Table 7.1: The Type IIA constituents and parameterization of the most general themelion with $\mathbb{T}^3$ invariance.

the radius of the ψ-circle, and so this determines the possible locations of the themelion. In particular, for the bubbling solutions of [33, 34, 212], this constraint is equivalent to the bubble equations [1]. The last linear equations (7.9) reflect the fact that, in the six-dimensional supergravity theories used to build superstrata and bubbling solutions, the tensor fields corresponding to $\alpha_{9,10,11,12}$ must be anti-self dual.

For bubbling solutions the quadratic constraints, like (7.10), correspond to smoothness conditions, giving exactly the quadratic constraints on the sources of harmonic functions needed to construct smooth horizonless solutions of [33, 34, 212].

As we noted earlier, a superstratum is made of two themelia: one at the supertube locus and one at the center of space. Using the correspondence between parameters in branes in Table 7.1, one can see that the supertube themelion has $\alpha_{3,4,5,6,11,12} = 0$ and $\alpha_7 + \alpha_8 = \alpha_9 + \alpha_{10} = 0$. The simplest way to identify the parameters of the center-of-space themelion is to perform a "spectral inversion," $\psi \leftrightarrow y$, [179] [2] and then one sees that this themelion has $\alpha_{1,2,7,8,9,10} = 0$ and $\alpha_{11} + \alpha_{12} = \alpha_3 + \alpha_4 = 0$.

Remembering that the supertube themelion has charge densities that depend on ψ, and the center-of-space themelion has charge densities that depend on y one sees that (7.10) imposes two independent constraints on these densities. Amazingly, these are exactly the coiffuring constraints [25], which were necessary to construct a smooth supergravity solutions.

[1] A similar relation between bubble equations and probe-brane constraints has been found for supertubes probing bubbling solutions [226]

[2] We note that spectral inversion is inconsistent with (7.7) and (7.8). Consistency can be restored by performing a large gauge transformation in supergravity to eliminate Wilson lines.

7.3 The hyperstratum

The themelia that enter in the construction of the superstrata actually belong to a much larger moduli space of themelia. Indeed, the Type IIB superstratum only had fields that preserve the $\mathbb{T}^4$ invariance, but when we dualize it to the Type IIA/M-Theory duality frame we use in this Chapter, it only has a $\mathbb{T}^3$ invariance, along the directions 234. This suggests one should consider a more general themelion which preserves this $\mathbb{T}^3$ invariance and has branes that can wrap $1, y, z$ and ψ. This themelion can have 20 possible species of branes:

$$\text{M2}(0ab)\,,\quad \text{M5}(0234ab)\,,\quad \text{P}(a)\,,\quad \text{KKM}(0234abc)\,, \tag{7.11}$$

where $a, b, c \in \{1, y, z, \psi\}$. The complete set of species is described in the IIA nomenclature in Table 7.1.

The projector is now constructed using $\widehat{P} = P + P'$ where P is given by (7.6) and

$$\begin{aligned} P' = {} & \alpha_{13}\Gamma^{0z} + \alpha_{14}\Gamma^{01234z} + \alpha_{15}\Gamma^{0y\psi} + \alpha_{16}\Gamma^{0y\psi1234} \\ & + \alpha_{17}\Gamma^{01z} + \alpha_{18}\Gamma^{01} + \alpha_{19}\Gamma^{0y\psi234} + \alpha_{20}\Gamma^{0y\psi234z}\,. \end{aligned} \tag{7.12}$$

We find that the null-space condition (7.5) now imposes eight linear constraints on the α_j, while the projection condition yields another 15 quadratic constraints. This is a hugely overdetermined system, and if we first use the linear constraints, we can re-parameterize the system in terms of three vectors in $\mathbb{C}^3$, defined by:

$$\begin{aligned} \boldsymbol{p}_1 &\equiv (u_1 + iu_2\,, -(w_1 - iw_2)\,, x_1 + ix_2)\,, \\ \boldsymbol{p}_2 &\equiv (-i(v_1 + iv_2)\,, -i(y_1 - iy_2)\,, -i(w_1 - iw_2))\,, \\ \boldsymbol{p}_3 &\equiv (-(z_1 + iz_2)\,, -(v_1 + iv_2)\,, u_1 + iu_2)\,. \end{aligned} \tag{7.13}$$

where $(u_1, \ldots, z_2)$ are real parameters. Note that each vector p_i has an entry in common with both other vectors and so there are twelve independent real parameters and their relationship with the α_j may be found in (D.1). The projection condition, $\widehat{P}^2 = \widehat{P}$, is equivalent to the statement that the $\boldsymbol{p}_j$ are orthonormal in $\mathbb{C}^3$. This means that one can then use $U(3)$ to rotate the $\boldsymbol{p}_j$ to a simple canonical form:

$$\boldsymbol{p}_1{}' \equiv (0\,, 0\,, 1)\,,\ \boldsymbol{p}_2{}' \equiv (0\,, \mp i\,, 0)\,,\ \boldsymbol{p}_3{}' \equiv (\mp 1\,, 0\,, 0)\,. \tag{7.14}$$

Note that this basis corresponds to $x_1 = 1$, $y_1 = z_1 = \pm 1$, with all the other parameters set to zero. From (D.1) one sees that this themelion corresponds to $\alpha_1 = 1$ (for $+$), or $\alpha_4 = 1$ (for $-$) with all the other α_j vanishing. Thus a $U(3)$ U-duality rotation can *locally* map this themelion onto a stack of F1 strings or a stack of coincident KKM's.

Using the U(3) one can parameterize the most general themelion, remembering that the rotation must be restricted by the constraints on interrelated components of the $\boldsymbol{p}_i$ in (7.13). The result is a six parameter family, (D.2), given by the angles, $\theta_1, \theta_2, \varphi_j$, $j = 1, 2, 3, 4$. As noted earlier, the projector of the supertube-locus themelion of the superstratum solution, based on (7.6), is given by $v_j = w_j = 0$, or $\theta_2 = \frac{\pi}{2}$ and $\varphi_2 = 0$.

It is not hard to see that our general themelion also include the themelia that enter the construction of the vector superstratum of [235] of which a subset can be built using only NS-NS fields. The "supertube-locus" themelion of these NS-NS vector superstratum is obtained by taking $u_j = v_j = 0$, or $\theta_2 = 0$.

To obtain a themelion with no components in the space-time (ψ) directions, a glance at Table 7.1 reveals that one must remove all the constituents in the second column, and hence all the second components must vanish. This is achieved by setting all the φ-phases in (D.2) to zero. This leaves a themelion with:

$$\begin{aligned} P =&(\beta_1\,\Gamma^{0yz} + \beta_2\,\Gamma^{01234y} + \beta_3\,\Gamma^{0y}) + \beta_4\,(\Gamma^{0z} - \Gamma^{01234z}) \\ &+ \beta_5\,(\Gamma^{01} - \Gamma^{01z}) + \beta_6\,(\Gamma^{01y} + \Gamma^{0234yz})\,. \end{aligned}$$

and

$$\begin{aligned} &\beta_1 = \cos^2\tfrac{1}{2}\theta_1\,,\ \ \beta_2 = \sin^2\tfrac{1}{2}\theta_1\sin^2\theta_2\,,\ \ \beta_3 = \sin^2\tfrac{1}{2}\theta_1\cos^2\theta_2\,, \\ &\beta_4 = \sin^2\tfrac{1}{2}\theta_1\sin\theta_2\cos\theta_2\,,\ \ \beta_5 + i\beta_6 = \tfrac{1}{2}\sin\theta_1\,e^{i\theta_2}\,. \end{aligned}$$

Amazingly, this is the projector of the super-maze [36]. Hence, the class of themelia we obtain from $\widehat{P}$ contains the themelia that govern both the original and vector superstrata, as well as the super-maze themelion. Therefore, we expect there to be supergravity solutions made of multiple generalized themelia, which we can call *hyperstrata*. These will contain all the existing superstrata and super-mazes. Since the momentum charge is carried by different excitations in the superstrata and the super-maze, we expect the *hyperstrata* to have a larger entropy than either subclass.

Moreover, it was argued in [36] that, because the super-maze captures brane fractionation, its entropy is expected to match that of the rotationally-invariant microstates of the black hole, $2\pi\sqrt{\frac{5}{6}Q_1Q_5Q_P}$. The *hyperstratum* will capture these microstates as well those that break the spacetime rotational invariance of the black-hole horizon. Given that the hyperstratum captures fractionation and restores democracy between the y-circle and a generic torus direction, we expect it to match the full black-hole entropy. It would be exciting to construct some *hyperstratum* solutions, to see whether this intuition is realized.

By breaking the torus invariance, we have found themelia that capture fractionated branes, and perhaps the full black-hole entropy. It is thus natural ask how the phase space of themelia will expand if we relax the $\mathbb{T}^3$ invariance imposed here and allow all possible branes wrapping the compactified dimensions. Given that the generic super-maze breaks this invariance, we suspect that relaxing the $\mathbb{T}^3$ invariance will lead to a phase space that is a combination of all superstrata and generic supermazes.

Armed with our knowledge of themelia and hyperstrata, we return to the resolution of a seeming paradox of the original superstratum: its moduli space appears to have a degenerate limit to a BTZ black hole with finite horizon area [25,26], and yet a themelion cannot have a horizon. This degenerate limit arises when one forces the two themelia of the superstratum to coincide. One of these themelia has only ψ fluctuations and a KKM that shrinks y, while the other one has only y fluctuations and a KKM that shrinks ψ. Forcing these two themelia to coincide turns off both the ψ and y fluctuations, and either

requires one to set the momentum charge to zero, or results in a configuration that is not a themelion.

However, we have seen that the themelia that give rise to the superstratum are part of a much larger family of themelia that can fluctuate not only along ψ and y, but also along z and the torus directions. The hyperstratum is built from these more generic themelia, and the coincidence limit is no longer degenerate: the momentum charge can be carried by fluctuations along z and the torus, and the resulting configuration will be another horizonless themelion, the super-maze. The presence of a black hole in the phase space of superstratum solutions is an artifact of objects made from enforcing $\mathbb{T}^4$ invariance and *smearing* the themelia. This illustrates, once again, the fuzzball precept: horizons only appear because of ensemble averaging.

Chapter 8

Maze Topiary in Supergravity

8.1 Introduction

The entropy of many classes of brane systems can be counted using perturbative String Theory in a regime of parameters in which gravity is turned off. The result matches the entropy of the black hole with the same charges in the regime of parameters in which gravity is turned on. This gives spectacular matches, both for the D1-D5 system [10, 12], for M5-M5-M5-P black holes [238], and also for Type IIA F1-NS5-P black holes [38].

These entropy-matching computations rest on the fact that the counting of index states essentially does not change[1] as couplings are varied from perturbative string states to black-hole microstructure. Such an approach fails to address the hugely important issue of what happens to particular individual microstates as one turns gravity on, and precisely what the microstate structure "looks like" at finite G_{Newton}? An alternative formulation of this question is: what distinguishes different black-hole microstates from each other in the regime of parameters where the classical black hole exists. There are strong arguments, coming from quantum information theory, that individual microstates should differ from each other and from the classical black-hole solution at the scale of the horizon [150, 233]. Indeed, several very large classes of microstate geometry solutions, dual to some families of pure states of the CFT that counts the black hole entropy, have been constructed, both for supersymmetric black holes [24–26, 152, 154, 156, 157, 168, 205, 224, 235, 239–243], and also, in fundamentally different approaches, for non-extremal ones [167, 176, 244] and [245–258].

Tracking the D1-D5 microstates from weak to strong coupling, as we have already seen in Chapter 6 is challenging, since the momentum is carried by bi-fundamental strings whose back-reaction is only known at the most rudimentary level. The construction of superstrata [24–26, 152, 154, 156, 157, 168, 205, 224, 235, 239–243] largely rests on collective string excitations in the untwisted sectors of the D1-D5 CFT. While these solutions describe a significant sector of the black-hole microstructure, they fall parametrically short of capturing the black-hole entropy [27, 28]. To obtain a geometric description of generic

[1] There can be jumps under "wall-crossing" but these are sub-leading.

microstructure one must capture coherent combinations of twisted-sector states of the CFT, and this seems to be easier in the Type IIA F1-NS5-P formulation of the brane system that leads to a black hole.

As we have seen in Chapter 6, in this formulation, the momentum is carried by little strings, which live on the NS5 world-volume. These little strings have a very simple geometric description: When uplifting the F1-NS5 system to M theory, each F1 uplifts to an M2 wrapping the M-theory direction. This M2 can break into N_5 strips (which correspond to the little strings on the NS5 world-volume) which carry momentum independently. The N_1N_5 resulting little strings form a complicated maze of intersecting M2 and M5 branes carrying momentum and whose entropy (upon taking into consideration fermionic partners) matches exactly that of the F1-NS5-P black hole. The beauty of this characterization of the microstructure is that it lends itself to a geometric description of the coherent states in terms of supergravity.

Since the momentum of such a "supermaze" is carried by waves on the little strings, the microstates of the black hole have coherent expression as momentum carried by components of a fractionated M2-M5 system. One can thus explore such structures in the regime of parameters where gravity is large and the classical black hole solution is valid. As we have seen in Chapter 6, upon taking into account brane-brane interaction, the supermaze has 16 supercharges locally, but only 4 supercharges globally. This is a property shared by all brane systems whose supergravity back-reaction gives a smooth horizonless solution [29], which makes us confident that the fully back-reacted supergravity solution sourced by the supermaze will not have a horizon. If the supergravity formulation of the supermaze turns out as we expect it will, it would finally provide a proof of the fuzzball conjecture.

The purpose of this Chapter is to make a crucial first step in developing the supergravity formulation of the supermaze. As one would expect, the supergravity solutions for generic intersecting branes are extremely complicated. Moreover, supergravity solutions for various intersecting branes have been extensively studied in the past. We start by pulling together, and unifying, earlier literature on the intersecting-brane solutions relevant to the supermaze. We obtain the supergravity equations governing supermaze solutions, and show how a "near-brane" limit is related to a certain class of warped $AdS_3\times S^3\times S^3$ solutions constructed in [40].

There are several stages in this construction, and several technical tools we will develop. The first is to construct the solution corresponding to the supermaze without momentum. We will do this from first principles in Section 8.2, and relate our equations and solutions to the construction in [259]. We also show that, if one imposes spherical $(SO(4)\times SO(4))$ symmetry, then our equations capture all the $\frac{1}{4}$-BPS M2-M5 solutions. This is described in Section 8.2.3 and Appendix E. Even without spherical symmetry, the results of [259] suggest that the results described in Section 8.2 capture all the possible pure intersecting M2-M5 solutions.

There is an important issue that we clarify in Appendix F. We are considering the $\frac{1}{4}$-BPS system (8 supersymmetries) of intersecting M2's and M5's. These branes have

one spatial direction in common, which we label by y. The combined M2 and M5 system therefore spans six spatial dimensions, and so has four transverse spatial dimensions. Because of the way that the supersymmetry projectors work, one can add, *without breaking the supersymmetry any further*, a complementary set of M5 branes, which we will denote as M5', whose world volume spans these four transverse dimensions and y. There is a complete democracy between the original M5 branes and the M5' branes. One can thus have $\frac{1}{4}$-BPS solutions with arbitrary numbers of M2, M5 and M5' branes, and the BPS equations respect this fact. However, the explicit eleven-dimensional metric involves a fibration that seemingly breaks the democracy. In Appendix F we discuss how this seeming asymmetry between the M5 branes and the M5' branes is simply an artifact of coordinate choices.

From the perspective of the supermaze, we want the M5 branes to wrap what will become compactified directions and *not fill the space-time*. We thus focus on solutions with no net M5' charge. However, because we do want net M2 and M5 charges, the Chern-Simons term of supergravity will generically require some, at least, "dipolar" distribution of M5' charge. These considerations play a major role in determining the solutions we consider in subsequent Sections.

In Section 8.3, we first look at a smeared, highly symmetric version of our supermaze and show how it is related to a brane-intersection solution found in [260]. We then consider a more general scaling limit of our system of equations that corresponds to a "near-brane-intersection" limit of the supermaze. We show that this reduces to a particular family of the $AdS_3\times S^3\times S^3$ solutions constructed in [40]. Our analysis provides the complete mapping between the near-brane supermaze, the results of [259] and the results of [40]. We re-derive the BPS equations of [40] from the perspective of the supermaze, thereby furnishing a description of the supersymmetries of the near-brane, AdS formulation in terms of projection matrices in M-theory.

In Section 8.4 and Appendix G, we show how our supermaze system can be smeared and dualized into various brane systems. In particular, we show how the supermaze solutions can be dualized to the F1-D1 string web, whose geometry was constructed in [261]. In Appendix H, we also use dualities to construct simple, new solutions to our original supermaze equations.

In Section 8.5 we consider "floating" M2 and M5 branes both in the original intersecting M2-M5 brane formulation and in the near-brane AdS formulation. Floating branes [262] reveal the probes that are mutually BPS with respect to the background brane configuration. While the floating brane analysis is relatively straightforward in the M2-M5 formulation, it is particularly revealing in the AdS formulation of [40]. Indeed it shows how the AdS directions emerge from combinations of natural brane coordinates and shows that only a particular family of the solutions considered in [40] correspond to brane configurations that are asymptotic to M2 or M5 branes at infinity.

In Section 8.6, we adapt and develop some of the examples of AdS solutions obtained in [40], mapping them across to the M2-M5 brane-intersection formulation. This reveals how the AdS space and the Riemann surface of [40] appear in the more intuitive brane

configurations that are inherent to the supermaze.

The primary core of this Chapter is the development of "momentum-free" supermazes, the equations that govern them and how to map the near-brane, AdS solutions onto the M2-M5 configurations. The next stage in this program is the addition of independent momenta to all the elements of this system. This is a challenging enterprise and the first real progress towards it is presented in the next Chapter. However, we could not resist exploring the addition of a simple momentum charge as a first step in this direction. In Section 8.7 we show that a singular momentum charge can indeed be added by a harmonic Ansatz for the distribution of BPS momentum charge. On top of the AdS, near-brane "momentum-free" supermaze, adding such a momentum distribution converts the AdS_3 factor into an extremal spinning BTZ black-hole geometry whose momentum charge depends on the two dimensions of the brane intersection locus. The fact that adding such a momentum charge involves such an extremely simple Ansatz makes us very optimistic about completing the far more ambitious project of adding independent momenta to each intersection locus. Even if the asymptotics of these solutions is not flat, it is also worth remarking that they give an infinite violation of black-hole uniqueness in this system.

We finish by making some concluding remarks in Section 8.8.

8.2 The most general solution describing M5-M2 intersections

We are interested in 8-supercharge, or $\frac{1}{4}$-BPS, supergravity solutions describing the uplift of momentum-free type IIA little strings inside NS5 branes. If we denote the direction of the little strings as x^1, and the M-theory direction as x^2, the M-theory solution will have the charges of M2 branes extended along 012 and of M5 branes extended along the directions 013456. Before the back-reaction of the branes, one can think about this configuration as describing M5 branes located at arbitrary positions in the M-theory direction, x^2, and M2 branes stretched between any of these M5 branes, and located at arbitrary locations inside the four-torus spanned by x^3, x^4, x^5, x^6.

However, we know that this picture is altered by the interaction between these branes [36]: the M2 branes will pull on the M5 branes, and the final brane configuration will consist of multiple spikes with M5 and M2 charge, extending from one M5 to another. Furthermore, we expect the back-reaction of these spikes to give rise, via a geometric transition, to a new geometry containing bubbles and fluxes, but no brane sources. However, both the brane interactions and the geometric transition will respect the symmetries and the supersymmetries of the original brane system.

Our strategy is to use the eight Killing spinors of the system, defined in terms of the frame components along the M2 and M5 directions:

$$\Gamma^{012}\,\varepsilon \;=\; -\,\varepsilon\,, \qquad \Gamma^{013456}\,\varepsilon \;=\; \varepsilon \tag{8.1}$$

to solve the gravitino equation

$$\delta\psi_\mu \;\equiv\; \nabla_\mu \epsilon \;+\; \frac{1}{288}\Big(\Gamma_\mu{}^{\nu\rho\lambda\sigma} \;-\; 8\,\delta_\mu^\nu\,\Gamma^{\rho\lambda\sigma}\Big)\,F_{\nu\rho\lambda\sigma} \;=\; 0\,, \tag{8.2}$$

and to determine the metric and three-form vector potential of this system. Before beginning we can observe that, since

$$\Gamma^{0123456789\,10} \;=\; \mathbb{1}\,, \tag{8.3}$$

equation (8.1) implies that

$$\Gamma^{01789\,10}\,\varepsilon \;=\; -\,\varepsilon\,, \tag{8.4}$$

and hence adding a set of M5 branes along 01789 10 does not break supersymmetry any further. We will denote this second possible set of branes by M5'.

8.2.1 The metric and the three-form potential.

We parametrize the M2 directions via $(x^0, x^1, x^2) = (t, y, z)$, and we denote the coordinates inside the M5 branes $(x^3, \ldots, x^6)$ by vectors $\boldsymbol{u} \in \mathbb{R}^4$. The transverse dimensions, $(x^7, \ldots, x^{10})$, will be parametrized by vectors $\boldsymbol{v} \in \mathbb{R}^4$. As we explain in Appendix E, upon using (8.2) and the equations of motion of eleven-dimensional supergravity we find that the eleven-dimensional metric ultimately has the form:

$$\begin{aligned} ds_{11}^2 \;=\; e^{2A_0}\Big[&-dt^2 \;+\; dy^2 \;+\; e^{-3A_0}\,(-\partial_z w)^{-\frac{1}{2}}\,d\boldsymbol{u}\cdot d\boldsymbol{u} \;+\; e^{-3A_0}\,(-\partial_z w)^{\frac{1}{2}}\,d\boldsymbol{v}\cdot d\boldsymbol{v} \\ &+\; (-\partial_z w)\Big(dz \;+\; (\partial_z w)^{-1}\,(\boldsymbol{\nabla}_{\boldsymbol{u}}\, w)\cdot d\boldsymbol{u}\Big)^2\Big]\,. \end{aligned} \tag{8.5}$$

This metric is conformally flat along time and the common M2-M5 direction, $(t, y) \in \mathbb{R}^{(1,1)}$, and also along the internal M5 torus (parameterized by $\boldsymbol{u}$) and the transverse $\mathbb{R}^4$ parameterized by $\boldsymbol{v} \in \mathbb{R}^4$. Since the equations we solve are local, the torus wrapped by the M5 branes can be replaced by $\mathbb{R}^4$. To obtain solutions with a compact four-torus one has to consider periodic sources in this $\mathbb{R}^4$. The metric involves a non-trivial fibration of the "M-theory direction," z, over this internal $\mathbb{R}^4$.

The constraints on, and relationships between, the functions $A_0(\boldsymbol{u}, \boldsymbol{v}, z)$ and $w(\boldsymbol{u}, \boldsymbol{v}, z)$ will be discussed below, and, for obvious reasons, we require $\partial_z w < 0$.

We will use the set of frames:

$$\begin{aligned} &e^0 \;=\; e^{A_0}\,dt\,, \qquad e^1 \;=\; e^{A_0}\,dy\,, \qquad e^2 \;=\; e^{A_0}(-\partial_z w)^{\frac{1}{2}}\Big(dz \;+\; (\partial_z w)^{-1}\Big(\boldsymbol{\nabla}_{\boldsymbol{u}}\, w\Big)\cdot d\boldsymbol{u}\Big)\,, \\ &e^{i+2} \;=\; e^{-\frac{1}{2}A_0}\,(-\partial_z w)^{-\frac{1}{4}}\,du_i\,, \qquad e^{i+6} \;=\; e^{-\frac{1}{2}A_0}\,(-\partial_z w)^{\frac{1}{4}}\,dv_i\,, \qquad i = 1, 2, 3, 4\,. \end{aligned} \tag{8.6}$$

The three-form vector potential is given by:

$$C^{(3)} \;=\; -\,e^0\wedge e^1\wedge e^2 \;+\; \frac{1}{3!}\,\epsilon_{ijk\ell}\Big((\partial_z w)^{-1}\,(\partial_{u_\ell} w)\,du^i\wedge du^j\wedge du^k \;-\; (\partial_{v_\ell} w)\,dv^i\wedge dv^j\wedge dv^k\Big)\,, \tag{8.7}$$

where $\epsilon_{ijk\ell}$ is the ϵ-symbol on $\mathbb{R}^4$.

This solution appears to be asymmetric between the two $\mathbb{R}^4$'s, and hence between the M5 and M5' branes. However, as we explain in detail in Appendix F, this is a coordinate artifact coming from the choice of fibration of the M-theory direction. One can flip the fibration from the $\boldsymbol{u}$-plane to the $\boldsymbol{v}$-plane by using w as a coordinate and thinking of z as a function, $z(w, \boldsymbol{u}, \boldsymbol{v})$.

8.2.2 The maze function

Denote the Laplacians on each $\mathbb{R}^4$ via:

$$\mathcal{L}_u \equiv \nabla_{\boldsymbol{u}} \cdot \nabla_{\boldsymbol{u}}\,, \qquad \mathcal{L}_v \equiv \nabla_{\boldsymbol{v}} \cdot \nabla_{\boldsymbol{v}}\,, \tag{8.8}$$

and suppose that $G_0(\boldsymbol{u}, \boldsymbol{v}, z)$ is a solution to what we will refer to as the "maze equation[2]:"

$$\mathcal{L}_v G_0 = (\mathcal{L}_u G_0)\,(\partial_z \partial_z G_0) - (\nabla_{\boldsymbol{u}} \partial_z G_0) \cdot (\nabla_{\boldsymbol{u}} \partial_z G_0)\,. \tag{8.9}$$

One then finds that there are eight solutions to the gravitino variation equations, (8.2), provided w and A_0 are given by :

$$w = \partial_z G_0\,, \qquad e^{-3A_0}\,(-\partial_z w)^{\frac{1}{2}} = \mathcal{L}_v G_0\,. \tag{8.10}$$

One can also verify that these equations along with (8.9) imply

$$e^{-3A_0}\,(\partial_z w)^{-\frac{1}{2}} - (\partial_z w)^{-1}\,(\nabla_{\boldsymbol{u}}\, w) \cdot (\nabla_{\boldsymbol{u}}\, w) = -\,\mathcal{L}_u G_0\,. \tag{8.11}$$

Hence, given a brane distribution specified by boundary conditions and sources, the "brane-intersection" equations, like (8.9), will have a unique solution and so (8.9) does indeed completely determine the M5-M2 intersections of interest to us

The differential equation (8.9) has a very interesting form but it is non-linear and cannot be explicitly solved in general. It also has variant, but very similar, forms for many other solutions describing $\frac{1}{4}$-BPS brane intersections [259, 261, 266]. Despite the non-linearity, it was argued in [261] using perturbation theory that once one has specified a brane distribution through its boundary conditions and sources, there is a unique solution to (8.9), and thus there is a one-to-one map between brane webs[3] and solutions to (8.9).

8.2.3 Imposing spherical symmetry

A supermaze generically has spherical symmetry in the transverse $\mathbb{R}^4$, but breaks all isometries in the internal $\mathbb{R}^4$. Since this solution is complicated, one can try focusing on a

[2]In other contexts, when a solution to a BPS system is governed by a single function satisfying one equation, this function and the equation have been referred to as a "master function" and a "master equation." (See, for example, [263–265].) Since G_0 completely encodes the structure of the "maze" of branes, we think "maze" is a more appropriate sobriquet here.

[3]Some of these brane webs are a special examples of the configurations we consider, where one smears over three directions of the internal four-torus.

simpler solution that has spherical symmetry in the internal $\mathbb{R}^4$ as well. This solution can describe either a single M2 spike ending on and pulling on an M5 brane, or an M2 brane stretching between two M5 branes, or multiple coincident M2 branes ending on multiple M5 branes.

The metric with spherical symmetry in the two $\mathbb{R}^4$'s is:

$$\begin{aligned} ds_{11}^2 \;=\; e^{2A_0}\Big[&-dt^2 \;+\; dy^2 \;+\; (-\partial_z w)\Big(dz \;+\; (\partial_z w)^{-1}\,(\partial_u w)\,du\Big)^2 \\ &+\; e^{-3A_0}\,(-\partial_z w)^{-\frac{1}{2}}\Big(du^2 \;+\; u^2\,d\Omega_3^2\Big) \;+\; e^{-3A_0}\,(-\partial_z w)^{\frac{1}{2}}\Big(dv^2 \;+\; v^2\,d\Omega_3'^2\Big)\Big]\,, \end{aligned} \tag{8.12}$$

where $u = |\boldsymbol{u}|$, $v = |\boldsymbol{v}|$ and $d\Omega_3^2$, $d\Omega_3'^2$ are the metrics of unit three-spheres in each $\mathbb{R}^4$ factor. The obvious choice for a set of frames is then:

$$\begin{aligned} e^0 \;&=\; e^{A_0}\,dt\,, \qquad e^1 \;=\; e^{A_0}\,dy\,, \qquad e^2 \;=\; e^{A_0}\,(-\partial_z w)^{\frac{1}{2}}\Big(dz \;+\; (\partial_z w)^{-1}\,(\partial_u w)\,du\Big)\,, \\ e^3 \;&=\; e^{-\frac{1}{2}A_0}\,(-\partial_z w)^{-\frac{1}{4}}\,du\,, \qquad e^4 \;=\; e^{-\frac{1}{2}A_0}\,(-\partial_z w)^{\frac{1}{4}}\,dv\,, \\ e^{i+4} \;&=\; e^{-\frac{1}{2}A_0}\,(-\partial_z w)^{-\frac{1}{4}}\,\sigma_i\,, \qquad e^{i+7} \;=\; e^{-\frac{1}{2}A_0}\,(-\partial_z w)^{\frac{1}{4}}\,\widetilde{\sigma}_i\,, \qquad i = 1,2,3\,. \end{aligned} \tag{8.13}$$

where σ_i and $\widetilde{\sigma}_i$ are left-invariant one-forms on the unit three-spheres.

Similarly one has the spherically symmetric 3-form potential:

$$C^{(3)} \;=\; -\,e^0\wedge e^1\wedge e^2 \;+\; (\partial_z w)^{-1}\Big(u^3\partial_u w\Big)\,\mathrm{Vol}(S^3) \;+\; \Big(v^3\partial_v w\Big)\,\mathrm{Vol}(S'^3)\,, \tag{8.14}$$

where $\mathrm{Vol}(S^3)$ and $\mathrm{Vol}(S'^3)$ are the volume forms of the unit three-spheres. Note there is a sign-flip of the flux along the S'^3 compared to (8.7). This is because of the orientation change in (8.13) compared to (8.6) where the e^4 is now the radial v-direction.

The spherically symmetric formulation is important because it is the one we use most directly, and because it is relatively easily to show that it is the most general $\frac{1}{4}$-BPS configuration for our intersecting M2 and M5 branes.

In Appendix E we derive this solution following the methodology developed in [263, 264, 267–269]. We will show that the solutions described above are the only possible ones with these symmetries.

8.3 Near-brane M5-M2 intersections

Perhaps rather surprisingly, the $\frac{1}{4}$-BPS geometry created by intersecting M2 and M5 branes has a near-brane limit that includes an AdS_3 factor. One can see this by searching for solutions with an $SO(2,2)\times SO(4)\times SO(4)$ isometry and whose geometry contains factors of $\mathrm{AdS}_3\times\mathrm{S}^3\times\mathrm{S}^3$. The most general such geometry can depend on two non-trivial variables that we will label as (ρ,ξ). Such solutions have been extensively studied in [40, 260, 266, 270–274].

8.3.1 Smeared solutions

One can smear along the M-theory direction and thereby find geometries that are ultimately independent of z. This results in the solution given in [260]. However one has to be a little careful in using the methodology of Section 8.2 to arrive at this result: smearing should make the solution independent of the M-theory direction but, as we will describe, this requires a judicious coordinate change.

There are two ways to proceed. The smearing will wash out the fibration and so one can re-work the approach of Appendix E but starting with $B_1 \equiv 0$.

In this instance one finds that the BPS equations only solve a subset of the equations of motion and so one must supplement the BPS system with one of the equations of motion. Alternatively, one can use the results of Section 8.2 while being careful about what it means to be independent of the M-theory direction. Specifically, we will see that to realize such independence one may have to change the z-coordinate via $\widehat{z} = z f(u)$ to get a metric that is then independent of $\widehat{z}$. In particular, such a coordinate change leads to a differential $d\widehat{z} = f(u)dz + zf'(u)du$ that can be used to absorb a z-dependent B_1 field into a coordinate re-definition.

To explore these possibilities, and cast the net a little wider, it is instructive to seek solutions to (8.9) with a power-series Ansatz in z:

$$G_0 \;=\; -\frac{1}{2}\, z^2\, \widehat{g}_2(u,v) \;+\; z\, \widehat{g}_1(u,v) \;+\; \widehat{g}_0(u,v)\,. \tag{8.15}$$

Substituting this into (8.9) results in a quadratic in z and hence three equations:

$$\begin{aligned}
&\mathcal{L}_{\boldsymbol{v}}\, \widehat{g}_2 \;+\; \widehat{g}_2\, \mathcal{L}_{\boldsymbol{u}}\, \widehat{g}_2 \;-\; 2\left(\boldsymbol{\nabla}_{\boldsymbol{u}}\, \widehat{g}_2\right)^2 \;=\; 0\,,\\
&\mathcal{L}_{\boldsymbol{v}}\, \widehat{g}_1 \;+\; \widehat{g}_2\, \mathcal{L}_{\boldsymbol{u}}\, \widehat{g}_1 \;-\; 2\left(\boldsymbol{\nabla}_{\boldsymbol{u}}\, \widehat{g}_1\right)\cdot\left(\boldsymbol{\nabla}_{\boldsymbol{u}}\, \widehat{g}_2\right) \;=\; 0\,,\\
&\mathcal{L}_{\boldsymbol{v}}\, \widehat{g}_0 \;+\; \widehat{g}_2\, \mathcal{L}_{\boldsymbol{v}}\, \widehat{g}_0 \;-\; \left(\boldsymbol{\nabla}_{\boldsymbol{u}}\, \widehat{g}_1\right)^2 \;=\; 0\,.
\end{aligned} \tag{8.16}$$

The first equation can be written

$$\mathcal{L}_{\boldsymbol{v}}\, \widehat{g}_2 \;-\; \widehat{g}_2^3\, \mathcal{L}_{\boldsymbol{u}}(\widehat{g}_2^{-1}) \;=\; 0\,, \tag{8.17}$$

which leads to an obvious "separable" solution:

$$\widehat{g}_2 \;=\; \frac{h_2(\boldsymbol{v})}{h_1(\boldsymbol{u})}\,, \tag{8.18}$$

where the h_j are harmonic. This is the near-brane, limiting boundary condition discussed in [259].

With this choice for $\widehat{g}_2$, the remaining equations in (8.16) are linear. There is also the gauge redundancy associated with a linear shift $z \to z + const.$. We will make the simple choice: $\widehat{g}_1 \equiv 0$, which also eliminates the redundancy. Hence we take

$$G_0 \;=\; -\frac{1}{2}\, z^2\, \frac{h_2(\boldsymbol{v})}{h_1(\boldsymbol{u})} \;+\; \widehat{g}_0(u,v)\,, \tag{8.19}$$

and the maze equation, (8.9), reduces to the requirement that the h_j are harmonic and that $\widehat{g}_0$ satisfy the linear equation:

$$\frac{1}{h_1(\boldsymbol{u})}\,\mathcal{L}_{\boldsymbol{u}}\,\widehat{g}_0 \;+\; \frac{1}{h_2(\boldsymbol{v})}\,\mathcal{L}_{\boldsymbol{v}}\,\widehat{g}_0 \;=\; 0\,, \tag{8.20}$$

Having got to this point we note that we now have:

$$w \;=\; \partial_z G_0 \;=\; -\,z\,\frac{h_2(\boldsymbol{v})}{h_1(\boldsymbol{u})}\,, \tag{8.21}$$

and this means that the non-diagonal frame in the metric can be greatly simplified. Specifically:

$$\begin{aligned} e^{-A_0}\,e^2 \;&=\; (-\partial_z w)^{\frac{1}{2}}\Big(dz \;+\; (\partial_z w)^{-1}\big(\boldsymbol{\nabla}_{\boldsymbol{u}}\,w\big)\cdot d\boldsymbol{u}\Big) \;=\; \left(\frac{h_2(\boldsymbol{v})}{h_1(\boldsymbol{u})}\right)^{\frac{1}{2}}\left[dz \;-\; \frac{z}{h_1(\boldsymbol{u})}\big(\boldsymbol{\nabla}_{\boldsymbol{u}}\,h_1(\boldsymbol{u})\big)\cdot d\boldsymbol{u}\right] \\ &=\; \big(h_1(\boldsymbol{u})h_2(\boldsymbol{v})\big)^{\frac{1}{2}}\left[\frac{dz}{h_1(\boldsymbol{u})} \;-\; \frac{z}{(h_1(\boldsymbol{u}))^2}\big(\boldsymbol{\nabla}_{\boldsymbol{u}}\,h_1(\boldsymbol{u})\big)\cdot d\boldsymbol{u}\right] \;=\; \big(h_1(\boldsymbol{u})h_2(\boldsymbol{v})\big)^{\frac{1}{2}}\,d\widehat{z}\,, \end{aligned} \tag{8.22}$$

where

$$\widehat{z} \;\equiv\; \frac{z}{h_1(\boldsymbol{u})}\,. \tag{8.23}$$

In other words, the fibration is "pure gauge." Hence, both the fibration and the z-dependence of the metric can be removed by a judicious change of variable. It is the $\widehat{z}$-coordinate that is the correct smeared M-theory direction.

There is probably a rich class of solutions to equation (8.20), but there is one interesting, non-trivial way to satisfy it. One first re-writes (8.20) as:

$$\mathcal{L}_{\boldsymbol{u}}\,\widehat{g}_0 \;=\; -\,h_0(\boldsymbol{u},\boldsymbol{v})\,h_1(\boldsymbol{u})\,, \qquad \mathcal{L}_{\boldsymbol{v}}\,\widehat{g}_0 \;=\; h_0(\boldsymbol{u},\boldsymbol{v})\,h_2(\boldsymbol{v})\,, \tag{8.24}$$

for some function, h_0. One then follows [260] by imposing the constraint $h_0 = h_1 h_2$ so that:

$$\widehat{g}_0 \;=\; f_2(\boldsymbol{v})\,h_1(\boldsymbol{u}) \;-\; f_1(\boldsymbol{u})\,h_2(\boldsymbol{v})\,, \quad \text{where} \quad \mathcal{L}_{\boldsymbol{u}}\,f_1 \;=\; h_1^2\,, \quad \mathcal{L}_{\boldsymbol{v}}\,f_2 \;=\; h_2^2\,, \tag{8.25}$$

and hence

$$G_0 \;=\; -\,\frac{1}{2}\,z^2\,\frac{h_2(\boldsymbol{v})}{h_1(\boldsymbol{u})} \;+\; f_2(\boldsymbol{v})\,h_1(\boldsymbol{u}) \;-\; f_1(\boldsymbol{u})\,h_2(\boldsymbol{v})\,. \tag{8.26}$$

Using this in (8.10), one obtains

$$w \;=\; -\,z\,\frac{h_2(\boldsymbol{v})}{h_1(\boldsymbol{u})}\,, \qquad e^{-3A_0}\left(\frac{h_2(\boldsymbol{v})}{h_1(\boldsymbol{u})}\right)^{\frac{1}{2}} \;=\; h_1(\boldsymbol{u})\,h_2^2(\boldsymbol{v}) \quad\Rightarrow\quad e^{-2A_0} \;=\; h_1(\boldsymbol{u})\,h_2(\boldsymbol{v})\,. \tag{8.27}$$

The end result is precisely the family of solutions constructed in [260] and, in particular, the metric reduces to:

$$ds_{11}^2 \;=\; (h_1(\boldsymbol{u})\,h_2(\boldsymbol{v}))^{-1}\,(-dt^2 \;+\; dy^2) \;+\; d\widehat{z}^2 \;+\; h_1(\boldsymbol{u})\,d\boldsymbol{u}\cdot d\boldsymbol{u} \;+\; h_2\,(\boldsymbol{v})\,d\boldsymbol{v}\cdot d\boldsymbol{v}\,. \tag{8.28}$$

One should note that, if one starts from the more general framework of Section 8.2, then the independence from the M-theory direction and the removal of the non-trivial fibration requires a re-definition of the z-coordinate.

8.3.2 More general families of solutions

There are more general, "unsmeared" solutions that have been obtained in a "near-brane" limit [40, 266, 270–274]. Here we summarize the key results of [40].

The Ansatz makes full use of the isometries:

$$\begin{aligned} ds_{11}^2 &= e^{2A}\left(\widehat{f}_1^2\, ds^2_{AdS_3} + \widehat{f}_2^2\, ds^2_{S^3} + \widehat{f}_3^2\, ds^2_{S'^3} + h_{ij} d\sigma^i d\sigma^j\right), \\ C^{(3)} &= b_1\, \widehat{e}^{012} + b_2\, \widehat{e}^{345} + b_3\, \widehat{e}^{678}, \end{aligned} \tag{8.29}$$

where the metrics $ds^2_{AdS_3}$, $s^2_{S^3}$ and $ds^2_{S'^3}$ are the metrics of unit radius on AdS_3 and the three-spheres and $\widehat{e}^{012}$, $\widehat{e}^{345}$ and $\widehat{e}^{678}$ are the corresponding volume forms.

The functions e^{2A}, $\widehat{f}_j$, b_j, and the two-dimensional metric, h_{ij}, are, *a priori*, arbitrary functions of (σ^1, σ^2) (and the e^{2A} factor is redundant). However, the final result in [40] is to pin down all these functions and express them in terms of a complex function, G, and a real function h.

First, the two dimensional metric must be that of a Riemann surface with Kähler potential, $\log(h)$:

$$h_{ij} d\sigma^i d\sigma^j = \frac{\partial_w h \partial_{\overline{w}} h}{h^2} |dw|^2, \tag{8.30}$$

where w is a complex coordinate and h is required to be harmonic:

$$\partial_w \partial_{\overline{w}} h = 0. \tag{8.31}$$

We will define real and imaginary parts of w via:

$$w = \xi + i\,\rho \quad \Rightarrow \quad \partial_w = \tfrac{1}{2}\left(\partial_\xi - i\,\partial_\rho\right), \qquad \partial_{\overline{w}} = \tfrac{1}{2}\left(\partial_\xi + i\,\partial_\rho\right). \tag{8.32}$$

It is also convenient to introduce the harmonic conjugate, $\widetilde{h}$, of h, defined by requiring that $-\widetilde{h} + ih$ is holomorphic:

$$\partial_{\overline{w}}(-\widetilde{h} + ih) = 0. \tag{8.33}$$

Since $-\widetilde{h}+ih$ is holomorphic we can use them as local coordinates on the Riemann surface, or, equivalently we can take

$$-\widetilde{h} + ih = \beta\, w = \beta\,(\xi + i\,\rho), \tag{8.34}$$

where β is a constant parameter introduced for later convenience.

Thus we may (locally) fix the Riemann surface metric to be a multiple of that of the Poincaré upper half-plane:

$$h_{ij} d\sigma^i d\sigma^j = \frac{d\xi^2 + d\rho^2}{4\,\rho^2}, \tag{8.35}$$

where the factor of 4 comes from the factors of $\frac{1}{2}$ in partial derivatives (8.32).

The complex function, G, is required to satisfy the equation:

$$\partial_w G = \tfrac{1}{2}\,(G + \overline{G})\,\partial_w \log(h). \tag{8.36}$$

If one writes G in terms of real and imaginary parts, $G = g_1 + ig_2$, and uses the local coordinates (8.34), then one has:

$$\partial_\xi g_1 \; + \; \partial_\rho g_2 \; = \; 0\,, \qquad \partial_\xi g_2 \; - \; \partial_\rho g_1 \; = \; -\,\frac{1}{\rho}\,g_1\,. \tag{8.37}$$

It is convenient to introduce potentials, Φ, and $\widetilde{\Phi}$, associated with G. First, one defines Φ via:

$$\partial_w\,\Phi \; = \; \overline{G}\,\partial_w h \qquad \Leftrightarrow \qquad \partial_\xi\Phi \; = \; -\,\beta\,g_2\,, \quad \partial_\rho\Phi \; = \; \beta\,g_1\,. \tag{8.38}$$

The existence of such a Φ is guaranteed by the first equation in (8.37). The second equation in (8.37) implies that Φ must satisfy

$$\Big(\partial_\xi^2 \; + \; \partial_\rho^2 \; - \; \frac{1}{\rho}\,\partial_\rho\Big)\,\Phi \; = \; 0\,. \tag{8.39}$$

Similarly, the second equation in (8.37) implies that there is a conjugate potential, $\widetilde{\Phi}$, defined by:

$$\partial_\xi\widetilde{\Phi} \; = \; -\,\frac{\beta}{\rho}\,g_1 \; = \; -\,\frac{1}{\rho}\,\partial_\rho\Phi\,, \qquad \partial_\rho\widetilde{\Phi} \; = \; -\,\frac{\beta}{\rho}\,g_2 \; = \; \frac{1}{\rho}\,\partial_\xi\Phi\,. \tag{8.40}$$

The first equation in (8.37) then implies that $\widetilde{\Phi}$ must satisfy

$$\partial_\xi^2\widetilde{\Phi} \; + \; \frac{1}{\rho}\,\partial_\rho\Big(\,\rho\,\partial_\rho\widetilde{\Phi}\,\Big) \; = \; 0\,. \tag{8.41}$$

If one introduces a dummy coordinate, χ, and considers Euclidean $\mathbb{R}^3$ with coordinates (ρ, χ, ξ), where ξ defines one of the axes and (ρ, χ) are polar coordinates in the remaining $\mathbb{R}^2$, then the equation (8.41) is simply the condition that $\widetilde{\Phi}$ is harmonic on $\mathbb{R}^3$. Moreover, if one defines a one-form, $\Phi d\chi$, then the relationship between Φ and $\widetilde{\Phi}$ in (8.40) can be summarized as $*_3(\Phi d\chi) = d\widetilde{\Phi}$. It remains to be seen if this is simply a coincidence or where there is some deeper physical meaning to this observation and the coordinate, χ.

Finally, define the functions:

$$W_\pm \; \equiv \; |G \; \pm \; i|^2 \; + \; \gamma^{\pm 1}\,(G\overline{G} \; - \; 1)\,, \tag{8.42}$$

where $-1 \leq \gamma \leq 1$ is a "deformation" parameter that defines the relevant exceptional superalgebra $D(2,1;\gamma) \oplus D(2,1;\gamma)$ [40].

The sign of gamma is related to the magnitude of G via:

$$\gamma\,(G\overline{G} \; - \; 1) \; \geq \; 0\,, \tag{8.43}$$

and to keep our presentation simple, we will henceforth restrict to:

$$\gamma \; > \; 0\,, \qquad |G| \; \geq \; 1\,. \tag{8.44}$$

With this choice, the parameters in [40] can be simplified to:

$$c_1 = \gamma^{1/2} + \gamma^{-1/2} > 0\,, \qquad c_2 = -\gamma^{1/2} < 0\,, \qquad c_3 = -\gamma^{-1/2} < 0\,, \qquad \sigma = +1\,. \tag{8.45}$$

The metric functions in (8.29) are given by:

$$\widehat{f}_1^{-2} \;=\; \gamma^{-1}\,(\gamma+1)^2\,(G\overline{G}\;-\;1)\,,\qquad \widehat{f}_2^{-2} \;=\; W_+\,,\qquad \widehat{f}_3^{-2} \;=\; W_-\,, \tag{8.46}$$

and

$$e^{6A} \;=\; h^2\,(G\overline{G}\;-\;1)\,W_+\,W_- \;=\; \gamma\,(\gamma+1)^{-2}\,h^2\,\widehat{f}_1^{-2}\,\widehat{f}_2^{-2}\,\widehat{f}_3^{-2}\,. \tag{8.47}$$

The flux functions, b_i, are given by:

$$\begin{aligned} b_1 \;&=\; \frac{\nu_1}{c_1^3}\left[\frac{h\,(G+\overline{G})}{(G\overline{G}\;-\;1)}\;+\;\gamma^{-1}\,(\gamma+1)^2\,\Phi\;-\;(\gamma-\gamma^{-1})\,\widetilde{h}\right],\\ b_2 \;&=\; \frac{\nu_2}{c_2}\left[-\frac{h\,(G+\overline{G})}{W_+}\;+\;(\Phi\;-\;\widetilde{h})\right],\qquad b_3 \;=\; \frac{\nu_3}{c_3}\left[\frac{h\,(G+\overline{G})}{W_-}\;-\;(\Phi\;+\;\widetilde{h})\right], \end{aligned} \tag{8.48}$$

where one has $|\nu_i| = 1$, with signs arranged so that $\nu_1\nu_2\nu_3 = -1$. Compared to the results in [40], we have used (8.45) and we have dropped some (irrelevant) additive constants in the b_i.

8.3.3 Mapping the AdS$_3$ solutions to M5-M2 intersections

Our goal here is to show how to map the AdS$_3$ solutions of Section 8.3.2 into the spherically-symmetric brane-intersection formulation of Section 8.2.3.

The first step is to remember that the AdS$_3$ solutions, supposed to correspond to a near-brane limit, depend non-trivially on only two coordinates, (ρ, ξ), whereas the formulation in Section 8.2.3 allows asymptotically-flat solutions that depend non-trivially on three variables, (u, v, z). We thus have to find a scaling limit for the solutions in Section 8.2.3.

To render the scaling properties more transparent, we introduce a Poincaré metric on AdS$_3$:

$$ds^2_{AdS_3} \;=\; \frac{d\mu^2}{\mu^2}\;+\;\mu^2\left(-\,dt^2\;+\;dy^2\right), \tag{8.49}$$

where the Poincaré $\mathbb{R}^{1,1}$ factor represents the common directions of the brane intersection, and it is to be identified with the same factor in (8.12).

We start by noting that the metric (8.29) is scale invariant under:

$$\mu\;\to\;\lambda\,\mu\,,\qquad (t,y)\;\to\;\lambda^{-1}(t,y)\,. \tag{8.50}$$

This must now be imposed on the more general class of solutions discussed in Section 8.2.3.

Scale invariance of (8.12) can be achieved by taking:

$$(u,v)\;\to\;\sqrt{\lambda}\,(u,v)\,,\qquad z\;\to\;\lambda^{-1}z\,, \tag{8.51}$$

and

$$e^{A_0}\;\to\;\lambda\,e^{A_0}\,,\qquad w\;\to\;\lambda^{-1}\,w\,. \tag{8.52}$$

There is a very important difference between (8.50), (8.51) and (8.52). The first two are simply prescriptions for the scaling of coordinates, while the (8.52) imposes strong constraints on the functional form of e^{A_0} and w. It is these constraints that lead to the near-brane limit. Indeed, this scaling invariance leads to the following Ansatz for the mapping we seek:

$$\begin{aligned} u &= \sqrt{\mu}\, m_1(\rho,\xi)\,, \qquad v = \sqrt{\mu}\, m_2(\rho,\xi)\,, \qquad z = \mu^{-1}\, m_3(\rho,\xi)\,, \\ w &= \mu^{-1}\, m_4(\rho,\xi)\,, \qquad e^{A_0} = \mu\, m_5(\rho,\xi)\,, \end{aligned} \tag{8.53}$$

for some functions, m_j.

A direct comparison of (8.12) and (8.29), using (8.49) and (8.35), leads to:

$$e^{2A}\,\widehat{f}_1^2\,\mu^2 = e^{2A_0}\,, \qquad e^{2A}\,\widehat{f}_2^2 = e^{-A_0}\,(-\partial_z w)^{-\frac{1}{2}}\,u^2\,, \qquad e^{2A}\,\widehat{f}_3^2 = e^{-A_0}\,(-\partial_z w)^{\frac{1}{2}}\,v^2\,, \tag{8.54}$$

along with

$$\begin{aligned} e^{2A}\left(\widehat{f}_1^2\,\frac{d\mu^2}{\mu^2} + \frac{d\xi^2 + d\rho^2}{4\,\rho^2}\right) &= e^{-A_0}\Big((-\partial_z w)^{-\frac{1}{2}}\,du^2 + (-\partial_z w)^{\frac{1}{2}}\,dv^2\Big) \\ &\quad + e^{2A_0}\,(-\partial_z w)\left(dz + (-\partial_z w)^{-1}\left(\partial_u w\right)du\right)^2. \end{aligned} \tag{8.55}$$

Using (8.34), (8.46), (8.47) and (8.54) in (8.55) one finds that one must have:

$$\begin{aligned} &\frac{\gamma}{(1+\gamma)^2}\,\frac{1}{(G\overline{G}-1)}\,\frac{d\mu^2}{\mu^2} + \frac{d\xi^2 + d\rho^2}{4\,\rho^2} \\ &\quad = \frac{1}{W_+}\,\frac{du^2}{u^2} + \frac{1}{W_-}\,\frac{dv^2}{v^2} + \frac{1}{\beta^2\,\rho^2\,(G\overline{G}-1)}\,\frac{W_+}{W_-}\left(u^2 dz + (-\partial_z w)^{-1}\left(u^3\partial_u w\right)\frac{du}{u}\right)^2. \end{aligned} \tag{8.56}$$

One can also manipulate (8.54), using (8.47) and (8.34), to obtain:

$$u^2 v^2 = \frac{\beta^2\,\gamma}{(\gamma+1)^2}\,\mu^2\,\rho^2\,, \qquad (-\partial_z w)\,\frac{v^2}{u^2} = \frac{W_+}{W_-}\,, \qquad e^{A_0} = \frac{\beta\sqrt{\gamma}\mu\rho}{(\gamma+1)}e^{-2A}(W_+W_-)^{\frac{1}{2}}\,. \tag{8.57}$$

The first identity in (8.57), and the form of the fibration on the right-hand side of (8.56), suggest a slightly more refined change of variables:

$$u = \sqrt{a\,\mu\,\rho}\,e^{\alpha(\rho,\xi)}\,, \qquad v = \sqrt{a\,\mu\,\rho}\,e^{-\alpha(\rho,\xi)}\,, \qquad z = \mu^{-1}\,e^{-2\alpha(\rho,\xi)}\,p(\rho,\xi)\,, \tag{8.58}$$

where α and p are functions to be determined, and the parameter a is given by:

$$a \equiv \frac{\beta\,\sqrt{\gamma}}{(\gamma+1)}\,. \tag{8.59}$$

Comparing the expressions (8.14) and (8.29) for the $C^{(3)}$ flux leads to:

$$(\partial_z w)^{-1}\left(u^3\partial_u w\right) = b_2\,, \qquad \left(v^3\partial_v w\right) = b_3\,. \tag{8.60}$$

where b_2 and b_3 are given in (8.48). The matching of the flux along the AdS direction involves non-trivial gauge transformations and we will return to this below.

From this we note that (8.56) can be re-written as

$$\begin{aligned}&\frac{\gamma}{(1+\gamma)^2}\,\frac{1}{(G\overline{G}-1)}\,\frac{d\mu^2}{\mu^2}\;+\;\frac{d\xi^2\;+\;d\rho^2}{4\,\rho^2}\\&\qquad=\;\frac{1}{W_+}\,\frac{du^2}{u^2}\;+\;\frac{1}{W_-}\,\frac{dv^2}{v^2}\;+\;\frac{1}{\beta^2\,\rho^2\,(G\overline{G}-1)}\,\frac{W_+}{W_-}\left(u^2dz\;+\;b_2\,\frac{du}{u}\right)^2.\end{aligned}\tag{8.61}$$

Substituting the change of variable (8.58) into this, one obtains an over-determined system of equations for b_2 and the derivatives of α and p. This system is very complicated, involving square-roots of a quadratic in $W_\pm$. However, for $\gamma=1$, the system dramatically simplifies and one finds:

$$\begin{aligned}\partial_\xi\alpha\;&=\;-\,\frac{\varepsilon_1}{2\rho}\,g_1\,,\quad\partial_\rho\alpha\;=\;\frac{1}{2\rho}\,g_2\,,\qquad b_2\;=\;2\,a\,\rho\,p\;+\;\frac{\varepsilon_2\,\beta\rho\,g_1}{g_1^2+g_2^2+g_2}\,,\\\partial_\xi p\;&=\;-\,\frac{\varepsilon_1\varepsilon_2\,\beta}{2\,a\rho}\,(g_2-1)\,,\quad\partial_\rho p\;=\;-\,\frac{1}{\rho}\left(p\;+\;\frac{\varepsilon_2\,\beta}{2\,a}\,g_1\right).\end{aligned}\tag{8.62}$$

where g_1 and g_2 are the real and imaginary parts of G, $G=g_1+ig_2$.

From (8.37) one sees that $\partial_\xi(\rho^{-1}g_2)=\partial_\rho(\rho^{-1}g_1)$ and hence we must take $\varepsilon_1=-1$, and then one can identify α with the potential $\widetilde{\Phi}$:

$$\alpha\;=\;-\,\frac{1}{2\,\beta}\,\widetilde{\Phi}\,.\tag{8.63}$$

Similarly, it is elementary to integrate the equations for p to arrive at:

$$p\;=\;-\,\frac{\varepsilon_2}{2\,a\,\rho}\left(\Phi\;+\;\beta\,\xi\right).\tag{8.64}$$

Using (8.62) one finds that b_2 must have the form:

$$b_2\;=\;\varepsilon_2\left(\frac{\beta\rho\,g_1}{g_1^2+g_2^2+g_2}\;-\;\left(\Phi+\beta\,\xi\right)\right)\;=\;\varepsilon_2\left(\frac{h\,(G+\overline{G})}{W_+}\;-\;\left(\Phi-\widetilde{h}\right)\right).\tag{8.65}$$

From (8.45) one sees that $c_2=-1$ for $\gamma=1$, and one finds a perfect match between (8.65) and (8.48) if $\nu_2=\varepsilon_2$.

To summarize, in order to map the solution in Section 8.3.2 to the near-brane limit of the spherically-symmetric brane-intersection of Section 8.2.3 one needs to take:

$$\gamma=1\,,\qquad u=\left(\tfrac{1}{2}\,\beta\mu\rho\right)^{\frac{1}{2}}e^{-\frac{1}{2\beta}\widetilde{\Phi}}\,,\qquad v=\left(\tfrac{1}{2}\,\beta\mu\rho\right)^{\frac{1}{2}}e^{+\frac{1}{2\beta}\widetilde{\Phi}}\,,\qquad z=-\frac{\varepsilon_2}{\beta\rho\mu}\,e^{\frac{1}{\beta}\widetilde{\Phi}}\left(\Phi+\beta\,\xi\right).\tag{8.66}$$

One can also compute w as a function of (μ,ρ,ξ). Indeed, from (8.57) and (8.60) one has

$$\partial_z w\;=\;-\,\frac{g_1^2+g_2^2+g_2}{g_1^2+g_2^2-g_2}\,e^{-\frac{2}{\beta}\widetilde{\Phi}}\,,\qquad(\partial_z w)^{-1}\left(u^3\partial_u w\right)\;=\;b_2\,,\qquad\left(v^3\partial_v w\right)\;=\;b_3\,,\tag{8.67}$$

from which one obtains:

$$dw \;=\; (\partial_z w)dz \;+\; (\partial_u w)du \;+\; (\partial_v w)dv \;=\; d\left[\frac{\varepsilon_2}{\beta\rho\mu}\, e^{-\frac{1}{\beta}\widetilde{\Phi}}(\Phi-\beta\xi)\right], \tag{8.68}$$

and hence:

$$w \;=\; \frac{\varepsilon_2}{\beta\rho\mu}\, e^{-\frac{1}{\beta}\widetilde{\Phi}}(\Phi-\beta\xi)\,. \tag{8.69}$$

To get an exact differential on the right-hand side of (8.68) it is essential that one has

$$b_3 \;=\; \varepsilon_2\left(\frac{\beta\rho\, g_1}{g_1^2+g_2^2-g_2} \;-\; \Big(\Phi-\beta\,\xi\Big)\right) \;=\; \varepsilon_2\left(\frac{h\,(G+\overline{G})}{W_-} \;-\; \Big(\Phi+\widetilde{h}\Big)\right). \tag{8.70}$$

From (8.45) one sees that $c_3 = -1$ for $\gamma = 1$, and one finds a perfect match between (8.70) and (8.48) if $\nu_3 = -\varepsilon_2$.

It is interesting to note that (8.66) and (8.69) imply

$$u^2\, z \;=\; -\tfrac{1}{2}\,\varepsilon_2\Big(\Phi+\beta\,\xi\Big)\,, \qquad v^2\, w \;=\; \tfrac{1}{2}\,\varepsilon_2\Big(\Phi-\beta\,\xi\Big)\,, \tag{8.71}$$

which, once again, illustrates the "democracy" in the fibration discussed in Appendix F. Additionally, it is interesting to observe that (8.66) and (8.69) imply that if one flips the signs of the potentials, then one flips the roles of u and v and the roles of z and w:

$$\Phi\to-\Phi\,,\quad \widetilde{\Phi}\to-\widetilde{\Phi} \quad\Rightarrow\quad u\leftrightarrow v\,,\quad z\leftrightarrow w\,. \tag{8.72}$$

Finally, consider the differential:

$$\omega \;\equiv\; e^{3A_0}\,(-\partial_z w)^{\frac{1}{2}}\left(dz \;+\; (\partial_z w)^{-1}\Big(\partial_u w\Big)\,du\right). \tag{8.73}$$

Using (8.47), (8.57) and (8.66) one finds:

$$\begin{aligned}
\omega \;&=\; \frac{W_+\,\mu^2}{4\,(G\overline{G}-1)}\left(u^2 dz \;+\; (\partial_z w)^{-1}\Big(u^3\partial_u w\Big)\,\frac{du}{u}\right)\\
&=\; \frac{\varepsilon_2}{4}\left[\left(\frac{\beta\rho\, g_1}{g_1^2+g_2^2-1} \;+\; 2\,\Phi\right)\mu\, d\mu \;-\; d\Big(\mu^2\,\Phi\Big)\right]\\
&=\; \frac{\varepsilon_2}{8}\left[\left(\frac{h(G+\overline{G})}{(G\overline{G}-1)} \;+\; 4\,\Phi\right)\mu\, d\mu \;-\; d\Big(2\,\mu^2\,\Phi\Big)\right] \;=\; \frac{\varepsilon_2}{\nu_1}\, b_1\,\mu\, d\mu \;-\; \frac{\varepsilon_2}{4}\, d\Big(\mu^2\,\Phi\Big)\,,
\end{aligned} \tag{8.74}$$

where the last expression follows from (8.48) and (8.45) for $\gamma = 1$. Thus one has

$$b_1 \;=\; \frac{\nu_1}{4}\left(\frac{\beta\rho\, g_1}{g_1^2+g_2^2-1} \;+\; 2\,\Phi\right), \tag{8.75}$$

as in (8.48) and [40] with $c_1 = 2$.

The important point here is that the three-form potential (8.7) along y (the common M2-M5 direction) and z (the M-theory direction) is:

$$C^{(3)}_{tyz} \;=\; -e^0\wedge e^1\wedge e^2 \;=\; -dt\wedge dy\wedge\omega \;=\; -\frac{\varepsilon_2}{\nu_1}\, b_1\,\mu\, dt\wedge dy\wedge d\mu + \frac{\varepsilon_2}{4}\, d\Big(\mu^2\,\Phi\, dt\wedge dy\Big)\,. \tag{8.76}$$

Using (8.29) and (8.49) one has:

$$C^{(3)}_{tyz} \;=\; b_1\,\mu\,dt\wedge dy\wedge d\mu\,, \tag{8.77}$$

and so these components of the flux match (8.76), up to a gauge transformation, provided that $\nu_1 = -\varepsilon_2$.

We have shown that there is perfect agreement if and only if $-\nu_1 = \nu_2 = -\nu_3 = \varepsilon_2$.

In [40] these is a further constraint $\nu_1\nu_2\nu_3 = -1$, which suggests $\varepsilon_2 = -1$, however this last constraint is related to the form of the unbroken supersymmetries. We will discuss all these signs in the next Section.

8.3.4 Verifying the BPS equations for the AdS_3 solutions

We can use the results of Section 8.3.3 to verify that the AdS_3 solutions satisfy directly the BPS equations in Section 8.2. Specifically, we have taken the following frames:

$$\begin{aligned}
e^0 &= \frac{\mu\, e^A}{2\sqrt{G\overline{G}-1}}\,dt\,, \qquad e^1 = \frac{\mu\, e^A}{2\sqrt{G\overline{G}-1}}\,dy\,,\\
e^2 &= \frac{\varepsilon_2\, e^A}{\rho\sqrt{(G\overline{G}-1)\,W_+\,W_-}}\left(\rho\, g_1\,\frac{d\mu}{\mu} + (G\overline{G}-1)\Big(g_2\,d\xi - g_1\,d\rho\Big)\right),\\
e^3 &= \frac{e^A}{2\sqrt{W_+}}\left(\frac{d\mu}{\mu}+\frac{d\rho}{\rho}+\frac{1}{\rho}\Big(g_1\,d\xi+g_2\,d\rho\Big)\right),\\
e^4 &= \frac{e^A}{2\sqrt{W_-}}\left(\frac{d\mu}{\mu}+\frac{d\rho}{\rho}-\frac{1}{\rho}\Big(g_1\,d\xi+g_2\,d\rho\Big)\right),\\
e^{i+4} &= \frac{e^A}{2\sqrt{W_+}}\,\sigma_i\,, \qquad e^{i+7} = \frac{e^A}{2\sqrt{W_-}}\,\widetilde{\sigma}_i\,, \qquad i=1,2,3\,.
\end{aligned} \tag{8.78}$$

These are, in fact, precisely the same frames as in (8.13); note, in particular, the possible sign choice, ε_2, in e^2. Using (8.29) to define the Ansatz for the flux, $C^{(3)}$, one finds that all the BPS equations can be satisfied if:

$$\begin{aligned}
\partial_\xi b_1 &= \varepsilon_2\,\partial_\xi\left[-\frac{\beta\,\rho\,g_1}{4\,(G\overline{G}-1)}\right] + \frac{1}{2}\,\varepsilon_2\,\beta\,g_2\,, \qquad \partial_\rho b_1 = \varepsilon_2\,\partial_\rho\left[-\frac{\beta\,\rho\,g_1}{4\,(G\overline{G}-1)}\right] - \frac{1}{2}\,\varepsilon_2\,\beta\,g_1\,,\\
\partial_\xi b_2 &= \varepsilon_2\,\partial_\xi\left[-\frac{2\,\beta\,\rho\,g_1}{W_+}+\beta\,\xi\right] - \varepsilon_2\,\beta\,g_2\,, \qquad \partial_\rho b_2 = \varepsilon_2\,\partial_\rho\left[-\frac{2\,\beta\,\rho\,g_1}{W_+}+\varepsilon_2\,\beta\,\xi\right] + \varepsilon_2\,\beta\,g_1\,,\\
\partial_\xi b_3 &= \varepsilon_2\,\partial_\xi\left[-\frac{2\,\beta\,\rho\,g_1}{W_-}-\beta\,\xi\right] - \varepsilon_2\,\beta\,g_2\,, \qquad \partial_\rho b_3 = \varepsilon_2\,\partial_\rho\left[-\frac{2\,\beta\,\rho\,g_1}{W_-}-\beta\,\xi\right] + \varepsilon_2\,\beta\,g_1\,.
\end{aligned} \tag{8.79}$$

which leads to:

$$b_1 = -\varepsilon_2\left(\frac{\beta\,\rho\,g_1}{4\,(G\overline{G}-1)}+\frac{1}{2}\,\Phi\right),\;\; b_2 = -\varepsilon_2\left(\frac{2\,\beta\,\rho\,g_1}{W_+}-(\Phi+\beta\,\xi)\right),\;\; b_3 = -\varepsilon_2\left(\frac{2\,\beta\,\rho\,g_1}{W_-}-(\Phi-\beta\,\xi)\right). \tag{8.80}$$

This is consistent with (8.48) for $c_1 = 2, c_2 = c_3 = -1$, if one takes $-\nu_1 = -\nu_2 = \nu_3 = \varepsilon_2$.

The signs of the fluxes determine the unbroken supersymmetries. Indeed, if we generalize (E.4) to

$$\Gamma^{012}\,\varepsilon \;=\; \eta_1\,\varepsilon\,, \qquad \Gamma^{013567}\,\varepsilon \;=\; \eta_2\,\varepsilon\,, \qquad \Gamma^{01489\,10}\,\varepsilon \;=\; -\,\eta_1\,\eta_2\,\varepsilon\,. \tag{8.81}$$

where η_j are signs, $\eta_j^2 = 1$, then one finds:

$$\begin{aligned} b_1 \;&=\; \varepsilon_2\,\eta_1\left(\frac{\beta\,\rho\,g_1}{4\,(G\overline{G}-1)}+\frac{1}{2}\,\Phi\right), \qquad b_2 \;=\; \varepsilon_2\,\eta_1\eta_2\left(\frac{2\,\beta\,\rho\,g_1}{W_+}-(\Phi+\beta\,\xi)\right), \\ b_3 \;&=\; -\,\varepsilon_2\,\eta_2\left(\frac{2\,\beta\,\rho\,g_1}{W_-}-(\Phi-\beta\,\xi)\right). \end{aligned} \tag{8.82}$$

This matches (8.48) for $c_1 = 2, c_2 = c_3 = -1$, if $\nu_1 = \varepsilon_2\eta_1$, $\nu_2 = \varepsilon_2\eta_1\eta_2$ and $\nu_3 = \varepsilon_2\eta_2$. Note that this implies $\nu_1\nu_2\nu_3 = \varepsilon_2$, and, as noted above, this matches the constraint in [40] if $\varepsilon_2 = -1$. This means that the frame, e^2, in (8.78) comes with a negative sign. Indeed, in Section 8.3.3 the matching required that $-\nu_1 = \nu_2 = -\nu_3 = \varepsilon_2$, which corresponds to $\eta_1 = \eta_2 = \varepsilon_2 = -1$.

The choices of signs η_1, η_2 and ε_2 are determined by the unbroken supersymmetry and frame orientations. We will persist with the choice that we started with in (8.1) and we will keep our frames positive. Thus we will take:

$$\eta_1 \;=\; -\,1\,, \qquad \eta_2 \;=\; +\,1\,, \qquad \varepsilon_2 \;=\; +\,1\ . \tag{8.83}$$

8.4 String webs

Some of the solutions we have constructed can be related, via dualities, to the (p, q) string-web solutions preserving eight supercharges that were obtained in [261]. This relation is expected: when the M2-M5 solutions are smeared over three of the internal torus directions, one can find a duality chain that relates the M2 and M5 branes to F1 and D1 strings. To illustrate this connection and some of the interesting properties of our solutions it reveals, we perform the explicit duality at the level of supergravity solutions, and relate the F1-D1 string-web solutions of [261] to the ones we obtained in Section 8.2.

We begin with the string-web solutions:

$$\begin{aligned} ds^2_{IIB} &= \sqrt{h_{11}}\left[-e^{3A}dt^2 + e^{3A}h_{ab}dr^a dr^b + \frac{e^{-3A}}{\det h}dw_2^2 + d\boldsymbol{y}_6^2\right], \\ e^{2\phi} &= \frac{h_{11}^2}{\det h}\,, \quad C_0 = -\frac{h_{12}}{h_{11}}\,, \quad B_2 = e^{3A}h_{1a}dt\wedge dr^a, \quad C_2 = e^{3A}h_{2a}dt\wedge dr^a \end{aligned} \tag{8.84}$$

which describe a web of F1-strings, D1-strings and more generic (p, q) strings in the plane spanned by (r^1, r^2), with w_2 and $\mathbf{y}_6$ being orthogonal directions. The two-dimensional metric h_{ab} can be expressed in terms of a Kähler potential:

$$h_{ab} = \frac{1}{2}\partial_a\partial_b K(r^1, r^2, \boldsymbol{y})\,, \tag{8.85}$$

which satisfies a Monge-Ampère equation

$$\Delta_y K + 2e^{-3A} = 0\,, \tag{8.86}$$

with $e^{-3A} = \det h$.

8.4.1 The D2-D4 frame

In order to dualize the solution (8.84) to the M2-M5 duality frame and compare it with our solution (8.5)-(8.7), we have to first go to the D2-D4 frame by performing T-dualities along w_2 and y_1, an S-duality, and finally another T-duality along y_2. Anticipating the mapping of this solution to the one of Section 8.2, we do the following coordinate relabeling:

$$r^1 \to z\,, \quad r^2 \to u_1\,, \quad w_2 \to u_2\,, \quad y_1 \to u_3\,, \quad y_2 \to y\,, \quad y_{3,4,5,6} \to v_{3,4,5,6}\,. \tag{8.87}$$

The procedure, explained in detail in Appendix G, involves working in the democratic formalism and using several times the Monge-Ampère equation (8.86). The final result for the solution describing a D2-D4 web is

$$\begin{aligned}
ds^2 &= \frac{1}{\sqrt{\det h}}(-dt^2+dy^2) + \frac{\sqrt{\det h}}{h_{11}}(du_2^2+du_3^2) + \sqrt{\det h}\left(e^{3A}h_{ab}dr^a dr^b + ds^2_{\mathbb{R}^4}\right)\,,\\
e^{2\phi} &= \frac{\sqrt{\det h}}{h_{11}}\,, \quad B_2 = \frac{h_{12}}{h_{11}}du_2\wedge du_3\,,\\
C_3 &= e^{3A}h_{1a}dt\wedge dr^a\wedge dy - \frac{v^3}{2}\partial_v\partial_z K\, d\Omega_3'\,,\\
C_5 &= \frac{1}{h_{11}}dt\wedge du_1\wedge du_2\wedge du_3\wedge dy + \frac{v^3}{2}\left(\frac{h_{12}}{h_{11}}\partial_v\partial_z K - \partial_v\partial_{u_1}K\right)du_2\wedge du_3\wedge d\Omega_3'\,.
\end{aligned} \tag{8.88}$$

8.4.2 Uplifting to M-theory

In order to go to M-theory we have to uplift the system (8.88) along a direction, x, that we will call $x = -u_4$. Using the usual relations between type IIA and 11-dimensional supergravity

$$ds^2_{11} = e^{\frac{-2\phi}{3}}ds^2_{10} + e^{\frac{4\phi}{3}}(dx + C_1)^2\,, \tag{8.89}$$

$$C_3' = C_3 + B_2\wedge dx\,, \tag{8.90}$$

where x is the uplifting direction, we arrive at the following M-theory solution:

$$\begin{aligned}
ds^2_{11} =& \frac{h_{11}^{1/3}}{(\det h)^{2/3}}(-dt^2+dy^2) + \frac{(\det h)^{1/3}}{h_{11}^{2/3}}(du_2^2+du_3^2+du_4^2)\\
&+ (\det h)^{1/3}h_{11}^{1/3}\left(e^{3A}h_{ab}dr^a dr^b + ds^2_{\mathbb{R}^4}\right)\,,
\end{aligned} \tag{8.91}$$

$$C_3 = \frac{h_{11}}{\det h}dt\wedge dz\wedge dy + \frac{h_{12}}{\det h}dt\wedge du_1\wedge dy - \frac{h_{12}}{h_{11}}du_2\wedge du_3\wedge du_4 - \frac{v^3}{2}\partial_v\partial_z K d\Omega_3'\,. \tag{8.92}$$

Remembering the re-labelling of the r^a coordinates in (8.87), and adding and subtracting $\frac{(\det h)^{1/3}}{h_{11}^{2/3}} du_1^2$ in (8.91), the foregoing metric becomes:

$$\begin{aligned} ds_{11}^2 =& \frac{h_{11}^{1/3}}{(\det h)^{2/3}}(-dt^2+dy^2) + \frac{(\det h)^{1/3}}{h_{11}^{2/3}}(du_1^2+du_2^2+du_3^2+du_4^2) \\ &+ \frac{h_{11}^{4/3}}{(\det h)^{2/3}}\left(dz+\frac{h_{12}}{h_{11}}du_1\right)^2 + (\det h)^{1/3}h_{11}^{1/3}\left(dv^2+v^2d\Omega_3'^2\right)\,, \end{aligned} \tag{8.93}$$

where we have written the $\mathbb{R}^4$ metric of (8.91) in hyperspherical coordinates,

Now, we would like to compare this solution with (8.5)-(8.7). In order to do that we have to assume spherical symmetry in $\mathbb{R}^4(\boldsymbol{v})$[4] and fiber the "original" M-theory direction, z, over a single direction of the $\mathbb{R}^4(\boldsymbol{u})$, which we pick, for obvious reasons, to be u_1. The metric and $C^{(3)}$ field then become:

$$\begin{aligned} ds_{11}^2 =& e^{2A_0}(-dt^2+dy^2) + e^{-A_0}(-\partial_z w)^{-\frac{1}{2}}\left(du_1^2+du_2^2+du_3^2+du_4^2\right) \\ &+ e^{2A_0}(-\partial_z w)\left(dz+(\partial_z w)^{-1}(\partial_{u_1}w)du_1\right)^2 + e^{-A_0}(-\partial_z w)^{\frac{1}{2}}\left(dv^2+v^2d\Omega_3'^2\right)\,, \end{aligned} \tag{8.94}$$

$$\begin{aligned} C^{(3)} =& -e^{3A_0}(-\partial_z w)^{\frac{1}{2}}dt\wedge dy\wedge dz + e^{3A_0}(-\partial_z w)^{-\frac{1}{2}}(\partial_{x_1}w)dt\wedge dy\wedge dx_1 \\ &+ (-\partial_z w)^{-1}(\partial_{u_1}w)du_2\wedge du_3\wedge du_4 + (v^3\partial_v w)d\Omega_3'\,. \end{aligned} \tag{8.95}$$

Comparing (8.94) with (8.91) it is easy to see that the following relations should hold for the two metrics to be the same:

$$e^{2A_0} = \frac{h_{11}^{1/3}}{(\det h)^{2/3}}\,,\quad h_{11} = -\partial_z w\,,\quad h_{12} = -\partial_{u_1}w\,. \tag{8.96}$$

Finally, comparing (8.95) with (8.92) we see that w should be equal to $-\frac{1}{2}\partial_z K$, and from (8.10) one finds that the maze function, G_0, is, up to signs and factors of 2, precisely the Kähler potential of the string-web solution.

8.5 Floating M2 and M5 branes

Even if the brane structure of the solutions we construct is obscured by the brane interactions and back-reaction, there is a very intuitive way to reveal this structure: one finds the brane probes that feel no force when inserted into these solutions. The orientation of the floating branes in the metric given by the frames in Section 8.2 is straightforward, and so is the evaluation of the appropriate DBI-like and Wess-Zumino-like terms in the M2-brane action. However, the action of M5 branes is rather complicated [275]; the easiest way to evaluate it is to use one of the isometries of the M-theory solution to formally write it as a Type IIA solution (as we did in the previous Section) and evaluate the action of probe D4 branes.

We now examine these brane probes in more detail.

[4]It is not necessary to assume spherical symmetry in $\mathbb{R}^4(\boldsymbol{v})$ in 8.4.1, but doing so simplifies considerably the transition to the democratic formalism.

8.5.1 Floating M2 branes in the intersecting M2-M5 Ansatz

It is easy to see the floating M2 branes in the brane-intersection formulation of the M2-M5 solutions of Section 8.2. Indeed, parametrizing the brane using coordinates (η_0, η_1, η_2), it is trivial to see that a brane with:

$$t \;=\; \eta_0\,, \qquad y \;=\; \eta_1\,, \qquad z \;=\; \eta_2\,, \qquad \boldsymbol{u}, \boldsymbol{v} \text{ constant}\,, \tag{8.97}$$

feels no force in all of the solutions in Section 8.2. This is because the (t, y, z)-components of $C^{(3)}$ are simply:

$$C^{(3)}_{tyz} \;=\; -\,e^0 \wedge e^1 \wedge e^2\,. \tag{8.98}$$

Since this is the form of the determinant of the frames along the probe directions, it means that the WZW term will precisely cancel the DBI action for the brane embedding defined by (8.97). Thus (8.97) defines floating M2 branes.

Using (8.66) we see that in the AdS_3 formulation, the floating M2 branes are given by:

$$\rho \;=\; k_1\,\mu^{-1}\,, \qquad \widetilde{\Phi}(\xi, \rho) \;=\; k_2\,, \tag{8.99}$$

where k_1 and k_2 are constants. The floating M2 branes thus follow the level-curves of $\widetilde{\Phi}$, with scale, μ, set by the radial coordinate, ρ, on the Riemann surface.

8.5.2 Floating M2 branes in the AdS_3 formulation

It is instructive to look for floating M2 branes directly in the AdS_3 solutions. We are going to start with a general value (though positive) value of $\gamma > 0$. Following (8.97) we use the parametrization

$$t \;=\; \eta_0\,, \qquad y \;=\; \eta_1\,, \qquad \mu \;=\; e^{\eta_2}\,, \qquad \xi \;=\; \sigma_1(\eta_2)\,, \qquad \rho \;=\; \sigma_2(\eta_2)\,, \tag{8.100}$$

for some functions, σ_1 and σ_2.

The pull-back of the metric defined by (8.29), (8.35) and (8.49) onto the M2 brane is:

$$d\widehat{s}_3^2 \;=\; e^{2A}\left[\widehat{f}_1^2\left(d\eta_2^2 \;+\; e^{2\eta_2}\left(-\,d\eta_0^2 + d\eta_1^2\right)\right) \;+\; \frac{(\sigma_1')^2 + (\sigma_2')^2}{4\,\sigma_2^2}\,d\eta_2^2\right]. \tag{8.101}$$

The DBI Lagrangian is given by the square-root of the determinant of this metric:

$$\begin{aligned}\mathcal{L}_{DBI} \;&=\; e^{3A}\,\widehat{f}_1^2\,e^{2\eta_2}\left(\widehat{f}_1^2 + \frac{(\sigma_1')^2 + (\sigma_2')^2}{4\,\sigma_2^2}\right)^{\frac{1}{2}} \\ &=\; h\;\widehat{f}_1^2\,e^{2\eta_2}\left[(\,G\overline{G}\;-\;1)\,W_+\,W_-\left(\widehat{f}_1^2 + \frac{(\sigma_1')^2 + (\sigma_2')^2}{4\,\sigma_2^2}\right)\right]^{\frac{1}{2}}.\end{aligned} \tag{8.102}$$

To be able to cancel this against the WZW term, the term in the square bracket needs to be a perfect square. For $\gamma = 1$, there is a simple way to achieve this. Suppose

$$\frac{(\sigma_1')^2 + (\sigma_2')^2}{\sigma_2^2} \;=\; \frac{g_1^2 + g_2^2}{g_1^2}\,, \tag{8.103}$$

then one finds that

$$\left[(G\overline{G} \;-\; 1)\, W_+\, W_- \left(\widehat{f}_1^2 + \frac{(\sigma_1')^2 + (\sigma_2')^2}{4\,\sigma_2^2}\right)\right] \;=\; \left(\frac{W_+ W_-}{4\,g_1}\right)^2, \tag{8.104}$$

and the DBI Lagrangian reduces to:

$$\mathcal{L}_{DBI} \;=\; e^{2\eta_2}\, \frac{\beta\,\sigma_2\left((g_1^2+g_2^2)^2 - g_2^2\right)}{4\,g_1\,(g_1^2+g_2^2-1)}\,, \tag{8.105}$$

where we have assumed $\gamma = 1$ and used (8.34) and (8.100).

The WZW action is the pull-back of $C^{(3)}$ onto the M2 brane:

$$\widehat{C}^{(3)} \;=\; b_1\, e^{2\eta_2}\, d\eta_0 \wedge d\eta_1 \wedge d\eta_2\,, \tag{8.106}$$

with b_1 given by (8.48). However, we must also allow for a possible gauge transformation of the form $C^{(3)} \to C^{(3)} + d[\mu^2 \Lambda(\rho,\xi)\, d\eta_0 \wedge d\eta_1]$, for some function, Λ, and so we take the WZW action to be:

$$\widetilde{C}^{(3)} \;=\; e^{2\eta_2}\left(b_1 \;+\; 2\,\Lambda \;+\; (\partial_\xi \Lambda)\,\sigma_1' \;+\; (\partial_\rho \Lambda)\,\sigma_2'\right) d\eta_0 \wedge d\eta_1 \wedge d\eta_2\,. \tag{8.107}$$

Taking $\gamma = 1$ and $\Lambda = -2\nu_1 c_1^{-3}\Phi$ yields

$$\begin{aligned}\widetilde{C}^{(3)} \;&=\; e^{2\eta_2}\,\frac{\nu_1}{c_1^3}\left[\frac{h\,(G+\overline{G})}{(G\overline{G} \;-\; 1)} \;-\; 2\,(\partial_\xi \Phi)\,\sigma_1' \;-\; 2\,(\partial_\rho \Phi)\,\sigma_2'\right] d\eta_0 \wedge d\eta_1 \wedge d\eta_2 \\ &=\; \nu_1\, e^{2\eta_2}\,\frac{\beta\,\sigma_2}{4}\left[\frac{g_1}{(g_1^2+g_2^2-1)} \;+\; g_2\,\frac{\sigma_1'}{\sigma_2} \;-\; g_1\,\frac{\sigma_2'}{\sigma_2}\right] d\eta_0 \wedge d\eta_1 \wedge d\eta_2\,,\end{aligned} \tag{8.108}$$

where we have used (8.40) and (8.45) for $\gamma = 1$.

The WZW term exactly matches the DBI Lagrangian, (8.105), if and only if:

$$\sigma_2 \;=\; k_1\, e^{-\eta_2}\,, \qquad \frac{\sigma_1'}{\sigma_2} \;=\; \frac{g_2}{g_1}\,, \tag{8.109}$$

which also satisfies (8.103). The constant, k_1 is the same as in (8.99).

Given that $\sigma_2 = -\sigma_2'$, the second equation can be written:

$$g_1\sigma_1' \;+\; g_2\,\sigma_2' \;=\; 0 \quad\Leftrightarrow\quad \partial_\xi\widetilde{\Phi}\,\sigma_1' \;+\; \partial_\rho\widetilde{\Phi}\,\sigma_2' \;=\; 0\,, \tag{8.110}$$

which means that the floating branes follow the level curves of $\widetilde{\Phi}$. This agrees with the shape of the floating M2 brane determined directly in Section 8.5.1 and changing from the M2-M5 coordinates to the coordinates proper to the AdS_3 solution (8.99).

8.5.3 Floating M5 branes in the intersecting M2-M5 Ansatz

As we mentioned above, evaluating the action of probe M5 branes in a complicated background is quite involved. The easiest strategy is to reduce the solution to Type IIA

and evaluate the action of probe D4 branes. Fortunately, we have already obtained the formulas for the IIA reduction of our M2-M5 solution when relating it to F1-D1 string webs (8.88).

We consider probe D4 branes whose volume is parametrized by $(\eta_0, \eta_1, \eta_2, \eta_3, \eta_4)$ embedded in spacetime as

$$\eta_0 = t\,,\ \ \eta_1 = -u_1\,,\ \ \eta_2 = u_2\,,\ \ \eta_3 = u_3\,,\ \ \eta_4 = y\,. \tag{8.111}$$

The induced metric on it is

$$d\tilde{s}_6^2 = \frac{1}{\sqrt{\det h}}(-dt^2 + dy^2) + \frac{h_{22}}{\sqrt{\det h}}du_1^2 + \frac{\sqrt{\det h}}{h_{11}}(du_2^2 + du_3^2) \tag{8.112}$$

and the induced NS-NS and RR fields are

$$\begin{aligned}
\widetilde{B}_2 &= \frac{h_{12}}{h_{11}}du_2 \wedge du_3\,,\\
\widetilde{C}_3 &= -\frac{h_{12}}{\det h}dt \wedge du_1 \wedge dy\,,\\
\widetilde{C}_5 &= -\frac{1}{h_{11}}dt \wedge du_1 \wedge du_2 \wedge du_3 \wedge dy\,.
\end{aligned} \tag{8.113}$$

It is straightforward now to see that the DBI and WZ actions are:

$$S_{DBI} = -T_4 \int d^5\sigma e^{-\phi}\sqrt{-\det\left(\widetilde{G}_{\alpha\beta} + F_{\alpha\beta} + \widetilde{B}_{\alpha\beta}\right)} = -T_5 \int d^5\sigma \frac{h_{22}}{\det h}\,, \tag{8.114}$$

$$S_{WZ} = -T_4 \int e^{\widetilde{B}_2 + \widetilde{F}_2} \wedge \oplus_n \widetilde{C}_n = T_4 \int d^5\sigma \frac{h_{22}}{\det h}\,, \tag{8.115}$$

and hence the D4-brane (8.111) feels no force in this solution. This in turn indicates that probe M5 branes extended along y and the four-torus parameterized by $\boldsymbol{u}$ feel no force in the M2-M5 solution (8.5-8.7).

8.6 Interesting examples of M2-M5 near-horizon solutions

The solutions of the M2-M5 system considered in Section 8.2 are determined by a non-linear Monge-Ampère-like maze equation (8.9), and obtaining generic solutions to this equation is prohibitively complicated. Even simpler solutions such as a single infinite M2 brane ending on (and pulling on) an M5 brane cannot be found. The only known solution to this maze equation is the one corresponding to an infinite tilted M5 brane with M2 charge. This solution can be obtained by dualizing a tilted D-brane system, and for the proper tilt and the proper M2 brane density it can be shown to fit precisely in the Ansatz (8.12). We present this solution in Appendix H.

In contrast, the near-horizon geometries corresponding to M2-M5 solutions with an $SO(4) \times SO(4)$ isometry have been shown in Section 8.3 to belong to the $\gamma = 1$ family

of $AdS_3 \times S^3 \times S^3 \times \Sigma$ solutions constructed in [40], where Σ is a Riemann surface. These solutions can be constructed systematically by solving a set of linear equations in two dimensions, and there are quite a few classes of solutions that one can try to relate to M2-M5 brane systems.

8.6.1 No-flip solutions

In Section 8.3 of [40], the authors consider "no-flip" solutions with:

$$h = -iw + i\overline{w}\,, \qquad G = \pm\left[i + \sum_{a=1}^{n+1} \frac{\zeta_a \,\mathrm{Im}(w)}{(\overline{w}-\xi_a)|w-\xi_a|}\right], \tag{8.116}$$

where ξ_a and ζ_a are real parameters. As noted in (8.72), the exchange of the plus and minus sign in the expression above exchanges the role of u and v and the role of z and w.

From (8.116), (8.32) and (8.34), we see that

$$\beta = 2\,, \tag{8.117}$$

and

$$g_1 = \pm \sum_{a=1}^{n+1} \frac{\zeta_a\, \rho\, (\xi-\xi_a)}{\left((\xi-\xi_a)^2+\rho^2\right)^{\frac{3}{2}}}\,, \qquad g_2 = \pm\left[1 + \sum_{a=1}^{n+1} \frac{\zeta_a\, \rho^2}{\left((\xi-\xi_a)^2+\rho^2\right)^{\frac{3}{2}}}\right]. \tag{8.118}$$

Such functions are familiar in the study of axi-symmetric Gibbons-Hawking metrics[5]. Indeed, one can easily compute the potentials from (8.40) (with $\beta = 2$):

$$\widetilde{\Phi} = \pm 2\left[-\log\rho + \sum_{a=1}^{n+1} \frac{\zeta_a}{\sqrt{(\xi-\xi_a)^2+\rho^2}}\right], \qquad \Phi = \mp 2\left[\xi + \sum_{a=1}^{n+1} \frac{\zeta_a\,(\xi-\xi_a)}{\sqrt{(\xi-\xi_a)^2+\rho^2}}\right]. \tag{8.119}$$

This gives a nice physical picture of these solutions: the non-logarithmic part of $\widetilde{\Phi}$ is simply the three-dimensional potential of charges, $\pm 2\,\zeta_a$, arrayed along the ξ-axis at the points $(\rho,\xi) = (0,\xi_a)$. The $\log\rho$ component of $\widetilde{\Phi}$ is also a harmonic function, and its role is to give the correct asymptotic behavior.

The floating M2 branes are given by (8.99). When $|k_2|$ is large, then either u or v must be small. The floating branes are thus given by the level-curves of $\widetilde{\Phi}$ and, as can be seen in Fig. 8.1, when ρ is small, they roughly circle half-way around each of of the singularities of $\widetilde{\Phi}$ located at $(\rho,\xi) = (0,\xi_a)$, and run roughly parallel to the boundary between the singularities. These infinite M2 branes are parallel to the M2 branes whose back-reaction gives rise to the solution, but in the coordinates adapted to the AdS_3 near-horizon geometry they have the shape given in Figure 8.1.

[5]This may not be a complete coincidence: Gibbons-Hawking metrics provide solutions to the Monge-Ampère equation in two variables with two $U(1)$ isometries.

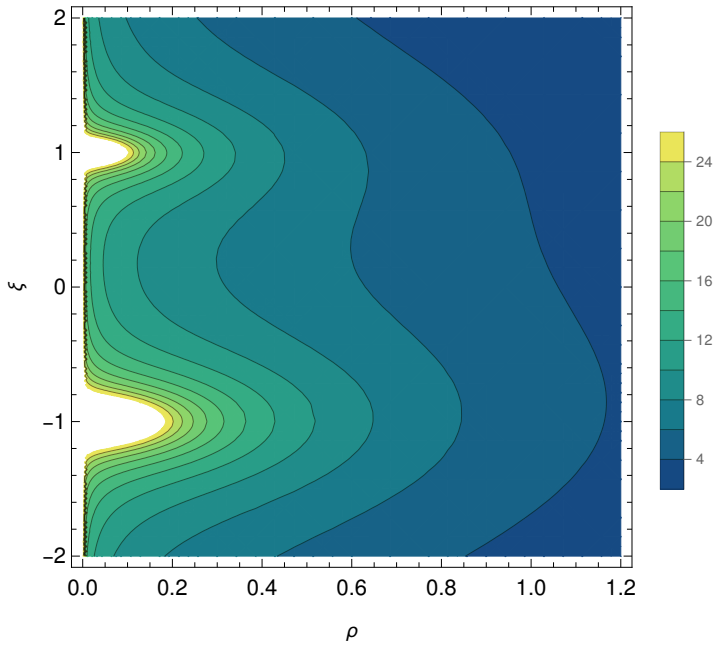

Figure 8.1: Contour plot of $\widetilde{\Phi}$ for two points, with $(\zeta_1 = 1, \xi_1 = 1)$ and $(\zeta_2 = 2, \xi_2 = -1)$. By (8.99), the lines of constant potential drawn in black are the floating M2 branes.

8.7 Adding momentum

To transform the M2-M5 supermaze we discussed in the previous Sections into a microstate of a three-charge black hole with a large horizon, one needs to add to it momentum along the common M2-M5 direction. As discussed in detail in [29,36], a momentum wave that preserves the locally-16-supercharge structure of the supermaze can only be added when accompanied by other brane dipole moments, which can modify the structure of our Ansatz. Our purpose here is to find the minimal modification of our Ansatz needed to add momentum, and to construct the resulting solution, even though this solution does not display local supersymmetry enhancement to 16 supercharges.

8.7.1 Adding momentum to spherically symmetric brane intersections

As we will see, the simplest $\frac{1}{8}$-BPS solutions that carry momentum charge have a singular momentum-charge source that gives rise to a momentum harmonic function that encodes the momentum density of the solution.

We start from the metric Ansatz:

$$\begin{aligned} ds_{11} = -e^{2A_0}\,dt^2 \;+\; e^{2A_1}\Big(dy - P\,dt\Big)^2 \;+\; e^{2A_2}\,du^2 \;+\; e^{2A_3}\,dv^2 \;+\; u^2\,e^{2A_4}\,d\Omega_3^2 \;+\; v^2\,e^{2A_5}\,d\Omega_3'^2 \\ +\; e^{2A_6}\Big(dz \;+\; B_1\,du\Big)^2\,, \end{aligned} \tag{8.120}$$

which reduces to the no-momentum Ansatz in equation (8.5) by taking $A_1 \equiv A_0$ and

$P \equiv 0$. We take the frames to be:

$$\begin{aligned} e^0 &= e^{A_0}\,dt\,, \qquad e^1 = e^{A_1}\Big(dy - P\,dt\Big)\,, \qquad e^2 = e^{A_6}\Big(dz + B_1\,du\Big)\,, \\ e^3 &= e^{A_2}\,du\,, \qquad e^4 = e^{A_3}\,dv\,, \qquad e^{i+4} = u\,e^{A_4}\,\sigma_i\,, \qquad e^{i+7} = v\,e^{A_5}\,\widetilde{\sigma}_i\,, \qquad i = 1,2,3\,. \end{aligned} \tag{8.121}$$

Based on the symmetries, we also use the Ansatz (E.9) for the field strength.

The supersymmetries of this system will be defined in terms of the frame components along the momentum direction, y, as well as the M2 and M5 directions:

$$\Gamma^{01}\,\varepsilon = -\,\varepsilon\,, \qquad \Gamma^{012}\,\varepsilon = -\,\varepsilon\,, \qquad \Gamma^{013456}\,\varepsilon = \varepsilon \tag{8.122}$$

There are thus four supersymmetries and the brane system is $\frac{1}{8}$-BPS.

As before, these projectors are compatible with

$$\Gamma^{01789\,10}\,\varepsilon = -\,\varepsilon\,, \tag{8.123}$$

and hence one can add another set of M5 branes along the directions 01789 10 without breaking supersymmetry any further.

As before, the goal is to solve

$$\delta\psi_\mu \equiv \nabla_\mu\,\epsilon + \tfrac{1}{288}\Big(\Gamma_\mu{}^{\nu\rho\lambda\sigma} - 8\,\delta^\nu_\mu\,\Gamma^{\rho\lambda\sigma}\Big)\,F_{\nu\rho\lambda\sigma} = 0\,, \tag{8.124}$$

subject to the foregoing projection conditions.

Solving these BPS equations proceeds as in Appendix E.2, except that one rapidly discovers that one must take $P = -e^{A_0 - A_1} + const.$ The constant can be absorbed through a shift of y, and we will take:

$$P \equiv 1 - e^{A_0 - A_1}\,. \tag{8.125}$$

With this choice, the solution with no momentum constructed in Appendix E.2 is simply given by taking $A_1 = A_0$.

It is convenient to define

$$\widehat{A}_0 \equiv \frac{1}{2}\,(A_0 + A_1)\,, \qquad \widehat{A}_1 \equiv \frac{1}{2}\,(A_0 - A_1)\,. \tag{8.126}$$

and one finds that all the remaining BPS equations are *exactly* as in Section E.2 with $\widehat{A}_0$ replacing by A_0 and A_6 replacing A_1. In particular, the BPS equations place no constraint whatsoever on $\widehat{A}_1$.

One thus finds that the BPS equations are identically satisfied if the metric takes the form

$$\begin{aligned} ds_{11} = e^{2\widehat{A}_0}\Bigg[&- e^{2\widehat{A}_1}\,dt^2 + e^{-2\widehat{A}_1}\Big(dy + \big(e^{2\,\widehat{A}_1} - 1\big)\,dt\Big)^2 + (-\partial_z w)\Big(dz + (\partial_z w)^{-1}\big(\partial_u w\big)\,du\Big)^2 \\ &+ e^{-3\widehat{A}_0}\,(-\partial_z w)^{-\frac{1}{2}}\Big(du^2 + u^2\,d\Omega_3^2\Big) + e^{-3\widehat{A}_0}\,(-\partial_z w)^{\frac{1}{2}}\Big(dv^2 + v^2\,d\Omega'^2_3\Big)\Bigg]\,, \end{aligned} \tag{8.127}$$

with the frames:

$$\begin{aligned}
e^0 &= e^{\widehat{A}_0+\widehat{A}_1}\,dt\,, \qquad e^1 = e^{\widehat{A}_0-\widehat{A}_1}\Big(dy+\big(e^{2\,\widehat{A}_1}-1\big)\,dt\Big)\,,\\
e^2 &= e^{\widehat{A}_0}\,(-\partial_z w)^{\frac{1}{2}}\Big(dz \;+\; (\partial_z w)^{-1}\big(\partial_u w\big)\,du\Big)\,,\\
e^3 &= e^{-\frac{1}{2}\widehat{A}_0}\,(-\partial_z w)^{-\frac{1}{4}}\,du\,, \qquad e^4 = e^{-\frac{1}{2}\widehat{A}_0}\,(-\partial_z w)^{\frac{1}{4}}\,dv\,,\\
e^{i+4} &= \frac{1}{2}\,u\,e^{-\frac{1}{2}\widehat{A}_0}\,(-\partial_z w)^{-\frac{1}{4}}\,\sigma_i\,, \qquad e^{i+7} = \frac{1}{2}\,v\,e^{-\frac{1}{2}\widehat{A}_0}\,(-\partial_z w)^{\frac{1}{4}}\,\widetilde{\sigma}_i\,, \qquad i=1,2,3\,.
\end{aligned} \tag{8.128}$$

One finds that $C^{(3)}$ is still given by given by (8.14):

$$C^{(3)} \;=\; -\,e^0\wedge e^1\wedge e^2 \;+\; (\partial_z w)^{-1}\Big(u^3\partial_u w\Big)\,\mathrm{Vol}(S^3) \;+\; \Big(v^3\partial_v w\Big)\,\mathrm{Vol}(S'^3)\,. \tag{8.129}$$

Note that $\widehat{A}_1$ cancels out entirely in $e^0\wedge e^1$. Thus the solution to the BPS equations is exactly as it was in the absence of momentum, except for the $\widehat{A}_1$-dependent terms in the metric.

As before the BPS solution is obtained by solving (E.24) and then w and $\widehat{A}_0$ are obtained from (E.23) and the appropriate re-labeling of (E.20):

$$F_1 \;\equiv\; (-\partial_z w)^{\frac{1}{2}}\,e^{-3\widehat{A}_0}\,, \qquad F_2 \;\equiv\; (-\partial_z w)^{-\frac{1}{2}}\,e^{-3\widehat{A}_0} \;+\; (-\partial_z w)^{-1}\,(\partial_u w)^2\,, \tag{8.130}$$

The function $\widehat{A}_1$ is not determined by the BPS equations, however it is determined by the equations of motion. To that end, it is useful to define the operator, $\mathcal{L}$, to be the Laplacian of the metric (8.127) with $\widehat{A}_1=0$. If $H(u,v,z)$, is only a function of (u,v,z), then one finds that the equations for w and $\widehat{A}_0$ enable one to simplify the Laplacian to:

$$\begin{aligned}
\mathcal{L}(H) \;=\; e^{2\widehat{A}_0}\,(-\partial_z w)^{-\frac{1}{2}}\Big[&(-\partial_z w)\,\frac{1}{u^3}\partial_u\Big(u^3\partial_u H\Big) \;+\; \frac{1}{v^3}\partial_v\Big(v^3\partial_v H\Big) \;+\; 2\,(\partial_u w)\partial_u\partial_z H\\
&+\;\Big((-\partial_z w)^{-\frac{1}{2}}\,e^{-3\widehat{A}_0} \;+\; (-\partial_z w)^{-1}\,(\partial_u w)^2\Big)\Big)\,\partial_z^2 H\Big]\,.
\end{aligned} \tag{8.131}$$

Note that, by definition (and as is manifest from the explicit expression), this is a linear operator on the background geometry defined by $\widehat{A}_0$ and w.

One can show that all the equations of motion are satisfied if $\widehat{A}_1$ solves:

$$\mathcal{L}\Big(e^{-2\widehat{A}_1}\Big) \;=\; 0\,. \tag{8.132}$$

Thus there is a simple harmonic Ansatz for adding pure momentum sources to the the M2-M5 brane intersections.

8.7.2 Adding momentum charge to the near-brane limit

From the results above, it is elementary to translate the effect of adding a source corresponding to momentum to the AdS near-brane limit described in Section 8.3. The metric

given by (8.29), (8.35) and (8.49) generalizes to:

$$\begin{aligned} ds_{11}^2 \;=\; e^{2A}\Big[\widehat{f}_1^2\Big(\frac{d\mu^2}{\mu^2} \;+\; \mu^2\Big(-e^{2\widehat{A}_1}\,dt^2 + e^{-2\widehat{A}_1}\Big(dy + \Big(e^{2\,\widehat{A}_1}-1\Big)\,dt\Big)^2\Big)\Big) \\ +\; \widehat{f}_2^2\,ds_{S^3}^2 \;+\; \widehat{f}_3^2\,ds_{S'^3}^2 \;+\; \frac{d\xi^2+d\rho^2}{4\rho^2}\Big]\,, \end{aligned} \tag{8.133}$$

and the flux, $C^{(3)}$, remains the same.

The function, $\widehat{A}_1$, is determined by the harmonic condition, (8.132), and in the coordinate system of the near-brane AdS limit of Section 8.3, this Laplacian becomes:

$$\mathcal{L}(H) \;=\; 4\,e^{-A}\Big[(G\overline{G}-1)\,\frac{1}{\mu}\,\partial_\mu\Big(\mu^3\partial_\mu H\Big) \;+\; \frac{1}{\rho}\,\partial_\rho\Big(\rho^3\partial_\rho H\Big) \;+\; \rho^2\partial_\xi^2 H\Big]\,. \tag{8.134}$$

on some function, $H(\mu,\xi,\rho)$.

If one seeks a scaling solution to $\mathcal{L}(H)=0$ with $H(\mu,\xi,\rho)=\mu^p K(\xi,\rho)$, then K must satisfy

$$\frac{1}{\rho}\,\partial_\rho\Big(\rho^3\partial_\rho K\Big) \;+\; \rho^2\partial_\xi^2 K \;+\; p(p+2)\,(G\overline{G}-1)\,K \;=\; 0\,. \tag{8.135}$$

One can easily verify that, for $p=-1$, this has solutions

$$K \;=\; \frac{c_1}{u^2} \;+\; \frac{c_2}{v^2} \;=\; \frac{2}{\beta\rho}\Big(c_1\,e^{\frac{1}{\beta}\widetilde{\Phi}} + c_2\,e^{-\frac{1}{\beta}\widetilde{\Phi}}\Big)\,. \tag{8.136}$$

where c_1 and c_2 are constants and we have used (8.66). This is also manifestly a solution to $\mathcal{L}(H)=0$ using (8.131). These correspond to smeared distributions of singular sources of the momentum harmonic function,

To get an isolated momentum source one would like a solution that falls off at spatial infinity as $(u^2+v^2)^{-3}$. In the μ,ρ coordinates this is

$$(u^2+v^2)^{-3} \;\sim\; \mu^{-3}\,\rho^{-3}\,. \tag{8.137}$$

It is useful to note that (8.135) may be written as

$$\frac{1}{\rho^3}\,\partial_\rho\Big(\rho^3\partial_\rho K\Big) \;+\; \partial_\xi^2 K \;+\; \frac{p(p+2)}{\rho^2}\,(G\overline{G}-1)\,K \;=\; 0\,, \tag{8.138}$$

and that

$$\mathcal{L}_4(K) \;\equiv\; \frac{1}{\rho^3}\,\partial_\rho\Big(\rho^3\partial_\rho K\Big) \;+\; \partial_\xi^2 K\,, \tag{8.139}$$

is the Laplacian of flat $\mathbb{R}^5$ with a metric:

$$ds_5^2 \;\equiv\; d\rho^2 \;+\; \rho^2 d\Omega_3^2 \;+\; d\xi^2\,. \tag{8.140}$$

This means that

$$\mathcal{L}_4\Big(\frac{1}{(\rho^2+\xi^2)^{\frac{3}{2}}}\Big) \;=\; 0\,. \tag{8.141}$$

Note that this falls off as ρ^{-3} at large ρ, which is consistent with (8.137).

Now observe that at large ρ and ξ, one generically has $(G\overline{G}-1)\to 0$. Indeed, in the example in Section 8.6.1 one has:

$$\frac{p(p+2)}{\rho^2}\,(G\overline{G}-1)\;\sim\;\frac{c_0}{(\rho^2+\xi^2)^{\frac{3}{2}}}\,, \tag{8.142}$$

for some constant c_0. One can then solve (8.135) perturbatively. Indeed, if one starts from the homogeneous solution (8.141), then, using (8.142), one obtains, at first order:

$$K\;=\;\frac{Q}{(\rho^2+\xi^2)^{\frac{3}{2}}}\left(1\;-\;\frac{c_0}{4}\,\frac{1}{\sqrt{\rho^2+\xi^2}}\;+\;\ldots\right), \tag{8.143}$$

for some constant, Q, that determines the momentum charge. Given the simplicity of the Laplacian and the forms of the solutions in Section 8.6.1, this perturbation expansion can be continued to arbitrarily high order.

8.7.3 An interesting family of solutions

A simple solution to (8.134) is:

$$e^{-2\widehat{A}_1}\;=\;V_0\;+\;V_1\,\mu^{-2}\,, \tag{8.144}$$

where

$$V_0\;=\;1\;+\;\sum_{a=1}^{m}\frac{k_a}{\left((\xi-\widetilde{\xi}_a)^2+\rho^2\right)^{\frac{3}{2}}}\,,\qquad V_1\;=\;q_0\;+\;\sum_{a=1}^{m'}\frac{q_a}{\left((\xi-\widehat{\xi}_a)^2+\rho^2\right)^{\frac{3}{2}}}\,, \tag{8.145}$$

for some charges k_a and q_a. Note that we have taken the constant term in V_0 to be 1 because we require $\widehat{A}_1\to 0$ at infinity. Furthermore, the locations of the poles of these harmonic functions, $\widetilde{\xi}_a$ and $\widehat{\xi}_a$ do not have to coincide with ξ_a, the locations of the poles of Φ and $\widetilde{\Phi}$ in Section 8.6.1, but it might be interesting if they did.

Amusingly enough, at fixed ρ and ξ, (8.144) gives

$$e^{-2\widehat{A}_1}\;=\;1+\alpha\;+\;Q\,\mu^{-2}\,, \tag{8.146}$$

for some parameters, $\alpha, Q>0$.

If one takes $k_a=0, a\geq 1$, then $\alpha=0$ and the metric in the AdS_3 directions becomes

$$\begin{aligned}
&\frac{d\mu^2}{\mu^2}\;+\;\mu^2\left(-e^{2\widehat{A}_1}\,dt^2+e^{-2\widehat{A}_1}\left(dy+\left(e^{2\,\widehat{A}_1}-1\right)dt\right)^2\right)\\
&=\;\frac{d\mu^2}{\mu^2}\;-\;\frac{\mu^4}{Q+\mu^2}\,dt^2\;+\;(Q+\mu^2)\left(dy-\frac{Q}{Q+\mu^2}\,dt\right)^2\\
&=\;\frac{d\mu^2}{\mu^2}\;+\;\mu^2\Big(-dt^2\;+\;dy^2\Big)\;+\;Q\,(dy-dt)^2\,,
\end{aligned} \tag{8.147}$$

which is simply the extremal BTZ metric. Thus, our solution describes a continuous family of extremal BTZ $\times\mathrm{S}^3\times\mathrm{S}^3$ solutions warped over a Riemann surface, where the (angular) momentum of the extremal BTZ solutions, Q, is a function of the Riemann-surface coordinates, ρ and ξ. The families of solutions we have constructed give an infinite violation of black hole uniqueness with our particular $\mathrm{AdS}_3\times\mathrm{S}^3\times\mathrm{S}^3\times\Sigma$ asymptotics.

8.8 Conclusions and future directions

We have constructed, from first principles, the eight-supercharge supergravity solutions corresponding to a system of parallel M5 branes with M2 stretched between them, and have related our solutions to those previously obtained in [259]. We have found that these solutions are entirely determined by a single "maze function" satisfying a Monge-Ampère-like "maze equation." We have used floating probe M2 and M5 branes to explore the structure of these solutions and have related a class of our solutions to F1-D1 (p,q) string-web solutions [261].

Solving the maze equation is non-trivial in general, but we have identified two ways of finding special classes of solutions. The first, is to consider an infinite M2-M5 bound state at a certain angle and with a certain ratio of M2 and M5 densities. This solution, obtained in Appendix H by dualities, can be shown to have a maze function that satisfies exactly the maze equation.

The second method to solve this equation is to take a near-horizon limit of our solutions, by imposing a certain scaling symmetry on the functions in the metric and 4-form field-strength Ansatz. This scaling symmetry allowed us, in Section 8.3, to relate our solutions to a family of the $AdS_3\times S^3\times S^3$ solutions warped over a Riemann surface constructed in [40]. As with other microstate geometries, these solutions can be constructed via a linear procedure.

We have also found a family of supergravity solutions that describe M2-M5 intersections carrying momentum. The momentum of these solutions has singular sources, but we have succeeded in extending the solutions of [40] to $BTZ^{extremal}\times S^3\times S^3$ solutions warped over a Riemann surface, where the momentum of the BTZ black hole is a function of the Riemann surface coordinates. From a higher-dimensional perspective, these solutions violate black-hole uniqueness copiously.

The primary focus of our work here has been the construction of the "static," or momentum-free supermazes. The important next step is to add momentum charge in such a manner that one obtains themelia [29]: fundamental brane systems that, while being $\frac{1}{8}$-BPS globally, actually have 16 supersymmetries locally, and thus represent states in the black-hole microstructure. As we remarked earlier, this will require the addition of fluxes and localized momentum excitations that go well beyond the simple Ansätze we have used here. On the other hand, our results in Section 8.7 give us considerable optimism that this can be achieved, and perhaps through a linear system of equations that supplements the maze equation.

To understand and appreciate this remark, it is useful to recall some of the history of microstate geometries and superstrata. In the earliest work on microstate geometries, it was clear that the most general such geometry in five dimensions would be based on a general four-dimensional ambi-polar hyper-Kähler geometry [33, 212, 276]. Similarly, in six-dimensions, the most general superstrata are based on a highly-non-trivial five-dimensional spatial fibration over a four-dimensional "almost hyper-Kähler" base [204, 277]. These geometries are generically determined by non-linear systems of equa-

tions. However, once these geometries are determined, one can add momentum charge to these backgrounds in a variety of ways, and the system of equations that determines the momentum excitations, as well as the entire phases space of such excitations, is actually *linear* [183,204,205,212,276]. Moreover, the momentum can be added in such a manner as to make themelia, like the superstratum, and this also enables the detailed construction of the corresponding holographic dictionary [20, 169–175].

In Chapter 9, we show that this pattern repeats with supermazes. The "static," or momentum-free supermazes is indeed governed by generically non-linear maze equations, as we have described here, but the addition of momentum excitations on top of this geometry is, once again, governed by linear systems of equations. Therefore, we should be able to add momentum while preserving the 16-local-supercharge structure of the supermaze and thus construct huge new families of themelia. Our results in Section 8.7 are a first step towards achieving of this ideal.

While the linear systems on the "static," or momentum-free supermazes are highly non-trivial and difficult to solve explicitly, these structures still establish the existence of momentum-carrying supermazes in supergravity, and provide a route to characterizing the phase space of such excitations, and especially the themelia that locally have sixteen supercharges. Ultimately, one would like to quantize this phase space to arrive at a semi-classical description of the fractionated branes that lie at the heart of black-hole microstructure.

This may seem like something of "an ask," but the nearly 20 year history of successes in microstate geometries suggests that such a miraculous outcome is really very plausible!

Chapter 9

Waves on Mazes

9.1 Introduction

Building the supergravity solutions corresponding to the super-maze involves several technical hurdles. The first is that the $\frac{1}{4}$-BPS momentum-less M2-M5 super-maze is governed by a non-linear Monge-Ampère-like equation [259, 261, 278] and finding cohomogeneity-three solutions (which is the smallest cohomogeneity that gives interesting solutions) is rather involved[1]. The second hurdle is to add momentum to this M2-M5 super-maze substrate. The latter will be the focus of this Chapter.

A first step in this direction was achieved in [279] using the Born-Infeld action. One can smear the M2 branes of the super-maze along one of the torus direction, and compactify the solutions to a Type-IIA super-maze consisting of D2 brane strips stretched between parallel D4 branes. The fundamental building block of this IIA super-maze consists of a single D2 brane strip stretched between two parallel D4 branes.

One can describe such an isolated component entirely in terms of the $SU(2)$ maximally-supersymmetric Yang-Mills theory living on the world-volume of the D4 branes. This solution is nothing other than the 't Hooft-Polyakov monopole [279–281] and this serves as a $\frac{1}{4}$-BPS substrate to which one can add momentum. Indeed, one can add a null wave in some additional world-volume fluxes. This wave is parameterized by an arbitrary shape function and it does not disturb any of the non-trivial fields of the original 't Hooft-Polyakov monopole [279]. Hence, the full $\frac{1}{8}$-BPS momentum-carrying solution is constructed in three steps: first, one builds the non-trivial $\frac{1}{4}$-BPS solution to a non-linear set of equations; second, one adds some "self-dual" fields that depend on an arbitrary function of the null variable, and lastly, one computes the momentum density of the system, which depends on the square of this arbitrary function.

Such a layered structure is also a feature of all systematic constructions of supersymmetric supergravity solutions with black-hole charges [33, 204, 205, 212, 253, 254, 276, 282,

[1] In Chapter 8, we have shown in the near-horizon limit of these solutions is related by a change of coordinates to a family of $AdS_3\times S^3\times S^3\times\Sigma_2$ solutions, where Σ_2 is a Riemann surface [40]. Since these solutions can be constructed using a linear algorithm, this raises the hope that at least the near-horizon region of certain M2-M5 super-maze geometries will be constructible analytically.

283]. The starting point is usually a two-charge, $\frac{1}{4}$-BPS background. In five and six dimensions, the most generic solutions start from hyper-Kähler, or almost hyper-Kähler, four-dimensional spatial base geometry [24–26, 33, 204, 212, 221, 284, 285]. Without imposing additional symmetries, such a base geometry is governed by some very non-trivial, non-linear equation, like the Monge-Ampère system.

The process of adding a third charge in such a manner as to create a themelion, requires the addition of further dipolar fields, which we think of as *glue*. The glue is dipolar, and so carries no net charge, but it binds the three fundamental charges together. As described in [30] and in [29, 36], the glue carries precisely the correct *local charges* so that, when combined with the global charges, each and every element of the configuration has 16 supersymmetries locally. The three overall global charges mean that the themelion is $\frac{1}{8}$-BPS but, as we have already noted, the sixteen local supercharges mean that one cannot break the configuration apart without breaking the supersymmetry. It is therefore a bound state and the glue really is glue.

In all these constructions, the BPS equations governing the addition of the glue and the third charge, which is usually momentum, are linear [33, 204, 205, 212, 276]. The only feedback between the overlay of the third charge, its glue and the original, possibly singular, $\frac{1}{4}$-BPS substrate, is that the glue smooths out the geometry and fixes some of its moduli. The $\frac{1}{4}$-BPS solution, and the non-linear equations underlying it, are otherwise unmodified.

The fact that the same substrate-glue-momentum layered structure appears both in the supergravity description of themelia and in their DBI description [279], leads us to formulate the "extended themelion conjecture:"

The addition of momentum on top of a $\frac{1}{4}$-BPS themelion substrate can be done using a layered set of linear equations.

9.1.1 Adding momentum to M2-M5 Intersections

The purpose of this Chapter is to show that this conjecture correctly describes the addition of momentum to the M2-M5 super-maze substrate. We use the same type of glue as in the DBI description of [279], and find that, given any M2-M5 $\frac{1}{4}$-BPS solution, one can add a momentum profile specified by an arbitrary function, and obtain a $\frac{1}{8}$-BPS solution by solving *a linear system of equations*. This does not mean that these equations are trivial. The equation that determines the glue is a homogeneous Laplace equation on a very complicated background. This solution must then be fed back, quadratically, as a source for another linear Poisson equation that determines the momentum charge distribution. Such an "upper triangular" structure of the linear system is familiar from earlier linear systems governing themelia [33, 204, 205, 212, 276].

There is another interesting feature (first observed in [224]) of our momentum-carrying solutions that greatly simplifies our construction. One can show that even if all the self-dual glue fields depend on a single, arbitrary function of the null coordinate, this function can be absorbed by a re-definition of the null coordinate so that it only appears in the

denominator of a single term in the metric ansatz. Thus, one can construct a much simpler solution where the arbitrary function is a constant, and then promote the constant to an arbitrary function. One can then check explicitly that this is still a solution.

We will use the most symmetric $\frac{1}{4}$-BPS super-maze solution as a substrate. This solution has an $SO(4) \times SO(4)$ symmetry and was presented in Chapter 8. The first $SO(4)$ corresponds to rotations in the four-dimensional space orthogonal to the M2 branes and the M5 brane, while the second $SO(4)$ corresponds to rotations in the plane of the M5 branes.

A momentum wave on the M2 brane strips breaks the second $SO(4)$. If the wave is polarized along one of the M5 directions, the symmetry is broken to $SO(3) \times U(1)$ and, upon smearing along the $U(1)$ and reducing to Type IIA String Theory, it becomes a momentum wave on the D4-D2 system. The construction of this momentum wave in the non-Abelian D4 world-volume theory [279] is reviewed in Section 9.2 and will help us find the glue needed to add momentum while maintaining the themelion structure. We also show that one can give the wave a circular polarization that breaks the symmetry to $SU(2) \times U(1)$. We will construct both types of waves in Section 9.3. Section 9.4 contains our final remarks.

9.2 Adding momentum to the M2-M5 system - the DBI analysis

An M2 brane strip stretched between two M5 branes can be smeared along one of the M5 brane directions and reduced to Type IIA String Theory, becoming a D2 strip stretched between two D4 branes. From the perspective of the $SU(2)$ non-Abelian D4-brane world-volume theory this solution is nothing other than a 't Hooft-Polyakov monopole solution in 3+1 dimensions [280] that is independent of the fourth D4 world-volume direction [279,281]. This is the common D2-D4 direction, along which one can add a null momentum wave involving several non-trivial fields in the D4 world-volume theory [279]. A simpler solution is a semi-infinite D2 ending on a D4 brane, to which one can also add a momentum wave using the same D4 world-volume fields. In this Section we review this construction and use it to reveal the fields that one must use in supergravity to add momentum to this brane system.

It is well known that a semi-infinite F1 or D1 string ending on a D3 brane pulls it and forms a spike [39, 227], and this can be described as an Abelian monopole in the Born-Infeld action. By T-duality, one can see that the same gauge configuration also describes a semi-infinite D2 furrow bending a D4 brane. This solution has sixteen supercharges locally[2] and eight globally, and so it is a $\frac{1}{4}$-BPS themelion. The furrow is extended along the D2-D4 common direction, y, and looks like a spike in the $\mathbb{R}^3$ spanned by the other three directions of the D4-brane world-volume.

[2] As do all solutions of the Abelian DBI action.

Since the solution is spherically symmetric in this $\mathbb{R}^3$ we use coordinates, (u, θ, ϕ) where u is the radius and (θ, ϕ) are angles on the S^2. We define $\widehat{\theta}, \widehat{\phi}$ to be flat indices for frames on the S^2. The D4 scalars and Maxwell fields that describe the D2 spike take the form:

$$\Phi \;=\; \frac{b}{u}\,, \qquad F_{\widehat{\theta}\widehat{\phi}} \;=\; \partial_u \Phi\,. \tag{9.1}$$

The scalar Φ determines the displacement of the D4-brane in the D2-brane direction, z, orthogonal to the D4 brane. The non-trivial profile of Φ describes the spike. This profile sources the monopole configuration of the Maxwell field, and the result is a solution to the DBI equations. Note that this solution is independent of the common D2-D4 direction, y.

One can add momentum to the D2-D4 brane solution by turning on a magnetic and an electric field in the D4 world-volume theory:

$$F_{uy} = -F_{u0} = \frac{f(y-t)}{u^2}\,, \tag{9.2}$$

with $f(y-t)$ an arbitrary function. One can check that adding these fields does not disturb the fields already present in the original D4-D2 solution (9.1). The non-trivial electric and magnetic fields generate a Poynting vector, giving rise to a momentum density along y, and a net global momentum charge.

Thus the global charges of this solution are:

$$Q^{\rm D4}_{\rm u\theta\phi y}\,, \qquad D^{\rm D2}_{\rm zy}\,, \qquad Q^{\rm P}_{\rm y}\,, \tag{9.3}$$

where the subscripts denote the directions.

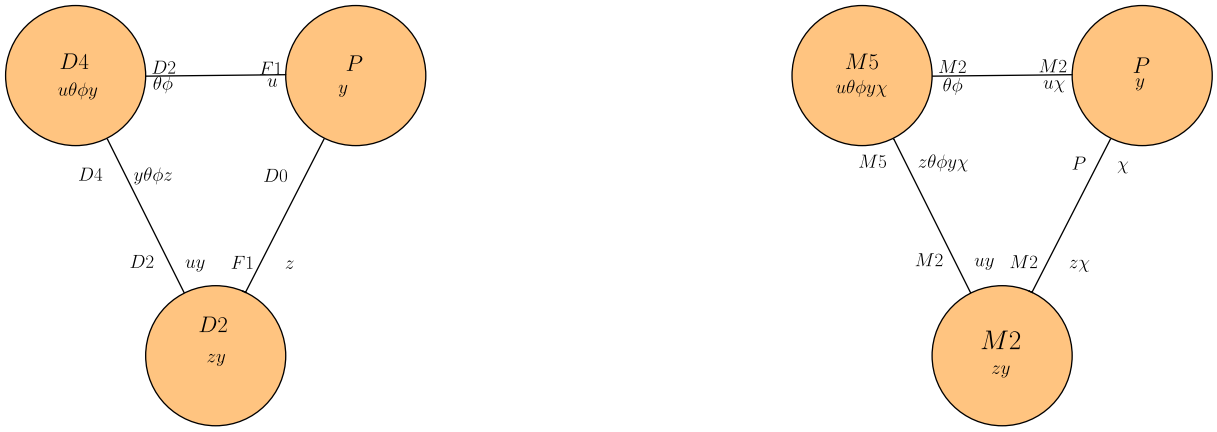

(a) Type-IIA charges and glue

(b) M theory charges and glue.

Figure 9.1: Global and local charges of our solution in Type IIA String Theory (a) and M theory (b). The brane charges in the circles are global charges. The branes on the branches are the "glue" one needs to add in order to have enhance the local supersymmetry to 16 supercharge. The two "glue" branes on a given branch have the same local charge.

The brane profile also sources a collection of dipole charges, the glue:

$$Q^{\rm D4}_{\rm z\theta\phi y}\,, \quad Q^{\rm D2}_{\rm uy}\,, \quad Q^{\rm D2}_{\theta\phi}\,, \quad Q^{\rm F1}_{\rm u}\,, \quad Q^{\rm D0}\,, \quad Q^{\rm F1}_{\rm z}\,. \tag{9.4}$$

It is easy to see the intuitive origin of these dipoles. The first two reflect the bending of the D4 brane pulled on by the D2 branes, and are also present in the absence of a momentum wave. They correspond to the left-hand side of the triangle in Figure 9.1(a). The remaining dipole charges are linear in the profile function and thus create no net charge. The $Q^{\rm D2}_{\theta\phi}$ charge comes from F_{uy}, which sources a $C_{0\theta\phi}$ through the WZ term. Similarly, $Q^{\rm D0}$ is sourced by $F_{uy}\wedge F_{\theta\phi}$ in the WZ term. The remaining F1 charge arises through the DBI action. Both are sourced by F_{0u}: B_{0u} couples directly, while B_{0z} couples via the pull-back $\partial_u\Phi$. The complete set of global and dipole charges are depicted in Figure 9.1, along with their M-theory uplifts.

A more precise analysis [279] enables one to read off the local charges of this solution directly from the $\kappa-$symmetry of the DBI action. The simplest way to express all the charges is to introduce two angles

$$\tan\alpha \equiv \partial_u\Phi\,, \tag{9.5}$$

$$\tan\beta \equiv \frac{F_{yu}}{\sqrt{1+(\partial_u\Phi)^2}}\,. \tag{9.6}$$

The angle α can be thought as the local slope of the D2-D4 spike, which parameterizes how much the D2 pulls on the D4 world-volume. The angle β can be thought as the local pitch of the momentum-carrying wave. The three charge densities that contribute to the global charges of the solution can be written as:

$$Q^{\rm D4}_{\rm u\theta\phi y} = M\cos^2\alpha\cos^2\beta\,, \tag{9.7}$$

$$D^{\rm D2}_{\rm zy} = M\sin^2\alpha\cos^2\beta\,, \tag{9.8}$$

$$Q^{\rm P}_{\rm y} = M\sin^2\beta\,. \tag{9.9}$$

The six local charges, that form the glue needed to give the themelion sixteen-local-supercharges structure to the solution are:

$$Q^{\rm D4}_{\rm z\theta\phi y} = M\cos^2\beta\cos\alpha\sin\alpha\,,\quad Q^{\rm D2}_{\rm uy} = -M\cos^2\beta\cos\alpha\sin\alpha\,, \tag{9.10}$$

$$Q^{\rm D2}_{\theta\phi} = M\cos\beta\sin\beta\cos\alpha\,,\quad Q^{\rm F1}_{\rm u} = -M\cos\beta\sin\beta\cos\alpha\,, \tag{9.11}$$

$$Q^{\rm D0} = M\cos\beta\sin\beta\sin\alpha\,,\quad Q^{\rm F1}_{\rm z} = -M\cos\beta\sin\beta\sin\alpha\,. \tag{9.12}$$

The uplift of this configuration to M-theory is a momentum wave on an M2 strip meeting an M5. This is depicted on the right-hand side of Figure 9.1, where χ is the M theory direction. Since the basic configuration is intersecting M2 and M5 branes carrying momentum we will think of this as a kind of super-maze [36], except that the glue of this system is not the same[3] as that of [36].

[3] In [36], the glue on the M5-M2 and the M2-P branch is the same, but the glue on the M5-P branch corresponds to M5 and P rather than two species of M2 branes, as depicted along the top of Figure 9.1(b).

9.3 The $\frac{1}{8}$-BPS M2-M5-P themelion

In this Section we want to add momentum to the supergravity solutions for M2-M5 intersections of Section 8.2. Such solutions are completely determined by the maze function G_0, which obeys the Monge-Ampere like equation (8.9). While this non-linear equation is daunting, it has been shown that solutions exist, and can be constructed in an iterative expansion [259, 261]. Moreover, by imposing spherical symmetry and taking a near-brane limit, one can reduce that maze function to two variables, and it can be re-cast as a linear system [40, 266, 270–274, 278, 286]. We will therefore take this solution as "given," and assume that we have some form of intersecting M2-M5 substrate on which we will erect momentum modes.

9.3.1 The Ansatz for the metric and flux

We will impose an $SO(4)$ symmetry transverse to the branes, and write the metric in the directions, (x^7, x^8, x^9, x^{10}), in terms of a radial coordinate v, and an S^3, with unit metric $d\Omega'^2_3$. We will not, *a priori*, assume that the metric in these directions is conformal to the $\mathbb{R}^4$ metric (9.13).

We are going to consider two possible structures along the 3456 directions of the M5 brane:

Choice (i):

We take these directions to have an $SO(3) \times \mathbb{R}$ symmetry, in which $x^6 = \chi$ is $\mathbb{R}$, or S^1, and the remaining directions are described by a radial coordinate, u, and spheres, S^2, with unit metric $d\Omega_2^2$. We allow the scale factors in front of du^2, $d\Omega_2^2$ and $d\chi^2$ to be independent arbitrary functions of (u, v, z). The polarization density of the null wave will be directed along $x^6 = \chi$. This solution can be compactified to Type IIA String Theory along χ to give the supergravity solution corresponding to the D2-D4-P configuration in Section 9.2.

Choice (ii):

We impose an $SU(2)_L \times U(1)$ symmetry by introducing a radial coordinate, u, and (possibly *squashed*) spheres, S^3, whose metric we take to be that of a Hopf fibration over S^2. We allow the scale factors in front of du^2, the S^2 base of the fibration, and the Hopf fiber to be independent arbitrary functions of (u, v, z). The polarization density of the null wave will be directed along the Hopf fiber.

Finally, following [266, 278] and, as in (8.5), we are also going to allow a non-trivial fibration of the z-direction over du.

To be more specific, we are going to analyze two possible geometries on the M5 branes:

$$\text{Choice (i)}: \; ds_4^2 \equiv du^2 + u^2\, d\Omega_2^2 + d\chi^2\,, \quad \text{or} \quad \text{Choice (ii)}: ds_4^2 \equiv du^2 + u^2\, d\Omega_3^2\,, \tag{9.13}$$

and the metric on the $\mathbb{R}^4$ orthogonal to the M5 branes

$$ds'^2_4 \equiv dv^2 + v^2\, d\Omega'^2_3\,. \tag{9.14}$$

Here, $d\Omega^2_n$ is the maximally symmetric metric on a unit-radius S^n, and χ is some flat direction of which the solution is independent. The corresponding Laplacians are:

$$\mathcal{L}_u G = \frac{1}{u^n}\partial_u\Big(u^n\partial_u G\Big)\,, \qquad \mathcal{L}_v G = \frac{1}{v^3}\partial_v\Big(v^3\partial_v G\Big)\,, \tag{9.15}$$

where $n = 2$ for Choice (i) and $n = 3$ for Choice (ii).

We want to construct a solution that has the charges of the super-maze constructed in Section 9.2, and not the charges of the super-maze of [36], so the momentum of the solution will only be along the common M2-M5 direction, y (and not along the pure M2-direction z). We therefore introduce null coordinates, ζ, ξ, and take $(x^0 + x^1, x^1 - x^0, x^2) = (\zeta, \xi, z)$, and assume the wave is a function of ξ. We also expect that the null wave profile can be an arbitrary function, $F(\xi)$, and we will show that this expectation is indeed correct.

We therefore use the metric Ansatz :

$$\begin{aligned} ds^2_{11} = e^{2A_0}\Bigg[d\xi\left(P\,d\xi + 2\left(\frac{d\zeta}{F(\xi)} + k\,\widehat{\sigma}_3\right)\right) + e^{2A_1}\,ds^2_4 + e^{2A_2}\,ds'^2_4 \\ + e^{2A_3}\Big(dz + B_1\,du\Big)^2\Bigg]\,, \end{aligned} \tag{9.16}$$

where the four-dimensional metrics are given by:

$$ds^2_4 \equiv du^2 + \tfrac{1}{4}u^2\,e^{2A_4}\left(\sigma_1^2 + \sigma_2^2\right) + \tfrac{1}{4}u^2\,e^{2A_5}\,\sigma_3^2\,, \tag{9.17}$$

and

$$ds'^2_4 \equiv dv^2 + \tfrac{1}{4}e^{2A_6}\,v^2\,\left(\sigma'^2_1 + \sigma'^2_2 + \sigma'^2_3\right). \tag{9.18}$$

For Choice (ii), we take the σ_i to be the left-invariant 1-forms on S^3:

$$\begin{aligned} \sigma_1 &= \cos\varphi_3\,d\varphi_1 + \sin\varphi_3\sin\varphi_1\,d\varphi_2\,,\\ \sigma_2 &= \sin\varphi_3\,d\varphi_1 - \cos\varphi_3\sin\varphi_1\,d\varphi_2\,,\\ \sigma_3 &= d\varphi_3 + \cos\varphi_1\,d\varphi_2\,, \end{aligned} \tag{9.19}$$

with the similar expressions for the σ'_i, but with $\varphi_j \to \varphi'_j$. The polarization vector, $\widehat{\sigma}_3$ is set equal to σ_3, pointing along the Hopf fiber:

$$\widehat{\sigma}_3 = \sigma_3\,. \tag{9.20}$$

For Choice (i), the σ_i are:

$$\sigma_1 = 2\,d\theta\,, \qquad \sigma_2 = 2\,\sin\theta\,d\phi\,, \qquad \sigma_3 = \frac{2}{u}\,d\chi\,, \tag{9.21}$$

so that the metric (9.17) is becomes

$$ds^2_4 = du^2 + u^2\,e^{2A_4}\left(d\theta^2 + \sin^2\theta\,d\phi^2\right) + e^{2A_5}\,d\chi^2\,. \tag{9.22}$$

The polarization vector, $\widehat{\sigma}_3$, now points along $d\chi$:

$$\widehat{\sigma}_3 \;=\; d\chi\,. \tag{9.23}$$

The metric ds'^2_4 remains the same for both choices, with σ'_i being the left-invariant 1-forms on S'^3.

In this Ansatz, the functions P, k and A_n, $n = 0, 1, \ldots, 6$ are, as yet arbitrary functions of (u, v, z). The only dependence on ξ appears through the single function, $F(\xi)$ in the metric.

We use the orthonormal frames:

$$\begin{aligned}
e^0 &= \frac{e^{A_0}}{\sqrt{P}}\left(\frac{d\zeta}{F(\xi)} + k\,\widehat{\sigma}_3\right), \qquad e^1 = \frac{e^{A_0}}{\sqrt{P}}\left(P\,d\xi + \frac{d\zeta}{F(\xi)} + k\,\widehat{\sigma}_3\right),\\
e^2 &= e^{A_0+A_3}\Big(dz + B_1\,du\Big), \qquad e^3 = e^{A_0+A_1}\,du\,, \qquad e^4 = e^{A_0+A_2}\,dv\,,\\
e^{5,6} &= \tfrac{1}{2}\,u\,e^{A_0+A_1+A_4}\,\sigma_{1,2}\,, \qquad e^7 = \tfrac{1}{2}\,u\,e^{A_0+A_1+A_5}\,\sigma_3\,, \qquad e^{8,9,10} = \tfrac{1}{2}\,v\,e^{A_0+A_2+A_6}\,\sigma'_{1,2,3}\,.
\end{aligned} \tag{9.24}$$

Rather than making a general Ansatz for the potential, $C^{(3)}$, we find it easier to make the most general possible Ansatz for the fluxes, $F^{(4)}$, in a manner that is consistent with all of the symmetries. The frames e^5 and e^6 must appear as $e^5 \wedge e^6$, and the frames e^8, e^9 and e^{10} must appear as $e^8 \wedge e^9 \wedge e^{10}$, while the remaining six frames, e^0, e^1, e^2, e^3, e^4 and e^7, can appear in any combination. This means that there are, in principle, 36 functions that can appear when $F^{(4)}$ is expanded in frames. We thus introduce 36 functions of (u, v, z) into our Ansatz.

One could use the general properties of null waves to simplify the Ansatz for $F^{(4)}$, but this turns out to be unnecessary. We will, however, note that in addition to the fluxes sourced by the background M2 and M5 branes, we expect momentum waves to involve flux components with legs along $d\xi$ and not $d\zeta$. In terms of frames, this means that the momentum waves source flux components involving only $e^1 - e^0$. This is indeed what we find from solving the BPS equations.

9.3.2 The supersymmetries

The four supersymmetries of the $\frac{1}{8}$-BPS system are defined by adding a momentum projector to the M2 and M5 brane projectors in (8.1):

$$\Gamma^{01}\,\varepsilon \;=\; -\,\varepsilon\,, \qquad \Gamma^{012}\,\varepsilon \;=\; -\,\varepsilon\,, \qquad \Gamma^{013456}\,\varepsilon \;=\; \varepsilon\,. \tag{9.25}$$

This is still consistent with the projector (8.4), allowing the addition of a set of M5' branes. One should also note that the sign in the momentum projector, Γ^{01}, is fixed implicitly by the choice of frames and the sign of P in (9.24).

The goal is, of course, to solve

$$\delta\psi_\mu \;\equiv\; \nabla_\mu\,\epsilon \;+\; \tfrac{1}{288}\Big(\Gamma_\mu{}^{\nu\rho\lambda\sigma} \;-\; 8\,\delta^\nu_\mu\,\Gamma^{\rho\lambda\sigma}\Big)\,F_{\nu\rho\lambda\sigma} \;=\; 0\,, \tag{9.26}$$

using the Ansatz for the metric and fluxes, subject to the foregoing projection conditions.

The dependence of the supersymmetries on the sphere directions is determined entirely by group theory. With our choices of projectors and frames, the supersymmetries, ε, are independent of ${\varphi'}_j$, and independent of φ_j for the Choice (ii) metric (9.17) with (9.19). For the Choice (i) metric (9.22) one must solve for Killing spinors on the S^2 and use the fact that χ is simply $\mathbb{R}$ or S^1.

This yields:

$$\partial_\theta \varepsilon \;=\; \frac{1}{2}\,\Gamma^{35}\,\varepsilon\,, \qquad \partial_\phi \varepsilon \;=\; \frac{1}{2}\Big(\sin\theta\,\Gamma^{36} + \cos\theta\,\Gamma^{56}\Big)\,\varepsilon\,, \qquad \partial_\chi \varepsilon \;=\; 0\,. \tag{9.27}$$

The dependence of the spinors on (ξ, u, v, z) follows from the fact that $K^\mu \equiv \bar{\varepsilon}\Gamma^\mu\varepsilon$ is the time-like Killing vector, $\frac{\partial}{\partial\zeta}$. This means that

$$\varepsilon \;=\; e^{\frac{1}{2}A_0}\,F^{-\frac{1}{2}}\,P^{-\frac{1}{4}}\,\varepsilon_0\,, \tag{9.28}$$

where ε_0 is independent of all the coordinates for the metric (9.17) with (9.19), or, for the metric (9.22), ε_0 only has the coordinate dependences implied by (9.27).

9.3.3 Outline of solving the BPS equations

Since we know the coordinate dependences of ε, it is now straightforward to solve the BPS equations, (9.26), using the metric and flux Ansatz described above. All but two of the 36 flux functions are determined algebraically in terms of the metric functions and their first derivatives (most of the fluxes are identically zero). One then finds simple sets of first-order equations that relate the metric functions to one another. The computation proceeds much as in [278]. There is still some gauge freedom left in redefining the coordinates and this can be used to fix some of the metric functions completely.

The form of the metric and fluxes

After solving the supersymmetry transformations we find the metric reduces to the form:

$$\begin{aligned} ds_{11}^2 \;=\; e^{2A_0}\Bigg[d\xi\,\Big(P\,d\xi \;+\; 2\,\Big(\frac{d\zeta}{F(\xi)} \;+\; k\,\widehat{\sigma}_3\Big)\Big) \;+\; e^{-3A_0}\,(-\partial_z w)^{-\frac{1}{2}}\,ds_4^2 \\ +\; e^{-3A_0}\,(-\partial_z w)^{\frac{1}{2}}\,ds'^2_4 \;+\; (-\partial_z w)\,\Big(dz \;+\; (\partial_z w)^{-1}\,(\partial_u w)\,du\Big)^2\Bigg]\,, \end{aligned} \tag{9.29}$$

where the four-dimensional metrics are those of flat space.

The BPS equations almost completely fix the relative scales, A_4, A_5 and A_6, of the various pieces within ds_4^2 and ds'^2_4 so that these metrics are flat. Note that, but for P and k, the functions appearing in this metric are exactly the same as those of the substrate momentum-less solution of Section 8.2.

There are some constants of integration that can be absorbed into coordinate re-definitions, but there is one constant that remains unfixed: one is allowed to have a

constant re-scaling to the Hopf fiber of ds_4^2 in Choice (ii). We found that allowing this Hopf fiber to become squashed away from its round value led to singularities in the solution, and so we fixed the metric to that of a round S^3 in Choice (ii). Thus,

$$ds'^2_4 \;=\; dv^2 \;+\; \tfrac{1}{4}\,v^2\,\left(\sigma'^2_1+\sigma'^2_2+\sigma'^2_3\right), \tag{9.30}$$

and for Choice (i)

$$ds_4^2 \;=\; du^2 \;+\; u^2\,\left(d\theta^2+\sin^2\theta\,d\phi^2\right) \;+\; d\chi^2\,, \tag{9.31}$$

while for Choice (ii)

$$ds_4^2 \;=\; du^2 \;+\; \tfrac{1}{4}\,u^2\,\left(\sigma_1^2+\sigma_2^2+\sigma_3^2\right). \tag{9.32}$$

The functions, P, k, w and A_0 are, as yet, arbitrary functions of (u, v, z). The function, $F(\xi)$, remains unconstrained.

As indicated earlier, almost all the flux functions are determined in terms of metric functions. Indeed, we find that the fluxes sourced by the M2 and M5 branes are related to metric functions exactly as they were in [278]. The new non-zero fluxes, again in frame indices, are:

$$\begin{aligned}
&F_{0237}=-F_{1237}\;=\;b_1\,,\qquad F_{0347}=-F_{1347}\;=\;b_2\,,\qquad F_{0247}=-F_{1247}\;=\;\frac{1}{2}\,\frac{e^{2A_0}}{\sqrt{P}}\,(\partial_v k)\,,\\
&F_{0256}=-F_{1256}\;=\;-\,b_1\;+\;\frac{1}{2}\,\frac{e^{2A_0}}{\sqrt{P}}\left((-\partial_z w)^{\frac{1}{2}}\,\partial_u k+\frac{\partial_u w}{(-\partial_z w)^{\frac{1}{2}}}\,\partial_z k\right),
\end{aligned} \tag{9.33}$$

where b_1, b_2 are arbitrary functions of (u, v, z). These new components of the flux satisfy $F_{1bcd} = -F_{2bcd}$, as one expects for null waves. In Section 9.3.3 we will show the charges of this solution are those of the DBI solution reviewed in Section 9.2.

The Bianchi Identities - I

The heavy lifting in solving the BPS equations is to solve the Bianchi identities. That is, we have made an Ansatz for all the possible terms in $F^{(4)}$, and determined these based on the supersymmetry, but one must now impose $dF^{(4)} = 0$. These equations fall into two parts: those of the $\frac{1}{4}$-BPS substrate and those for the new fluxes. Most significantly, the equations governing the $\frac{1}{4}$-BPS brane substrate completely decouple from the equations relating to the addition of the momentum wave.

Thus, the first set of Bianchi equations turn out to be exactly the same as those for the $\frac{1}{4}$-BPS background "maze" described in Section 8.2 and their solution proceeds in an identical manner to that described in [278]. That is, these equations determine the functions A_0 and w by solving (8.9) and using (8.10).

The remaining Bianchi identities determine the new fluxes and polarization vector, and depend on the functions w and A_0. However, the latter functions are now to be considered as part of the *known* background of the substrate branes.

The Bianchi Identities - II

The Bianchi equations for the new fluxes are rather non-trivial, but they are *linear* in the fluxes. We consider Choice (i) and Choice (ii) separately, as the equations are slightly different.

For Choice (i), one of the Bianchi identities can be written as:

$$\partial_u\Big[\, u^2\, e^{-\frac{1}{2}A_0}(-\partial_z w)^{-\frac{1}{4}}\,\sqrt{P}\, b_2\,\Big]$$
$$= \partial_v\Big[\frac{u^2}{(\partial_z w)}\,\Big(\frac{1}{2}\,\partial_z k - e^{A_0}(\partial_u w)\Big(\sqrt{P}\, b_1 - \frac{1}{2}e^{2A_0}\Big((-\partial_z w)^{\frac{1}{2}}\,\partial_u k + (-\partial_z w)^{-\frac{1}{2}}\,(\partial_u w)\,\partial_z k\,\Big)\Big)\Big)\Big]\,. \tag{9.34}$$

This can be satisfied by introducing a pre-potential, q, defined by:

$$\begin{aligned}\partial_v q &= u^2\, e^{-\frac{1}{2}A_0}(-\partial_z w)^{-\frac{1}{4}}\,\sqrt{P}\, b_2\,,\\ \partial_u q &= \frac{u^2}{(\partial_z w)}\,\Big(\frac{1}{2}\,\partial_z k - e^{A_0}(\partial_u w)\Big(\sqrt{P}\, b_1 - \frac{1}{2}e^{2A_0}\Big((-\partial_z w)^{\frac{1}{2}}\,\partial_u k + (-\partial_z w)^{-\frac{1}{2}}\,(\partial_u w)\,\partial_z k\,\Big)\Big)\Big)\,.\end{aligned} \tag{9.35}$$

Using these identities to replace b_1 and b_2 in the remaining Bianchi identities leads to two more equations, one of which is relatively simple, and can be solved by introducing another pre-potential, p, defined by:

$$\partial_u p \;=\; u^2\, k \;+\; 2\,(\partial_u w)\, q\,, \qquad \partial_v p \;=\; 2\,(\partial_z w)\, q\,. \tag{9.36}$$

One then finds that this pre-potential, p also solves the remaining Bianchi identity.

Note that the polarization vector of the null momentum wave is given by:

$$k \;=\; \frac{1}{u^2}\,\Big(\partial_u p \;-\; \frac{(\partial_u w)}{(\partial_z w)}\,\partial_v p\Big)\,. \tag{9.37}$$

The analysis for Choice (ii) is almost identical, except that the pre-potentials are defined by

$$\begin{aligned}\partial_v q &= u^4\, e^{-\frac{1}{2}A_0}(-\partial_z w)^{-\frac{1}{4}}\,\sqrt{P}\, b_2\,,\\ \partial_u q &= \frac{u^3}{(\partial_z w)}\,\Big(\partial_z k - e^{A_0}(\partial_u w)\Big(u\,\sqrt{P}\, b_1 - e^{2A_0}\Big((-\partial_z w)^{\frac{1}{2}}\,\partial_u k + (-\partial_z w)^{-\frac{1}{2}}\,(\partial_u w)\,\partial_z k\,\Big)\Big)\Big)\,,\end{aligned} \tag{9.38}$$

and

$$\partial_u p \;=\; 2\Big(u^3\, k \;+\; (\partial_u w)\, q\Big)\,, \qquad \partial_v p \;=\; 2\,(\partial_z w)\, q\,, \tag{9.39}$$

and hence one has

$$k \;=\; \frac{1}{2u^3}\,\Big(\partial_u p \;-\; \frac{(\partial_u w)}{(\partial_z w)}\,\partial_v p\Big)\,. \tag{9.40}$$

As with Choice (i), one finds that using the pre-potential, p solves the remaining Bianchi identities.

We have thus reduced the solving of the fluxes and polarization vector, k, to finding a single, undetermined function, p. Indeed, the rest of the solution is contained by two undetermined functions: The momentum density, P, and the pre-potential p, both of which will be governed by the equations of motion.

The gauge potential

Given that we have solved the Bianchi identities, we can now integrate the flux Ansatz to obtain an expression for the gauge potential. For Choice (i) we find:

$$\begin{aligned} C^{(3)} \;=\; & -\, e^0 \wedge e^1 \wedge e^2 \\ & -\left(\frac{\partial_u w}{\partial_z w}\right) u^n \sin\theta \, d\theta \wedge d\phi \wedge d\chi + \frac{1}{8}\,(\partial_v w)\, v^3 \sin\varphi'_1 \, d\varphi'_1 \wedge d\varphi'_2 \wedge d\varphi'_3 \\ & + \frac{1}{u^\ell \sqrt{P}\,(-\partial_z w)^{\frac{1}{2}}} \Big(\partial_z p\Big)\,(e^1 - e^0) \wedge \Big(e^3 \wedge e^7 \;-\; e^5 \wedge e^6\Big)\,, \end{aligned} \tag{9.41}$$

with $\ell = 2, n = 2$, while for Choice (ii) we find

$$\begin{aligned} C^{(3)} \;=\; & -\, e^0 \wedge e^1 \wedge e^2 \\ & + \frac{1}{8}\left(\frac{\partial_u w}{\partial_z w}\right) u^n \sin\varphi_1 \, d\varphi_1 \wedge d\varphi_2 \wedge d\varphi_3 + \frac{1}{8}\,(\partial_v w)\, v^3 \sin\varphi'_1 \, d\varphi'_1 \wedge d\varphi'_2 \wedge d\varphi'_3 \\ & + \frac{1}{u^\ell \sqrt{P}\,(-\partial_z w)^{\frac{1}{2}}} \Big(\partial_z p\Big)\,(e^1 - e^0) \wedge \Big(e^3 \wedge e^7 \;-\; e^5 \wedge e^6\Big)\,, \end{aligned} \tag{9.42}$$

with $\ell = 4, n = 3$.

Naively, the first three terms in these expressions are exactly what one expects for the fluxes of the $\frac{1}{4}$-BPS background maze solution [278] discussed in Section 8.2. However, this perspective is a little oversimplified because one should remember that the frames e^0 and e^1 now involve a momentum density and a polarization vector, and are therefore significantly more complicated than those of [278].

Matching to the Born-Infeld construction

It is interesting to try to connect the features of the supergravity solution to those of the DBI description of the D4-D2 momentum wave [279] reviewed in Section 9.2.

To do this, one first has to re-define the null coordinates, such that the $d\zeta\; d\xi$ term in the metric is ξ independent. This is done by introducing a new null coordinate, η, such that

$$d\eta = \frac{d\xi}{F(\xi)} \equiv \frac{d\xi}{f(\eta)}\,. \tag{9.43}$$

The function $f(\eta)$ is defined implicitly above and, since $F(\xi)$ is an arbitrary function, one can also consider $f(\eta)$ as the defining arbitrary function of our solution, which is now written as

$$\begin{aligned} ds_{11}^2 \;=\; & e^{2A_0}\, d\eta \Big[2\, d\zeta \;+\; 2k f(\eta)\, d\chi \;+\; P f(\eta)^2\, d\eta\Big] \;+\; e^{-A_0}\,(-\partial_z w)^{-\frac{1}{2}}\, ds_4^2 \\ & +\; e^{-A_0}\,(-\partial_z w)^{\frac{1}{2}}\, ds'^2_4 \;+\; e^{2A_0}\,(-\partial_z w)\Big(dz \;+\; (\partial_z w)^{-1}\,(\partial_u w)\; du\Big)^2\,, \end{aligned} \tag{9.44}$$

where we have explicitly used the Choice (i) metric, which is related to the brane construction in Section 9.2. The metric already allows us to see one of the components of

the glue, corresponding to momentum along the χ direction (depicted on the right side of the triangle in Figure 9.1(b)). As expected from the DBI construction, this glue charge is parameterized by the arbitrary function $f(\eta)$.

To see the other components of the glue, it is best to explicitly expand the vielbeins in the Choice (1) gauge potential (9.41) and use the null coordinate η introduced in (9.43)

$$\begin{aligned} C^{(3)} \;=\; & e^{3A_0}\,(-\partial_z w)^{\frac{1}{2}}\,d\eta\wedge\Big(d\zeta + k f(\eta)\,d\chi\Big)\wedge\Big(dz \;+\; (\partial_z w)^{-1}\,(\partial_u w)\;du\Big) \\ & - \left(\frac{\partial_u w}{\partial_z w}\right) u^2\sin\theta\,d\theta\wedge d\phi\wedge d\chi + \frac{1}{8}\,(\partial_v w)\,v^3\sin\varphi'_1\,d\varphi'_1\wedge d\varphi'_2\wedge d\varphi'_3 \\ & + \frac{\big(\partial_z p\big)}{u^2}\,f(\eta)\,d\eta\wedge\Big(du\wedge d\chi - u^2\sin\theta\,d\theta\wedge d\phi\Big)\;, \end{aligned} \tag{9.45}$$

On can see from the first line of this potential that the solution also has the other glue charge depicted on the right side of the triangle in Figure 9.1(b), corresponding to M2 branes extended along the χ and z directions.

The last line of this expression also makes explicit the equality of the $\mathrm{M2}_{\theta,\phi}$ and $\mathrm{M2}_{u,\chi}$ glue charges, shown on the top line of triangle in Figure 9.1(b). These charges are the M-theory uplift of the charges (9.11) of the DBI construction in Section 9.2, and their equality is also a consequence of the DBI construction.

9.3.4 The equations of motion

Having solved the BPS equations, one must still check the equations of motion. This will determine the remaining functions, p and P.

It is useful to compute the Laplacian, $\widehat{\mathcal{L}}$, for the substrate metric (8.5) acting on a function H that only depends on (u,v,z). Using symmetries we have imposed, and the equations for w and A_0, one can simplify the Laplacian to obtain the following operator:

$$\begin{aligned} \mathcal{L}(H) \;\equiv\; & e^{-A_0}\,(-\partial_z w)^{-\frac{1}{2}}\,\widehat{\mathcal{L}}(H) \\ =\; & \left[\frac{1}{u^n}\,\partial_u\Big(u^n\partial_u H\Big) \;+\; \frac{1}{(-\partial_z w)}\,\frac{1}{v^3}\partial_v\Big(v^3\partial_v H\Big) \;+\; 2\,\frac{(\partial_u w)}{(-\partial_z w)}\,\partial_u\partial_z H\right. \\ & \left. +\; \Big((-\partial_z w)^{-\frac{3}{2}}\,e^{-3A_0} \;+\; (-\partial_z w)^{-2}\,(\partial_u w)^2\Big)\,\partial_z^2 H\right], \end{aligned} \tag{9.46}$$

with $n=2$ or $n=3$ for choices (i) or (ii), respectively. It is interesting to note that one could also have replaced $\widehat{\mathcal{L}}$ by the Laplacian for the final metric (9.29) because *on functions of (u,v,z) alone*, these two Laplacians agree. Here, however, we wish to emphasize that $\mathcal{L}$ is a Laplacian operator on a known substrate background that does not depend upon the functions we are trying to determine.

The Maxwell equations actually give rise to two rather different-looking *third-order* linear equations for p. Fortunately, these two equations are compatible, and can be solved by requiring p to be the solution of a *single, second order, linear equation*:

$$\mathcal{L}\left(\frac{p}{u^\ell}\right) \;-\; \frac{2\,m}{u^2}\,\frac{p}{u^\ell} \;=\; 0\,, \tag{9.47}$$

with $\ell = 2, m = 1$ or $\ell = 4, m = 4$ for choices (i) or (ii), respectively. To be more specific, the two seemingly-independent Maxwell equations are actually combinations of the differential equation (9.47) and either the u-derivative, or the z-derivative, of this differential equation.

The Einstein equations produce second-order differential equations for k and P. The former is identically satisfied if one uses (9.37), or (9.40), to rewrite k in terms of p, and then employs (9.47) (or the combinations of (9.47) that arise in the Maxwell equations).

The equation for P can also be written as:

$$\mathcal{L}\Big(P\Big) \;=\; s_{(x)}\,, \tag{9.48}$$

where, for the two choices, one has:

$$\begin{aligned}
s_{(\mathrm{i})} &= -4\,e^{-A_0}\,(-\partial_z w)^{-\frac{1}{2}}\,\Big[2\,\Big(\big(\sqrt{P}\,b_1\big)^2 + \big(\sqrt{P}\,b_2\big)^2\Big) \\
&\qquad - e^{2A_0}\,\Big(\sqrt{P}\,b_1\Big)\Big((-\partial_z w)^{\frac{1}{2}}\,\partial_u k \;+\; (\partial_u w)\,(-\partial_z w)^{-\frac{1}{2}}\,\partial_z k\Big)\Big]\,, \\
s_{(\mathrm{ii})} &= -8\,e^{-A_0}\,(-\partial_z w)^{-\frac{1}{2}}\,\Big[\big(\sqrt{P}\,b_2\big)^2 \;+\; \Big(\big(\sqrt{P}\,b_1\big) \;-\; \frac{2\,e^{2A_0}}{u^2}\,(-\partial_z w)^{\frac{1}{2}}\,k\Big) \\
&\qquad \times\Big(\big(\sqrt{P}\,b_1\big) \;-\; \frac{e^{2A_0}}{u}\,\Big((-\partial_z w)^{\frac{1}{2}}\,\partial_u k \;+\; (-\partial_z w)^{-\frac{1}{2}}\,(\partial_u w)\,\partial_z k\Big)\Big)\Big]\,.
\end{aligned} \tag{9.49}$$

The important point here is that $\sqrt{P}\,b_{1,2}$ can be eliminated via (9.35) and (9.36) or (9.38) and (9.39), to obtain sources, $s_{(x)}$, that are completely independent of P, and only depend on the known fields, w, A_0, and p. This means that the equation for P, (9.48), is *linear*, and sourced by the background fluxes and metric components that have already been determined.

9.3.5 An interesting footnote

The equation for P, (9.48), is inhomogeneous and the sources, (9.49), are very complicated once they are expanded using (9.35) and (9.36), or (9.38) and (9.39). However, motivated by similar equations in other microstate geometries, one can make a simple guess for part of the required "particular solution." We find:

$$\begin{aligned}
&\mathcal{L}\Big(\frac{(\partial_z p)^2}{u^4(\partial_z w)}\Big) \;-\; s_{(\mathrm{i})} \\
&\quad = \;\frac{2}{u^6(\partial_z w)}\,\Big(6(\partial_z p)^2 - 4u(\partial_z p)(\partial_u\partial_z p) + 2u(\partial_z^2 p)(\partial_u p) \;+\; u^2\Big((\partial_u\partial_z p)^2 - (\partial_u^2 p)(\partial_z^2 p)\Big)\Big)\,, \\
&\mathcal{L}\Big(\frac{(\partial_z p)^2}{u^8(\partial_z w)}\Big) \;-\; s_{(\mathrm{ii})} \\
&\quad = \;\frac{1}{u^{10}(\partial_z w)}\,\Big(24(\partial_z p)^2 - 8u(\partial_z p)(\partial_u\partial_z p) + 5u(\partial_z^2 p)(\partial_u p) \;+\; u^2\Big((\partial_u\partial_z p)^2 - (\partial_u^2 p)(\partial_z^2 p)\Big)\Big)\,.
\end{aligned} \tag{9.50}$$

These partial solutions to the inhomogeneous terms represent a very substantial simplification of the source terms, but we have not found a simple expression for a particular solution that generates the right-hand sides of (9.50).

9.3.6 Summary of the solution

The $\frac{1}{8}$-BPS solution carrying momentum waves starts from a $\frac{1}{4}$-BPS M2-M5 substrate whose metric is given by (8.5) and fluxes are given by (8.7). The unknown functions, w and A_0 are obtained by solving (8.9) and using (8.10).

Imposing symmetries as described in Section 9.3.1, the metric with momentum waves is given by (9.29) and the frames are defined in (9.24). The fluxes are now determined in terms of a pre-potential, p, via (9.41) and (9.42) and the polarization function, k, is determined in terms of p through (9.37), or (9.40), depending upon the imposed symmetries.

The pre-potential, p, is determined by a modified Laplace equation, (9.47) with operator (9.46) defined by the substrate metric (8.5). The momentum density, P, is fixed by a Poisson equation, (9.48), also with operator (9.46), but now with sources, (9.49). The crucial fact is that this last set of equations in actually *linear*. Indeed, the only non-linear equation to be solved is (8.9) which defines the $\frac{1}{4}$-BPS substrate.

The wave profile, $F(\xi)$, is a freely choosable (arbitrary) function.

The sources of the Poisson equation for the momentum density, P, are quadratic in terms that define the momentum flux. This is a vestige of the Chern-Simons interaction in the equation for $F^{(4)}$. A partial particular solution to the inhomogeneous equation can be obtained from the squares of derivatives of the pre-potential as demonstrated in (9.50).

9.3.7 A conjecture about multiple momentum waves.

The fact that the full momentum-carrying solution is constructed on top of a substrate by null waves in the "glue" fields which can be added in a linear procedure suggests a very obvious generalization of our solution.

First, note that the substrate in equations (8.6),(8.7) does not need to have any spherical symmetry, and can describe in principle a multitude of M2 brane strips stretching between M5 branes. Our linear system also suggests an obvious covariantization.

The fundamental object will be an anti-self-dual form on the $\mathbb{R}^4$ wrapped by the M5 branes. In the third line of equation (9.41) this appears as

$$\mathcal{P} \equiv \left(\partial_z p\right)\left(e^3 \wedge e^7 \; - \; e^5 \wedge e^6\right), \tag{9.51}$$

and one can see from (9.45) that it can be multiplied by an arbitrary function of η. The homogeneous equation for p, (9.47) will emerge from the anti-self-duality. Equation (9.36) shows that the one-form k will emerge as a combination of the divergence of p and the inner product of ∇w and p. The function q and hence the fluxes $\sqrt{P}b_1$ and $\sqrt{P}b_2$ are also 2-forms, which we will denote schematically as "$\mathcal{B}$". All these fields are part of the

"glue" and is parameterized again by an arbitrary function of η. Finally, equations (9.48) and (9.49) show that the momentum density is sourced by terms of the form $*_4(\mathcal{B}\wedge\mathcal{B})$, $*_4(k\wedge\nabla w\wedge\mathcal{B})$ and $*_4(dk\wedge\mathcal{B})$.

It is reasonable to assume that one can source the anti-self-dual form p independently on each strip, and that the corresponding waves will be parameterized by different arbitrary functions of η. Hence, the metric will become

$$\begin{aligned} ds_{11}^2 \;=\; & e^{2A_0}\, d\eta \left[2\, d\zeta \;+\; 2 f^i(\eta) \boldsymbol{k_i}\cdot d\boldsymbol{u} \;+\; P_{ij} f^i(\eta) f^j(\eta)\, d\eta\right] \;+\; e^{-A_0}\, (-\partial_z w)^{-\frac{1}{2}}\, ds_4^2 \\ & +\; e^{-A_0}\, (-\partial_z w)^{\frac{1}{2}}\, ds_4'^2 \;+\; e^{2A_0}\, (-\partial_z w) \left(dz \;+\; (\partial_z w)^{-1} \left(\boldsymbol{\nabla_u}\, w\right)\cdot d\boldsymbol{u}\right), \end{aligned} \tag{9.52}$$

where we have used the label i to enumerate different strips and their sources. Since P is sourced quadratically, it will carry two of these enumeration indices. Furthermore, the potential will be

$$\begin{aligned} C^{(3)} \;=\; & e^{3A_0}\, (-\partial_z w)^{\frac{1}{2}}\, d\eta \wedge \left(d\zeta + f^i(\eta) \boldsymbol{k_i}\cdot d\boldsymbol{u}\right) \wedge \left(dz \;+\; (\partial_z w)^{-1} \left(\boldsymbol{\nabla_u}\, w\right)\cdot d\boldsymbol{u}\right) \\ & + \frac{1}{3!}\, \epsilon_{ijk\ell} \left((\partial_z w)^{-1}\, (\partial_{u_\ell} w)\, du^i\wedge du^j\wedge du^k \;-\; (\partial_{v_\ell} w)\, dv^i\wedge dv^j\wedge dv^k\right) + f^i(\eta)\, d\eta\wedge\mathcal{P}_i\,, \end{aligned} \tag{9.53}$$

where $\mathcal{P}_i$ is the suitable generalization of (9.51).

Obviously, there is much here that needs to be verified, but we are optimistic based on the linearity and our experience with superstrata.

9.4 Final comments

The construction of Microstate Geometries for black holes started almost 20 years ago with [211, 212]. This work was motivated by the desire to extend Mathur's remarkable fuzzball program from two-charge solutions, to the "three-charge problem," for which the corresponding black holes have macroscopic horizons. Ironically, the expectation of one of the authors of [212] was that the BPS equations would be hopelessly non-linear because having three independent sets of charges and magnetic fluxes would activate the Chern-Simons interaction, and this would make the Maxwell equation non-linear. To their very great surprise, the system of BPS equations governing the fluxes turned out to be linear [276]: the non-linearities were confined to the source terms that were quadratic in known solutions to other linear equations.

This result opened up the analysis of the phase space of five-dimensional microstate geometries. While there were very large numbers of solutions [22, 210, 212, 213, 216–221], and some of them had the mass gap of the typical states of the dual CFT, such geometries could only account for a tiny fraction of the black-hole microstates. These five-dimensional microstate geometries were only accessing CFT states that had a $U(1)\times U(1)$ isometry. It became imperative to break these symmetries and add more degrees of freedom. The obvious extension was to go to six dimensions and incorporate and generalize the supertubes that had been such an integral part of the two-charge fuzzballs.

In yet another irony, the other author of the Microstate Geometry program was deeply skeptical that the equations [202, 277] governing six-dimensional microstate geometries could also be linear. But they were [204]!

More precisely, in both five and six-dimensions, the equations governing the substrate geometries were non-linear (Monge-Ampère) equations governing either hyper-Kähler, or almost hyper-Kähler substrate geometries [277, 284]. Adding momentum, and the fluxes to carry the momentum, is entirely governed by a linear system of equations [204,205,276]. From a thorough analysis of the CFT duals of these six-dimensional geometries, it became clear that the substrate geometry was determining the CFT, or IR ground state and the linearly determined fluxes and momentum carriers were dual to families of CFT excitations of these ground states [24, 171].

The linearity of the supergravity solutions was essential to both the development of the holographic dictionary and the analysis of the CFT excitations.

Over the last few years, the six-dimensional system has been extensively mapped out with precision holography [155, 162, 172–175, 287–293]. We know the strengths and limitations of this system and we know exactly what states it can capture and what it is missing. There are a vast number of states accessible to the six-dimensional system, but their entropy grows, at most, as $\sqrt{Q_1 Q_5}\sqrt[4]{Q_p}$, [27, 28] which is parametrically short of the black-hole entropy, $\sqrt{Q_1 Q_5 Q_p}$. The shortfall comes from the fact that six-dimensional supergravity cannot resolve the brane fractionation that is essential to accessing the twisted sector states.

This has led to a new thrust in which one tries to resolve brane fractionation using supergravity in ten or eleven dimensions. The simple idea is that since there are a truly vast number of microstates, then there should also be an exceptional number of coherent expressions of those microstates that will be visible in supergravity. Hence brane fractionation should have a supergravity avatar. In much the same way that the analysis of supersymmetric brane configurations [30] led to *superstrata* in six-dimensional supergravity [24–26], a similar analysis of super-mazes and themelia [29, 36, 279] led to the work presented here, and once again we seem to be finding the same miracles.

The $\frac{1}{4}$-BPS substrate geometries are determined by complicated, non-linear equations. However, the momentum excitations, and the fluxes that carry them, appear to be governed by linear systems. This strongly suggests that the substrate geometries (and their non-linear equations) determine the particular twisted, or fractionated, sector of the dual field theory, and once again the momentum excitations, and the states that carry them, are determined by a linear system. What remains to be done is much like the story of superstrata: we need to find the most general families of momentum excitations, and geometric transitions of the super-maze geometries and map out the states accessible to supergravity. The linearity we have discovered here and the discussion in Section 9.3.7 suggests that this is going to be a feasible undertaking.

This would mean that supergravity can access the twisted sectors of the CFT *and* enable one to fully analyze the phase space of the momentum excitations within those

twisted sectors. As a result, supergravity could be used to sample all the essential sectors of the underlying CFT and see the details of the states that make up the black-hole microstructure. The entropy of such microstate geometries should grow as $Q^{3/2}$.

The linear description of this phase space will not only prove critical to counting the microstates, but it may well enable the development of precision holography of those states.

In retrospect, we now believe we understand the "why" of all the linear systems emerging from microstate geometries, and this is the heart of the extended themelion conjecture: the linear systems are a feature of the "glue" that welds the momentum to the branes to create an object that has sixteen local supersymmetries. The sixteen local supersymmetries are responsible for the local phenomenon of linearity of the equations that govern the excitations.

Chapter 10

The M2-M5 Mohawk

10.1 Introduction

The study of intersecting brane systems has a vast and diverse history in String Theory. One can gain significant insight by treating the branes perturbatively, or using the brane actions to determine their dynamics, while the fully back-reacted supergravity solutions for intersecting branes can be very challenging. This problem can be simplified by smearing the brane distribution, but this can wipe out essential dynamical details, especially if one is trying to describe black-hole microstructure [23, 224, 234]. Ideally one would like supergravity solutions that describe unsmeared brane intersections, but such solutions typically involve metrics and fluxes that are characterized by complicated systems of non-linear equations.

There are two ways in which such non-linear systems can be rendered manageable. The first is to try to arrange a very high level of symmetry so that the configuration only depends on one or two variables. In this situation, the equations sometimes simplify to a linear system. However, such a high level of symmetry often involves smearing out structures that one wants to investigate. The second approach is to consider some form of "near-brane" limit in which some of the functional dependence of the solution is controlled by scale invariance, while the remaining equations can be reduced to a linear system. In this Chapter we will make a detailed exploration of an example of such a near-brane limit.

We focus on stacks of M2 and M5 branes that intersect along a common $\mathbb{R}^{1,1}$. The intersection is thus co-dimension 4 in the M5 branes, and we will impose spherical symmetry in these directions along the stack of M5 branes. The intersecting M2-M5 system also has co-dimension 4 in the complete space time, and we will also impose spherical symmetry in these transverse directions. The solution therefore has an $\mathbb{R}^{1,1} \times SO(4) \times SO(4)$ symmetry, and depends on three variables, (u, v, z), where u, v are, respectively, radial coordinates in the M5 branes and the transverse space, while z is the remaining coordinate along the M2 branes. This class of brane intersections has been extensively studied, and the general solution is governed by a non-linear Monge-Ampère-like equation [259–261, 278, 294].

As an offshoot of the study of Janus solutions, a near-brane limit of intersecting M2 and M5 branes was constructed by seeking out solutions with an $SO(2,2) \times SO(4) \times SO(4)$

symmetry [40,270–274,286]. These solutions contain a warped product of $\mathrm{AdS}_3 \times S^3 \times S^3$, with the remaining two dimensions described by a Riemann surface, coordinatized by (ξ, ρ). The underlying BPS equations were also simplified to a linear system. In [278] it was shown how a class of these solutions could be mapped onto a near-brane limit of the M2-M5 intersections described in [259, 261]. In particular, it was shown how, in such a limit, the coordinates (u, v, z) can be recast in terms of the scale coordinate, μ, of a Poincaré AdS_3 and the coordinates (ξ, ρ) of the Riemann surface. This work also implicitly implies that, by reducing the problem to only two non-trivial variables, the Monge-Ampère-like system can be reduced to a linear set of equations.

Despite this mapping, it remained unclear what kind of M2-M5 systems the solutions of [40] describe. The complication is that the solutions of [40] involve choices of the Riemann surface and choices of poles and residues in a single function, G, that defines the flux sources. These choices are inextricably linked by requiring regularity of the solution. In this Chapter we will make a detailed analysis of certain families of solutions constructed in [40] and show that they describe, what appears from infinity, to be a *single stack* of semi-infinite M2 branes ending on, and deforming, a *single stack* of M5 branes. More precisely, the brane stacks are all coincident at infinity but, because the M2 branes pull on the M5 branes, the back-reaction causes these stacks to resolve into physically separated spikes (a "mohawk"), with the distance between each spike being controlled by the number of M2's and M5's making up each spike.

More generally, we suspect that any near-brane limit that leads to such an AdS_3 factor is necessarily limited to a single intersection. The argument is simple: a more complicated intersection must involve a scale that would violate the symmetries of the AdS_3. Consider, for example, a supergravity solution for an M2 brane stretched between two M5 branes. As we will see, the supergravity solution for a single intersection faithfully reproduces a geometry consistent with the spike created by an F1 ending on a D-brane [39, 227]. An M2 brane stretched between M5's must look like two spikes that meet one another, as depicted in Fig. 10.1, creating a two-sided tube between the M5's. Around this tube there will be a 7-cycle that is a Gaussian surface for the M2 charge. In the configuration shown in Fig. 10.1, this 7-cycle will reach a minimum size at some value of the putative AdS radius. This will break the scale invariance of the AdS.

The near-brane AdS_3 geometries that we investigate are limited to a single intersection, but the solutions are far from being featureless. Once the back-reaction is incorporated via a supergravity solution, we find spikes created by M2 branes ending on M5 branes that have a profile [39, 227, 259]:

$$z \sim \frac{c}{u^2}\,. \tag{10.1}$$

The right-hand side is generically a harmonic function sourced by the M2's ending on the M5's, and is thus proportional to u^{-2} given the spherical symmetry. The steepness of the spike, c, is determined by the ratio of the number, Q_{M2}, of M2 branes that are pulling and the number, Q_{M5}, of M5 branes being deformed. Indeed, $c \sim \frac{Q_{M2}}{Q_{M5}}$. However, as we will show, the AdS_3 can accommodate any number of spikes with different steepnesses and the

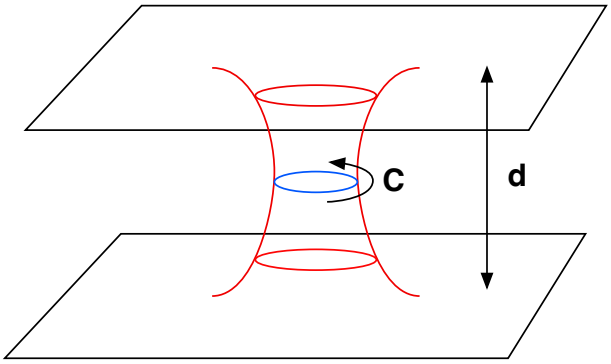

Figure 10.1: An M2 brane stretched between two M5 branes. In the back-reacted solution, the branes will be stretched and the minimum circumference, C, around the M2 branes will depend on the separation, d, of the M5 branes.

self-similarity of (10.1) is what leads to the scale invariance. Thus we can partition the stack of M5 branes into groups, and choose the number of M2's that end on each group. This results in different spikes whose steepness is controlled by the value of $\frac{Q_{M2}}{Q_{M5}}$ in each group.

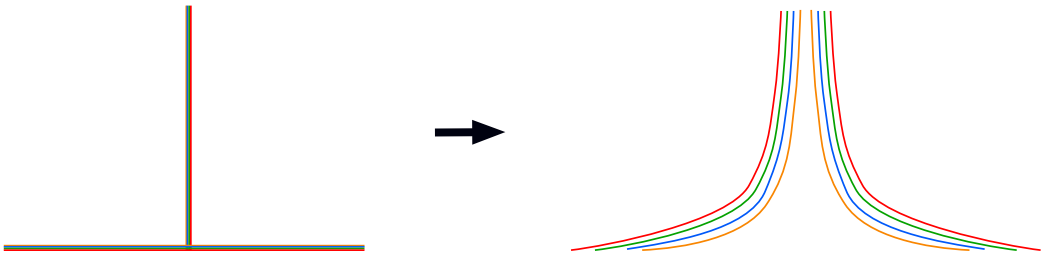

Figure 10.2: Brane fractionation at a single intersection as a result of back-reacted brane bending. If the bent branes are self-similar, preserving a scale invariance, then the near-brane description can result in an AdS geometry.

Upon turning on the back-reaction, the different groups spatially separate according to their steepness. This is depicted in Fig. 10.2. The residues of the function, G, control the number of M5's in each group, while the location of the poles of G on the Riemann surface is controlled by the steepness, and thus encodes the M2 charge in each group. In this way, a "single intersection" of non-back-reacted branes actually resolves into a complex of multiple, self-similar intersections whose components localize at different points on the Riemann surface. At infinity, the brane configuration converges to a stack of coincident M5's in one direction and M2's in another, but as one zooms into the intersection, the M2's and M5's resolve into physically separated groups.

It is interesting to note that this brane picture describes the solutions of [40] that have $AdS_4/\mathbb{Z}_2$ asymptotics, as well as the solutions that have AdS_7 asymptotics. The $AdS_4/\mathbb{Z}_2$ asymptotics is not surprising: after all, as one goes up the semi-infinite M2 branes, far away from the M5 branes, one expects the geometry they source to be $AdS_4 \times S^7$. However, for the asymptotically-AdS_7 geometries one might naively hope that they describe M2

branes sandwiched between M5 branes [40]. However, as we will discuss in Section 10.3, these solutions are simply a zoom-in limit at the bottom of the spike depicted in Fig. 10.2, and hence are degenerate limit of an M2-M5 infinite spike.

In Section 10.2 we review the known supergravity solutions for M2-M5 intersections, focusing on the geometry that emerges in the near-intersection limit. We follow this, in Section 10.3, with our primary example because it has all the essential features of a single intersection. In Section 10.4 we return to the general near-intersection solutions and compute, in detail, the M2-brane charge density function, and evaluate it at all the sources in the example. This gives us the picture of the M2-M5 mohawk: a collection of self-similar spikes separated according to steepness. Section 10.5 contains some final comments. In Appendix I we show how M5-brane probes reproduce a key characteristic of the mohawk. That is, given a supergravity solution M2-M5 mohawk, one can analyze the forces experienced by a probe component of the mohawk (an M5-brane with an M2 spike, which in the coordinates of [40] is extended along the $AdS_3 \times S_3$ part of the geometry). We show that the probe has an equilibrium position on the boundary of the Riemann surface depends linearly on the amount of M2 flux along the probe world-volume. This implies that the relation between the M2 charge and the steepness of the spike is that same as that in the spikes whose backreaction gives rise to the background $AdS_3 \times S_3 \times S_3$ solution.

10.2 General M2-M5 intersections and AdS$_3$ limits

As described in the previous Section, the brane configuration becomes much clearer in the original formulation of [259, 261], and here we will use the language of the previous two Chapters. As usual, the M2 directions correspond to the coordinates $(x^0, x^1, x^2) = (t, y, z)$, while the coordinates along the M5 branes are $(t, y, x^3, \ldots, x^6)$. The transverse directions are thus $(x^7, \ldots, x^{10})$, and will be denoted by $\boldsymbol{v} \in \mathbb{R}^4$. Similarly, we use a vector, $\boldsymbol{u} \in \mathbb{R}^4$, to denote the directions, $(x^3, \ldots, x^6)$, transverse to the M2 inside in M5. Since we are going to focus on a single brane intersection, we will impose spherical symmetry in both these $\mathbb{R}^4$'s. Therefore, the $\frac{1}{4}$-BPS solution will have the metric of the form (8.12) and the fluxes will be given by (8.14).

As for the "near-brane" limit of M2-M5 intersections, which is also an implicit part of the work on Janus solutions in M-theory [40, 266, 270–274, 278, 286], we will take the metric and fluxes to have the form (8.29). For the analysis in the next Sections we will use the results presented in Section 8.3.2, we will take $\beta = 2$ in (8.34) and we will choose the following set of signs in (8.48):

$$\nu_1 = \nu_2 = -\nu_3 = \sigma = 1\,. \tag{10.2}$$

Therefore, the flux functions, b_i, which are also determined by G and its potentials, will

be:

$$\begin{aligned} b_1 &= \frac{1}{2}\left[\frac{\rho\, g_1}{(G\overline{G}\ -\ 1)} + \Phi\right], \qquad b_2 = \frac{4\,\rho\, g_1}{W_+} - (\Phi + 2\,\xi)\,, \\ b_3 &= \frac{4\,\rho\, g_1}{W_-} - (\Phi - 2\,\xi)\,. \end{aligned} \tag{10.3}$$

As we will discuss extensively below, these are well-defined locally and up to the addition of constants.

Finally, in order to map the solution in Section 8.3.2 to the near-brane limit of the spherically-symmetric brane-intersection of Section 8.2.3 we will take:

$$\gamma = 1\,, \qquad u = (\mu\rho)^{\frac{1}{2}}\, e^{-\frac{1}{4}\widetilde{\Phi}}\,, \qquad v = (\mu\rho)^{\frac{1}{2}}\, e^{+\frac{1}{4}\widetilde{\Phi}}\,, \qquad z = \frac{1}{2\rho\mu}\, e^{\frac{1}{2}\widetilde{\Phi}}\left(\Phi + 2\,\xi\right), \tag{10.4}$$

$$w = -\frac{1}{2\rho\mu}\, e^{-\frac{1}{2}\widetilde{\Phi}}(\Phi - 2\xi)\,. \tag{10.5}$$

10.3 Primary example

Our primary example is designed to produce the near-brane limit of a stack of M2's ending on a stack of M5's. We will choose a very simple Riemann surface, the Poincaré upper half plane, which corresponds to taking h to have a single zero and a pole $w = \infty$:

$$h = -i(w - \overline{w})\,. \tag{10.6}$$

The choice of G is more complicated. The most general solution can involve three species of branes: M5 branes with non-back-reacted world-volume along $(t, y, x^3, \ldots, x^6)$, M5 branes, (usually denoted M5') along $(t, y, x^7, \ldots, x^{10})$ and M2 branes along (t, y, z). We wish to exclude the M5' branes but want M5 sources, and this determines the pole structure of G. Moreover to get an $\mathrm{AdS}_4 \times S^7$ geometry, corresponding to semi-infinite M2 branes, the function G must contain a "flip-term" on the boundary of the Riemann surface [40]:

$$h = -i(w - \overline{w}), \qquad G = -\left(i\frac{w - \alpha}{|w - \alpha|} + \sum_{a=1}^{n+1} \frac{\zeta_a \mathrm{Im}(w)}{(\overline{w} - \xi_a)|w - \xi_a|}\right), \tag{10.7}$$

where the parameters α, ξ_a and ζ_a are real. Without loss of generality we will also take

$$\alpha < \xi_1 < \xi_2 \cdots < \xi_{n+1}. \tag{10.8}$$

The flip term changes the boundary value of G from $+i$ to $-i$ at $w = \alpha$ and $w = \infty$. We have included the flip parameter, α, so that it is easy to pass to a no-flip solution (in which $G = -i$ on the entire boundary) by taking $\alpha \to -\infty$. In this way one can easily see that the no-flip solution is a degenerate limit of the solution with a flip.

The poles in G lie on the boundary ($\rho = 0$) at $w = \xi_a$, and the residue parameters, ζ_a, represent the M5 charges sourced by these poles. As depicted in Fig. 10.3, we have

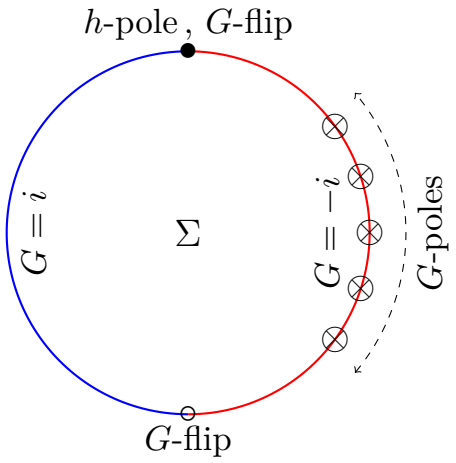

Figure 10.3: Schematic representation of the Riemann surface Σ with the topology of a disc. The red arc denotes the region on the boundary of Σ where $G = -i$ and the blue arc denotes the region on the boundary where $G = i$. The solid dot $\bullet$ marks the pole in h at $w = \infty$, the poles in G at $w = \xi_a$ are denoted by the symbol $\otimes$ on the red arc and the circle $\circ$ denotes the flip in G at $w = \alpha$.

chosen the poles to lie in the interval $\alpha < \xi < \infty$, where $G = -i$. This implements the choice of only M5 (and not M5') sources. Metric regularity then requires[1] $\zeta_a > 0$.

Using the coordinates (8.32), one can write the real and the imaginary parts of $G = g_1 + ig_2$ as:

$$\begin{aligned} g_1 &= \frac{\rho}{\sqrt{(\xi-\alpha)^2+\rho^2}} - \sum_{a=1}^{n+1} \frac{\zeta_a \rho (\xi-\xi_a)}{((\xi-\xi_a)^2+\rho^2)^{3/2}}\,, \\ g_2 &= -\left(\frac{(\xi-\alpha)}{\sqrt{(\xi-\alpha)^2+\rho^2}} + \sum_{a=1}^{n+1} \frac{\zeta_a \rho^2}{((\xi-\xi_a)^2+\rho^2)^{3/2}} \right). \end{aligned} \tag{10.9}$$

One then easily obtains the potentials (8.40):

$$\begin{aligned} \widetilde{\Phi} &= 2\left(\log(\alpha\,\rho) - \log\left(\xi - \alpha + \sqrt{(\xi-\alpha)^2+\rho^2}\right) - \sum_{a=1}^{n+1} \frac{\zeta_a}{\sqrt{(\xi-\xi_a)^2+\rho^2}} \right), \\ \Phi &= 2\left(\alpha + \sqrt{(\xi-\alpha)^2+\rho^2} + \sum_{a=1}^{n+1} \frac{\zeta_a(\xi-\xi_a)}{\sqrt{(\xi-\xi_a)^2+\rho^2}} \right). \end{aligned} \tag{10.10}$$

The potentials $\Phi, \widetilde{\Phi}$ are defined up to a constant shift. In the expressions above we have adjusted the constant part of the potentials so that they have a smooth $\alpha \to -\infty$ limit. It is easy to check that in the $\alpha \to -\infty$ limit, one obtains the potentials discussed in [278].

[1] More generally, regularity requires $\zeta_a(\xi_a - \alpha) > 0$, but since we only have M5 sources, this means $\zeta_a > 0$.

To obtain a more geometric picture of the brane layout, it is useful to express the solution in terms of the u, v, z coordinates given in (10.4):

$$\begin{aligned} u &= \sqrt{\frac{\mu}{|\alpha|}}\left(\xi-\alpha+\sqrt{(\xi-\alpha)^2+\rho^2}\right)^{1/2} e^{\frac{1}{2}\widehat{\Phi}}, \\ v &= \rho\sqrt{\mu|\alpha|}\left(\xi-\alpha+\sqrt{(\xi-\alpha)^2+\rho^2}\right)^{-1/2} e^{-\frac{1}{2}\widehat{\Phi}}, \\ z &= \frac{|\alpha|}{\mu}\left(\xi-\alpha+\sqrt{(\xi-\alpha)^2+\rho^2}\right)^{-1} e^{-\widehat{\Phi}}\left(\xi+\alpha+\sqrt{(\xi-\alpha)^2+\rho^2}+\sum_{a=1}^{n+1}\frac{\zeta_a(\xi-\xi_a)}{\sqrt{(\xi-\xi_a)^2+\rho^2}}\right), \end{aligned} \tag{10.11}$$

where we have defined:

$$\widehat{\Phi} \equiv \sum_{a=1}^{n+1}\frac{\zeta_a}{\sqrt{(\xi-\xi_a)^2+\rho^2}}\,. \tag{10.12}$$

It is also useful to introduce polar coordinates at the flip point:

$$\xi-\alpha = \lambda^2\cos\theta\,, \qquad \rho = \lambda^2\sin\theta\,, \tag{10.13}$$

which leads to:

$$\begin{aligned} u &= \sqrt{\frac{2\,\mu}{|\alpha|}}\,\lambda\cos\left(\frac{\theta}{2}\right)e^{\frac{1}{2}\widehat{\Phi}}\,, \qquad v = \sqrt{\frac{2\,\mu}{|\alpha|}}\,\lambda\sin\left(\frac{\theta}{2}\right)e^{-\frac{1}{2}\widehat{\Phi}}, \\ z &= \frac{|\alpha|}{2\,\mu}\left(\lambda\cos\left(\frac{\theta}{2}\right)\right)^{-2} e^{-\widehat{\Phi}}\left(2\,\alpha \;+\; \lambda^2\cos^2\left(\frac{\theta}{2}\right) \;+\; \sum_{a=1}^{n+1}\frac{\zeta_a(\xi-\xi_a)}{\sqrt{(\xi-\xi_a)^2+\rho^2}}\right). \end{aligned} \tag{10.14}$$

Note that $\rho \geq 0$ corresponds to $0 \leq \theta \leq \pi$. Also note that

$$\begin{aligned} \widehat{z} \equiv u^2\,z &= \xi+\alpha+\sqrt{(\xi-\alpha)^2+\rho^2} \;+\; \sum_{a=1}^{n+1}\frac{\zeta_a(\xi-\xi_a)}{\sqrt{(\xi-\xi_a)^2+\rho^2}} \\ &\to \quad (\xi+\alpha) \;+\; |\xi-\alpha| \;+\; \sum_{a=1}^{n+1}\zeta_a\,\mathrm{sign}(\xi-\xi_a) \quad \text{as} \quad \rho\to 0\,. \end{aligned} \tag{10.15}$$

These coordinate changes reveal much about the configuration.

First, the brane sources all lie along $\rho = 0$, which corresponds to $v = 0$. It is evident from (8.12) that $v = 0$ defines the origin of the $\mathbb{R}^4$ transverse to the M2-M5 system.

The M5 sources are defined by $(\xi = \xi_a, \rho = 0)$. From (10.15), one has at these points:

$$\widehat{z}|_{\xi=\xi_a,\rho=0} = 2\xi_a \;-\; \sum_{b=1}^{a-1}\zeta_b \;+\; \sum_{b=a+1}^{n+1}\zeta_b\,, \tag{10.16}$$

which is a constant on each brane. Indeed, the M5 brane world-volume is defined by (t, y) and the $\mathbb{R}^4$ with radial coordinate u. One sees from (10.11) that along this world volume one has:

$$z \sim \frac{1}{\mu}\,, \qquad u \sim \sqrt{\mu}\,. \tag{10.17}$$

This shows that the M5 brane is deformed into a "spike" in the M2 direction, z, with the AdS scale sweeping the radial coordinate in the combined world-volume. As expected from the results of [39, 227, 259], the spike profile is determined by the harmonic function (u^{-2}) sourced by the M2 branes inside the M5 world-volume. One also sees how the AdS scale invariance arises: It represents the scaling self-similarity (10.17) of all the spike profiles. In Appendix I, we use M5-brane probes to confirm this picture of the solution described by (10.7). That is, we show that an M5-brane probe with a world-volume along $AdS_3 \times S_3$, and carrying M2 flux, feels no force when located at a point on the boundary of Σ that is determined by the probe's M2 flux.

As discussed in the Introduction, in more complicated multi-intersections of branes, the M2 brane profile becomes more complicated, such as in Fig. 10.1, and the self-similarity is lost. It is this that defines, and restricts the range of, the near-brane, AdS limit.

The constant of proportionality in (10.17) determines the steepness of the spike profile, and this is determined by (10.16). Observe that these values are monotonically increasing in a because $\zeta_a > 0$ and because of (10.8). The M5 brane sources are thus a separated collection of spikes (at different values of ξ_a) and each such collection is progressively steeper, as depicted in Fig. 10.2. It is this picture (and Fig. 10.4) that led to us refer to this configuration as a "mohawk." We will discuss the steepness more extensively in Section 10.4.4.

Far from the M5 sources, the function $\widehat{\Phi}$ vanishes, and one has

$$u^2 \ + \ v^2 \ \approx \ \frac{2\,\mu}{|\alpha|}\,\lambda^2\,. \tag{10.18}$$

This defines the asymptotic radial coordinate, and S^7, in the $\mathbb{R}^4 \times \mathbb{R}^4$ factors of (8.12). This S^7 is the Gaussian surface surrounding the M2 branes.

In the limit $\lambda \to 0$, the metric (8.29) takes the form:

$$ds_{11}^2 \ = \ B_1\,ds^2_{AdS_3} \ + \ B_2\left[d\lambda^2 + \lambda^2\left(d\Big(\frac{\theta}{2}\Big)^2 + \cos^2\Big(\frac{\theta}{2}\Big)\,ds^2_{S^3} + \sin^2\Big(\frac{\theta}{2}\Big)\,ds^2_{S'^3}\right)\right], \tag{10.19}$$

where

$$B_1 \ = \ \frac{4}{B_2^2} \ = \ \left(4\sum_{a=1}^{n+1}\frac{\zeta_a}{(\xi_a-\alpha)^2}\right)^{-2/3}\,. \tag{10.20}$$

Since $0 \le \theta \le \pi$, the factor in square brackets in (10.19) is precisely the metric of flat $\mathbb{R}^8$. There are no sources at $\lambda = 0$.

As $\lambda \to \infty$, the metric (8.29) takes the form:

$$ds^2 \ = \ \left[B'_1\,\lambda^4\,ds^2_{AdS_3} \ + \ B'_2\,\frac{d\lambda^2}{\lambda^2}\right] \ + \ B'_2\left[d\Big(\frac{\theta}{2}\Big)^2 + \cos^2\Big(\frac{\theta}{2}\Big)\,ds^2_{S^3} + \sin^2\Big(\frac{\theta}{2}\Big)\,ds^2_{S'^3}\right], \tag{10.21}$$

where

$$B'_1 \ = \ \frac{4}{B'^2_2} \ = \ \left[2\left(\sum_{a=1}^{n+1}\zeta_a\right)^2 + 4\sum_{a=1}^{n+1}\zeta_a\,(\xi_a-\alpha)\right]^{-2/3}\,. \tag{10.22}$$

The second factor in (10.21) is exactly the round metric on S^7, but now the metric has stabilized to a fixed radius given by (10.22). In Section 10.4.4, we will show that the term in the square brackets of (10.22) is a simple multiple of the total M2 charge of the system.

The first factor in (10.21) is a section of the metric on an AdS_4. The easiest way to see this is to note that if $\widehat{ds}^2_{AdS_3}$ denotes the metric on a unit global AdS_3, then the metric on a unit global AdS_4 may be written as:

$$\widehat{ds}^2_{AdS_4} \;=\; d\sigma^2 \;+\; \cosh^2\sigma\, \widehat{ds}^2_{AdS_3}\,, \tag{10.23}$$

where $-\infty < \sigma < \infty$. In the same way that one can scale global AdS metrics to get Poincaré AdS metrics, one can scale (10.23) to arrive at the first factor of (10.21). In this sense the latter metric, with $0 < \lambda < \infty$, defines an $AdS_4/\mathbb{Z}_2$.

The important point here is that the large-λ region of the metric is precisely that of a stack of M2 branes with a radius of curvature determined by the M2-charge.

10.4 Computing the M2 Charges

The equations of motion for $C^{(3)}$ are

$$d * F^{(4)} \;=\; -\frac{1}{2} F^{(4)} \wedge F^{(4)}\,, \tag{10.24}$$

which imply the existence of an M2-charge density, $C^{(6)}$, defined by:

$$dC^{(6)} \;=\; * F^{(4)} \;+\; \frac{1}{2} C^{(3)} \wedge F^{(4)} \;+\; \text{exact}\,. \tag{10.25}$$

One should note that this is a Page charge: it is conserved, because of (10.24), but it is gauge dependent. For the near-intersection limit of Section 8.3.2, one can write this as:

$$dC^{(6)} \;=\; -\, d\Omega_1\, \widehat{e}^{345678} \;+\; d\Omega_2\, \widehat{e}^{678012} \;+\; d\Omega_3\, \widehat{e}^{345012}\,, \tag{10.26}$$

where the six-forms, $\widehat{e}^{adcdef}$, are the wedge products of the volume forms introduced in (8.29), and the $d\Omega_j$ are one-forms on the Riemann surface, Σ. The M2 charge is determined by the first term in (10.26), and so we focus on this.

10.4.1 The flux functions

Computing $C^{(6)}$ turns out to involve a few subtleties and so we provide some details here. There is a discussion of this in [40], however we will elucidate this further and make some (minor) corrections. To facilitate comparison with [40], we will adopt their notation and conventions (except we set $\gamma = 1$), and use their slightly different normalization of the flux functions.

We introduce the potentials, $\widehat{b}_i$:

$$\begin{aligned}
\widehat{b}_1 \;&\equiv\; \frac{h\,(G+\overline{G})}{(G\overline{G}\;-\;1)} + 4\,\Phi \;+\; \widehat{b}_1^0\,,\\
\widehat{b}_2 \;&\equiv\; -\,\frac{h\,(G+\overline{G})}{W_+} + (\Phi - \widetilde{h}) \;+\; \widehat{b}_2^0\,, \qquad \widehat{b}_3 \;\equiv\; \frac{h\,(G+\overline{G})}{W_-} - (\Phi + \widetilde{h}) \;+\; \widehat{b}_3^0\,,
\end{aligned} \tag{10.27}$$

where we have also included constants of integration[2], $\widehat{b}_j^0$, as they will be important in constructing the M2-charge densities.

Using (10.25) and (10.26), one finds that the normalized one-form, $d\widehat{\Omega}_1$, is given by:

$$\partial_w\widehat{\Omega}_1 \;=\; \frac{i\,h\,(G\overline{G}-1)^2}{W_+W_-}\,\partial_w\widehat{b}_1 \;-\; \frac{1}{2}\left(\widehat{b}_2\,\partial_w\widehat{b}_3 - \widehat{b}_3\,\partial_w\widehat{b}_2\right) \;+\; \partial_w\widehat{\eta}_1\,, \tag{10.28}$$

and its complex conjugate. The function, $\widehat{\eta}_1$, reflects the fact that $d\widehat{\Omega}_1$ is ambiguous up to an exact piece. With the normalizations of (10.27) and the choices in (10.3) (see, also, the footnote), it turns out that the original $C^{(6)}$ is obtained from (10.26) and $\Omega_1 = \widehat{\Omega}_1$.

10.4.2 Non-trivial cycles and smooth fluxes

To compute the M2-charges, we need to determine the non-trivial 7-cycles, and then choose $\widehat{\eta}_1$ so that $d\widehat{\Omega}_1$ is well-defined on each such cycle. Having done that, we integrate $dC^{(6)}$ over that 7-cycle by using Stokes' theorem and the values $\widehat{\Omega}_1$ at the endpoints of carefully chosen curves.

The 7-cycles are either S^7 or $S^4\times S^3$, and they can be described using the two S^3's of the geometry and a curve in Σ that we will parametrize by θ. Along this curve, the relevant part of the geometry has the schematic form:

$$ds_7^2 \;=\; d\theta^2 \;+\; k_1(\theta)^2\,ds^2_{S^3} \;+\; k_2(\theta)^2\,ds^2_{S'^3}\,, \tag{10.29}$$

for some functions $k_j(\theta)$. One obtains an S^7 if k_1 vanishes at one end of the θ-curve and k_2 vanishes at the other end. One obtains $S^4\times S^3$ if one of the k_i remains strictly positive along the curve while the other k_j vanishes at both ends.

In the geometry (8.29), the S^3's pinch off at the boundary of Σ, ($\rho\to 0$), where $G\to\pm i$. A curve running between any two points on the boundary of Σ thus describes a 7-cycle, and it is topologically non-trivial if the curve is non-contractible, which happens if the curve surrounds singular points of G or h. We will only consider situations in which such singular points also lie at the boundary of Σ. Because of the symmetry, the integrals over the S^3's are trivial, giving a factor of $4\pi^4$, which we will largely ignore. The only non-trivial aspect of the calculation is the integral of $d\widehat{\Omega}_1$ along the curve in Σ. If $\widehat{\Omega}_1$ is continuous along the curve, the integral reduces to the difference of values of $\widehat{\Omega}_1$ at the end points of the curve:

$$\int_{X_7} dC^{(6)} \;=\; 4\pi^4\;\widehat{\Omega}_1\Big|_{\xi=\xi_-}^{\xi=\xi_+}\,, \tag{10.30}$$

[2]In [40] these constants of integration are denoted b_j^0. Moreover, the flux functions b_i in (10.3) are related to the ones in (10.27) by $b_i = \frac{\nu_i}{c_i^3}\widehat{b}_i$, with $c_1 = 2, c_2 = c_3 = -1$, and ν_i given by (10.2).

where the endpoints of the curve are at $\rho = 0$ and $\xi = \xi_\pm$.

As one approaches the boundary of Σ, the potentials, $\widehat{b}_j$, generically remain finite, and so there is a danger that $d\widehat{\Omega}_1$ will be singular because the right-hand-side of (10.28) is finite while a sphere metric is pinching off. One can adjust the constants, $\widehat{b}_2^0$ and $\widehat{b}_3^0$, so that $\widehat{b}_2$ vanishes at one point and $\widehat{b}_3$ vanishes at some other point. In this way, one can use the constants to ensure that $d\widehat{\Omega}_1$ is well-defined on any topological S^7. However, a problem can arise for cycles that are topologically $S^4 \times S^3$: smoothness seems to require that the same $\widehat{b}_j$ must vanish at two different points.

To resolve this problem, one has to use a non-trivial exact part, $d\widehat{\eta}_1$. Specifically, if $G \to -i\epsilon$ at both ends of the curve, one can obtain a smooth $d\widehat{\Omega}_1$ by setting:

$$\partial_w \widehat{\Omega}_1 \;=\; \frac{i\,h\,(G\overline{G}-1)^2}{W_+W_-}\,\partial_w\widehat{b}_1 \;-\; \frac{1}{2}\left(\widehat{b}_2\,\partial_w\widehat{b}_3 - \widehat{b}_3\,\partial_w\widehat{b}_2\right) \;-\; \frac{1}{2}\,\epsilon\,\partial_w\Big(\widehat{b}_2\,\widehat{b}_3\Big)\,. \tag{10.31}$$

To see how this works, observe that as $G \to -i$, the metric on S^3 remains finite, while S'^3 pinches off. This means that $\widehat{b}_2$ is non-singular (for any $\widehat{b}_2^0$) on the cycle, while finite $\widehat{b}_3$ will lead to a singular $d\widehat{\Omega}_1$ at the pinch-off points. Taking $\epsilon = 1$ in (10.31) converts the source to $\widehat{b}_2\,\partial_w\widehat{b}_3$, with no "bare" $\widehat{b}_3$, thus obviating the effects of a finite $\widehat{b}_3$. Similarly, as $G \to +i$, the metric on S'^3 remains finite and S^3 pinches off, making finite $\widehat{b}_2$ dangerous, but taking $\epsilon = -1$ cancels the bare $\widehat{b}_2$ in (10.31).

We now see how this works in detail by computing $\widehat{\Omega}_1$ explicitly.

10.4.3 Computing the flux potential, $\widehat{\Omega}_1$

Again, following [40], the solution to (10.31) has the form

$$\begin{aligned}\widehat{\Omega}_1 \;=\; &\frac{h}{2\,W_+}\Big[h\,(G\overline{G}-1) \;+\; (\Phi+\widetilde{h})(G+\overline{G})\Big] \;-\; \frac{h}{2\,W_-}\Big[h\,(G\overline{G}-1) \;+\; (\Phi-\widetilde{h})(G+\overline{G})\Big]\\ &-\; \frac{1}{2}\,\widehat{b}_2^0\left[\frac{h\,(G+\overline{G})}{W_-} - (\Phi+\widetilde{h})\right] \;-\; \frac{1}{2}\,\widehat{b}_3^0\left[\frac{h\,(G+\overline{G})}{W_+} - (\Phi-\widetilde{h}))\right]\\ &-\; \widetilde{h}\,\Phi \;+\; \Lambda \;-\; \frac{1}{2}\,\epsilon\,\widehat{b}_2\,\widehat{b}_3\,,\end{aligned} \tag{10.32}$$

where Λ satisfies:

$$\partial_w\Lambda \;=\; i\,h\,\partial_w\Phi \;-\; 2i\,\Phi\,\partial_w h\,. \tag{10.33}$$

The integrability condition for the equation for Λ follows from the equation (8.39) for Φ. Specifically, one can write (10.33) as

$$\partial_\xi\Lambda \;=\; 2\rho\,\partial_\rho\Phi \;-\; 4\,\Phi\,, \qquad \partial_\rho\Lambda \;=\; -\,2\rho\,\partial_\xi\Phi\,. \tag{10.34}$$

Eliminating Λ from these equations gives (8.39), while eliminating Φ leads to:

$$\partial_\xi^2\Lambda \;+\; \partial_\rho^2\Lambda \;-\; \frac{3}{\rho}\,\partial_\rho\Lambda \;=\; 0\,. \tag{10.35}$$

Finally, using (10.27), observe that

$$
\begin{aligned}
-\frac{1}{2}\,\epsilon\,\widehat{b}_2\,\widehat{b}_3 \;&=\; \frac{1}{2}\,\epsilon\,\frac{h^2\,(G+\overline{G})^2}{W_+W_-} \;+\; \frac{1}{2}\,\epsilon\,\Big(\Phi-\widetilde{h}+\widehat{b}_2^0\Big)\Big(\Phi+\widetilde{h}-\widehat{b}_3^0\Big)\\
&\quad-\;\epsilon\left[\frac{h}{2\,W_+}\Big(\Phi+\widetilde{h}-\widehat{b}_3^0\Big)(G+\overline{G}) \;+\; \frac{h}{2\,W_-}\Big(\Phi-\widetilde{h}+\widehat{b}_2^0\Big)(G+\overline{G})\right]
\end{aligned}
\tag{10.36}
$$

and hence

$$
\begin{aligned}
\widehat{\Omega}_1 \;&=\; \frac{1}{2}\,\epsilon\,\frac{h^2\,(G+\overline{G})^2}{W_+W_-} \;+\; \frac{i\,h^2\,(G\overline{G}-1)(G-\overline{G})}{W_+W_-}\\
&\quad-\;\frac{1}{2}\,(1-\epsilon)\,\Big(\widehat{b}_3^0-(\Phi+\widetilde{h})\Big)\left[\frac{h}{W_+}\,(G+\overline{G})-\Big(\Phi-\widetilde{h}\Big)\right]\\
&\quad-\;\frac{1}{2}\,(1+\epsilon)\,\Big(\widehat{b}_2^0+(\Phi-\widetilde{h})\Big)\left[\frac{h}{W_-}\,(G+\overline{G})-\Big(\Phi+\widetilde{h}\Big)\right]\\
&\quad-\;\frac{1}{2}\,\epsilon\,\Big(\Phi^2-\widetilde{h}^2\Big) \;-\; \widetilde{h}\,\Phi \;+\; \Lambda \;-\; \frac{1}{2}\,\epsilon\,\widehat{b}_2^0\,\widehat{b}_3^0\,.
\end{aligned}
\tag{10.37}
$$

Consider the limit of $\widehat{\Omega}_1$ as $\rho\to 0$. Recall that, in this limit, one has $G\to\mp i$ which means $W_\pm\sim\mathcal{O}(\rho^2)$ and $W_\mp\to 4$. It follows that the first two terms in (10.37) vanish. If one has M5 brane sources in the $G\to -i$ region, as we do in the example of Section 10.3, then, as we discussed above, we use the gauge with $\epsilon=+1$ for Ω_1 to be well-defined. This leaves:

$$
\begin{aligned}
\widehat{\Omega}_1\Big|_{\rho=0} \;&=\; \Big(\Lambda \;-\; \widetilde{h}\,\Phi \;+\; \frac{1}{2}\,\Big(\Phi^2-\widetilde{h}^2\Big) \;+\; \widehat{b}_2^0\,\Big(\Phi+\widetilde{h}\Big)\\
&\qquad-\;\frac{1}{2}\,\widehat{b}_2^0\,\widehat{b}_3^0 \;-\; \Big(\widehat{b}_2^0+(\Phi-\widetilde{h})\Big)\frac{h}{W_-}\,(G+\overline{G})\Big)\Big|_{\rho=0}\,.
\end{aligned}
\tag{10.38}
$$

Conversely, if the M5 brane source lies in the $G\to +i$ region, one must use the gauge with $\epsilon=-1$, and one is left with:

$$
\begin{aligned}
\widehat{\Omega}_1\Big|_{\rho=0} \;&=\; \Big(\Lambda \;-\; \widetilde{h}\,\Phi \;-\; \frac{1}{2}\,\Big(\Phi^2-\widetilde{h}^2\Big) \;+\; \widehat{b}_3^0\,\Big(\Phi-\widetilde{h}\Big)\\
&\qquad+\;\frac{1}{2}\,\widehat{b}_2^0\,\widehat{b}_3^0 \;-\; \Big(\widehat{b}_3^0-(\Phi+\widetilde{h})\Big)\,\frac{h}{W_+}(G+\overline{G})\Big)\Big|_{\rho=0}\,.
\end{aligned}
\tag{10.39}
$$

Since we want to focus on the example in Section 10.3, we will use (10.38) and we will drop the constant term $\widehat{b}_2^0\,\widehat{b}_3^0$ as this can be absorbed into the definition of Λ.

In our example, all the M5 brane sources lie in the $G\to -i$ region and we can actually choose a gauge in which $\widehat{\Omega}_1$ is globally well-defined. As discussed above, we need to arrange for $\widehat{b}_2$ to vanish at the boundary where $G\to +i$. From (10.27), one therefore must choose:

$$
\widehat{b}_2^0 \;=\; -\,\Big(\Phi-\widetilde{h}\Big)\Big|_{\rho=0,\,G\to+i}\,.
\tag{10.40}
$$

The left-hand side of this equation is a constant, while the right-hand side is potentially a function of ξ, however we will see that, the right-hand side is a constant in the $G\to +i$

region ($\xi < \alpha$). Moreover, for $\xi > \alpha$, $W_- \to 4$, and hence the non-trivial term of the second line of (10.38) vanishes for all ξ to give:

$$\widehat{\Omega}_1\Big|_{\rho=0} \;=\; \Big(\Lambda \;-\; \widetilde{h}\,\Phi \;+\; \frac{1}{2}\left(\Phi^2 - \widetilde{h}^2\right) \;+\; \widehat{b}_2^0\left(\Phi + \widetilde{h}\right)\Big)\Big|_{\rho=0}. \tag{10.41}$$

The value of $\widehat{b}_2^0$-term reflects another gauge choice: observe that if one makes a shift $\Phi \to \Phi + \beta$, where β is a constant, then (10.34) implies that $\Lambda \to \Lambda - 4\,\beta\xi = \Lambda + 2\,\beta\widetilde{h}$ and therefore

$$\widehat{\Omega}_1\Big|_{\rho=0} \;\to\; \widehat{\Omega}_1\Big|_{\rho=0} \;+\; \beta\left(\Phi + \widetilde{h}\right) \;+\; \frac{1}{2}\,\beta^2 \;+\; \widehat{b}_2^0\,\beta\,. \tag{10.42}$$

Thus shifting Φ by a constant results in a shift of $\widehat{b}_2^0$, and an irrelevant constant shift in Λ.

10.4.4 Computing the flux potential, $\widehat{\Omega}_1$ for the example

For the solution described in Section 10.3, with Φ given by (10.10), we find:

$$\begin{aligned}\Lambda = -4\Bigg[\,&2\,\alpha\,\xi + (\xi-\alpha)\sqrt{(\xi-\alpha)^2+\rho^2} \;-\; \alpha^2 \\ &-\; \sum_{a=1}^{n+1}\zeta_a\left(\frac{\rho^2}{\sqrt{(\xi-\xi_a)^2+\rho^2}} - 2\sqrt{(\xi-\xi_a)^2+\rho^2}\right)\Bigg],\end{aligned} \tag{10.43}$$

where we have added a constant term, $4\alpha^2$, so as to make the $\alpha \to -\infty$ limit finite. Taking $\rho \to 0$ in this example, we find:

$$\begin{aligned} g_2\Big|_{\rho=0} \;&=\; -\,\mathrm{sign}(\xi-\alpha)\,, \\ \Phi\Big|_{\rho=0} \;&=\; 2\left(\alpha + |\xi-\alpha| + \sum_{a=1}^{n+1}\zeta_a\,\mathrm{sign}(\xi-\xi_a)\right), \\ \Lambda\Big|_{\rho=0} \;&=\; -\,4\left[2\,\alpha\,\xi + |\xi-\alpha|\,(\xi-\alpha) \;-\; \alpha^2 \;+\; 2\sum_{a=1}^{n+1}\zeta_a\,|\xi-\xi_a|\right]. \end{aligned} \tag{10.44}$$

From (10.9) one has, as $\rho \to 0$,

$$G \;\to\; -\,\mathrm{sign}(\xi-\alpha)\,i. \tag{10.45}$$

We have computed (10.41) with the gauge choice (10.40), which reduces to:

$$\widehat{b}_2^0 \;=\; -\left(\Phi - \widetilde{h}\right)\Big|_{\rho=0,\,\xi<\alpha} \;=\; -\,2\left(2\,\alpha \;-\; \sum_{a=1}^{n+1}\zeta_a\right), \tag{10.46}$$

and we find:

$$\begin{aligned}\widehat{\Omega}_1\Big|_{\rho=0} \;=\; &2\left(\sum_{a=1}^{n+1}\mathrm{sign}(\xi-\xi_a)\,\zeta_a\right)^2 \;+\; 8\sum_{a=1}^{n+1}\mathrm{sign}(\xi-\xi_a)\,\zeta_a\,\xi_a \;+\; 2\,\widehat{b}^0\sum_{a=1}^{n+1}\zeta_a\,\mathrm{sign}(\xi-\xi_a) \\ &-\; 4\left(1-\mathrm{sign}(\xi-\alpha)\right)(\xi-\alpha)\left(\frac{1}{2}\,\widehat{b}^0 \;+\; 2\,\alpha \;+\; \sum_{a=1}^{n+1}\zeta_a\,\mathrm{sign}(\xi-\xi_a)\right).\end{aligned} \tag{10.47}$$

Observe that the second line manifestly vanishes for $\alpha < \xi < \infty$. Moreover, for $-\infty < \xi < \alpha$, one has $\text{sign}(\xi - \xi_a) = -1$, for all a, because of (10.8), and so the second line vanishes as a result of the gauge choice (10.46). Therefore, with our gauge choices, the result may be written:

$$\widehat{\Omega}_1\Big|_{\rho=0} \;=\; 2\left(\sum_{a=1}^{n+1}\Big(1+\text{sign}(\xi-\xi_a)\Big)\,\zeta_a\right)^2 \;+\; 8\sum_{a=1}^{n+1}\Big(1+\text{sign}(\xi-\xi_a)\Big)\,\zeta_a\,(\xi_a-\alpha)\,, \quad (10.48)$$

where we have adjusted the constant term to recast the expression in a simple form that vanishes as $\xi \to -\infty$, and in which every term is positive (recall that $\zeta_a > 0$).

This expression for $\widehat{\Omega}_1\big|_{\rho=0}$ is globally defined for $-\infty < \xi < \infty$, $\xi \neq \xi_a$, and it is *locally constant*, as required by conservation of the Page charge.

Using this, one can compute the M2 charge[3] sourced at each singular point, ξ_a:

$$Q_{M2,a} \;\equiv\; \widehat{\Omega}_1\Big|_{\rho=0,\,\xi=\xi_a+\varepsilon} \;-\; \widehat{\Omega}_1\Big|_{\rho=0,\,\xi=\xi_a-\varepsilon} \;=\; 8\,\zeta_a\left(2\,(\xi_a-\alpha) \;+\; \zeta_a \;+\; 2\sum_{b=1}^{a-1}\zeta_b\right), \quad (10.49)$$

for some small $\varepsilon > 0$. Note that, with our gauge choices, all these charges are positive.

The total M2 charge is given by:

$$Q_{M2,total} \;=\; \widehat{\Omega}_1\Big|_{\rho=0,\,\xi\to+\infty} \;-\; \widehat{\Omega}_1\Big|_{\rho=0,\,\xi\to-\infty} \;=\; 8\left(\sum_{a=1}^{n+1}\zeta_a\right)^2 \;+\; 16\sum_{a=1}^{n+1}\zeta_a\,(\xi_a-\alpha)\,, \quad (10.50)$$

and one can easily check see that this is also given by the sum of the contributions (10.49), as required by conservation.

Returning to the metric at infinity, (10.21) and (10.22), we see that radius of curvature is determined by $Q_{M2,total}$.

10.4.5 The brane-intersection mohawk

As we discussed in Section 10.3, it is very useful to define the spike-profile coordinate, $\widehat{z}$:

$$\widehat{z} \;\equiv\; u^2\,z \;=\; \tfrac{1}{2}\Big(\Phi+2\,\xi\Big) \;=\; (\xi+\alpha) \;+\; \sqrt{(\xi-\alpha)^2 \;+\; \rho^2}+\sum_{a=1}^{n+1}\frac{\zeta_a(\xi-\xi_a)}{\sqrt{(\xi-\xi_a)^2+\rho^2}}\,. \quad (10.51)$$

Note that, for $\rho = 0$, $\widehat{z}$ is constant for $\xi < \alpha$, and is linear in ξ for $\xi > \alpha$ except for jumps at each M5 source by $2\zeta_a$. The heights of these jumps are essentially the M5 charge of the source. Moreover, the spike-profile at each source can be written as:

$$\lim_{\rho\to 0}\Big(\widehat{z}+\tfrac{1}{2}\,\widehat{b}_2^0\Big)\Big|_{\xi=\xi_a} \;=\; 2\,(\xi_a-\alpha) \;+\; \left(\zeta_a \;+\; 2\sum_{b=1}^{a-1}\zeta_b\right) \;=\; \frac{Q_{M2,a}}{8\,\zeta_a}\,. \quad (10.52)$$

[3]The sign of this charge depends on contour orientation and also does not take into account the negative sign in (4.9) of [40], and so there can be differences in signs that depend upon these conventions. We have chosen to make $Q_{M2,a}$ positive.

This means that the spike-profile at each source has the form:

$$\lim_{\rho\to 0}\left(\widehat{z}+\tfrac{1}{2}\,\widehat{b}_2^0\right)\Big|_{\xi=\xi_a} \;=\; \frac{Q_{M2,a}}{2\,Q_{M5,a}}\,. \tag{10.53}$$

where we have used the fact that the M5 charge is $4\,\zeta_a$ [40]. This equation has a very simple meaning: the spike is caused by M2's pulling on the M5's, and the steepness of the spike is determined by the number of M2's pulling on the M5's divided by the number of M5's being pulled. Note that we have written the offset in $\widehat{z}$ in terms of $\widehat{b}_2^0$ to reflect the fact that the offset is part of a gauge choice.

One can also write this formula as:

$$\lim_{\rho\to 0}\widehat{z}\,\Big|_{\xi=\xi_a} \;\sim\; \frac{\left(Q_{M2,a} \;-\; \tfrac{1}{2}\,\widehat{b}_2^0\,Q_{M5,a}\right)}{Q_{M5,a}}\,. \tag{10.54}$$

From the perspective of brane intersections, the coordinates (u, v, z), and hence $\widehat{z}$, are universal, and necessarily gauge invariant. This means that the right-hand side of (10.54) is gauge invariant. Indeed, observe that the combination in the numerator has the form of the gauge invariant brane charge associated with each spike.

As noted in Section 10.3, another very important feature of (10.49) and (10.53) is that these quantities increase monotonically with a, because $\zeta_a > 0$ and $\xi_{a+1} > \xi_a$. This leads to an intuitively satisfying picture of the back-reacted brane intersection. Before back-reaction, one has a stack of coincident M2 branes ending on a stack of coincident M5 branes. One can partition the M5's into groups, with the number in each such group determined by ζ_a. One is then allowed to choose how many M2's terminate on and dissolve into each of the these groups of M5's. This is determined by the number in the numerator of (10.54). The more M2's terminating on each group of M5's, the greater the bending of the M5 branes: the groups of M5's bend according to the value of each term in (10.54). This causes the groups of M5's to physically separate into distinct localized sources at $\xi = \xi_a$, as determined by (10.54). The sources are ordered according to steepness, with the steepest localized at $\xi = \xi_{n+1}$ and the least steep localized at $\xi = \xi_1$. The M2 charges thus determine the parameters, ξ_a. This is depicted schematically in Fig. 10.4.

10.5 Final comments

Our primary interest in brane fractionation is to capture the twisted sectors of the CFT's that arise on coincident stacks of two species of brane. The standard work-horse for CFT's on brane intersections is the D1-D5 system in which the CFT has a well-understood, weak-coupling limit. Here we have focussed on M2-M5 intersections because the structure of the solutions on the internal manifold is simpler.

In the standard picture, the twisted sectors, and the majority of microstates, emerge from some form of fractionation leading to a "Higgs Branch." In the D1-D5 system one gets $4N_1N_5$ scalars from the instanton moduli space of D1's inside D5's. For the M2-M5

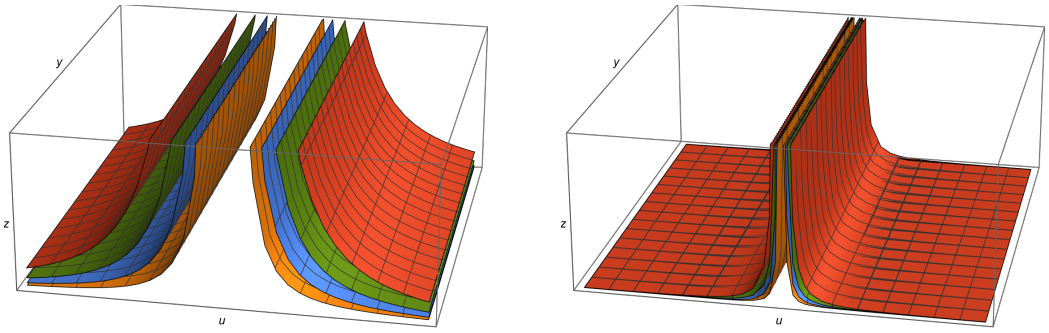

Figure 10.4: The "Mohawk:" the bending of the groups of M5 branes by intersecting M2 branes. The groups are separated and bent according to the value of $\frac{Q_{M2}}{Q_{M5}}$. At infinity, the M2 and M5 branes limit to coincident stacks, as depicted in the figure on the right. The two plots show the mohawk closer in and zoomed out, revealing the separation of the branes and their asymptotic convergence.

system, these scalars come from the $4N_2N_5$ positions of the fractionated branes depicted in the first part of Fig. 10.5.

To capture this fractionation with supergravity, one has to fractionate the branes only partially, so that each "brane segment" still has a sufficiently large number of branes to produce a significant gravitational back-reaction. We also have to choose the compactification scale to be sufficiently large so that the supergravity approximation is valid.

In this Chapter we have shown that brane fractionation can happen at two qualitatively different levels. The first is the one we just described. However, we have shown that there is a second fractionation, depicted in Fig. 10.2 and the second part of Fig. 10.5, which occurs at each individual intersection. This fractionation preserves an AdS isometry, creating what we have called the M2-M5 mohawk. Since this second fractionation occurs within a single AdS_3, its holographic interpretation should be captured by the *conformal* field theory dual to a single brane intersection.

Consider one such intersection with N_2 M2 branes and N_5 M5 branes, and the "intersection CFT" that it creates. This can result in many different mohawk configurations that are characterized by all the possible sets of $\frac{N_{2,a}}{N_{5,a}}$ consistent with the total brane charges. We conjecture that each of these different mohawk configurations corresponds to a ground state of this CFT. It would be interesting to count how many such configurations exist for a total N_2 and N_5. This is given by the total number of ways one can write families of fractions of the type $\frac{N_{2,a}}{N_{5,a}}$ with $\sum_a N_{2,a} = N_2$ and $\sum_a N_{5,a} = N_5$. We leave the evaluation of this number and its large-N growth to mathematics aficionados. More broadly, one would like to obtain a more complete understanding of the underlying CFT and its ground-state structure.

The results presented here suggest a number of very interesting follow-up projects. First, following on from [294], it would be very interesting to add momentum waves to these mohawk solutions so as to obtain $\frac{1}{8}$-BPS microstate geometries. More specifically, the goal of studying supergravity solutions that describe fractionated branes is to see

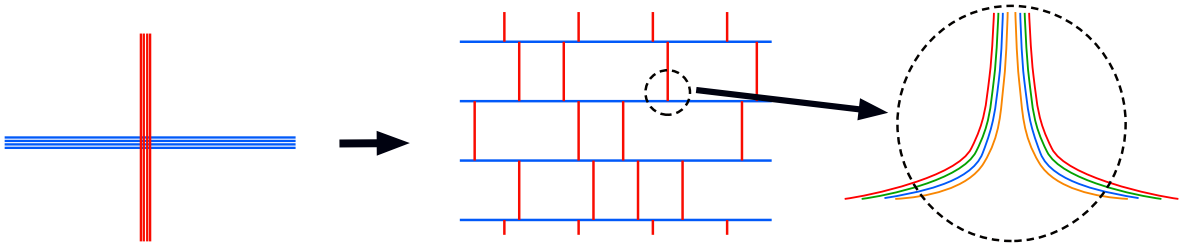

Figure 10.5: Brane fractionation. The first step shows "standard" brane fractionation in flat space. The second step shows "second-level" fractionation in a near-brane limit in which the back-reaction creates self-similar spikes whose scale invariance is transmogrified into an AdS_3 space. In the first step the moduli are the positions of each brane segment, while, in the second step, the position of each spike is controlled by the charge ratio in the spike.

how supergravity can access the twisted sectors of the CFT. If one can add independent momentum waves to each and every intersection point, then one will obtain a coherent supergravity model of the fractionated black-hole microstructure. As it was originally envisaged [23, 29, 36, 278, 279, 294], this momentum partitioning was to be done at the "first level" of partitioning as depicted in the first part of Fig. 10.5. The challenge in this approach is that the intersecting brane system is governed by a non-linear system of equations. (Nevertheless, the equations governing the momentum excitations and related fluxes were shown to be linear in [294].)

The new opportunity presented by this work is the emergence of the second level of fractionation in a near-brane limit, depicted in the second part of Fig. 10.5. These solutions are simpler, the background is governed by linear equations, and the brane intersections are characterized via the geometry of a Riemann surface. These near-brane geometries and their fractionation will thus provide a simpler setting for the investigation of momentum partitioning at fractionated intersections.

While we believe our example in Section 10.3 is representative, it is, from the perspective of [40], only a small subset of a diverse family of solutions. In particular, there is the parameter, γ, that determines the representation of the underlying superalgebra, and there is also the option to consider more general Riemann surfaces with more general flux functions, G. Indeed, there is a discussion of "Lego pieces" in [40] that suggests that one might be able to plumb together more complicated brane intersections using multiply punctured Riemann surfaces.

In this Chapter, we took the Riemann surface to be the entire Poincaré half plane. Moreover, as noted in [278, 294], the residual supersymmetry also allows one to include additional M5-brane sources, usually denoted as M5', that share (t, y) but fill the spatial directions transverse to the original M2 and M5 branes. These directions are described by v and the sphere S'^3 in Section 10.2. We have excluded such M5' sources[4]. (This is

[4]There is, of course, a dielectric distribution of M5' fluxes that, together with the M5 sources, give rise to the M2 charges through the Chern-Simons term.

why we chose all the sources in Section 10.3 to be in the region $G \to -i$.) Based on the analysis in [294], we also set the supersymmetry parameter, γ, to 1.

All of this greatly limits the "Lego pieces" described in [40], and excluding M5' brane sources places further limitations. It would be interesting to see if one can do something more general by freeing up the γ-parameter, and allowing a more general geometry for the common intersection of the branes. On the other hand, there has to be a price for taking the near-brane limit and getting an AdS factor in the geometry. As we have discussed in our example, the scaling of the AdS arises from the self-similarity of the bending of brane intersections. There must be a similar scale invariance in other brane intersections described by the results in [40], and, as we remarked in the Introduction, this will still limit the possibilities.

The near-brane limits of the intersecting M2-M5 system that can be incorporated as components of microstate geometries will therefore be a restricted sub-class of the families of solutions obtained in [40]. Nevertheless, we suspect that one can generalize beyond the example presented here, and even in this example we have seen that there is a rich structure to the "mohawk" that will prove invaluable to understanding momentum-carrying black-hole microstates.

Appendices

Appendix A

Chain of dualities

In this Appendix we present the explicit solutions for the intermediate steps in the two duality chains that we discussed in Section 5.3. In the first part we present the steps (5.9) that lead from the F1-P system with a non-trivial profile (5.7) to the NS5-P system with local D0-D4 charges (5.10). In the second subsection we then present the chain of dualities (5.13) which is used to write the latter solution in the D1-D5 frame of [183]. This allows us to consistently add a D1-brane charge which corresponds to adding an F1 charge in the F1-NS5 frame.

A.1 Generating the NS5-P-(D0-D4) solution

F1-P

The starting point is the F1-P configuration in Type IIB theory depicted in figure 5.2: Take the fundamental string to wrap the $S^1(y)$ circle and have a non-trivial profile $F(v)$ along one of the directions of the T^4, which we call z_9. Add momentum along the y direction and distribute (smear) the string charge along the four-torus while keeping all the charge localized at a point in $\mathbb{R}^4$. The supergravity solution corresponding to such a configuration is given by [181, 182]

$$ds^2 = -\frac{2}{H_5}\, dv \left[du - \frac{\dot{F}^2(v)}{2}\,(H_5-1)\, dv + \dot{F}(v)\,(H_5-1)\, dz^9\right] + dx^i\, dx^i + dz^a\, dz^a\,, \tag{A.1a}$$

$$B = -\left(1-\frac{1}{H_5}\right)\left[du\wedge dv + \dot{F}(v)\, dv\wedge dz^9\right], \qquad e^{2\phi} = \frac{1}{H_5}\,, \tag{A.1b}$$

with all other fields vanishing. In the above, u and v are null coordinates (5.5) and H_5 is a harmonic function associated with the F1-string and is given by (5.8).

S-duality to D1-P

The next step is to perform an S-duality (B.8) which yields

$$ds^2 = -\frac{2}{\sqrt{H_5}}\, dv \left(du + \frac{\dot{F}^2(v)}{2}\, (1-H_5)\, dv - \dot{F}(v)\, (1-H_5)\, \dot{F}(v)\, dz^9 \right) + \sqrt{H_5} \left(dx^i\, dx^i + dz^a\, dz^a \right) , \tag{A.2a}$$

$$B = 0\,, \qquad e^{2\phi} = H_5\,, \tag{A.2b}$$

$$C_0 = 0\,, \tag{A.2c}$$

$$C_2 = \left(1 - \frac{1}{H_5}\right) du \wedge dv + \dot{F}(v) \left(1 - \frac{1}{H_5}\right) dv \wedge dz^9\,, \tag{A.2d}$$

$$C_4 = 0\,, \tag{A.2e}$$

$$C_6 = \gamma \wedge \left(\dot{F}(v)\, dv \wedge dz^6 \wedge dz^7 \wedge dz^8 + \widehat{\mathrm{vol}}_4 \right) , \tag{A.2f}$$

where we have introduced a two-form γ such that

$$d\gamma \equiv *_4 dH\,, \tag{A.3}$$

and used the volume form of the T^4

$$\widehat{\mathrm{vol}}_4 \equiv dz^6 \wedge dz^7 \wedge dz^8 \wedge dz^9\,. \tag{A.4}$$

This solution describes a D1-brane wrapping the $S^1(y)$ circle and carrying momentum along that direction. The D1-brane is smeared along the T^4, with a non-trivial profile along the z_9, while being located at the origin or the base space. We use the democratic formalism (see Appendix B), which we have used to determine C_6 by imposing the duality condition between F_3 and F_7.

T-dual along z_9 to D2-P with local D0-F1 charges

Next we perform T-dualities (B.14) along all four directions of the torus, and we begin with the "special" direction z_9. When performing this duality, following Figure 5.3, the decomposition of the local charges into those along the y and the z_9 direction become important. The result is a configuration in Type IIA theory: a D2-brane (wrapping the y and z_9 directions) with a momentum along y, on which we find D0 and F1 charges (the latter wrapping the z_9 direction), which have varying densities along the y direction. The

corresponding supergravity solution is

$$ds^2 = -\frac{2}{\sqrt{H_5}}\,dv\,\left[du - \frac{\dot{F}^2(v)}{2}\left(1-\frac{1}{H_5}\right)\,dv\right] + \sqrt{H_5}\left(dx^i\,dx^i + \sum_{a=6}^{8} dz^a\,dz^a\right) + \frac{1}{\sqrt{H_5}}\left(dz^9\right)^2\,, \tag{A.5a}$$

$$B_2 = \dot{F}(v)\left(1-\frac{1}{H_5}\right)dv\wedge dz^9\,, \qquad e^{2\phi} = \sqrt{H_5}\,. \tag{A.5b}$$

$$C_1 = \dot{F}(v)\left(1-\frac{1}{H_5}\right)dv\,, \tag{A.5c}$$

$$C_3 = \left(1-\frac{1}{H_5}\right)du\wedge dv\wedge dz^9\,, \tag{A.5d}$$

$$C_5 = \gamma\wedge dz^6\wedge dz^7\wedge dz^8\,, \tag{A.5e}$$

$$C_7 = \frac{\dot{F}(v)}{H_5}\,\gamma\wedge dv\wedge\widehat{\mathrm{vol}}_4\,. \tag{A.5f}$$

In the above solution, the y-, or more appropriately v-, dependent distribution of D0 and F1 charges is seen in the dependence on $\dot{F}(v)$ that appears in B_2, which is sourced by fundamental strings, and C_1 (C_7) which is electrically (magnetically) sourced by D0-branes. On the other hand, C_3 and C_5, which are sourced by D2-branes, are independent of $\dot{F}(v)$.

T-dualities along z_8, z_7 and z_6 to the D5-P with local D3-F1 charges

The three T-dualities along z_8, z_7, and z_6 (in that order) are very similar and thus we perform them together. The final result is a configuration in Type IIB theory where the D2-brane now becomes a D5-brane wrapping the $S^1(y)$ circle and all four directions of the T^4, while the $\dot{F}(v)$ dependent fields are now sourced by local D3 and F1 charges:

$$ds^2 = -\frac{2}{\sqrt{H_5}}\,dv\,\left[du - \frac{\dot{F}^2(v)}{2}\left(1-\frac{1}{H_5}\right)\,dv\right] + \sqrt{H_5}dx^i\,dx^i + \frac{1}{\sqrt{H_5}}\,dz^a\,dz^a\,, \tag{A.6a}$$

$$B_2 = \dot{F}(v)\left(1-\frac{1}{H_5}\right)dv\wedge dz^9\,, \qquad e^{2\phi} = \frac{1}{H_5}\,, \tag{A.6b}$$

$$C_0 = 0\,, \tag{A.6c}$$

$$C_2 = \gamma\,, \tag{A.6d}$$

$$C_4 = -\frac{\dot{F}(v)}{H_5}\,\gamma\wedge dv\wedge dz^9 - \dot{F}(v)\left(1-\frac{1}{H_5}\right)dv\wedge dz^6\wedge dz^7\wedge dz^8\,, \tag{A.6e}$$

$$C_6 = \left(1-\frac{1}{H_5}\right)du\wedge dv\wedge\widehat{\mathrm{vol}}_4\,, \tag{A.6f}$$

$$C_8 = 0\,. \tag{A.6g}$$

S-duality to NS5-P with local D3-D1 charges

Since our aim is to obtain a solution corresponding to a configuration with NS5-P charges, we continue with another S-duality. Essentially, this only exchanges the D5-brane for an

NS5-brane and the D1 local charges with F1 charge distribution:

$$ds^2 = -2dv\left[du - \frac{\dot{F}^2(v)}{2}\left(1-\frac{1}{H_5}\right)dv\right] + H_5\, dx^i\, dx^i + dz^a\, dz^a\,, \tag{A.7a}$$

$$B_2 = \gamma\,, \qquad e^{2\phi} = H_5\,, \tag{A.7b}$$

$$C_0 = 0\,, \tag{A.7c}$$

$$C_2 = -\dot{F}(v)\left(1-\frac{1}{H_5}\right)dv\wedge dz^9\,, \tag{A.7d}$$

$$C_4 = -\dot{F}(v)\,\gamma\wedge dv\wedge dz^9 - \dot{F}(v)\left(1-\frac{1}{H_5}\right)dv\wedge dz^6\wedge dz^7\wedge dz^8\,, \tag{A.7e}$$

$$C_6 = -\dot{F}(v)\,\gamma\wedge dv\wedge dz^6\wedge dz^7\wedge dz^8\,, \tag{A.7f}$$

$$C_8 = 0\,. \tag{A.7g}$$

T-duality to NS5-P with local D0-D4 charges

Finally, we perform another T-duality along z_9, which lands us in the desired configuration: an NS5-brane with momentum along the y-direction with D0- and D4-brane charges which vary along the $S^1(y)$ circle

$$ds^2 = -2dv\left[du - \frac{\dot{F}(v)^2}{2}\left(1-\frac{1}{H_5}\right)dv\right] + H\, dx^i\, dx^i + dz^a\, dz^a\,, \tag{A.8a}$$

$$B_2 = \gamma\,, \qquad e^{2\phi} = H_5\,, \tag{A.8b}$$

$$C_1 = -\dot{F}(v)\left(1-\frac{1}{H_5}\right)dv\,, \tag{A.8c}$$

$$C_3 = -\dot{F}(v)\,\gamma\wedge dv\,, \tag{A.8d}$$

$$C_5 = -\dot{F}(v)\left(1-\frac{1}{H_5}\right)dv\wedge\widehat{\mathrm{vol}}_4 = C_1\wedge\widehat{\mathrm{vol}}_4\,, \tag{A.8e}$$

$$C_7 = -\dot{F}(v)\,\gamma\wedge dv\wedge\widehat{\mathrm{vol}}_4 = C_3\wedge\widehat{\mathrm{vol}}_4\,, \tag{A.8f}$$

which is the solution (5.10) presented in the main text. Unlike any of the previous solutions presented in this Appendix, (A.8) depends on the T^4 only through its volume form (A.4).

A.2 Adding F1 charge by using a Gibbons-Hawking base

The solution (A.8) (or equivalently (5.10) of the main text) is asymptotically a two-charge solution. To make contact with the microstate geometries programme, we would like to construct a solution which has three charges. We choose to add to the configuration an additional fundamental string that wraps the $S^1(y)$ circle and is smeared along the T^4.

We do so in a roundabout way: We write the four-dimensional flat metric in Gibbons-Hawking form and T-dualize along the Gibbons-Hawking fiber. If we then perform an

S-duality, the resulting configuration should be described in terms of the complete ansatz for the D1-D5 system constructed in [183]. Adding a source corresponding to a D1-brane in this duality frame is equivalent to adding a fundamental string in the NS5-P frame, only that in the former frame we know all fields which get excited as a consequence of adding a new object into the configuration.

Begin by writing the flat base space metric in (A.8) as[1]

$$dx^i\, dx^i = \frac{1}{V}(d\psi + A)^2 + V\, ds_3^2\,, \tag{A.10}$$

where ds_3^2 denotes the flat metric on $\mathbb{R}^3$. Recall that we need to impose the following constraints on the function V and one-form A

$$*_3 dA = dV\,, \quad \Longrightarrow \quad *d*dV = 0\,, \qquad d*dA = 0\,, \tag{A.11}$$

which also means that the warp factor, V, is a harmonic function in $\mathbb{R}^3$. The metric (A.10) is invariant under a simultaneous rescaling of the coordinates, the function V, and one-form A, which we can fix by setting the periodicity of ψ to be 4π.

Now assume that ψ denotes an isometry direction of the solution. Then one can decompose

$$*_4 dH_5 = (d\psi + A) \wedge *_3 dH_5\,, \tag{A.12}$$

and[2]

$$\gamma \equiv -\,(d\psi + A) \wedge \gamma^{(1)} + \gamma^{(2)}\,, \tag{A.13}$$

where the one-form $\gamma^{(1)}$ and the two-form $\gamma^{(2)}$ are determined from the definition (5.11) by

$$d\gamma^{(1)} = *_3 dH_5\,, \qquad d\gamma^{(2)} = *_3 dV \wedge \gamma^{(1)}\,. \tag{A.14}$$

[1] In what follows we do not specify the coordinates used in the Gibbons-Hawking ansatz. However, one can introduce spherical coordinates for $\mathbb{R}^4$ whose metric can be written as

$$ds_4^2 = dr^2 + r^2\left(d\theta^2 + \sin^2\theta\, d\varphi_1^2 + \cos^2\theta\, d\varphi_2^2\right).$$

To rewrite this metric in the Gibbons-Hawking form, we introduce new coordinates as $r \equiv 2\sqrt{\rho}$, $\widetilde{\theta} \equiv 2\theta$, $\psi \equiv \varphi_1 + \varphi_2$, and $\phi \equiv \varphi_2 - \varphi_1$, where the ranges of various coordinates are taken to be $\varphi_{1,2} \in [0, 2\pi)$, $\psi \in [0, 4\pi)$, and $\phi \in [0, 2\pi)$, while r and ρ are both taken to be non-negative. The metric becomes

$$ds_4^2 = \rho\,(d\psi + \cos\widetilde{\theta}\, d\phi)^2 + \frac{1}{\rho}\left(d\rho^2 + \rho^2\left(d\widetilde{\theta}^2 + \sin^2\widetilde{\theta}\, d\phi^2\right)\right), \tag{A.9}$$

and one can read off that $V = \rho^{-1}$ and $A = \cos\widetilde{\theta}\, d\phi$. Furthermore $H_5 = 1 + \frac{Q_5}{4\rho}$, and is thus harmonic even in $\mathbb{R}^3$.

[2] For example, in spherical coordinates (see footnote 1) $\gamma^{(1)} = \frac{1}{4}\, Q_5\, \cos\widetilde{\theta}\, d\phi$ and $\gamma^{(2)} = 0$.

T-duality along the Gibbons-Hawking fiber

We now use the T-duality rules to dualize along the Gibbons-Hawking fiber ψ. However, after performing the transformation, we need to change the sign of ψ

$$\psi \to -\psi\,, \tag{A.15}$$

to obtain

$$ds^2 = -2\,dv\left[du - \frac{\dot{F}^2(v)}{2}\left(1-\frac{1}{H_5}\right)dv\right] + V\left[\frac{1}{H_5}\left(d\psi+\gamma^{(1)}\right)^2 + H_5\,ds_3^2\right] + ds_4^2\,, \tag{A.16a}$$

$$B_2 = A\wedge d\psi + \gamma^{(2)}\,, \qquad e^{2\phi} = V\,, \tag{A.16b}$$

$$C_0 = 0\,, \tag{A.16c}$$

$$C_2 = \dot{F}(v)\left(1-\frac{1}{H_5}\right)dv\wedge(d\psi+\gamma^{(1)}) - \dot{F}\,dv\wedge\gamma^{(1)}\,, \tag{A.16d}$$

$$C_4 = \dot{F}(v)\,dv\wedge\left(d\psi+\gamma^{(1)}\right)\wedge\gamma^{(2)}\,, \tag{A.16e}$$

where the sign flip (A.15) ensures that the first equation of (A.14) now serves as the constraint between the one-form and scalar function in the new Gibbons-Hawking base-space metric.

S-duality to the D1-D5 frame

S-dualizing the above solution puts us in the D1-D5 frame, and the resulting configuration fits within the ansatz of [183]. In this transformation, and only in this transformation alone, we choose $b=-c=-1$ when performing the S-duality (B.8). This allows us to compare the resulting solution with the complete ansatz of [183] without changing the signs of the fields and furthermore, when transforming back to the NS5-P system we can take $b=-c=1$ which is the inverse transformation. We find

$$\begin{aligned} ds^2 = &-\frac{2}{\sqrt{V}}\,dv\left[du - \frac{\dot{F}^2(v)}{2}\left(1-\frac{1}{H_5}\right)dv\right] + \sqrt{V}\left[\frac{1}{H_5}\left(d\psi+\gamma^{(1)}\right)^2 + H_5\,ds_3^2\right] \\ &+\frac{1}{\sqrt{V}}\,d\hat{s}_4^2\,, \end{aligned} \tag{A.17a}$$

$$B_2 = \dot{F}(v)\left[\left(1-\frac{1}{H_5}\right)\left(d\psi+\gamma^{(1)}\right)-\gamma^{(1)}\right]\wedge dv\,, \qquad e^{2\phi} = \frac{1}{V}\,, \tag{A.17b}$$

$$C_0 = 0\,, \tag{A.17c}$$

$$C_2 = A\wedge\left(d\psi+\gamma^{(1)}\right) + \gamma^{(2)} - A\wedge\gamma^{(1)}\,, \tag{A.17d}$$

$$C_4 = -\dot{F}(v)\left[\frac{1}{H_5}\left(d\psi+\gamma^{(1)}\right)\wedge\left(\gamma^{(2)}-A\wedge\gamma^{(1)}\right)+\gamma^{(1)}\wedge\gamma^{(2)}\right]\wedge dv\,. \tag{A.17e}$$

At this point one can recombine the Gibbons-Hawking decomposition of the base space (including the forms), compare the solution (A.17) with the complete ansatz of [183] and read off the ansatz quantities,[3] however, this is not central to our analysis.

[3] Once this is done, one can check that the read-off quantities solve the BPS equations [183, 204].

Adding a D1 charge

What is important for us is that the harmonic function corresponding to D1-brane sources is precisely known in the complete ansatz [183].[4] Thus denoting this harmonic function with H_1 (see (5.15)), we find that the new solution is given by

$$ds^2 = -\frac{2}{\sqrt{V\,H_1}}\,dv\,\left[du - \frac{\dot{F}^2(v)}{2}\left(1-\frac{1}{H_5}\right)dv\right] + \sqrt{V\,H_1}\,\left[\frac{1}{H_5}\left(d\psi+\gamma^{(1)}\right)^2 + H_5\,ds_3^2\right] + \sqrt{\frac{H_1}{V}}\,d\hat{s}_4^2\,, \tag{A.18a}$$

$$B_2 = \dot{F}(v)\left[\left(1-\frac{1}{H_5}\right)\left(d\psi+\gamma^{(1)}\right)-\gamma^{(1)}\right]\wedge dv\,, \qquad e^{2\phi} = \frac{H_1}{V}\,, \tag{A.18b}$$

$$C_0 = 0\,, \tag{A.18c}$$

$$C_2 = -\frac{1}{H_1}du\wedge dv + A\wedge\left(d\psi+\gamma^{(1)}\right)+\gamma^{(2)} - A\wedge\gamma^{(1)}\,, \tag{A.18d}$$

$$C_4 = -\dot{F}(v)\,\left[\frac{1}{H_5}\,\left(d\psi+\gamma^{(1)}\right)\wedge\left(\gamma^{(2)}-A\wedge\gamma^{(1)}\right)+\gamma^{(1)}\wedge\gamma^{(2)}\right]\wedge dv\,. \tag{A.18e}$$

It is straightforward to check that this supersymmetric torus-independent D1-D5-frame solution (A.18) solves the equations governing all such solutions [183].

S-dual to F1-NS5 frame in Type IIB

To return to the NS5-P system, we need to first perform an S-duality and then a T-duality along ψ. Using $b=-c=1$, which ensures that this is the inverse transformation of the one used to arrive at (A.17), we obtain

$$ds^2 = -\frac{2}{H_1}\,dv\left[du - \frac{\dot{F}^2(v)}{2}\left(1-\frac{1}{H_5}\right)dv\right] + V\left[\frac{1}{H_5}\left(d\psi+\gamma^{(1)}\right)^2 + H_5\,ds_3^2\right] + ds_4^2\,, \tag{A.19a}$$

$$B_2 = -\frac{1}{H_1}du\wedge dv + A\wedge d\psi+\gamma^{(2)}\,, \qquad e^{2\phi} = \frac{V}{H_1}\,, \tag{A.19b}$$

$$C_0 = 0\,, \tag{A.19c}$$

$$C_2 = -\dot{F}(v)\left[\left(1-\frac{1}{H_5}\right)\left(d\psi+\gamma^{(1)}\right)-\gamma^{(1)}\right]\wedge dv\,, \tag{A.19d}$$

$$C_4 = -\dot{F}(v)\,\left(d\psi+\gamma^{(1)}\right)\wedge\gamma^{(2)}\wedge dv\,. \tag{A.19e}$$

T-dual to the F1-NS5 system in Type IIA

To return to the original system we perform a final T-duality along the ψ direction, which has to be again followed by a sign flip (A.15). Furthermore, in order to compare the final

[4] In the notation commonly used in the microstate geometries literature dealing with the D1-D5 system [24, 26, 204, 240] (see also Appendix E.7 of [183]), this is the scalar function Z_1. Note that in addition one would need to turn on a contribution to the gauge field C_6, which would ensure, in the democratic formalism, appropriate self-duality properties of the gauge field strengths. However, we will determine higher-order gauge fields only after the last duality transformation.

solution to the two-charge case (A.8), we also exchange $\dot{F}(v) \to -\dot{F}(v)$. Then one finds

$$ds^2 = -\frac{2}{H_1} dv \left[du - \frac{\dot{F}(v)^2}{2} \left(1 - \frac{1}{H_5}\right) dv \right] + H_5 \, dx^i \, dx^i + dz^a \, dz^a \,, \tag{A.20a}$$

$$B_2 = -\frac{1}{H_1} \, du \wedge dv + \gamma \,, \qquad e^{2\phi} = \frac{H_5}{H_1} \,, \tag{A.20b}$$

$$C_1 = -\dot{F}(v) \left(1 - \frac{1}{H_5}\right) dv \,, \tag{A.20c}$$

$$C_3 = -\dot{F}(v) \, \gamma \wedge dv \,, \tag{A.20d}$$

where we have recombined the decompositions along the Gibbons-Hawking fiber. After the remaining RR gauge fields are computed, this solution matches the one presented in the main text in Equation (5.14).

Appendix B

Conventions for Chapter 5

Democratic formalism

When dealing with brane sources it is useful to introduce the democratic formalism [121] which effectively doubles the number of gauge fields in the theory, but introduces self-duality constraints on the field strengths so that the number of degrees of freedom remains unchanged. This democracy is imposed only on the Ramond-Ramond gauge fields C_p, while we keep only one NS-NS gauge field B, with a three-form field strength

$$H_3 = dB\,. \tag{B.1}$$

The RR field strengths are defined as

$$F_p \equiv dC_{p-1} - H_3 \wedge C_{p-3}\,, \tag{B.2}$$

which satisfy modified Bianchi identities $dF_p = H_3 \wedge F_{p-2}$.

In each of the Type II theories, we introduce additional RR gauge field potentials, so that for Type IIA we consider $\{C_1, C_3, C_5, C_7\}$ and $\{C_0, C_2, C_4, C_6, C_8\}$ for Type IIB. However, the number of degrees of freedom is kept constant by imposing

$$(IIA): \quad F_2 = *F_8\,, \quad F_4 = -*F_6\,, \quad F_6 = *F_4\,, \quad F_8 = -*F_2\,, \tag{B.3a}$$

$$(IIB): \quad F_1 = *F_9, \quad F_3 = -*F_7, \quad F_5 = *F_5, \quad F_7 = -*F_3, \quad F_9 = *F_1\,, \tag{B.3b}$$

which imply that the field strengths F_p and F_{10-p} essentially convey the same information. Note that we follow the conventions of [183], where the Hodge dual of a k-form in a D-dimensional spacetime is given by

$$*X_k \equiv \frac{1}{k!(D-k)!}\,\epsilon_{m_1\ldots m_{D-k},n_{D-k+1}\ldots n_D}\,X^{n_{D-k+1}\ldots n_D}\,e^{m_1}\wedge\ldots e^{m_{D-k}}\,. \tag{B.4}$$

Furthermore, we choose the orientation

$$\epsilon^{+-12346789} = \epsilon^{1234} = 1\,. \tag{B.5}$$

S-duality

Define a complex field as a combination of the axion field and the dilaton and combine the two-form gauge potentials into a vector

$$\lambda \equiv C_0 + i\, e^{-\phi}\,, \qquad T = \begin{pmatrix} B_2 \\ C_2 \end{pmatrix}\,. \tag{B.6}$$

Type IIB theories are invariant under a transformation generated by $U \in SL(2,\mathbb{R})$

$$U = \begin{pmatrix} a & b \\ c & d \end{pmatrix}\,, \quad \text{with} \quad a\,d - b\,c = 1\,, \tag{B.7}$$

such that

$$\lambda \to \widetilde{\lambda} = \frac{a\lambda + b}{c\lambda + d}\,, \qquad T \to \widetilde{T} = U\,T\,, \tag{B.8}$$

while the five-form gauge field strength, F_5, and the ten-dimensional metric in the Einstein frame are invariant.

In the main text we consider only a $\mathbb{Z}_2$ subgroup of $SL(2,\mathbb{R})$ transformations where

$$a = d = 0\,, \qquad b = -c = \pm 1. \tag{B.9}$$

Unless explicitly stated otherwise, we choose $b = -c = 1$ whenever we perform an S-duality transformation. In addition, in all of the solutions considered, the axion field C_0 is vanishing. Then the effect of such a transformation, with either choice of sign for b and c, results in the inversion of the dilaton field

$$\widetilde{\phi} = -\phi\,, \tag{B.10}$$

and the following change of the metric in the string frame

$$\widetilde{G}_{\mu\nu} = e^{-\phi}\,G_{\mu\nu}\,. \tag{B.11}$$

Furthermore, the two-form gauge fields are interchanged up to a minus sign

$$\widetilde{B}_2 = \pm C_2\,, \qquad\qquad \widetilde{C}_2 = \mp B_2\,, \tag{B.12}$$

where the upper (lower) sign corresponds to $b = +1$ ($b = -1$). For either sign, the invariance of F_5 implies that the four-form gauge field transforms as

$$\widetilde{C}_4 = C_4 - B_2 \wedge C_2\,. \tag{B.13}$$

Higher-form gauge fields can be calculated by using the duality rules of the democratic formalism (B.3) and (B.2). The effect of this particular transformation is thus to effectively exchange the two-form gauge potentials.

T-duality

For performing T-duality transformations we use the conventions of [295], which are convenient when one works in the democratic formalism. Assume that we are performing a T-duality along an isometry direction coordinatized by y. Rewrite the initial string frame metric and gauge fields as

$$ds^2 = G_{yy}\,(dy + A_\mu\,dx^\mu)^2 + \widehat{g}_{\mu\nu}\,dx^\mu\,dx^\nu \tag{B.14a}$$

$$B_2 = B_{\mu y} dx^\mu \wedge (dy + A_\mu\,dx^\mu) + \widehat{B}_2\,, \tag{B.14b}$$

$$C_p = C^y_{p-1} \wedge (dy + A_\mu\,dx^\mu) + \widehat{C}_p\,, \tag{B.14c}$$

where the forms $\widehat{B}_2$, $\widehat{C}_p$ and $\widehat{C}^y_{p-1}$ do not have any legs along y. After applying the rules of a T-duality transformation [296, 297], the new fields (denoted with the tilde) are

$$d\widetilde{s}^2 = G^{-1}_{yy}\,(dy - B_{\mu y}\,dx^\mu)^2 + \widehat{g}_{\mu\nu}\,dx^\mu\,dx^\nu \tag{B.15a}$$

$$\widetilde{B}_2 = -A_\mu dx^\mu \wedge dy + \widehat{B}_2\,, \tag{B.15b}$$

$$\widetilde{C}_p = \widehat{C}_{p-1} \wedge (dy - B_{\mu y}\,dx^\mu) + C^y_p\,, \tag{B.15c}$$

$$e^{2\widetilde{\phi}} = G^{-1}_{yy}\,e^{2\phi}\,. \tag{B.15d}$$

Appendix C

Projectors and involutions for branes

In this Appendix we list the involutions associated to common brane type. In Type II string theory, they are:

$$\begin{aligned}
P_{\mathrm{P}} &= \Gamma^{01}\,, & P_{\mathrm{F1}} &= \Gamma^{01}\sigma_3\,, \\
P^{\mathrm{IIA}}_{\mathrm{NS5}} &= \Gamma^{012345}\,, & P^{\mathrm{IIB}}_{\mathrm{NS5}} &= \Gamma^{012345}\sigma_3\,, \\
P^{\mathrm{IIA}}_{\mathrm{KKM}(12345;6)} &= \Gamma^{012345}\sigma_3\,, & P^{\mathrm{IIB}}_{\mathrm{KKM}(12345;6)} &= \Gamma^{012345}\,, \\
P_{\mathrm{D0}} = \Gamma^{0} i\sigma_2\,, \quad P_{\mathrm{D2}} &= \Gamma^{012}\sigma_1\,, & P_{\mathrm{D4}} &= \Gamma^{01234} i\sigma_2\,, \quad P_{\mathrm{D6}} = \Gamma^{0123456}\sigma_1\,, \\
P_{\mathrm{D1}} = \Gamma^{01}\sigma_1\,, \quad P_{\mathrm{D3}} &= \Gamma^{0123} i\sigma_2\,, & P_{\mathrm{D5}} &= \Gamma^{012345}\sigma_1\,.
\end{aligned} \tag{C.1}$$

The projectors in M-theory are given by:

$$P_{\mathrm{P}} = \Gamma^{01}\,, \qquad P_{\mathrm{M2}} = \Gamma^{012}\,, \qquad P_{\mathrm{M5}} = \Gamma^{012345}\,, \qquad P^{\mathrm{IIB}}_{\mathrm{KKm}} = \Gamma^{0123456}\,. \tag{C.2}$$

Appendix D

Parameterizing the themelia

In the interest of efficiency we parameterize the most general themelion considered in Chapter 7, which should be the building block of hyperstrata, via:

$$\begin{aligned}
&\alpha_1 = \tfrac{1}{4}\,(1 + x_1 + y_1 + z_1)\,,\ \alpha_2 = \tfrac{1}{4}\,(1 - x_1 + y_1 - z_1)\,,\\
&\alpha_3 = \tfrac{1}{4}\,(1 - x_1 - y_1 + z_1)\,,\ \alpha_4 = \tfrac{1}{4}\,(1 + x_1 - y_1 - z_1)\,,\\
&\alpha_5 = \tfrac{1}{4}\,(x_2 + y_2 + z_2)\,,\ \alpha_6 = \tfrac{1}{4}\,(-x_2 + y_2 - z_2)\,,\\
&\alpha_7 = \tfrac{1}{4}\,(-x_2 - y_2 + z_2)\,,\ \alpha_8 = \tfrac{1}{4}\,(x_2 - y_2 - z_2)\,,\\
&\alpha_9 = \alpha_{10} = \tfrac{1}{2}\,u_1\,,\ \alpha_{11} = \alpha_{12} = \tfrac{1}{2}\,u_2\,,\ \alpha_{13} = -\alpha_{14} = \tfrac{1}{2}\,v_1\,,\\
&\alpha_{15} = -\alpha_{16} = \tfrac{1}{2}\,v_2, \alpha_{17} = -\alpha_{18} = \tfrac{1}{2}\,w_1, \alpha_{19} = -\alpha_{20} = \tfrac{1}{2}\,w_2.
\end{aligned} \tag{D.1}$$

and the solution to the projection conditions is:

$$\begin{aligned}
&u_1 + iu_2 = s_1 s_2\, e^{i\varphi_1}\,,\\
&v_1 + iv_2 = s_2 c_2\, e^{i(\varphi_1 - \varphi_2 - \varphi_3)}(e^{-2i\varphi_4} - c_1)\,,\\
&w_1 + iw_2 = s_1 c_2\, e^{i\varphi_2}\,, \quad x_1 + ix_2 = c_1 e^{i\varphi_3}\,,\\
&y_1 + iy_2 = e^{i(2\varphi_2 + \varphi_3)}\,(c_1 c_2^2 + s_2^2\, e^{-2i\varphi_4})\,,\\
&z_1 + iz_2 = e^{i(2\varphi_1 - \varphi_3)}\,(c_2^2\, e^{2i\varphi_4} + c_1 s_2^2)\,,
\end{aligned} \tag{D.2}$$

where $c_j \equiv \cos\theta_j$ and $s_j \equiv \sin\theta_j$. The quadratic terms appear because some $U(3)$ rotation angles must be fixed in terms of others to preserve the relationships between the components, (7.13) of the $\boldsymbol{p}_j$.

Appendix E

Spherically symmetric $\frac{1}{4}$-BPS M5-M2 intersections

Here we show that our spherically symmetric configurations are, in fact, the most $\frac{1}{4}$-BPS general solutions with such symmetries and with supersymmetries defined by (8.1). That is, we will impose Poincaré symmetry on the common (t, y) directions of the branes and require an $SO(4) \times SO(4)$ symmetry that sweeps out two three spheres. We will write down the most general configurations that satisfies these symmetry requirements and, following the methodology developed in [263, 264, 267–269], we will show that the solutions defined in Section 8.2.3 are the only possibilities.

E.1 The Ansatz

The most general metric satisfying the symmetry requirements must have the form:

$$ds_{11} = e^{2\alpha_0}\left(-dt^2 + dy^2\right) + e^{2\alpha_1}\, d\Omega_3^2 + e^{2\alpha_2}\, d\Omega_3'^2 + g_{ij}\, dz^i dz^j\,, \tag{E.1}$$

where α_0, α_1 and α_2 are arbitrary functions of three remaining coordinates, z^i, and g_{ij} is a general metric in these three dimensions. There is, of course, a remaining diffeomorphism invariance, $z^i \to \widetilde{z}^i(z^j)$, and this can, in principle, be fixed by taking the metric, g_{ij}, to be diagonal [298–300]. It is therefore tempting to write $(z^1, z_2, z_3) = (z, u, v)$ and take:

$$ds_3 = g_{ij}\, dz^i dz^j = e^{2\alpha_3}\, dz^2 + e^{2\alpha_4}\, du^2 + e^{2\alpha_5}\, dv^2\,. \tag{E.2}$$

One is then tempted to use a set of frames:

$$\begin{aligned} e^0 &= e^{\alpha_0}\, dt\,, \qquad e^1 = e^{\alpha_0}\, dy\,, \qquad e^2 = e^{\alpha_1}\, dz \qquad e^3 = e^{\alpha_2}\, du\,, \qquad e^4 = e^{\alpha_3}\, dv\,, \\ e^{i+4} &= e^{\alpha_4}\, \sigma_i\,, \qquad e^{i+7} = e^{\alpha_5}\, \widetilde{\sigma}_i\,, \qquad i = 1, 2, 3\,, \end{aligned} \tag{E.3}$$

however, this misses a very important physical point. The choice of frames also fixes the meaning of the supersymmetry projectors of the form (8.1) and (8.4), which in the current frame labelling become:

$$\Gamma^{012}\,\varepsilon = -\varepsilon\,, \qquad \Gamma^{013567}\,\varepsilon = \varepsilon\,, \qquad \Gamma^{01489\,10}\,\varepsilon = -\varepsilon\,. \tag{E.4}$$

The M5, M5' and M2 branes are thereby required to follow the coordinate axes, and this is not the most general possibility because brane intersections typically result in deformations of the underlying branes. The most general possibility is to use frames, and hence Γ-matrices that are an arbitrary $SO(3)$ rotation (depending on (u, v, z)) of the frames (e^2, e^3, e^4) in (E.3). This is a little too challenging to analyze here, and so we make a more physical choice.

If one thinks in terms the IIA theory, we have a system of NS5, NS5' branes and F1 strings. The former are much heavier than the latter, and so they can be fixed along the coordinate axes while the M2 brane direction can be fibered over the M5 and M5' directions. This leads to the Ansatz we will use here:

$$\begin{aligned} e^0 &= e^{A_0}\,dt\,, \qquad e^1 = e^{A_0}\,dy\,, \qquad e^2 = e^{A_1}\Big(dz + B_1\,du + B_2\,dv\Big)\,,\\ e^3 &= e^{A_2}\,du\,, \qquad e^4 = e^{A_3}\,dv\,, \qquad e^{i+4} = u\,e^{A_4}\,\sigma_i\,, \qquad e^{i+7} = v\,e^{A_5}\,\widetilde{\sigma}_i\,, \qquad i = 1,2,3\,. \end{aligned} \tag{E.5}$$

where $A_0, \ldots, A_5$ and B_1, B_2 are arbitrary functions of (z, u, v). We have, for convenience, introduced factors of u and v into the definitions of the e^{i+4} and e^{i+7} respectively. Finally, one can also make a re-parametrization $z \to \widetilde{z}(z, u, v)$ so as to gauge away B_2 (or B_1). Therefore, without loss of generality, one can take:

$$B_2 \equiv 0\,. \tag{E.6}$$

We will therefore adopt the frames:

$$\begin{aligned} e^0 &= e^{A_0}\,dt\,, \qquad e^1 = e^{A_0}\,dy\,, \qquad e^2 = e^{A_1}\Big(dz + B_1\,du\Big)\,,\\ e^3 &= e^{A_2}\,du\,, \qquad e^4 = e^{A_3}\,dv\,, \qquad e^{i+4} = u\,e^{A_4}\,\sigma_i\,, \qquad e^{i+7} = v\,e^{A_5}\,\widetilde{\sigma}_i\,, \qquad i = 1,2,3\,, \end{aligned} \tag{E.7}$$

and metric:

$$\begin{aligned} ds_{11}^2 = e^{2A_0}\Big(-dt^2 + dy^2\Big) + e^{2A_2}\,du^2 + e^{2A_3}\,dv^2 + u^2\,e^{2A_4}\,d\Omega_3^2 + v^2\,e^{2A_5}\,d\Omega_3'^2 \\ + e^{2A_1}\Big(dz + B_1\,du\Big)^2\,. \end{aligned} \tag{E.8}$$

Within this Ansatz there remains the freedom to re-parametrize $z \to \widehat{z}(z, u)$, and to re-define $u \to \widehat{u}(u)$, $v \to \widehat{v}(v)$.

It is simpler to make an appropriately invariant Ansatz for the four-form field strength:

$$\begin{aligned} F^{(4)} &= e^0 \wedge e^1 \wedge \Big(b_1\,e^2 \wedge e^3 + b_2\,e^2 \wedge e^4 + b_3\,e^3 \wedge e^4\Big)\\ &\quad + \Big(b_4\,e^2 + b_5\,e^3 + b_6\,e^4\Big) \wedge e^5 \wedge e^6 \wedge e^7 + \Big(b_7\,e^2 + b_8\,e^3 + b_9\,e^4\Big) \wedge e^8 \wedge e^9 \wedge e^{10}\,, \end{aligned} \tag{E.9}$$

where $b_1, \ldots, b_9$ are arbitrary functions of (u, v, z). One will ultimately have to impose the Bianchi identities on $F^{(4)}$.

E.2 Solving the BPS system

If one uses the fact that $\bar{\epsilon}\Gamma^{\mu}\epsilon$ is necessarily the time-like Killing vector $\frac{\partial}{\partial t}$ one finds that the (u, v, z) dependence of the Killing vector is determined by:

$$\epsilon \;=\; e^{-\frac{1}{2}A_0}\,\epsilon_0\,, \tag{E.10}$$

where ϵ_0 is independent of t, y, z, u, v. The dependence of the supersymmetries on the sphere coordinates is determined entirely by the representations of $SO(4) \times SO(4)'$, or $(SU(2))^4$: four out of the eight supersymmetries are independent of the sphere angles and four rotate in the vector representation of each $SO(4)$ (or as bi-fundamentals of each pair of $SU(2)$'s).

Using this, the projectors (E.4) and the Ansatz (E.8) and (E.9), it is straightforward to solve the hugely over-determined system (8.2).

A first pass through this system determines the functions b_i algebraically in terms of the A_j and B_1 and the first derivatives of the A_j and B_1. One then eliminates the b_i entirely to arrive at a collection of first-order differential constraints on the A_j and B_1.

This collection includes:

$$\partial_u\Big(A_5 - A_3\Big) \;=\; \partial_z\Big(A_5 - A_3\Big) \;=\; 0\,, \qquad \partial_v\Big(A_4 - A_2\Big) \;=\; \partial_z\Big(A_4 - A_2\Big) \;=\; 0\,. \tag{E.11}$$

This means that $(A_5 - A_3)$ is only a function of v and $(A_4 - A_2)$ is only a function of u. Remembering that the Ansatz still allows the re-definition $u \to \widehat{u}(u)$, $v \to \widehat{v}(v)$, we can absorb these functional dependences of $(A_5 - A_3)$ and $(A_4 - A_2)$ into such a coordinate re-definition and assume, without loss of generality, that

$$A_4 \;=\; A_2\,, \qquad A_5 \;=\; A_3\,, \tag{E.12}$$

which means that the sphere metrics in ds_{11}^2 extend to the metrics of two conformally flat $\mathbb{R}^4$'s:

$$\begin{aligned} ds_{11}^2 \;=\; e^{2A_0}\Big(-dt^2 \;+\; dy^2\Big) \;+\; e^{2A_2}\Big(du^2 \;+\; u^2\,d\Omega_3^2\Big) \;+\; e^{2A_3}\Big(dv^2 \;+\; v^2\,d\Omega_3'^2\Big) \\ +\; e^{2A_1}\Big(dz \;+\; B_1\,du\Big)^2\,. \end{aligned} \tag{E.13}$$

Using (E.12), some of the other first-order equations show that $(A_0 + A_2 + A_3)$ is a constant. This constant can be taken to be zero by scaling u and v, and so we can take:

$$A_3 \;=\; -\,(A_0 + A_2)\,. \tag{E.14}$$

The first order system then gives $\partial_v(A_1 + 2A_2) = 0$, which means that $A_1 = -2A_2 + a_1(z, u)$ for some arbitrary function, a_1. However there is still the freedom to re-define $z \to \widehat{z}(z, u)$, and so we can take $a_1 \equiv 0$, to arrive at:

$$A_1 \;=\; -\,2A_2\,. \tag{E.15}$$

We have thus simplified the eleven-dimensional metric to the form:

$$ds_{11}^2 \;=\; e^{2A_0}\Big[\Big(-dt^2 \;+\; dy^2\Big) \;+\; e^{2(A_2-A_0)}\Big(du^2 \;+\; u^2\, d\Omega_3^2\Big) \;+\; e^{-2(A_2+2A_0)}\Big(dv^2 \;+\; v^2\, d\Omega_3'^2\Big) \\ +\; e^{-2(A_0+2A_2)}\Big(dz \;+\; B_1\, du\Big)^2\Big]\,. \tag{E.16}$$

There remains one last differential constraint in the first-order system:

$$\partial_z\Big(B_1\, e^{-2(A_0+2A_2)}\Big) \;=\; \partial_u\Big(e^{-2(A_0+2A_2)}\Big)\,. \tag{E.17}$$

This can be solved by introducing a potential, $w(u,v,z)$, with:

$$B_1\, e^{-2(A_0+2A_2)} \;=\; -\,\partial_u w\,, \qquad e^{-2(A_0+2A_2)} \;=\; -\,\partial_z w\,, \tag{E.18}$$

which leads to

$$B_1 \;=\; (\partial_z w)^{-1}\,\partial_u w\,, \qquad e^{-2(A_0+2A_2)} \;=\; -\,\partial_z w\,, \tag{E.19}$$

and the metric (E.16) becomes exactly that of (8.12).

One then finds that all the BPS equations are satisfied. However, one still has to solve the Bianchi conditions on $F^{(4)}$.

E.3 Solving the Bianchi equations

Solving the BPS equations led to expressions for the b_i in terms of the A_j and B_1 and their first derivatives. One thus obtains expressions for the b_i in terms of the A_j, the first derivatives of A_j and the first and second derivatives of w. The Bianchi identities thus lead to equations that are third-order in derivatives of w. Amazingly enough, these equations can be integrated.

Define:

$$F_1 \;\equiv\; (-\partial_z w)^{\frac{1}{2}}\, e^{-3A_0}\,, \qquad F_2 \;\equiv\; (-\partial_z w)^{-\frac{1}{2}}\, e^{-3A_0} \;+\; (-\partial_z w)^{-1}\,(\partial_u w)^2\,, \tag{E.20}$$

and then set:

$$H_1 \;\equiv\; \mathcal{L}_v w \;-\; \partial_z F_1\,, \qquad H_2 \;\equiv\; \mathcal{L}_u w \;+\; \partial_z F_2\,, \tag{E.21}$$

where $\mathcal{L}_u$ and $\mathcal{L}_v$ are the Laplacians on the $\mathbb{R}^4$'s.

The Bianchi identities can be summarized as

$$\partial_z H_1 \;=\; \partial_u H_1 \;=\; \partial_z H_2 \;=\; \partial_v H_2 \;=\; 0\,, \tag{E.22}$$

and hence $H_1 = H_1(v)$ and $H_2 = H_2(u)$.

One should note that (E.18) only defines w up to the addition of an arbitrary function of v, and so we can take $H_1(v) \equiv 0$. We will simplify life by taking $H_2(u) \equiv 0$. Having set $H_1 \equiv H_2 \equiv 0$, one can satisfy (E.21) by introducing a pre-potential, $G_0(u,v,z)$, with:

$$w \;=\; \partial_z G_0\,, \qquad F_1 \;=\; \mathcal{L}_v G_0\,, \qquad F_2 \;=\; -\,\mathcal{L}_u G_0\,. \tag{E.23}$$

From this and (E.20), one can determine e^{-3A_0} in terms of $\mathcal{L}_v G_0$ and $(-\partial_z w)^{\frac{1}{2}}$. Substituting this into the second expression in (E.20) and using (E.23), one obtains an equation that determines G_0:

$$\mathcal{L}_v G_0 \;=\; (\partial_z^2 G_0)\,(\mathcal{L}_u G_0) \;-\; (\partial_u \partial_z G_0)^2\,, \tag{E.24}$$

which is precisely the spherically symmetric form of (8.9).

Appendix F

The democracy of M5 and M5' branes

The metric (8.6) and fluxes (8.7) given in Section 8.2.1 appear to be asymmetric between the two $\mathbb{R}^4$'s, and hence between the M5 and M5' branes.

The purpose of this Appendix is to show that this is a coordinate artifact inherent in the fibration of the M-theory direction. Following a discussion in [259], we will show that one can flip the fibration from the $\boldsymbol{u}$-plane to the $\boldsymbol{v}$-plane by exchanging the role of w and z. In the $\boldsymbol{u}$-plane fibration (8.6), w is a function and z is a coordinate. In the $\boldsymbol{v}$-plane fibration we will construct here, w is a coordinate and z is a function appearing in the solution, $z(w, \boldsymbol{u}, \boldsymbol{v})$.

It is useful to introduce the notation, familiar from thermodynamics, in which subscripts on parentheses specify the variables that are being held fixed. For example, given a function, F, and some variables η, ζ, ξ, the expression

$$\left(\frac{\partial F}{\partial \eta}\right)_{\zeta,\xi} \tag{F.1}$$

specifically indicates that the derivative with respect to η is being taken while ζ and ξ are held fixed.

Consider the complete differential of the function $w(z, \boldsymbol{u}, \boldsymbol{v})$:

$$dw \;=\; \left(\frac{\partial w}{\partial z}\right)_{\boldsymbol{u},\boldsymbol{v}} dz \;+\; \left(\frac{\partial w}{\partial u_i}\right)_{z,\boldsymbol{v}} du_i \;+\; \left(\frac{\partial w}{\partial v_i}\right)_{z,\boldsymbol{u}} dv_i\,. \tag{F.2}$$

If one holds w fixed, then this must vanish and one then obtains:

$$\left(\frac{\partial z}{\partial u_i}\right)_{w,\boldsymbol{v}} \;=\; -\left(\left(\frac{\partial w}{\partial z}\right)_{\boldsymbol{u},\boldsymbol{v}}\right)^{-1}\left(\frac{\partial w}{\partial u_i}\right)_{z,\boldsymbol{v}}, \qquad \left(\frac{\partial z}{\partial v_i}\right)_{w,\boldsymbol{u}} \;=\; -\left(\left(\frac{\partial w}{\partial z}\right)_{\boldsymbol{u},\boldsymbol{v}}\right)^{-1}\left(\frac{\partial w}{\partial v_i}\right)_{z,\boldsymbol{u}}, \tag{F.3}$$

and

$$\left(\frac{\partial z}{\partial w}\right)_{\boldsymbol{u},\boldsymbol{v}} \;=\; \left(\left(\frac{\partial w}{\partial z}\right)_{\boldsymbol{u},\boldsymbol{v}}\right)^{-1}. \tag{F.4}$$

Using this one finds:

$$\begin{aligned} e^2 &= (-\partial_z w)^{\frac{1}{2}} \Big(dz \ + \ (\partial_z w)^{-1} \Big(\boldsymbol{\nabla}_{\boldsymbol{u}} \, w \Big) \cdot d\boldsymbol{u} \Big) \\ &= \ - \, (-\partial_z w)^{-\frac{1}{2}} \Big((\partial_z w) dz \ + \ \Big(\boldsymbol{\nabla}_{\boldsymbol{u}} \, w \Big) \cdot d\boldsymbol{u} \Big) \ = \ - \, (-\partial_z w)^{-\frac{1}{2}} \Big(dw \ - \ \Big(\boldsymbol{\nabla}_{\boldsymbol{v}} \, w \Big) \cdot d\boldsymbol{v} \Big) \\ &= \ - \Big((-\partial_w z)_{\boldsymbol{u},\boldsymbol{v}} \Big)^{\frac{1}{2}} \Big(dw \ + \ \Big(\Big(\frac{\partial z}{\partial w} \Big)_{\boldsymbol{v},\boldsymbol{u}} \Big)^{-1} \Big(\frac{\partial z}{\partial v_i} \Big)_{w,\boldsymbol{v}} \Big) dv_i \Big) \\ &= \ - \, (-\partial_w z)^{\frac{1}{2}} \Big(dw \ + \ (\partial_w z)^{-1} \Big(\boldsymbol{\nabla}_{\boldsymbol{v}} \, z \Big) \cdot d\boldsymbol{v} \Big) \ . \end{aligned} \tag{F.5}$$

One also obtains:

$$C^{(3)} \ = \ - e^0 \wedge e^1 \wedge e^2 \ + \ \frac{1}{3!} \, \epsilon_{ijk\ell} \Big(- (\partial_{u_\ell} z) \, du^i \wedge du^j \wedge du^k \ + \ (\partial_w z)^{-1} \, (\partial_{v_\ell} z) \, dv^i \wedge dv^j \wedge dv^k \Big) . \tag{F.6}$$

One therefore finds that by using w as a coordinate and using $z(w, \boldsymbol{u}, \boldsymbol{v})$ as a function appearing in the metric, the fibration is now over the $\mathbb{R}^4$ defined by $\boldsymbol{v}$ and the form of $C^{(3)}$ is similarly inverted compared to (F.6).

Thus the BPS solution generically requires a non-trivial fibration over one of the $\mathbb{R}^4$'s but which $\mathbb{R}^4$ is a matter of a coordinate choice. We will remain with the formulation in Section 8.2.1 where the M-theory direction is fibered over $\mathbb{R}^4(\boldsymbol{u})$.

Appendix G

Dualities from the F1-D1 string web to the D2-D4 string web

In this Appendix we describe in detail the dualities we perform to relate the F1-D1 string-web solution constructed in [261] to the M2-M5 solutions we construct in Section 8.2.

In order to perform a T-duality along an isometry direction x, we initially have to express the various fields in the following form:

$$\begin{aligned} ds^2 &= G_{xx}(dx + A_\mu dx^\mu)^2 + \widehat{g}_{\mu\nu}dx^\mu dx^\nu \,, \\ B_2 &= B_{\mu x}dx^\mu \wedge (dx + A_\mu dx^\mu) + \widehat{B}_2 \,, \\ C_p &= C_{(p-1)\,x} \wedge (dx + A_\mu dx^\mu) + \widehat{C}_p \,, \end{aligned} \tag{G.1}$$

where the hatted forms have no leg along x. Then, the transformed fields will be given by

$$\begin{aligned} d\widetilde{s}^2 &= G_{xx}^{-1}(dx + B_{\mu x}dx^\mu)^2 + \widehat{g}_{\mu\nu}dx^\mu dx^\nu \,, \\ e^{2\widetilde{\phi}} &= G_{xx}^{-1}e^{2\phi} \,, \\ \widetilde{B}_2 &= A_\mu dx^\mu \wedge dx + \widehat{B}_2 \,, \\ \widetilde{C}_p &= \widehat{C}_{p-1} \wedge (dx + B_{\mu x}dx^\mu) + C_{(p)x} \,. \end{aligned} \tag{G.2}$$

As for the S-duality, the conventions we use for the S-dual fields of a given Type IIB supergravity solution are the following[1]:

$$\begin{aligned} &\widetilde{g}_{\mu\nu} = \sqrt{C_0^2 + e^{-2\phi}}\, g_{\mu\nu} \,, \quad e^{-\widetilde{\phi}} = \frac{e^{-\phi}}{C_0^2 + e^{-2\phi}} \,, \quad \widetilde{C}_0 = -\frac{C_0}{C_0^2 + e^{-2\phi}} \,, \\ &\widetilde{B}_2 = -C_2 \,, \quad \widetilde{C}_2 = B_2 \,, \quad \widetilde{C}_4 = C_4 + B_2 \wedge C_2 \,. \end{aligned} \tag{G.3}$$

Using now (G.2) and (G.3), the solution obtained by the duality chain mentioned in the

[1] Note that the conventions for the T- and S-dualities are slightly different from those in Appendix B.

beginning of this Section is:

$$
\begin{aligned}
ds^2 &= \frac{\sqrt{\det h}}{h_{11}}(du_2^2+du_3^2)+\frac{1}{\sqrt{\det h}}(-dt^2+dy^2)+\sqrt{\det h}\left(e^{3A}h_{ab}dr^a dr^b+ds^2_{\mathbb{R}^4}\right)\,,\\
e^{2\phi} &= \frac{\sqrt{\det h}}{h_{11}}\,,\quad B_2=\frac{h_{12}}{h_{11}}du_2\wedge du_3\,,\\
C_3 &= e^{3A}h_{1a}dt\wedge dr^a\wedge dy\,,\quad C_5=\frac{1}{h_{11}}dt\wedge du_1\wedge du_2\wedge du_3\wedge dy\,.
\end{aligned}
\tag{G.4}
$$

In order to uplift the solution to M-theory we need to determine the magnetic dual of the C_5 field. Even though this is enough for our purposes we will for completeness determine the magnetic dual of the C_3 field as well. Our conventions for the democratic formalism are the following[2]:

$$
\begin{aligned}
&F_p = dC_{p-1} && \text{for } p<3\,,\\
&F_p = dC_{p-1}+H_3\wedge C_{p-3} && \text{for } p\geq 3\,,\\
&F_6=\star F_4\,, \qquad F_8=\star F_2\,.
\end{aligned}
$$

For simplicity, we will assume spherical symmetry in the $\mathbb{R}^4$ spanned by υ_i and use hyperspherical coordinates to describe it:

$$
\begin{aligned}
\upsilon_3 &= \upsilon\cos\phi_1\,,\\
\upsilon_4 &= \upsilon\sin\phi_1\cos\phi_2\,,\\
\upsilon_5 &= \upsilon\sin\phi_1\sin\phi_2\cos\phi_3\,,\\
\upsilon_6 &= \upsilon\sin\phi_1\sin\phi_2\sin\phi_3\,,\\
ds^2_{\mathbb{R}^4} &= d\upsilon^2+\upsilon^2\left(d\phi_1^2+\sin^2\phi_1\left(d\phi_2^2+\sin^2\phi_2\,d\phi_3^2\right)\right)
\end{aligned}
\tag{G.5}
$$

Now the metric h_{ab} is a function of z, u_1 and υ.

In order to find the C_3 field dual to the C_5 of (G.4) we need to compute $F_6^e = dC_5^e + H_3\wedge C_3^e$ [3]:

$$
dC_5^e = -\frac{1}{h_{11}^2}\left(\partial_z h_{11}dz+\partial_\upsilon h_{11}d\upsilon\right)\wedge dt\wedge du_1\wedge du_2\wedge du_3\wedge dy\,,
\tag{G.6}
$$

$$
\begin{aligned}
H_3\wedge C_3^e = &\left[\partial_z\left(\frac{h_{12}}{h_{11}}\right)e^{3A}h_{12}-\partial_{u_1}\left(\frac{h_{12}}{h_{11}}\right)e^{3A}h_{11}\right]dt\wedge du_1\wedge du_2\wedge du_3\wedge dz\wedge dy\\
&-\partial_\upsilon\left(\frac{h_{12}}{h_{11}}\right)e^{3A}h_{11}\,dz\wedge dt\wedge d\upsilon\wedge du_2\wedge du_3\wedge dy\\
&-\partial_\upsilon\left(\frac{h_{12}}{h_{11}}\right)e^{3A}h_{12}\,du_1\wedge dt\wedge d\upsilon\wedge du_2\wedge du_3\wedge dy\,.
\end{aligned}
\tag{G.7}
$$

[2]Note that these conventions are slightly different from those used in Appendix B.

[3]The superscripts e and m will be used to denote respectively the electric and magnetic parts of the RR fields.

Summing these two expressions we obtain:

$$\begin{aligned} F_6^e = & f_1\, dt \wedge dz \wedge du_1 \wedge du_2 \wedge du_3 \wedge dy \\ & + f_2\, dt \wedge du_1 \wedge du_2 \wedge du_3 \wedge dy \wedge d\upsilon \\ & - f_3\, dt \wedge dz \wedge du_2 \wedge du_3 \wedge dy \wedge d\upsilon\,, \end{aligned} \tag{G.8}$$

where the f_i are given by

$$\begin{aligned} f_1 &= \frac{1}{h_{11}^2}\partial_z h_{11} - \partial_z\left(\frac{h_{12}}{h_{11}}\right) e^{3A} h_{12} + \partial_{u_1}\left(\frac{h_{12}}{h_{11}}\right) e^{3A} h_{11}\,, \\ f_2 &= \frac{1}{h_{11}^2}\partial_\upsilon h_{11} - \partial_\upsilon\left(\frac{h_{12}}{h_{11}}\right) e^{3A} h_{12}\,, \\ f_3 &= \partial_\upsilon\left(\frac{h_{12}}{h_{11}}\right) e^{3A} h_{11}\,. \end{aligned} \tag{G.9}$$

We can now compute F_4^m by $F_4^m = -\star F_6^e$:

$$\begin{aligned} F_4^m = & -\upsilon^3 h_{11}\left(f_2 h_{11} + f_3 h_{12}\right) dz \wedge d\Omega_3' - \upsilon^3 h_{11}\left(f_2 h_{12} + f_3 h_{22}\right) du_1 \wedge d\Omega_3' \\ & + r^3 f_1 h_{11} \det h\, dr \wedge d\Omega_3'\,, \end{aligned} \tag{G.10}$$

where $d\Omega_3' = \sin^2\phi_1 \sin\phi_2\, d\phi_1 \wedge d\phi_2 \wedge d\phi_3$. Using the explicit form of the f_i, F_4^m becomes:

$$\begin{aligned} F_4^m = & -\left(\upsilon^3 \partial_\upsilon h_{11}\, dz + \upsilon^3 \partial_\upsilon h_{12}\, du_1\right) \wedge d\Omega_3' \\ & + \upsilon^3\left(h_{22}\partial_z h_{11} - h_{12}\partial_z h_{12} - h_{12}\partial_{u_1} h_{11} + h_{11}\partial_{u_1} h_{12}\right) d\upsilon \wedge d\Omega_3'\,. \end{aligned} \tag{G.11}$$

In order to further simplify this expression we substitute (8.85) to the first line of (G.11) (from now on we ignore $d\Omega_3'$) and get:

$$\begin{aligned} & -\frac{1}{2}\upsilon^3\partial_\upsilon\partial_z^2 K\, dz - \frac{1}{2}\upsilon^3\partial_\upsilon\partial_z\partial_{u_1} K\, du_1 = -\frac{1}{2}d(\upsilon^3\partial_\upsilon\partial_z K) + \frac{1}{2}\partial_\upsilon(\upsilon^3\partial_\upsilon\partial_z K)d\upsilon \\ & = -\frac{1}{2}d(\upsilon^3\partial_\upsilon\partial_z K) + \frac{\upsilon^3}{2}\partial_z\left(\frac{1}{\upsilon^3}\partial_\upsilon(\upsilon^3\partial_\upsilon K)\right) d\upsilon = -\frac{1}{2}d(\upsilon^3\partial_\upsilon\partial_z K) + \frac{\upsilon^3}{2}\partial_z\Delta_y K\, d\upsilon\,. \end{aligned} \tag{G.12}$$

Plugging (8.85) in the second line of (G.11) we get

$$\frac{\upsilon^3}{4}\left(\partial_{u_1}^2 K\partial_z^3 K - 2\partial_z\partial_{u_1} K\partial_z^2\partial_{u_1} K + \partial_z^2 K\partial_z\partial_{u_1}^2 K\right) d\upsilon = \upsilon^3\partial_z(\det h)\,. \tag{G.13}$$

Finally, putting (G.12) and (G.13) together we find

$$F_4^m = -\frac{1}{2}d(\upsilon^3\partial_\upsilon\partial_z K) \wedge d\Omega_3' + \frac{\upsilon^3}{2}\partial_z\left(\Delta_y K + 2\det h\right) d\upsilon \wedge d\Omega_3'\,. \tag{G.14}$$

The second term vanishes due to the Monge-Ampère equation (8.86) and therefore, from $F_4^m = dC_3^m + H \wedge C_1^m$ and because $C_1 = 0$, we can easily see that C_3^m is given by

$$C_3^m = -\frac{1}{2}\upsilon^3\partial_\upsilon\partial_z K\, d\Omega_3'\,. \tag{G.15}$$

Let us now find the C_5 field dual to the C_3 of (G.4), for which we need to compute $F_4^e = dC_3^e$:

$$\begin{aligned} dC_3^e = &-\left[\partial_{u_1}\left(e^{3A}h_{11}\right) - \partial_z\left(e^{3A}h_{12}\right)\right] dt\wedge du_1\wedge dz\wedge dy \\ &-\left[\partial_v\left(e^{3A}h_{11}\right) dz + \partial_v\left(e^{3A}h_{12}\right) du_1\right]\wedge dt\wedge dv\wedge dy\,. \end{aligned} \tag{G.16}$$

F_6^m will then be given by $F_6^m = \star F_4^e$:

$$\begin{aligned} F_6^m =&\frac{v^3\det h}{h_{11}}\left[h_{12}\partial_v\left(e^{3A}h_{11}\right) - h_{11}\partial_v\left(e^{3A}h_{12}\right)\right] dz\wedge du_2\wedge du_3\wedge d\Omega_3' \\ &+\frac{v^3\det h}{h_{11}}\left[h_{22}\partial_v\left(e^{3A}h_{11}\right) - h_{12}\partial_v\left(e^{3A}h_{12}\right)\right] du_1\wedge du_2\wedge du_3\wedge d\Omega_3' \\ &-\frac{v^3(\det h)^2}{h_{11}}\left[\partial_{u_1}\left(e^{3A}h_{11}\right) - \partial_z\left(e^{3A}h_{12}\right)\right] du_2\wedge du_3\wedge dv\wedge d\Omega_3'\,, \end{aligned} \tag{G.17}$$

which can be simplified to

$$\begin{aligned} F_6^m = &\, v^3\left(\frac{h_{12}}{h_{11}}\partial_v h_{11} - \partial_v h_{12}\right) dz\wedge du_2\wedge du_3\wedge d\Omega_3' \\ &+v^3\left(\frac{h_{12}}{h_{11}}\partial_v h_{12} - \partial_v h_{22}\right) du_1\wedge du_2\wedge du_3\wedge d\Omega_3' \\ &+v^3\left(\partial_{u_1}(\det h) - \frac{h_{12}}{h_{11}}\partial_z(\det h)\right) dv\wedge dx_2\wedge du_3\wedge d\Omega_3'\,. \end{aligned} \tag{G.18}$$

Using (8.85) the first two terms of (G.18) can be written as

$$\frac{1}{2}\frac{h_{12}}{h_{11}} d_\Sigma\left(v^3\partial_v\partial_z K\right)\wedge du_2\wedge du_3\wedge d\Omega_3' - \frac{1}{2} d_\Sigma\left(v^3\partial_v\partial_1 K\right)\wedge du_2\wedge du_3\wedge d\Omega_3'\,, \tag{G.19}$$

where by Σ we denote the two-dimensional space spanned by z and u_1.

We can now compute C_5^m from $F_6^m = dC_5^m + H_3\wedge C_3^m$, where C_3^m is given in (G.15):

$$\begin{aligned} F_6^m - H\wedge C_3^m = &\left[\frac{h_{12}}{h_{11}} d_\Sigma\left(\frac{v^3}{2}\partial_v\partial_z K\right) + d\left(\frac{h_{12}}{h_{11}}\right)\frac{v^3}{2}\partial_v\partial_z K\right]\wedge du_2\wedge du_3\wedge d\Omega_3' \\ &-d_\Sigma\left(\frac{v^3}{2}\partial_v\partial_{u_1} K\right)\wedge du_2\wedge du_3\wedge d\Omega_3' \\ &+v^3\left(\partial_{u_1}(\det h) - \frac{h_{12}}{h_{11}}\partial_z(\det h)\right) dv\wedge dx_2\wedge dx_3\wedge d\Omega_3'\,. \end{aligned} \tag{G.20}$$

The first two terms of (G.20) give

$$\begin{aligned} &d\left(\frac{v^3}{2}\frac{h_{12}}{h_{11}}\partial_v\partial_z K\right)\wedge du_2\wedge du_3\wedge d\Omega_3' - \frac{h_{12}}{h_{11}}\partial_v\left(\frac{v^3}{2}\partial_v\partial_z K\right) dv\wedge du_2\wedge du_3\wedge d\Omega_3' \\ &-d\left(\frac{v^3}{2}\partial_v\partial_{u_1} K\right)\wedge du_2\wedge du_3\wedge d\Omega_3' + \partial_v\left(\frac{v^3}{2}\partial_v\partial_{u_1} K\right) dv\wedge du_2\wedge du_3\wedge d\Omega_3'\,. \end{aligned} \tag{G.21}$$

Now if we combine the terms of (G.21) that are not total derivatives with the third term of (G.20) we get

$$\frac{v^3}{2}\partial_{u_1}\left[2\det h+\frac{1}{v^3}\partial_v\left(v^3\partial_v K\right)\right]-\frac{v^3}{2}\frac{h_{12}}{h_{11}}\partial_z\left[2\det h+\frac{1}{v^3}\partial_v\left(v^3\partial_v K\right)\right] \tag{G.22}$$

and we see that the Monge-Ampère equation (8.86) appeared again. Therefore, (G.20) reduces to:

$$F_6^m-H\wedge C_3^m=d\left(\frac{v^3}{2}\frac{h_{12}}{h_{11}}\partial_v\partial_z K-\frac{v^3}{2}\partial_v\partial_{u_1}K\right)\wedge du_2\wedge du_3\wedge d\Omega_3' \tag{G.23}$$

and C_5^m is

$$C_5^m=\frac{v^3}{2}\left(\frac{h_{12}}{h_{11}}\partial_v\partial_z K-\partial_v\partial_{u_1}K\right)du_2\wedge du_3\wedge d\Omega_3'\,. \tag{G.24}$$

To sum up, the final form of the D2-D4 string-web solution is:

$$\begin{aligned}
ds^2&=\frac{1}{\sqrt{\det h}}(-dt^2+dy^2)+\frac{\sqrt{\det h}}{h_{11}}(du_2^2+du_3^2)+\sqrt{\det h}\left(e^{3A}h_{ab}dr^a dr^b+ds^2_{\mathbb{R}^4}\right)\,,\\
e^{2\phi}&=\frac{\sqrt{\det h}}{h_{11}}\,,\quad B_2=\frac{h_{12}}{h_{11}}du_2\wedge du_3\,,\\
C_3&=e^{3A}h_{1a}dt\wedge dr^a\wedge dy-\frac{v^3}{2}\partial_v\partial_z K\,d\Omega_3'\,,\\
C_5&=\frac{1}{h_{11}}dt\wedge du_1\wedge du_2\wedge du_3\wedge dy+\frac{v^3}{2}\left(\frac{h_{12}}{h_{11}}\partial_v\partial_z K-\partial_v\partial_{u_1}K\right)du_2\wedge du_3\wedge d\Omega_3'\,.
\end{aligned} \tag{G.25}$$

Appendix H

The infinite tilted M2-M5 bound state.

The Ansatz for the M5-M2 intersections described in Section 8.2 is a complicated one. To construct asymptotically-flat solutions, one needs to solve the Monge-Ampère-like equation (8.9) with the appropriate boundary conditions. In this Appendix, we consider an alternative approach to construct a simple solution to these equations. We start with a stack of tilted D2-branes, and follow a chain of dualities to obtain a tilted M5-brane solution with M2 flux. We will see how this construction fits the Ansatz of Section 8.2.

A stack of D2 branes is described in Type IIA by the following system:

$$ds^2 = Z^{-1/2}(-dt^2 + dx_1^2 + dx_2^2) + Z^{1/2}(dx_3^2 + \cdots + dx_9^2)\,, \tag{H.1}$$

$$e^{\Phi} = Z^{1/4}\,, \tag{H.2}$$

$$C_3 = Z^{-1} dt \wedge dx_1 \wedge dx_2\,, \tag{H.3}$$

where Z is a harmonic function. The branes are smeared along the directions $x_{3,4,5}$, and located at an arbitrary point in the directions $x_{6,7,8,9}$, that we will take to be the center of space. Noting r the distance to the branes in these last four directions, the harmonic function Z takes the form:

$$Z \;=\; 1 + \frac{Q}{r^2}\,, \qquad r^2 \equiv x_6^2 + \cdots + x_9^2\,. \tag{H.4}$$

We now tilt the system in the $x_{2,3}$ plane by an angle θ. We define the new coordinates (x_2', x_3') by:

$$\begin{aligned} x_2 &= x_2' c + x_3' s\,, \\ x_3 &= -x_2' s + x_3' c\,, \end{aligned} \tag{H.5}$$

where $c \equiv \cos\theta$, $s \equiv \sin\theta$. In the following we will always use the new rotated coordinate and omit the primes. We also introduce the function W as:

$$W \equiv c^2 Z + s^2\,. \tag{H.6}$$

In the new coordinates, the metric and gauge field of the tilted-brane solution can be expressed as a fibration over the direction $x_3 (\equiv x_3')$:

$$\begin{aligned} ds^2 &= Z^{-1/2}(-dt^2 + dx_1^2) + Z^{1/2}(dx_4^2 + \cdots + dx_9^2) \\ &\quad + Z^{-1/2} W \Big(dx_3 - cs(Z-1)W^{-1} dx_2\Big)^2 + Z^{1/2} W^{-1} dx_2^2 \,, \end{aligned} \tag{H.7}$$

$$e^{2\Phi} = Z^{1/2} \,, \tag{H.8}$$

$$\begin{aligned} C_3 &= Z^{-1} s\, dt \wedge dx_1 \wedge \Big(dx_3 - cs(Z-1)W^{-1} dx_2\Big) \\ &\quad + W^{-1} c\, dt \wedge dx_1 \wedge dx_2 \,. \end{aligned} \tag{H.9}$$

The goal is now to dualize this solution to a solution of M-theory, by first performing two T-dualities, and then uplifting the solution.

H.1 Performing two T-dualities

We start by performing two T-dualities, along x_3 and x_4, using the standard T-duality rules (G.1,G.2). After the first T-duality along x_3, we obtain:

$$ds^2 = Z^{-1/2}(-dt^2 + dx_1^2) + Z^{1/2}(dx_4^2 + \cdots + dx_9^2) + Z^{1/2} W^{-1} \Big(dx_2^2 + dx_3^2\Big) \,, \tag{H.10}$$

$$e^{2\Phi} = W^{-1} Z \,, \qquad B_2 = -cs(Z-1)W^{-1}\, dx_2 \wedge dx_3 \,, \tag{H.11}$$

$$C_2 = Z^{-1} s\, dt \wedge dx_1 \,, \qquad C_4 = W^{-1} c\, dt \wedge dx_1 \wedge dx_2 \wedge dx_3 \,. \tag{H.12}$$

This a solution of Type IIB corresponding to a stack of D1-D3 branes, where the D3 branes extend along (x_1, x_2, x_3) and the D1 branes extend along x_1.

We then perform the second T-duality, along the x_4 direction. Since the solution presents no fibration or B-field in this direction, this is a trivial operation, it yields:

$$ds^2 = Z^{-1/2}(-dt^2 + dx_1^2 + dx_4^2) + Z^{1/2}(dx_5^2 + \cdots + dx_9^2) + Z^{1/2} W^{-1} \Big(dx_2^2 + dx_3^2\Big) \,, \tag{H.13}$$

$$e^{2\Phi} = Z^{1/2} W^{-1} \,, \qquad B_2 = -cs(Z-1)W^{-1}\, dx_2 \wedge dx_3 \,, \tag{H.14}$$

$$C_3 = Z^{-1} s\, dt \wedge dx_1 \wedge dx_4 \,, \qquad C_5 = W^{-1} c\, dt \wedge dx_1 \wedge dx_2 \wedge dx_3 \wedge dx_4 \,. \tag{H.15}$$

This is a $D2(014) - D4(01234)$ system. Recall that T-dualities preserves the amount of supersymmetries, all the solutions presented here have 16 supersymmetries.

Note that this solution can be embedded in the ansatz (8.88) by making a rotation in the x_{45} plane and relabelling the coordinates. One then identifies

$$\begin{gathered} h_{11} = c^2 Z + s^2 \,, \quad h_{22} = s^2 Z + c^2 \\ h_{12} = cs(Z-1) \,, \quad \text{and} \quad \det h = Z \,. \end{gathered} \tag{H.16}$$

We will nonetheless recompute the uplift of the solution to M-theory in this specific instance, as a cross-check to the previous computation, and to identify the solution to the maze equation.

H.2 The democratic formalism

To uplift the solution to M-theory, we need to know the full expression of the C_3 gauge field in the democratic formalism. That is to say, we need to determine the magnetic dual of the C_5 gauge field of (H.15).

Let us first compute the 6-form field strength $F_6 = dC_5 + dB_2 \wedge C_3$. We have

$$\begin{aligned} dB_2 \wedge C_3 &= \Big[-cs\,\partial_l\Big((Z-1)W^{-1}\Big)\,dx_l \wedge dx_2 \wedge dx_3\Big] \wedge \Big[Z^{-1}s\,dt \wedge dx_1 \wedge dx_4\Big] && \text{(H.17)} \\ &= cs^2\,W^{-2}Z^{-1}(\partial_l Z)\,dt \wedge dx_1 \wedge dx_2 \wedge dx_3 \wedge dx_4 \wedge dx_l\,, && \text{(H.18)} \end{aligned}$$

and

$$\begin{aligned} dC_5 &= c\,\partial_l\Big(W^{-1}\Big)\,dx_l \wedge dt \wedge dx_1 \wedge \cdots \wedge dx_4 && \text{(H.19)} \\ &= c^3\,W^{-2}(\partial_l Z)\,dt \wedge dx_1 \wedge dx_2 \wedge dx_3 \wedge dx_4 \wedge dx_l\,. && \text{(H.20)} \end{aligned}$$

where there is an implicit summation over $l \in \{5,6,7,8,9\}$, and to compute the derivatives we have used the expression of W in (H.6).

Summing the two results, we thus obtain

$$\begin{aligned} F_6 &= c\,W^{-1}Z^{-1}(\partial_l Z)\,dt \wedge dx_1 \wedge dx_2 \wedge dx_3 \wedge dx_4 \wedge dx_l && \text{(H.21)} \\ &= cZ^{-1}(\partial_l Z)\,e^0 \wedge e^1 \wedge e^2 \wedge e^3 \wedge e^4 \wedge e^l\,, && \text{(H.22)} \end{aligned}$$

where $e^i \propto dx^i$ are the natural diagonal frames of the metric (H.13).

We can now compute the dual four-form $F_4^{(m)} = -\star F_6$:

$$\begin{aligned} F_4^{(m)} &= c\,\frac{\partial_l Z}{Z}\,\frac{\epsilon_{(l-4),abcd}}{4!}e^{4+a} \wedge e^{4+b} \wedge e^{4+c} \wedge e^{4+d} && \text{(H.23)} \\ &= c\,(\partial_l Z)\,\frac{\epsilon_{(l-4),abcd}}{4!}dx^{4+a} \wedge dx^{4+b} \wedge dx^{4+c} \wedge dx^{4+d} && \text{(H.24)} \end{aligned}$$

where ϵ is the rank-5 antisymmetric tensor, the index l still runs between 5 and 9, while the indices a, b, c, d are summed over $1, \ldots, 5$. The exponent "(m)" of the four-form denotes the magnetic part.

We can further simplify this expression by using the fact that the harmonic function (H.4) does not depend on x_5, and depends only on the radial direction r:

$$F_4^{(m)} = -\,c\,\frac{x_l}{r}(\partial_r Z)\,\frac{\epsilon_{(l-5),abc}}{3!}dx^5 \wedge dx^{5+a} \wedge dx^{5+b} \wedge dx^{5+c} \qquad \text{(H.25)}$$

where now 5 is excluded from the sum over l, $l \in \{6,7,8,9\}$, while the indices a, b, c still run from 1 to 4. We then obtain the potential by integrating the field strength:

$$\begin{aligned} C_3^{(m)} &= -\,c\frac{x_5 x_l}{r}(\partial_r Z)\,\frac{\epsilon_{(l-5),abc}}{3!}dx^{5+a} \wedge dx^{5+b} \wedge dx^{5+c} && \text{(H.26)} \\ &= -\,c\,x_5\,r^3(\partial_r Z)\,d\Omega_3'\,. && \text{(H.27)} \end{aligned}$$

where $d\Omega_3'$ is the volume form of the unit 3-sphere defined by $x_6^2 + \cdots + x_9^2 = 1$.

H.3 M-theory uplift and matching

We can now uplift the solution to M-theory, calling the new direction x_{11}:

$$ds^2 = Z^{-1/6}W^{1/3}\Big[Z^{-1/2}(-dt^2+dx_1^2+dx_4^2)+Z^{1/2}(dx_5^2+\cdots+dx_9^2)\Big] + Z^{1/3}W^{-2/3}\Big(dx_2^2+dx_3^2+dx_{11}^2\Big)\,, \tag{H.28}$$

$$C_3 = Z^{-1}s\,dt\wedge dx_1\wedge dx_4 - cs(Z-1)W^{-1}\,dx_2\wedge dx_3\wedge dx_{11} - c\,x_5\,r^3(\partial_r Z)\,d\Omega_3'\,. \tag{H.29}$$

The system is now that of M2 branes extending in the directions (t, x_1, x_4), and M5 branes extending in $(t, x_1, x_2, x_3, x_4, x_{11})$. To make contact with the Ansatz of Section 8.2, there remains to apply a rotation in the plane $x_{4,5}$, by the same angle θ as the first tilt, and to relabel the coordinates to match the notations:

$$x_4 \to cu_1 + sz\,, \quad x_5 \to -su_1 + cz \tag{H.30}$$

$$x_1 \to y\,, \quad x_2 \to u_2\,, \quad x_3 \to u_3\,, \quad x_{11} \to -u_4\,, \quad x_{6,7,8,9} \to v_{1,2,3,4}\,. \tag{H.31}$$

where, as previously, $c = \cos\theta, s = \sin\theta$. The final result is

$$ds^2 = W^{1/3}Z^{-2/3}\Big(-dt^2+dy^2\Big) + W^{4/3}Z^{-2/3}\Big(dz - cs(Z-1)W^{-1}du_1\Big)^2 + W^{1/3}Z^{1/3}\Big(dv_1^2+\cdots+dv_4^2\Big) + W^{-2/3}Z^{1/3}\Big(du_1^2+du_2^2+du_3^2+du_4^2\Big)\,, \tag{H.32}$$

$$C_3 = Z^{-1}s\,dt\wedge dy\wedge(s\,dz+c\,du_1) + cs(Z-1)W^{-1}\,du_2\wedge du_3\wedge du_4 + c\,(su_1-cz)\,v^3(\partial_v Z)\,d\Omega_3'\,, \tag{H.33}$$

where $v \equiv (v_i v_i)^{1/2}$, the harmonic function is $Z = 1 + Q/v^2$, and $d\Omega_3'$ is the volume form of the unit 3-sphere defined by $\{v^2 = 1\}$. This solution has 4 charges in total: $M2(0y1)$, $M2(0yz)$, $M5(0y1234)$, $M5(0yz234)$. The charges cannot be independently dialed, they are related because the solution preserves 16 supersymmetries. The M2 branes are smeared over the direction $u_{2,3,4}$, and are parallel to the M5 branes in the plane (z, u_1).

Let us now compare this solution with the metric (8.5), and with the 3-form potential (8.7), of the Ansatz. To match the metrics, one needs the following identifications:

$$\begin{aligned} e^{A_0} &= W^{1/6}Z^{-1/3}\,, \quad (-\partial_z w) = W\,, \\ (\partial_{u_1} w) &= cs(Z-1)\,. \end{aligned} \tag{H.34}$$

As for the potential (H.33), one finds that they can be matched up to a simple gauge transformation, provided we identify:

$$(\partial_{v_l} w) = c\,(su_1 - cz)\,v_l\,\frac{\partial_v Z}{v}\,. \tag{H.35}$$

The gauge transformation in question is:

$$\delta C_3 = -c^2 dt\wedge dy\wedge dz + cs\,dt\wedge dy\wedge du_1\,. \tag{H.36}$$

This confirms that this tilted D2 brane solution can be dualized to the Ansatz considered in Chapter 8. This gives an explicit solution of the maze equation. To see this, first integrate the equations (H.34) and (H.35), and determine the function w:

$$w \equiv -zW + cs(Z-1)u_1 \,. \tag{H.37}$$

Then we use (8.10) and (8.11) to compute G_0:

$$G_0 = -\frac{1}{2}Z(cz - su_1)^2 - \frac{1}{2}(sz + cu_1)^2 + f(v) \,, \tag{H.38}$$

where f satisfies $\mathcal{L}_v f \equiv v^{-3}\partial_v(v^3\partial_v f) = Z$. This function satisfies the maze equation (8.9).

Appendix I

Probe M5-branes

We demonstrated in the main text that the solutions in Section 10.3 correspond to a single stack of semi-infinite M2-branes ending on a single stack of M5 branes, which, as one gets closer to their intersection, separate into different M2-M5 spikes depending on the values of ξ_a and ζ_a. The AdS radius, μ, sweeps the radial direction in the combined world-volume. In this Appendix, we would like to underline and elucidate our interpretation of the supergravity geometry by using probes that are M5 branes with an M2 spike. These probes have nontrivial M5 worldvolume fluxes. We expect that one can add such a "spiked" brane probe to the background determined by (10.7) and, because of (10.49), we anticipate that such probe branes will feel no force when located on the boundary of the Riemann surfaces at a ξ-position that scales linearly with the amount of M2 world-volume charge. We show that both of these expectations are correct.

Instead of working with the M5-brane action, which is rather complicated [275], we will reduce the M-theory background to a Type-IIA one and evaluate the action of a spiked D4 brane. We start with the metric and fluxes in (8.29) and use the Poincaré AdS_3 metric:

$$\begin{aligned} ds_{11}^2 &= f_1^2\left(\frac{d\mu^2}{\mu^2}+\mu^2\left(-dt^2+dy^2\right)\right) + f_2^2\, ds_{S^3}^2 + f_3^2\, ds_{S'^3}^2 + f_4^2|dw|^2\,, \\ C^{(3)} &= b_1\,\hat{e}^{012} + b_2\,\hat{e}^{345} + b_3\,\hat{e}^{678}\,, \end{aligned} \tag{I.1}$$

where we have absorbed the overall e^{2A} factor into the f_i's, which are given by:

$$\begin{aligned} f_1^6 &= \frac{h^2 W_+ W_-}{64(G\overline{G}-1)^2}\,, & f_2^6 &= \frac{h^2(G\overline{G}-1)W_-}{W_+^2}\,, \\ f_3^6 &= \frac{h^2(G\overline{G}-1)W_+}{W_-^2}\,, & f_4^6 &= \frac{|\partial_w h|^6}{h^4}(G\overline{G}-1)W_+W_-\,. \end{aligned} \tag{I.2}$$

In order to go to a Type IIA duality frame, we reduce the 11-dimensional solution along the y direction. Using the usual relations between type IIA and 11-dimensional supergravity solutions (8.89) (with x the direction along which we reduce) we arrive at the following type IIA solution:

$$\begin{aligned} ds_{10}^2 &= -\mu^3 f_1^3 dt^2 + \frac{f_1^3}{\mu}d\mu^2 + \mu f_1 f_2^2 ds_{S^3}^2 + \mu f_1 f_3^2 ds_{S'^3}^2 + \mu f_1 f_4^2|dw|^2\,, \\ C_3 &= b_2\,\hat{e}^{345} + b_3\,\hat{e}^{678}\,, \qquad B_2 = -\mu b_1 dt\wedge d\mu\,, \qquad e^{2\phi} = \mu^3 f_1^3\,. \end{aligned} \tag{I.3}$$

We consider a probe M5-brane extending along $AdS_3 \times S^3$ with world-volume M2 flux on it. We will take the worldvolume of the brane to be along the AdS_3 factor of the metric, since this is the only way for the probe to preserve the symmetries of the background. However, since we reduce along y we will instead study a D4-brane with world-volume F1 flux along it. We will take the world-volume of the D4 to be parametrized by $(\eta_0, \eta_1, \eta_2, \eta_3, \eta_4)$ with (η_0, η_1) identified respectively with t and μ and (η_2, η_3, η_4) identified with the coordinates on S^3. The induced metric on our probe brane is therefore:

$$d\widetilde{s}_5^2 = -\mu^3 f_1^3 dt^2 + \frac{f_1^3}{\mu} d\mu^2 + \mu f_1 f_2^2 ds_{S^3}^2 \tag{I.4}$$

and the induced NS-NS and RR fields are

$$\widetilde{B}_2 = -\mu b_1 dt \wedge d\mu \,, \qquad \widetilde{C}_3 = b_2 \widehat{e}^{345} \,. \tag{I.5}$$

In order to account for the F1 charge, we turn on a world-volume 2-form field of the form:

$$F_2 \;=\; \mathcal{F} dt \wedge d\mu \;=\; (\partial_t A_\mu - \partial_\mu A_0)\, dt \wedge d\mu \,, \tag{I.6}$$

where the gauge potential, A, and the Maxwell field, $\mathcal{F}$, are, in principle, functions of μ and the Riemann surface coordinates (ξ, ρ).

It is then straightforward to compute the DBI and WZ actions:

$$\begin{aligned} S_{DBI} &= -T_4 \int d^5\eta e^{-\phi} \sqrt{-\det\left(\widetilde{G}_{\alpha\beta} + F_{\alpha\beta} + \widetilde{B}_{\alpha\beta}\right)} = -T_4 \int dt\, dy\, d\Omega_3\, f_2^3 \sqrt{\mu^2 f_1^6 - (\mathcal{F} - \mu b_1)^2} \,, \\ S_{WZ} &= -T_4 \int e^{\widetilde{B}_2 + \widetilde{F}_2} \wedge \oplus_n \widetilde{C}_n = -T_4 \int dt\, dy\, d\Omega_3\, (F - \mu b_1) b_2 - T_4 \int \widetilde{C}_5 \,. \end{aligned} \tag{I.7}$$

In order to determine $\widetilde{C}_5$, we need to use the fact that:

$$\begin{aligned} &F_p = dC_{p-1} && \text{for } p < 3 \,, \\ &F_p = dC_{p-1} + H_3 \wedge C_{p-3} && \text{for } p \geq 3 \,, \\ &F_6 = \star F_4 \,, \qquad F_8 = \star F_2 \,. \end{aligned} \tag{I.8}$$

Employing these and noting that $C_1 = 0$ we arrive at

$$\begin{aligned} dC_5 = &\star \left(db_2 \wedge \widehat{e}^{345}\right) + \mu b_3 db_1 \wedge dt \wedge d\mu \wedge \widehat{e}^{678} \\ &\star \left(db_3 \wedge \widehat{e}^{678}\right) + \mu b_2 db_1 \wedge dt \wedge d\mu \wedge \widehat{e}^{345} \,, \end{aligned} \tag{I.9}$$

where $\star$ denotes the 10-dimensional Hodge star operator. The first term of the expression above gives a C_5 along the Riemann surface, Σ, and $dt \wedge d\mu \wedge \widehat{e}^{678}$, while the second gives a C_5 along Σ and $dt \wedge d\mu \wedge \widehat{e}^{345}$. Since we only need the pullback of C_5 to the D4-brane probe world-volume, we only need the terms of the second line, which give the following contribution:

$$-\mu \frac{f_1^3 f_2^3}{f_3^3} \left(\partial_\xi b_3\, d\rho - \partial_\rho b_3\, d\xi\right) \wedge dt \wedge d\mu \wedge d\Omega_3 + \mu b_2 \left(\partial_\xi\, d\xi + \partial_\rho\, d\rho\right) \wedge dt \wedge d\mu \wedge d\Omega_3 \,. \tag{I.10}$$

Integrating this expression is quite complicated and since we will eventually only care about the derivative of C_5 along the ξ direction we will leave (I.10) as it is.

The conjugate momentum to $\mathcal{F}$ captures the number of F1 strings (or equivalently M2 branes) that form the spike that ends to the D4 (or M5) branes:

$$\Pi = \frac{\partial \mathcal{L}}{\partial(\partial_t A_\mu)} = \left(-b_2 + \frac{f_2^3 \left(\mathcal{F} - \mu b_1\right)}{\sqrt{\mu^2 f_1^6 - \left(\mathcal{F} - \mu b_1\right)^2}} \right) . \tag{I.11}$$

The Hamiltonian density is now easily obtained:

$$\mathcal{H} \;=\; \Pi\left(\partial_t A_\mu\right) \;-\; \mathcal{L} \;=\; -\mu b_1 b_2 + f_2^3 \frac{\mu b_1 \left(\mathcal{F} - \mu b_1\right) + \mu^2 f_1^6}{\sqrt{\mu^2 f_1^6 - \left(\mathcal{F} - \mu b_1\right)^2}} + \widetilde{C}_5 \, . \tag{I.12}$$

The equation of motion obtained by varying the action, (I.7), with respect to A_0, yields $\partial_\mu \Pi = 0$. This is satisfied if one chooses $\mathcal{F} = \mu F(\rho, \xi)$. Solving for F in (I.11), we obtain

$$F \;=\; b_1 \pm \frac{f_1^3 |b_2 + \Pi|^2}{\sqrt{f_2^6 + \left(b_2 + \Pi\right)^2}} \, , \tag{I.13}$$

which we use to express the Hamiltonian only in terms of Π:

$$\mathcal{H}/\mu \;=\; -b_1 b_2 + f_1^3 \sqrt{f_2^6 + \left(b_2 + \Pi\right)^2} \pm b_1 |b_2 + \Pi| + \widetilde{C}_5 \, . \tag{I.14}$$

This Hamiltonian is a function of the Riemann-surface coordinates (ξ, ρ), but we are interested in putting probes on $\partial\Sigma$ and so we will take its $\rho \to 0$ limit. We will then interpret it as a potential in the ξ direction and find its minima for a given value of Π in a given background geometry. The expression in (I.14) has two possible forms depending on which solution of F we choose in (I.13) and on whether $b_2 + \Pi$ is less or greater than zero. This choice depends on whether we add M2 or anti-M2 charge to the M5-world-volume. For the particular example we will study here we will take the minus solution and assume that $b_2 + \Pi < 0$ to arrive at

$$\mathcal{H}/\mu = \Pi \, b_1 + f_1^3 \sqrt{f_2^6 + \left(b_2 + \Pi\right)^2} + \widetilde{C}_5 \, . \tag{I.15}$$

Moreover, we will express b_i in terms of $\widehat{b}_i$ (see the discussion below (10.27)) and we will factor out $\frac{\nu_3 \sigma}{c_1^3 c_2^3}$ to simplify our computation. Keeping only the $d\xi$ terms in (I.10) and noting that $c_1 c_2 c_3 f_1 f_2 f_3 = \sigma h$ we arrive at:

$$\partial_\xi \mathcal{H} = \frac{\nu_3 \sigma}{c_1^3 c_2^3} \partial_\xi \widehat{\mathcal{H}} = \frac{1}{8} \left(8 \, \partial_\xi \left(f_1^3 \sqrt{f_2^6 + (\Pi + \widehat{b}_2)^2} \right) + (\Pi + \widehat{b}_2) \, \partial_\xi \widehat{b}_1 - \frac{h^3}{f_3^6} \partial_\rho \widehat{b}_3 \right) . \tag{I.16}$$

In Fig. I.1 we depict the function $\partial_\xi \mathcal{H}$ for various values of Π and for solutions with two and three poles in G. By explicitly computing the zeros of this function we observe that they follow a linear growth in Π. In particular, we find that

$$\xi_0 = -\frac{1}{4} \Pi + c \, , \tag{I.17}$$

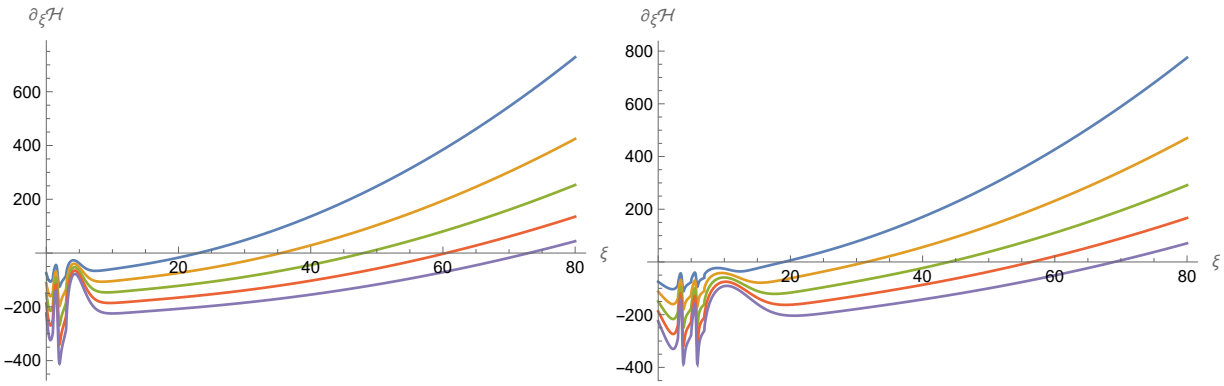

(a) Two-pole solution

(b) Three-pole solution

Figure I.1: Solution with two poles in G with parameters $(\xi_1, \xi_2, \zeta_1, \zeta_2, \alpha, \widehat{b}_2^0) = (1, 3, 1, 1, 0, 4)$ (a) and solution with three poles in G with parameters $(\xi_1, \xi_2, \xi_3, \zeta_1, \zeta_2, \zeta_3, \alpha, \widehat{b}_2^0) = (3, 5, 7, 1, 2, 3, 0, 12)$ (b). In both graphs Π takes the values $(-100, -150, -200, -250, -300)$ from left to right.

where ξ_0 denotes the minimum of $\mathcal{H}$ and c is a constant that depends on our gauge choices and the parameters of the particular solution we are probing.

The relation, (I.17), is expected since Π roughly corresponds to $\sim Q_{M2}/Q_{M5}$ and if we think of our probe as another spike in the solution we are examining, we expect from (10.49) that its position on the ξ axis will scale with Q_{M2} in the following way[1]:

$$\frac{Q_{M2,0}}{Q_{M5,0}} \sim -\frac{16\zeta_0}{4\zeta_0}\xi_0 \quad \Rightarrow \quad \xi_0 \sim -\frac{1}{4}\Pi\,. \tag{I.18}$$

For the values of Π and solution parameters we used in Fig. I.1 there are only minima to the right of the background spikes. However, for smaller values of Π one can generally find a minimum also to the left of the spikes, and for sufficient separation between the location of the various poles it is also possible to find a minimum in between them. We therefore find that the equilibrium positions of our probes match precisely with the supergravity solution and our interpretation of it.

[1]The signs of the M2 charges here are the opposite of those in the main text, but this simply reflects our choices of convention.

Bibliography

[1] **Supernova Search Team** , A. G. Riess *et al.*, "Observational evidence from supernovae for an accelerating universe and a cosmological constant," *Astron. J.* **116** (1998) 1009–1038, arXiv:astro-ph/9805201.

[2] **Supernova Cosmology Project** , S. Perlmutter *et al.*, "Measurements of Ω and Λ from 42 High Redshift Supernovae," *Astrophys. J.* **517** (1999) 565–586, arXiv:astro-ph/9812133.

[3] S. Weinberg, "Anthropic Bound on the Cosmological Constant," *Phys. Rev. Lett.* **59** (1987) 2607.

[4] S. Kachru, R. Kallosh, A. D. Linde, and S. P. Trivedi, "De Sitter vacua in string theory," *Phys. Rev.* **D68** (2003) 046005, arXiv:hep-th/0301240 [hep-th].

[5] G. Obied, H. Ooguri, L. Spodyneiko, and C. Vafa, "De Sitter Space and the Swampland," arXiv:1806.08362 [hep-th].

[6] H. Ooguri, E. Palti, G. Shiu, and C. Vafa, "Distance and de Sitter Conjectures on the Swampland," *Phys. Lett. B* **788** (2019) 180–184, arXiv:1810.05506 [hep-th].

[7] J. D. Bekenstein, "Black holes and entropy," *Phys. Rev.* **D7** (1973) 2333–2346.

[8] S. W. Hawking, "Particle Creation by Black Holes," *Commun. Math. Phys.* **43** (1975) 199–220. [Erratum: Commun.Math.Phys. 46, 206 (1976)].

[9] I. Bena, S. El-Showk, and B. Vercnocke, "Black Holes in String Theory," *Springer Proc. Phys.* **144** (2013) 59–178.

[10] A. Sen, "Extremal black holes and elementary string states," *Mod. Phys. Lett.* **A10** (1995) 2081–2094, arXiv:hep-th/9504147.

[11] A. Dabholkar, "Exact counting of black hole microstates," *Phys. Rev. Lett.* **94** (2005) 241301, arXiv:hep-th/0409148.

[12] A. Strominger and C. Vafa, "Microscopic Origin of the Bekenstein-Hawking Entropy," *Phys. Lett.* **B379** (1996) 99–104, arXiv:hep-th/9601029.

[13] S. D. Mathur, "The fuzzball proposal for black holes: An elementary review," *Fortsch. Phys.* **53** (2005) 793–827, arXiv:hep-th/0502050.

[14] D. Mateos and P. K. Townsend, "Supertubes," *Phys. Rev. Lett.* **87** (2001) 011602, arXiv:hep-th/0103030.

[15] B. Cabrera Palmer and D. Marolf, "Counting supertubes," *JHEP* **06** (2004) 028, arXiv:hep-th/0403025.

[16] O. Lunin and S. D. Mathur, "Metric of the multiply wound rotating string," *Nucl. Phys.* **B610** (2001) 49–76, arXiv:hep-th/0105136.

[17] O. Lunin and S. D. Mathur, "AdS/CFT duality and the black hole information paradox," *Nucl. Phys.* **B623** (2002) 342–394, arXiv:hep-th/0109154.

[18] O. Lunin, J. M. Maldacena, and L. Maoz, "Gravity solutions for the D1-D5 system with angular momentum," arXiv:hep-th/0212210.

[19] V. S. Rychkov, "D1-D5 black hole microstate counting from supergravity," *JHEP* **01** (2006) 063, arXiv:hep-th/0512053.

[20] I. Kanitscheider, K. Skenderis, and M. Taylor, "Fuzzballs with internal excitations," *JHEP* **06** (2007) 056, arXiv:0704.0690 [hep-th].

[21] P. Heidmann, *Black-Hole Microstates in String Theory: Black is the Color but Smooth are the Geometries?* PhD thesis, Orsay, 2019.

[22] N. P. Warner, "Lectures on Microstate Geometries," arXiv:1912.13108 [hep-th].

[23] I. Bena, E. J. Martinec, S. D. Mathur, and N. P. Warner, "Fuzzballs and Microstate Geometries: Black-Hole Structure in String Theory," arXiv:2204.13113 [hep-th].

[24] I. Bena, S. Giusto, R. Russo, M. Shigemori, and N. P. Warner, "Habemus Superstratum! A constructive proof of the existence of superstrata," *JHEP* **05** (2015) 110, arXiv:1503.01463 [hep-th].

[25] I. Bena, S. Giusto, E. J. Martinec, R. Russo, M. Shigemori, D. Turton, and N. P. Warner, "Smooth horizonless geometries deep inside the black-hole regime," *Phys. Rev. Lett.* **117** no. 20, (2016) 201601, arXiv:1607.03908 [hep-th].

[26] I. Bena, S. Giusto, E. J. Martinec, R. Russo, M. Shigemori, D. Turton, and N. P. Warner, "Asymptotically-flat supergravity solutions deep inside the black-hole regime," *JHEP* **02** (2018) 014, arXiv:1711.10474 [hep-th].

[27] M. Shigemori, "Counting Superstrata," *JHEP* **10** (2019) 017, arXiv:1907.03878 [hep-th].

[28] D. R. Mayerson and M. Shigemori, "Counting D1-D5-P microstates in supergravity," *SciPost Phys.* **10** no. 1, (2021) 018, arXiv:2010.04172 [hep-th].

[29] I. Bena, N. Čeplak, S. D. Hampton, A. Houppe, D. Toulikas, and N. P. Warner, "Themelia: the irreducible microstructure of black holes," arXiv:2212.06158 [hep-th].

[30] I. Bena, J. de Boer, M. Shigemori, and N. P. Warner, "Double, Double Supertube Bubble," *JHEP* **10** (2011) 116, arXiv:1107.2650 [hep-th].

[31] B. C. Palmer and D. Marolf, "Counting supertubes," *JHEP* **06** (2004) 028, arXiv:hep-th/0403025.

[32] I. Bena and N. P. Warner, "Resolving the Structure of Black Holes: Philosophizing with a Hammer," arXiv:1311.4538 [hep-th].

[33] I. Bena and N. P. Warner, "Bubbling supertubes and foaming black holes," *Phys. Rev.* **D74** (2006) 066001, arXiv:hep-th/0505166.

[34] P. Berglund, E. G. Gimon, and T. S. Levi, "Supergravity microstates for BPS black holes and black rings," *JHEP* **0606** (2006) 007, arXiv:hep-th/0505167 [hep-th].

[35] V. Balasubramanian, E. G. Gimon, and T. S. Levi, "Four Dimensional Black Hole Microstates: From D-branes to Spacetime Foam," *JHEP* **0801** (2008) 056, arXiv:hep-th/0606118 [hep-th].

[36] I. Bena, S. D. Hampton, A. Houppe, Y. Li, and D. Toulikas, "The (amazing) super-maze," *JHEP* **03** (2023) 237, arXiv:2211.14326 [hep-th].

[37] G. T. Horowitz and D. L. Welch, "Duality invariance of the Hawking temperature and entropy," *Phys. Rev. D* **49** (1994) 590–594, arXiv:hep-th/9308077.

[38] R. Dijkgraaf, E. P. Verlinde, and H. L. Verlinde, "BPS spectrum of the five-brane and black hole entropy," *Nucl. Phys. B* **486** (1997) 77–88, arXiv:hep-th/9603126.

[39] C. G. Callan and J. M. Maldacena, "Brane death and dynamics from the Born-Infeld action," *Nucl. Phys. B* **513** (1998) 198–212, arXiv:hep-th/9708147.

[40] C. Bachas, E. D'Hoker, J. Estes, and D. Krym, "M-theory Solutions Invariant under $D(2,1;\gamma) \oplus D(2,1;\gamma)$," *Fortsch. Phys.* **62** (2014) 207–254, arXiv:1312.5477 [hep-th].

[41] S. Sethi, "Supersymmetry Breaking by Fluxes," *JHEP* **10** (2018) 022, arXiv:1709.03554 [hep-th].

[42] M. Demirtas, M. Kim, L. Mcallister, and J. Moritz, "Vacua with Small Flux Superpotential," *Phys. Rev. Lett.* **124** no. 21, (2020) 211603, arXiv:1912.10047 [hep-th].

[43] M. Demirtas, M. Kim, L. McAllister, and J. Moritz, "Conifold Vacua with Small Flux Superpotential," *Fortsch. Phys.* **68** (2020) 2000085, arXiv:2009.03312 [hep-th].

[44] B. Bastian, T. W. Grimm, and D. van de Heisteeg, "Engineering Small Flux Superpotentials and Mass Hierarchies," arXiv:2108.11962 [hep-th].

[45] S. Kachru, R. Nally, and W. Yang, "Supersymmetric Flux Compactifications and Calabi-Yau Modularity," arXiv:2001.06022 [hep-th].

[46] P. Candelas, X. de la Ossa, P. Kuusela, and J. McGovern, "Flux Vacua and Modularity for $\mathbb{Z}_2$ Symmetric Calabi-Yau Manifolds," arXiv:2302.03047 [hep-th].

[47] R. Schimmrigk, "On flux vacua and modularity," *JHEP* **09** (2020) 061, arXiv:2003.01056 [hep-th].

[48] I. R. Klebanov and M. J. Strassler, "Supergravity and a confining gauge theory: Duality cascades and chi SB resolution of naked singularities," *JHEP* **0008** (2000) 052, arXiv:hep-th/0007191 [hep-th].

[49] G. Papadopoulos and A. A. Tseytlin, "Complex geometry of conifolds and five-brane wrapped on two sphere," *Class. Quant. Grav.* **18** (2001) 1333–1354, arXiv:hep-th/0012034.

[50] J. M. Maldacena and C. Nunez, "Towards the large N limit of pure N=1 superYang-Mills," *Phys. Rev. Lett.* **86** (2001) 588–591, arXiv:hep-th/0008001 [hep-th].

[51] A. Butti, M. Grana, R. Minasian, M. Petrini, and A. Zaffaroni, "The Baryonic branch of Klebanov-Strassler solution: A supersymmetric family of SU(3) structure backgrounds," *JHEP* **03** (2005) 069, arXiv:hep-th/0412187 [hep-th].

[52] I. Bena, M. Grana, and N. Halmagyi, "On the Existence of Meta-stable Vacua in Klebanov-Strassler," *JHEP* **1009** (2010) 087, arXiv:0912.3519 [hep-th].

[53] I. Bena, G. Giecold, M. Grana, N. Halmagyi, and S. Massai, "On Metastable Vacua and the Warped Deformed Conifold: Analytic Results," *Class.Quant.Grav.* **30** (2013) 015003, arXiv:1102.2403 [hep-th].

[54] I. Bena, G. Giecold, M. Grana, N. Halmagyi, and S. Massai, "The backreaction of anti-D3 branes on the Klebanov-Strassler geometry," *JHEP* **1306** (2013) 060, arXiv:1106.6165 [hep-th].

[55] I. Bena, M. Grana, S. Kuperstein, and S. Massai, "Giant Tachyons in the Landscape," arXiv:1410.7776 [hep-th].

[56] M. Grana and J. Polchinski, "Supersymmetric three form flux perturbations on AdS(5)," *Phys.Rev.* **D63** (2001) 026001, arXiv:hep-th/0009211 [hep-th].

[57] S. Gukov, C. Vafa, and E. Witten, "CFT's from Calabi-Yau four folds," *Nucl. Phys.* **B584** (2000) 69–108, arXiv:hep-th/9906070 [hep-th]. [Erratum: Nucl. Phys.B608,477(2001)].

[58] I. R. Klebanov and E. Witten, "Superconformal field theory on three-branes at a Calabi-Yau singularity," *Nucl. Phys. B* **536** (1998) 199–218, arXiv:hep-th/9807080.

[59] S. Massai, "A Comment on anti-brane singularities in warped throats," arXiv:1202.3789 [hep-th].

[60] I. Bena, E. Dudas, M. Grana, and S. Luest, "Uplifting Runaways," *Fortsch. Phys.* **67** no. 1-2, (2019) 1800100, arXiv:1809.06861 [hep-th].

[61] R. Blumenhagen, D. Kläwer, and L. Schlechter, "Swampland Variations on a Theme by KKLT," *JHEP* **05** (2019) 152, arXiv:1902.07724 [hep-th].

[62] E. Dudas and S. Lüst, "An update on moduli stabilization with antibrane uplift," *JHEP* **03** (2021) 107, arXiv:1912.09948 [hep-th].

[63] M. R. Douglas, J. Shelton, and G. Torroba, "Warping and supersymmetry breaking," arXiv:0704.4001 [hep-th].

[64] I. Antoniadis, E. Dudas, S. Ferrara, and A. Sagnotti, "The Volkov-Akulov-Starobinsky supergravity," *Phys. Lett.* **B733** (2014) 32–35, arXiv:1403.3269 [hep-th].

[65] S. Ferrara, R. Kallosh, and A. Linde, "Cosmology with Nilpotent Superfields," *JHEP* **10** (2014) 143, arXiv:1408.4096 [hep-th].

[66] B. V. Bento, D. Chakraborty, S. L. Parameswaran, and I. Zavala, "A new de Sitter solution with a weakly warped deformed conifold," *JHEP* **12** (2021) 124, arXiv:2105.03370 [hep-th].

[67] X. Gao, A. Hebecker, and D. Junghans, "Control issues of KKLT," *Fortsch. Phys.* **68** (2020) 2000089, arXiv:2009.03914 [hep-th].

[68] I. Bena, J. Blåbäck, M. Graña, and S. Lüst, "The tadpole problem," *JHEP* **11** (2021) 223, arXiv:2010.10519 [hep-th].

[69] U. H. Danielsson and T. Van Riet, "Fatal attraction: more on decaying anti-branes," *JHEP* **03** (2015) 087, arXiv:1410.8476 [hep-th].

[70] L. Randall, "The Boundaries of KKLT," *Fortsch. Phys.* **68** no. 3-4, (2020) 1900105, arXiv:1912.06693 [hep-th].

[71] I. R. Klebanov and A. A. Tseytlin, "Gravity duals of supersymmetric SU(N) x SU(N+M) gauge theories," *Nucl. Phys. B* **578** (2000) 123–138, arXiv:hep-th/0002159.

[72] S. Lüst and L. Randall, "Effective Theory of Warped Compactifications and the Implications for KKLT," *Fortsch. Phys.* **70** no. 7-8, (2022) 2200103, arXiv:2206.04708 [hep-th].

[73] A. Buchel, "Klebanov-Strassler black hole," *JHEP* **01** (2019) 207, arXiv:1809.08484 [hep-th].

[74] I. Bena, A. Buchel, and S. Lüst, "Throat destabilization (for profit and for fun)," arXiv:1910.08094 [hep-th].

[75] I. Bena, E. Dudas, M. Graña, G. L. Monaco, and D. Toulikas, "Bare-Bones de Sitter," arXiv:2202.02327 [hep-th].

[76] I. Affleck, M. Dine, and N. Seiberg, "Dynamical Supersymmetry Breaking in Supersymmetric QCD," *Nucl. Phys. B* **241** (1984) 493–534.

[77] P. G. Camara, L. E. Ibanez, and A. M. Uranga, "Flux-induced SUSY-breaking soft terms on D7-D3 brane systems," *Nucl. Phys.* **B708** (2005) 268–316, arXiv:hep-th/0408036 [hep-th].

[78] H. Jockers and J. Louis, "The Effective action of D7-branes in N = 1 Calabi-Yau orientifolds," *Nucl. Phys.* **B705** (2005) 167–211, arXiv:hep-th/0409098 [hep-th].

[79] M. Graña, N. Kovensky, and A. Retolaza, "Gaugino mass term for D-branes and Generalized Complex Geometry," *JHEP* **06** (2020) 047, arXiv:2002.01481 [hep-th].

[80] C. Crinò, F. Quevedo, and R. Valandro, "On de Sitter String Vacua from Anti-D3-Branes in the Large Volume Scenario," *JHEP* **03** (2021) 258, arXiv:2010.15903 [hep-th].

[81] D. Junghans, "LVS de Sitter vacua are probably in the swampland," *Nucl. Phys. B* **990** (2023) 116179, arXiv:2201.03572 [hep-th].

[82] E. Witten, "Nonperturbative superpotentials in string theory," *Nucl. Phys.* **B474** (1996) 343–360, arXiv:hep-th/9604030 [hep-th].

[83] E. Bergshoeff, R. Kallosh, A.-K. Kashani-Poor, D. Sorokin, and A. Tomasiello, "An Index for the Dirac operator on D3 branes with background fluxes," *JHEP* **10** (2005) 102, arXiv:hep-th/0507069.

[84] D. Lust, S. Reffert, W. Schulgin, and P. K. Tripathy, "Fermion zero modes in the presence of fluxes and a non-perturbative superpotential," *JHEP* **08** (2006) 071, arXiv:hep-th/0509082.

[85] D. Robbins and S. Sethi, "A Barren landscape?," *Phys. Rev. D* **71** (2005) 046008, arXiv:hep-th/0405011.

[86] P. K. Tripathy and S. P. Trivedi, "D3 brane action and fermion zero modes in presence of background flux," *JHEP* **06** (2005) 066, arXiv:hep-th/0503072.

[87] R. Kallosh, A.-K. Kashani-Poor, and A. Tomasiello, "Counting fermionic zero modes on M5 with fluxes," *JHEP* **06** (2005) 069, arXiv:hep-th/0503138.

[88] N. Saulina, "Topological constraints on stabilized flux vacua," *Nucl. Phys. B* **720** (2005) 203–210, arXiv:hep-th/0503125.

[89] L. Martucci, J. Rosseel, D. Van den Bleeken, and A. Van Proeyen, "Dirac actions for D-branes on backgrounds with fluxes," *Class. Quant. Grav.* **22** (2005) 2745–2764, arXiv:hep-th/0504041.

[90] P. Berglund and P. Mayr, "Non-perturbative superpotentials in F-theory and string duality," *JHEP* **01** (2013) 114, arXiv:hep-th/0504058.

[91] A. Dymarsky, I. R. Klebanov, and N. Seiberg, "On the moduli space of the cascading SU(M+p) x SU(p) gauge theory," *JHEP* **01** (2006) 155, arXiv:hep-th/0511254.

[92] K. Intriligator, N. Seiberg, and D. Shih, "Dynamical SUSY breaking in meta-stable vacua," *JHEP* **04** (2006) 021, hep-th/0602239.

[93] R. Argurio, M. Bertolini, S. Franco, and S. Kachru, "Meta-stable vacua and D-branes at the conifold," *JHEP* **06** (2007) 017, arXiv:hep-th/0703236.

[94] N. Seiberg, "Private communication,".

[95] M. Grana and J. Polchinski, "Gauge / gravity duals with holomorphic dilaton," *Phys. Rev. D* **65** (2002) 126005, arXiv:hep-th/0106014.

[96] S. Kuperstein and J. Sonnenschein, "Analytic nonsupersymmtric background dual of a confining gauge theory and the corresponding plane wave theory of hadrons," *JHEP* **02** (2004) 015, arXiv:hep-th/0309011.

[97] O. Aharony, A. Buchel, and A. Yarom, "Holographic renormalization of cascading gauge theories," *Phys. Rev. D* **72** (2005) 066003, arXiv:hep-th/0506002.

[98] A. Dymarsky, "On gravity dual of a metastable vacuum in Klebanov-Strassler theory," *JHEP* **05** (2011) 053, arXiv:1102.1734 [hep-th].

[99] A. Dymarsky and S. Massai, "Uplifting the baryonic branch: a test for backreacting anti-D3-branes," *JHEP* **11** (2014) 034, arXiv:1310.0015 [hep-th].

[100] V. Borokhov and S. S. Gubser, "Nonsupersymmetric deformations of the dual of a confining gauge theory," *JHEP* **05** (2003) 034, arXiv:hep-th/0206098.

[101] I. Bena, M. Graña, N. Kovensky, and A. Retolaza, "Kähler moduli stabilization from ten dimensions," *JHEP* **10** (2019) 200, arXiv:1908.01785 [hep-th].

[102] O. DeWolfe and S. B. Giddings, "Scales and hierarchies in warped compactifications and brane worlds," *Phys. Rev. D* **67** (2003) 066008, arXiv:hep-th/0208123.

[103] F. F. Gautason, V. Van Hemelryck, and T. Van Riet, "The Tension between 10D Supergravity and dS Uplifts," *Fortsch. Phys.* **67** no. 1-2, (2019) 1800091, arXiv:1810.08518 [hep-th].

[104] M. Demirtas, M. Kim, L. McAllister, J. Moritz, and A. Rios-Tascon, "Small cosmological constants in string theory," *JHEP* **12** (2021) 136, arXiv:2107.09064 [hep-th].

[105] M. Demirtas, M. Kim, L. McAllister, J. Moritz, and A. Rios-Tascon, "Exponentially Small Cosmological Constant in String Theory," *Phys. Rev. Lett.* **128** no. 1, (2022) 011602, arXiv:2107.09065 [hep-th].

[106] M. Grana, R. Minasian, M. Petrini, and A. Tomasiello, "Generalized structures of N=1 vacua," *JHEP* **11** (2005) 020, arXiv:hep-th/0505212 [hep-th].

[107] P. Koerber and L. Martucci, "Warped generalized geometry compactifications, effective theories and non-perturbative effects," *Fortsch. Phys.* **56** (2008) 862–868, arXiv:0803.3149 [hep-th].

[108] A. Dymarsky and L. Martucci, "D-brane non-perturbative effects and geometric deformations," *JHEP* **04** (2011) 061, arXiv:1012.4018 [hep-th].

[109] S. Kachru, M. Kim, L. McAllister, and M. Zimet, "de Sitter Vacua from Ten Dimensions," arXiv:1908.04788 [hep-th].

[110] P. Koerber and L. Martucci, "D-branes on AdS flux compactifications," *JHEP* **01** (2008) 047, arXiv:0710.5530 [hep-th].

[111] P. Koerber and L. Martucci, "From ten to four and back again: How to generalize the geometry," *JHEP* **08** (2007) 059, arXiv:0707.1038 [hep-th].

[112] I. Benmachiche and T. W. Grimm, "Generalized N=1 orientifold compactifications and the Hitchin functionals," *Nucl. Phys. B* **748** (2006) 200–252, arXiv:hep-th/0602241.

[113] F. Apers, M. Montero, T. Van Riet, and T. Wrase, "Comments on classical AdS flux vacua with scale separation," *JHEP* **05** (2022) 167, arXiv:2202.00682 [hep-th].

[114] Y. Hamada, A. Hebecker, G. Shiu, and P. Soler, "On brane gaugino condensates in 10d," *JHEP* **04** (2019) 008, arXiv:1812.06097 [hep-th].

[115] Y. Hamada, A. Hebecker, G. Shiu, and P. Soler, "Understanding KKLT from a 10d perspective," *JHEP* **06** (2019) 019, arXiv:1902.01410 [hep-th].

[116] F. F. Gautason, V. Van Hemelryck, T. Van Riet, and G. Venken, "A 10d view on the KKLT AdS vacuum and uplifting," *JHEP* **06** (2020) 074, arXiv:1902.01415 [hep-th].

[117] R. Kallosh, "Gaugino Condensation and Geometry of the Perfect Square," *Phys. Rev.* **D99** no. 6, (2019) 066003, arXiv:1901.02023 [hep-th].

[118] Y. Hamada, A. Hebecker, G. Shiu, and P. Soler, "Completing the D7-brane local gaugino action," *JHEP* **11** (2021) 033, arXiv:2105.11467 [hep-th].

[119] D. Lust, F. Marchesano, L. Martucci, and D. Tsimpis, "Generalized non-supersymmetric flux vacua," *JHEP* **11** (2008) 021, arXiv:0807.4540 [hep-th].

[120] P. Koerber, "Lectures on Generalized Complex Geometry for Physicists," *Fortsch. Phys.* **59** (2011) 169–242, arXiv:1006.1536 [hep-th].

[121] E. Bergshoeff, R. Kallosh, T. Ortin, D. Roest, and A. Van Proeyen, "New formulations of D = 10 supersymmetry and D8 - O8 domain walls," *Class. Quant. Grav.* **18** (2001) 3359–3382, arXiv:hep-th/0103233.

[122] P. Koerber and D. Tsimpis, "Supersymmetric sources, integrability and generalized-structure compactifications," *JHEP* **08** (2007) 082, arXiv:0706.1244 [hep-th].

[123] M. Grana, J. Louis, and D. Waldram, "Hitchin functionals in N=2 supergravity," *JHEP* **01** (2006) 008, arXiv:hep-th/0505264 [hep-th].

[124] M. Grana, J. Louis, and D. Waldram, "SU(3) x SU(3) compactification and mirror duals of magnetic fluxes," *JHEP* **04** (2007) 101, arXiv:hep-th/0612237 [hep-th].

[125] D. Cassani and A. Bilal, "Effective actions and N=1 vacuum conditions from SU(3) x SU(3) compactifications," *JHEP* **09** (2007) 076, arXiv:0707.3125 [hep-th].

[126] M. Grana, "Flux compactifications in string theory: A Comprehensive review," *Phys. Rept.* **423** (2006) 91–158, arXiv:hep-th/0509003.

[127] G. Veneziano and S. Yankielowicz, "An Effective Lagrangian for the Pure N=1 Supersymmetric Yang-Mills Theory," *Phys. Lett.* **113B** (1982) 231.

[128] A. R. Frey and M. Lippert, "AdS strings with torsion: Non-complex heterotic compactifications," *Phys. Rev.* **D72** (2005) 126001, arXiv:hep-th/0507202 [hep-th].

[129] R. Minasian, M. Petrini, and E. E. Svanes, "On Heterotic Vacua with Fermionic Expectation Values," *Fortsch. Phys.* **65** no. 3-4, (2017) 1700010, arXiv:1702.01156 [hep-th].

[130] J. Held, D. Lust, F. Marchesano, and L. Martucci, "DWSB in heterotic flux compactifications," *JHEP* **06** (2010) 090, arXiv:1004.0867 [hep-th].

[131] L. Martucci, "D-branes on general N=1 backgrounds: Superpotentials and D-terms," *JHEP* **06** (2006) 033, arXiv:hep-th/0602129 [hep-th].

[132] F. Cachazo, K. A. Intriligator, and C. Vafa, "A Large N duality via a geometric transition," *Nucl. Phys. B* **603** (2001) 3–41, arXiv:hep-th/0103067.

[133] M. Atiyah, J. M. Maldacena, and C. Vafa, "An M theory flop as a large N duality," *J. Math. Phys.* **42** (2001) 3209–3220, arXiv:hep-th/0011256 [hep-th].

[134] J. Maldacena and D. Martelli, "The Unwarped, resolved, deformed conifold: Fivebranes and the baryonic branch of the Klebanov-Strassler theory," *JHEP* **01** (2010) 104, arXiv:0906.0591 [hep-th].

[135] B. Heidenreich, L. McAllister, and G. Torroba, "Dynamic SU(2) Structure from Seven-branes," *JHEP* **05** (2011) 110, arXiv:1011.3510 [hep-th].

[136] D. Baumann, A. Dymarsky, S. Kachru, I. R. Klebanov, and L. McAllister, "D3-brane Potentials from Fluxes in AdS/CFT," *JHEP* **06** (2010) 072, arXiv:1001.5028 [hep-th].

[137] O. DeWolfe, A. Giryavets, S. Kachru, and W. Taylor, "Type IIA moduli stabilization," *JHEP* **07** (2005) 066, arXiv:hep-th/0505160.

[138] D. Junghans, "O-Plane Backreaction and Scale Separation in Type IIA Flux Vacua," *Fortsch. Phys.* **68** no. 6, (2020) 2000040, arXiv:2003.06274 [hep-th].

[139] F. Marchesano, E. Palti, J. Quirant, and A. Tomasiello, "On supersymmetric AdS_4 orientifold vacua," *JHEP* **08** (2020) 087, arXiv:2003.13578 [hep-th].

[140] J. Gray, A. S. Haupt, and A. Lukas, "Topological Invariants and Fibration Structure of Complete Intersection Calabi-Yau Four-Folds," *JHEP* **09** (2014) 093, arXiv:1405.2073 [hep-th].

[141] P. Candelas, E. Perevalov, and G. Rajesh, "Toric geometry and enhanced gauge symmetry of F theory / heterotic vacua," *Nucl. Phys. B* **507** (1997) 445–474, arXiv:hep-th/9704097.

[142] S. Lüst, C. Vafa, M. Wiesner, and K. Xu, "Holography and the KKLT Scenario," arXiv:2204.07171 [hep-th].

[143] A. Retolaza, J. Rogers, R. Tatar, and F. Tonioni, "Branes, fermions, and superspace dualities," *JHEP* **10** (2021) 243, arXiv:2106.02090 [hep-th]. [Erratum: JHEP 11, 124 (2021)].

[144] G. T. Horowitz and J. Polchinski, "A correspondence principle for black holes and strings," *Phys. Rev.* **D55** (1997) 6189–6197, arXiv:hep-th/9612146.

[145] T. Damour and G. Veneziano, "Selfgravitating fundamental strings and black holes," *Nucl. Phys.* **B568** (2000) 93–119, arXiv:hep-th/9907030 [hep-th].

[146] Y. Chen, J. Maldacena, and E. Witten, "On the black hole/string transition," arXiv:2109.08563 [hep-th].

[147] I. Bena and P. Kraus, "Three Charge Supertubes and Black Hole Hair," *Phys. Rev.* **D70** (2004) 046003, arXiv:hep-th/0402144.

[148] G. Gibbons and N. Warner, "Global structure of five-dimensional fuzzballs," *Class.Quant.Grav.* **31** (2014) 025016, arXiv:1305.0957 [hep-th].

[149] S. D. Mathur, "Fuzzballs and the information paradox: A Summary and conjectures," arXiv:0810.4525 [hep-th].

[150] A. Almheiri, D. Marolf, J. Polchinski, and J. Sully, "Black Holes: Complementarity or Firewalls?," *JHEP* **1302** (2013) 062, arXiv:1207.3123 [hep-th].

[151] I. Bena, P. Heidmann, and D. Turton, "AdS_2 holography: mind the cap," *JHEP* **12** (2018) 028, arXiv:1806.02834 [hep-th].

[152] I. Bena, E. Martinec, D. Turton, and N. P. Warner, "M-theory Superstrata and the MSW String," *JHEP* **06** (2017) 137, arXiv:1703.10171 [hep-th].

[153] I. Bena, E. J. Martinec, R. Walker, and N. P. Warner, "Early Scrambling and Capped BTZ Geometries," *JHEP* **04** (2019) 126, arXiv:1812.05110 [hep-th].

[154] N. Čeplak, R. Russo, and M. Shigemori, "Supercharging Superstrata," *JHEP* **03** (2019) 095, arXiv:1812.08761 [hep-th].

[155] I. Bena, P. Heidmann, R. Monten, and N. P. Warner, "Thermal Decay without Information Loss in Horizonless Microstate Geometries," *SciPost Phys.* **7** no. 5, (2019) 063, arXiv:1905.05194 [hep-th].

[156] P. Heidmann and N. P. Warner, "Superstratum Symbiosis," *JHEP* **09** (2019) 059, arXiv:1903.07631 [hep-th].

[157] P. Heidmann, D. R. Mayerson, R. Walker, and N. P. Warner, "Holomorphic Waves of Black Hole Microstructure," *JHEP* **02** (2020) 192, arXiv:1910.10714 [hep-th].

[158] D. R. Mayerson, R. A. Walker, and N. P. Warner, "Microstate Geometries from Gauged Supergravity in Three Dimensions," *JHEP* **10** (2020) 030, arXiv:2004.13031 [hep-th].

[159] M. Shigemori, "Superstrata," *Gen. Rel. Grav.* **52** no. 5, (2020) 51, arXiv:2002.01592 [hep-th].

[160] I. Bena, F. Eperon, P. Heidmann, and N. P. Warner, "The Great Escape: Tunneling out of Microstate Geometries," *JHEP* **04** (2021) 112, arXiv:2005.11323 [hep-th].

[161] I. Bena, A. Houppe, and N. P. Warner, "Delaying the Inevitable: Tidal Disruption in Microstate Geometries," *JHEP* **02** (2021) 103, arXiv:2006.13939 [hep-th].

[162] S. Giusto, M. R. Hughes, and R. Russo, "The Regge limit of AdS_3 holographic correlators," arXiv:2007.12118 [hep-th].

[163] E. J. Martinec and N. P. Warner, "The Harder They Fall, the Bigger They Become: Tidal Trapping of Strings by Microstate Geometries," *JHEP* **04** (2021) 259, arXiv:2009.07847 [hep-th].

[164] A. Houppe and N. P. Warner, "Supersymmetry and Superstrata in Three Dimensions," arXiv:2012.07850 [hep-th].

[165] N. Ceplak and M. R. R. Hughes, "The Regge limit of AdS_3 holographic correlators with heavy states: towards the black hole regime," *JHEP* **07** (2021) 021, arXiv:2102.09549 [hep-th].

[166] N. Ceplak, S. Hampton, and Y. Li, "A Helix Down the Throat: Internal Tidal Effects," arXiv:2106.03841 [hep-th].

[167] B. Ganchev, A. Houppe, and N. Warner, "Q-Balls Meet Fuzzballs: Non-BPS Microstate Geometries," arXiv:2107.09677 [hep-th].

[168] B. Ganchev, A. Houppe, and N. P. Warner, "New Superstrata from Three-Dimensional Supergravity," arXiv:2110.02961 [hep-th].

[169] I. Kanitscheider, K. Skenderis, and M. Taylor, "Holographic anatomy of fuzzballs," *JHEP* **04** (2007) 023, arXiv:hep-th/0611171.

[170] M. Taylor, "Matching of correlators in AdS(3) / CFT(2)," *JHEP* **06** (2008) 010, arXiv:0709.1838 [hep-th].

[171] S. Giusto, E. Moscato, and R. Russo, "AdS_3 holography for 1/4 and 1/8 BPS geometries," *JHEP* **11** (2015) 004, arXiv:1507.00945 [hep-th].

[172] A. Bombini, A. Galliani, S. Giusto, E. Moscato, and R. Russo, "Unitary 4-point correlators from classical geometries," arXiv:1710.06820 [hep-th].

[173] S. Giusto, S. Rawash, and D. Turton, "Ads_3 holography at dimension two," *JHEP* **07** (2019) 171, arXiv:1904.12880 [hep-th].

[174] J. Garcia i Tormo and M. Taylor, "One point functions for black hole microstates," *Gen. Rel. Grav.* **51** no. 7, (2019) 89, arXiv:1904.10200 [hep-th].

[175] S. Rawash and D. Turton, "Supercharged AdS_3 Holography," arXiv:2105.13046 [hep-th].

[176] B. Ganchev, S. Giusto, A. Houppe, and R. Russo, "AdS_3 holography for non-BPS geometries," arXiv:2112.03287 [hep-th].

[177] S. G. Avery, "Using the D1D5 CFT to Understand Black Holes," arXiv:1012.0072 [hep-th].

[178] F. Chen, B. Michel, J. Polchinski, and A. Puhm, "Journey to the Center of the Fuzzball," *JHEP* **02** (2015) 081, arXiv:1408.4798 [hep-th].

[179] B. E. Niehoff and N. P. Warner, "Doubly-Fluctuating BPS Solutions in Six Dimensions," *JHEP* **1310** (2013) 137, arXiv:1303.5449 [hep-th].

[180] R. Emparan, D. Mateos, and P. K. Townsend, "Supergravity supertubes," *JHEP* **07** (2001) 011, arXiv:hep-th/0106012.

[181] C. G. Callan, J. M. Maldacena, and A. W. Peet, "Extremal Black Holes As Fundamental Strings," *Nucl. Phys.* **B475** (1996) 645–678, arXiv:hep-th/9510134.

[182] A. Dabholkar, J. P. Gauntlett, J. A. Harvey, and D. Waldram, "Strings as Solitons & Black Holes as Strings," *Nucl. Phys.* **B474** (1996) 85–121, arXiv:hep-th/9511053.

[183] S. Giusto, L. Martucci, M. Petrini, and R. Russo, "6D microstate geometries from 10D structures," *Nucl.Phys.* **B876** (2013) 509–555, arXiv:1306.1745 [hep-th].

[184] G. W. Gibbons and S. W. Hawking, "Gravitational Multi - Instantons," *Phys. Lett. B* **78** (1978) 430.

[185] A. A. Tseytlin, "Harmonic superpositions of M-branes," *Nucl. Phys. B* **475** (1996) 149–163, arXiv:hep-th/9604035.

[186] R. C. Myers and M. Perry, "Black Holes in Higher Dimensional Space-Times," *Annals Phys.* **172** (1986) 304.

[187] J. M. Maldacena, "The large N limit of superconformal field theories and supergravity," *Adv. Theor. Math. Phys.* **2** (1998) 231–252, arXiv:hep-th/9711200.

[188] E. J. Martinec and S. Massai, "String Theory of Supertubes," *JHEP* **07** (2018) 163, arXiv:1705.10844 [hep-th].

[189] E. J. Martinec, S. Massai, and D. Turton, "String dynamics in NS5-F1-P geometries," *JHEP* **09** (2018) 031, arXiv:1803.08505 [hep-th].

[190] D. Bufalini, S. Iguri, N. Kovensky, and D. Turton, "Black hole microstates from the worldsheet," *JHEP* **08** (2021) 011, arXiv:2105.02255 [hep-th].

[191] D. Kutasov, "Introduction to little string theory," *ICTP Lect. Notes Ser.* **7** (2002) 165–209.

[192] I. Bena, S. F. Ross, and N. P. Warner, "On the Oscillation of Species," *JHEP* **1409** (2014) 113, arXiv:1312.3635 [hep-th].

[193] F. C. Eperon, H. S. Reall, and J. E. Santos, "Instability of supersymmetric microstate geometries," *JHEP* **10** (2016) 031, arXiv:1607.06828 [hep-th].

[194] D. Marolf, B. Michel, and A. Puhm, "A rough end for smooth microstate geometries," *JHEP* **05** (2017) 021, arXiv:1612.05235 [hep-th].

[195] E. J. Martinec, S. Massai, and D. Turton, "Little Strings, Long Strings, and Fuzzballs," *JHEP* **11** (2019) 019, arXiv:1906.11473 [hep-th].

[196] E. J. Martinec, "AdS3's with and without BTZ's," arXiv:2109.11716 [hep-th].

[197] J. de Boer, F. Denef, S. El-Showk, I. Messamah, and D. Van den Bleeken, "Black hole bound states in AdS3 x S2," *JHEP* **11** (2008) 050, arXiv:0802.2257 [hep-th].

[198] Y. Li, "Black holes and the swampland: the deep throat revelations," *JHEP* **06** (2021) 065, arXiv:2102.04480 [hep-th].

[199] Y. Li, "An Alliance in the Tripartite Conflict over Moduli Space," arXiv:2112.03281 [hep-th].

[200] I. Bena and D. R. Mayerson, "Black Holes Lessons from Multipole Ratios," *JHEP* **03** (2021) 114, arXiv:2007.09152 [hep-th].

[201] I. Bah, I. Bena, P. Heidmann, Y. Li, and D. R. Mayerson, "Gravitational footprints of black holes and their microstate geometries," *JHEP* **10** (2021) 138, arXiv:2104.10686 [hep-th].

[202] M. Cariglia and O. A. P. Mac Conamhna, "The General form of supersymmetric solutions of N=(1,0) U(1) and SU(2) gauged supergravities in six-dimensions," *Class. Quant. Grav.* **21** (2004) 3171–3196, arXiv:hep-th/0402055 [hep-th].

[203] P. A. Cano and T. Ortín, "The structure of all the supersymmetric solutions of ungauged $\mathcal{N} = (1,0), d = 6$ supergravity," *Class. Quant. Grav.* **36** no. 12, (2019) 125007, arXiv:1804.04945 [hep-th].

[204] I. Bena, S. Giusto, M. Shigemori, and N. P. Warner, "Supersymmetric Solutions in Six Dimensions: A Linear Structure," *JHEP* **1203** (2012) 084, arXiv:1110.2781 [hep-th].

[205] N. Čeplak, S. Hampton, and N. P. Warner, "Linearizing the BPS equations with vector and tensor multiplets," *JHEP* **03** (2023) 145, arXiv:2204.07170 [hep-th].

[206] E. Bakhshaei and A. Bombini, "Three-charge superstrata with internal excitations," arXiv:1811.00067 [hep-th].

[207] P. Heidmann, "Non-BPS Floating Branes and Bubbling Geometries," arXiv:2112.03279 [hep-th].

[208] J. M. Maldacena, "Black holes in string theory," arXiv:hep-th/9607235.

[209] S. Giusto and S. D. Mathur, "Geometry of D1-D5-P bound states," *Nucl. Phys.* **B729** (2005) 203–220, arXiv:hep-th/0409067.

[210] I. Bena, C.-W. Wang, and N. P. Warner, "The foaming three-charge black hole," *Phys. Rev.* **D75** (2007) 124026, arXiv:hep-th/0604110.

[211] I. Bena, C.-W. Wang, and N. P. Warner, "Mergers and Typical Black Hole Microstates," *JHEP* **11** (2006) 042, arXiv:hep-th/0608217.

[212] I. Bena and N. P. Warner, "Black holes, black rings and their microstates," *Lect. Notes Phys.* **755** (2008) 1–92, arXiv:hep-th/0701216.

[213] I. Bena, C.-W. Wang, and N. P. Warner, "Plumbing the Abyss: Black Ring Microstates," *JHEP* **07** (2008) 019, arXiv:0706.3786 [hep-th].

[214] I. Bena, N. Bobev, and N. P. Warner, "Spectral Flow, and the Spectrum of Multi-Center Solutions," *Phys. Rev.* **D77** (2008) 125025, arXiv:0803.1203 [hep-th].

[215] I. Bena, N. Bobev, S. Giusto, C. Ruef, and N. P. Warner, "An Infinite-Dimensional Family of Black-Hole Microstate Geometries," *JHEP* **1103** (2011) 022, arXiv:1006.3497 [hep-th].

[216] M. Bianchi, J. F. Morales, and L. Pieri, "Stringy origin of 4d black hole microstates," *JHEP* **06** (2016) 003, arXiv:1603.05169 [hep-th].

[217] M. Bianchi, J. F. Morales, L. Pieri, and N. Zinnato, "More on microstate geometries of 4d black holes," *JHEP* **05** (2017) 147, arXiv:1701.05520 [hep-th].

[218] P. Heidmann, "Four-center bubbled BPS solutions with a Gibbons-Hawking base," *JHEP* **10** (2017) 009, arXiv:1703.10095 [hep-th].

[219] I. Bena, P. Heidmann, and P. F. Ramirez, "A systematic construction of microstate geometries with low angular momentum," *JHEP* **10** (2017) 217, arXiv:1709.02812 [hep-th].

[220] J. Avila, P. F. Ramirez, and A. Ruiperez, "One Thousand and One Bubbles," *JHEP* **01** (2018) 041, arXiv:1709.03985 [hep-th].

[221] A. Tyukov, R. Walker, and N. P. Warner, "The Structure of BPS Equations for Ambi-polar Microstate Geometries," *Class. Quant. Grav.* **36** no. 1, (2019) 015021, arXiv:1807.06596 [hep-th].

[222] N. Seiberg, "New theories in six-dimensions and matrix description of M theory on T^5 and $T^5/\mathbb{Z}_2$," *Phys. Lett.* **B408** (1997) 98–104, arXiv:hep-th/9705221.

[223] I. Bena, M. Shigemori, and N. P. Warner, "Black-Hole Entropy from Supergravity Superstrata States," *JHEP* **1410** (2014) 140, arXiv:1406.4506 [hep-th].

[224] I. Bena, N. Ceplak, S. Hampton, Y. Li, D. Toulikas, and N. P. Warner, "Resolving black-hole microstructure with new momentum carriers," *JHEP* **10** (2022) 033, arXiv:2202.08844 [hep-th].

[225] S. D. Mathur and D. Turton, "Oscillating supertubes and neutral rotating black hole microstates," *JHEP* **1404** (2014) 072, arXiv:1310.1354 [hep-th].

[226] I. Bena, N. Bobev, C. Ruef, and N. P. Warner, "Supertubes in Bubbling Backgrounds: Born-Infeld Meets Supergravity," *JHEP* **07** (2009) 106, arXiv:0812.2942 [hep-th].

[227] N. R. Constable, R. C. Myers, and O. Tafjord, "The Noncommutative bion core," *Phys. Rev. D* **61** (2000) 106009, arXiv:hep-th/9911136.

[228] I. Bena, J. Blåbäck, R. Minasian, and R. Savelli, "There and back again: A T-brane's tale," *JHEP* **11** (2016) 179, arXiv:1608.01221 [hep-th].

[229] B. Bates and F. Denef, "Exact solutions for supersymmetric stationary black hole composites," *JHEP* **1111** (2011) 127, arXiv:hep-th/0304094 [hep-th].

[230] H. W. Lin, J. Maldacena, L. Rozenberg, and J. Shan, "Holography for people with no time," *SciPost Phys.* **14** no. 6, (2023) 150, arXiv:2207.00407 [hep-th].

[231] Z. Wei and Y. Yoneta, "Counting atypical black hole microstates from entanglement wedges," *JHEP* **05** (2024) 251, arXiv:2211.11787 [hep-th].

[232] P. Hayden and G. Penington, "Black hole microstates vs. the additivity conjectures," arXiv:2012.07861 [hep-th].

[233] S. D. Mathur, "The information paradox: A pedagogical introduction," *Class. Quant. Grav.* **26** (2009) 224001, arXiv:0909.1038 [hep-th].

[234] I. Bena, E. J. Martinec, S. D. Mathur, and N. P. Warner, "Snowmass White Paper: Micro- and Macro-Structure of Black Holes," arXiv:2203.04981 [hep-th].

[235] N. Čeplak, "Vector Superstrata," *JHEP* **08** (2023) 047, arXiv:2212.06947 [hep-th].

[236] I. Bena and P. Kraus, "Microstates of the D1-D5-KK system," *Phys. Rev.* **D72** (2005) 025007, arXiv:hep-th/0503053.

[237] I. Bena, P. Kraus, and N. P. Warner, "Black rings in Taub-NUT," *Phys. Rev.* **D72** (2005) 084019, arXiv:hep-th/0504142.

[238] J. M. Maldacena, A. Strominger, and E. Witten, "Black hole entropy in M-theory," *JHEP* **12** (1997) 002, arXiv:hep-th/9711053.

[239] M. Shigemori, "Perturbative 3-charge microstate geometries in six dimensions," *JHEP* **1310** (2013) 169, arXiv:1307.3115.

[240] S. Giusto and R. Russo, "Superdescendants of the D1D5 CFT and their dual 3-charge geometries," *JHEP* **1403** (2014) 007, arXiv:1311.5536 [hep-th].

[241] I. Bena, D. Turton, R. Walker, and N. P. Warner, "Integrability and Black-Hole Microstate Geometries," *JHEP* **11** (2017) 021, arXiv:1709.01107 [hep-th].

[242] R. Walker, "D1-D5-P superstrata in 5 and 6 dimensions: separable wave equations and prepotentials," *JHEP* **09** (2019) 117, arXiv:1906.04200 [hep-th].

[243] B. Ganchev, A. Houppe, and N. P. Warner, "Elliptical and Purely NS Superstrata," arXiv:2207.04060 [hep-th].

[244] B. Ganchev, S. Giusto, A. Houppe, R. Russo, and N. P. Warner, "Microstrata," *JHEP* **10** (2023) 163, arXiv:2307.13021 [hep-th].

[245] V. Jejjala, O. Madden, S. F. Ross, and G. Titchener, "Non-supersymmetric smooth geometries and D1-D5-P bound states," *Phys. Rev.* **D71** (2005) 124030, arXiv:hep-th/0504181.

[246] I. Bena, S. Giusto, C. Ruef, and N. P. Warner, "A (Running) Bolt for New Reasons," *JHEP* **11** (2009) 089, arXiv:0909.2559 [hep-th].

[247] N. Bobev, B. Niehoff, and N. P. Warner, "Hair in the Back of a Throat: Non-Supersymmetric Multi-Center Solutions from Káhler Manifolds," *JHEP* **1110** (2011) 149, arXiv:1103.0520 [hep-th].

[248] O. Vasilakis and N. P. Warner, "Mind the Gap: Supersymmetry Breaking in Scaling, Microstate Geometries," *JHEP* **1110** (2011) 006, arXiv:1104.2641 [hep-th].

[249] I. Bena, G. Bossard, S. Katmadas, and D. Turton, "Non-BPS multi-bubble microstate geometries," *JHEP* **02** (2016) 073, arXiv:1511.03669 [hep-th].

[250] I. Bena, G. Bossard, S. Katmadas, and D. Turton, "Bolting Multicenter Solutions," *JHEP* **01** (2017) 127, arXiv:1611.03500 [hep-th].

[251] G. Bossard, S. Katmadas, and D. Turton, "Two Kissing Bolts," arXiv:1711.04784 [hep-th].

[252] I. Bah and P. Heidmann, "Topological Stars and Black Holes," *Phys. Rev. Lett.* **126** no. 15, (2021) 151101, arXiv:2011.08851 [hep-th].

[253] I. Bah and P. Heidmann, "Topological Stars, Black holes and Generalized Charged Weyl Solutions," arXiv:2012.13407 [hep-th].

[254] I. Bah and P. Heidmann, "Smooth Bubbling Geometries Without Supersymmetry," arXiv:2106.05118 [hep-th].

[255] I. Bah, A. Dey, and P. Heidmann, "Stability of topological solitons, and black string to bubble transition," *JHEP* **04** (2022) 168, arXiv:2112.11474 [hep-th].

[256] I. Bah, P. Heidmann, and P. Weck, "Schwarzschild-like topological solitons," *JHEP* **08** (2022) 269, arXiv:2203.12625 [hep-th].

[257] I. Bah and P. Heidmann, "Non-BPS bubbling geometries in AdS_3," *JHEP* **02** (2023) 133, arXiv:2210.06483 [hep-th].

[258] I. Bah and P. Heidmann, "Geometric Resolution of Schwarzschild Horizon," arXiv:2303.10186 [hep-th].

[259] O. Lunin, "Strings ending on branes from supergravity," *JHEP* **09** (2007) 093, arXiv:0706.3396 [hep-th].

[260] J. de Boer, A. Pasquinucci, and K. Skenderis, "AdS / CFT dualities involving large 2-D N=4 superconformal symmetry," *Adv. Theor. Math. Phys.* **3** (1999) 577–614, arXiv:hep-th/9904073 [hep-th].

[261] O. Lunin, "Brane webs and 1/4-BPS geometries," *JHEP* **0809** (2008) 028, arXiv:0802.0735 [hep-th].

[262] I. Bena, S. Giusto, C. Ruef, and N. P. Warner, "Supergravity Solutions from Floating Branes," *JHEP* **03** (2010) 047, arXiv:0910.1860 [hep-th].

[263] K. Pilch and N. P. Warner, "N = 1 supersymmetric solutions of IIB supergravity from Killing spinors," arXiv:hep-th/0403005.

[264] D. Nemeschansky and N. P. Warner, "A Family of M theory flows with four supersymmetries," arXiv:hep-th/0403006.

[265] I. Bena and N. P. Warner, "A Harmonic family of dielectric flow solutions with maximal supersymmetry," *JHEP* **0412** (2004) 021, arXiv:hep-th/0406145 [hep-th].

[266] O. Lunin, "1/2-BPS states in M theory and defects in the dual CFTs," *JHEP* **10** (2007) 014, arXiv:0704.3442 [hep-th].

[267] C. N. Gowdigere and N. P. Warner, "Flowing with eight supersymmetries in M theory and F theory," *JHEP* **12** (2003) 048, arXiv:hep-th/0212190.

[268] K. Pilch and N. P. Warner, "Generalizing the N=2 supersymmetric RG flow solution of IIB supergravity," *Nucl. Phys. B* **675** (2003) 99–121, arXiv:hep-th/0306098.

[269] C. N. Gowdigere, D. Nemeschansky, and N. P. Warner, "Supersymmetric solutions with fluxes from algebraic Killing spinors," *Adv. Theor. Math. Phys.* **7** no. 5, (2003) 787–806, arXiv:hep-th/0306097.

[270] E. D'Hoker, J. Estes, M. Gutperle, and D. Krym, "Exact Half-BPS Flux Solutions in M-theory. I: Local Solutions," *JHEP* **08** (2008) 028, arXiv:0806.0605 [hep-th].

[271] E. D'Hoker, J. Estes, M. Gutperle, and D. Krym, "Exact Half-BPS Flux Solutions in M-theory II: Global solutions asymptotic to AdS(7) x S**4," *JHEP* **12** (2008) 044, arXiv:0810.4647 [hep-th].

[272] E. D'Hoker, J. Estes, M. Gutperle, D. Krym, and P. Sorba, "Half-BPS supergravity solutions and superalgebras," *JHEP* **12** (2008) 047, arXiv:0810.1484 [hep-th].

[273] E. D'Hoker, J. Estes, M. Gutperle, and D. Krym, "Janus solutions in M-theory," *JHEP* **06** (2009) 018, arXiv:0904.3313 [hep-th].

[274] E. D'Hoker, J. Estes, M. Gutperle, and D. Krym, "Exact Half-BPS Flux Solutions in M-theory III: Existence and rigidity of global solutions asymptotic to AdS(4) x S**7," *JHEP* **09** (2009) 067, arXiv:0906.0596 [hep-th].

[275] I. A. Bandos, K. Lechner, A. Nurmagambetov, P. Pasti, D. P. Sorokin, and M. Tonin, "Covariant action for the superfive-brane of M theory," *Phys. Rev. Lett.* **78** (1997) 4332–4334, arXiv:hep-th/9701149.

[276] I. Bena and N. P. Warner, "One ring to rule them all ... and in the darkness bind them?," *Adv. Theor. Math. Phys.* **9** (2005) 667–701, arXiv:hep-th/0408106.

[277] J. B. Gutowski, D. Martelli, and H. S. Reall, "All supersymmetric solutions of minimal supergravity in six dimensions," *Class. Quant. Grav.* **20** (2003) 5049–5078, arXiv:hep-th/0306235.

[278] I. Bena, A. Houppe, D. Toulikas, and N. P. Warner, "Maze Topiary in Supergravity," arXiv:2312.02286 [hep-th].

[279] I. Bena and R. Dulac, "Born-Infeld supermaze waves," *JHEP* **05** (2024) 063, arXiv:2312.13447 [hep-th].

[280] M. K. Prasad and C. M. Sommerfield, "An Exact Classical Solution for the 't Hooft Monopole and the Julia-Zee Dyon," *Phys. Rev. Lett.* **35** (1975) 760–762.

[281] K. Hashimoto and W. Taylor, "Strings between branes," *JHEP* **10** (2003) 040, arXiv:hep-th/0307297.

[282] G. Bossard and S. Katmadas, "Duality covariant non-BPS first order systems," *JHEP* **09** (2012) 100, arXiv:1205.5461 [hep-th].

[283] G. Bossard and S. Katmadas, "Floating JMaRT," *JHEP* **04** (2015) 067, arXiv:1412.5217 [hep-th].

[284] J. P. Gauntlett, J. B. Gutowski, C. M. Hull, S. Pakis, and H. S. Reall, "All supersymmetric solutions of minimal supergravity in five- dimensions," *Class.Quant.Grav.* **20** (2003) 4587–4634, arXiv:hep-th/0209114 [hep-th].

[285] J. B. Gutowski and H. S. Reall, "General supersymmetric AdS(5) black holes," *JHEP* **04** (2004) 048, arXiv:hep-th/0401129.

[286] N. Bobev, K. Pilch, and N. P. Warner, "Supersymmetric Janus Solutions in Four Dimensions," *JHEP* **06** (2014) 058, arXiv:1311.4883 [hep-th].

[287] A. Galliani, S. Giusto, E. Moscato, and R. Russo, "Correlators at large c without information loss," *JHEP* **09** (2016) 065, arXiv:1606.01119 [hep-th].

[288] A. Bombini and A. Galliani, "AdS_3 four-point functions from $\frac{1}{8}$ -BPS states," *JHEP* **06** (2019) 044, arXiv:1904.02656 [hep-th].

[289] J. Tian, J. Hou, and B. Chen, "Holographic Correlators on Integrable Superstrata," *Nucl. Phys. B* **948** (2019) 114766, arXiv:1904.04532 [hep-th].

[290] S. Giusto, R. Russo, A. Tyukov, and C. Wen, "Holographic correlators in AdS_3 without Witten diagrams," *JHEP* **09** (2019) 030, arXiv:1905.12314 [hep-th].

[291] O. Hulik, J. Raeymaekers, and O. Vasilakis, "Information recovery from pure state geometries in 3D," *JHEP* **06** (2020) 119, arXiv:1911.12309 [hep-th].

[292] N. Ceplak, S. Giusto, M. R. R. Hughes, and R. Russo, "Holographic correlators with multi-particle states," arXiv:2105.04670 [hep-th].

[293] M. Shigemori, "Interpolating between multi-center microstate geometries," *JHEP* **09** (2021) 010, arXiv:2105.11639 [hep-th].

[294] I. Bena, R. Dulac, A. Houppe, D. Toulikas, and N. P. Warner, "Waves on Mazes," arXiv:2404.14477 [hep-th].

[295] G. Dall'Agata, S. Giusto, and C. Ruef, "U-duality and non-BPS solutions," *JHEP* **02** (2011) 074, arXiv:1012.4803 [hep-th].

[296] T. H. Buscher, "Path Integral Derivation of Quantum Duality in Nonlinear Sigma Models," *Phys. Lett. B* **201** (1988) 466–472.

[297] T. H. Buscher, "A Symmetry of the String Background Field Equations," *Phys. Lett. B* **194** (1987) 59–62.

[298] D. M. De Turck and D. Yang, "Existence of elastic deformations with prescribed principal strains and triply orthogonal systems," *Duke Math. J.* **51** no. 2, (1984) 243–260.

[299] K. Tod, "On choosing coordinates to diagonalize the metric," *Class. Quant. Grav.* **9** no. 7, (1992) 1693.

[300] O. Kowalski and M. Sekizawa, "Diagonalization of three-dimensional pseudo-riemannian metrics," *Journal of Geometry and Physics* **74** (2013) 251–255. https://www.sciencedirect.com/science/article/pii/S0393044013001575.